



---

**Universidad de Valladolid**

Escuela de Ingenierías Industriales

Departamento de Ingeniería Química y Tecnología del  
Medio Ambiente

**Intensification of Cellulose Hydrolysis Process by  
Supercritical Water. Obtaining of Added Value  
Products**

Danilo Alberto Cantero Sposetti

Presentada por Danilo Alberto Cantero Sposetti  
para optar al grado de  
Doctor por la Universidad de Valladolid

Dirigida por:

Doctora María Dolores Bermejo Roda  
Profesora Doctora María José Cocero Alonso





---

# Universidad de Valladolid

Escuela de Ingenierías Industriales

Departamento de Ingeniería Química y Tecnología del  
Medio Ambiente

## Intensificación del Proceso de Hidrólisis de Celulosa para la Obtención de Productos de Valor Añadido mediante el uso de Agua Supercrítica.

Danilo Alberto Cantero Sposetti

Presentada por Danilo Alberto Cantero Sposetti  
para optar al grado de  
Doctor por la Universidad de Valladolid

Dirigida por:  
Doctora María Dolores Bermejo Roda  
Profesora Doctora María José Cocero Alonso



Memoria para optar al grado de Doctor,  
con Mención Doctor Internacional,  
presentada por el Ingeniero Químico:  
Danilo Alberto Cantero Sposetti

Siendo los tutores en la Universidad de Valladolid

Dra. María Dolores Bermejo Roda

y

Prof. Dra. D<sup>a</sup> María José Cocero Alonso

Y en el Lehrstuhl für Prozessmaschinen und Anlagentechnik,  
University of Erlangen (Alemania)

Prof. Dr.-Ing. E. Schlücker

Valladolid, Marzo de 2014



UNIVERSIDAD DE VALLADOLID  
ESCUELA DE INGENIERIAS INDUSTRIALES  
Secretaría

La presente tesis doctoral queda registrada en el folio número \_\_\_\_\_ del correspondiente libro de registro numero \_\_\_\_\_.

Valladolid, a \_\_\_ de \_\_\_\_\_ de 2014

Fdo. El encargado de registro



María Dolores Bermejo Roda  
Profesora de Universidad  
Departamento de Ingeniería Química y Tecnología del Medio Ambiente  
Universidad de Valladolid  
y  
María José Cocero Alonso  
Catedrática de Universidad  
Departamento de Ingeniería Química y Tecnología del Medio Ambiente  
Universidad de Valladolid

Certifican que:

El ingeniero químico DANILO ALBERTO CANTERO SPOSETTI ha realizado en el Departamento de Ingeniería Química y Tecnología del Medio Ambiente de la Universidad de Valladolid, bajo nuestra dirección, el trabajo: "Intensification of Cellulose Hydrolysis Process by Supercritical Water. Obtaining of Added Value Products", cuyo título en castellano es "Intensificación del Proceso de Hidrólisis de Celulosa para la Obtención de Productos de Valor Añadido mediante el uso de Agua Supercrítica". Considerando que dicho trabajo reúne los requisitos para ser presentado como Tesis Doctoral expresan su conformidad con dicha presentación.

Valladolid, a \_\_\_\_ de \_\_\_\_\_ de 2014

Fdo. María Dolores Bermejo Roda

Fdo. María José Cocero Alonso



Reunido el tribunal que ha juzgado la Tesis Doctoral titulada "Intensification of Cellulose Hydrolysis Process by Supercritical Water. Obtaining of Added Value Products" presentada por el Ingeniero Químico Danilo Alberto Cantero Sposetti y en cumplimiento con lo establecido en el Real Decreto 1393/2007 de 29 Octubre ha acordado conceder por \_\_\_\_\_ la calificación de \_\_\_\_\_.

Valladolid, a \_\_\_\_ de \_\_\_\_\_ de 2014

PRESIDENTE

SECRETARIO

1er VOCAL

2º VOCAL

3er VOCAL



Contents	
<b>Abstract</b> .....	5
<b>Symbols</b> .....	13
<b>State of the Art: Biomass refining processes intensification by supercritical water</b> .....	15
<b>Aims and Contents</b> .....	61
<b>Chapter 1. High glucose selectivity in pressurized water hydrolysis of cellulose using ultra-fast reactors.</b> .....	67
<b>Chapter 2. Kinetics analysis of cellulose depolymerization reactions in near critical water</b> .....	85
<b>Chapter 3. Tunable Selectivity on Cellulose Hydrolysis in Supercritical Water</b> .....	111
<b>Chapter 4. Pressure and Temperature Effect on Cellulose Hydrolysis Kinetic in Pressurized Water</b> .....	125
<b>Chapter 5. Selective Transformation of Fructose into Pyruvaldehyde in Supercritical Water. Reaction Pathway Development</b> .....	151
<b>Chapter 6. Transformation of Glucose in Added Value Compounds in a Hydrothermal Reaction Media</b> .....	165
<b>Chapter 7. Simultaneous and Selective Recovery of Cellulose and Hemicellulose Fractions from Wheat Bran by Supercritical Water Hydrolysis</b> .....	185
<b>Chapter 8. On the Energetic Approach of Biomass Hydrolysis in Supercritical Water</b> .....	205
<b>Conclusions</b> .....	229
<b>Resumen</b> .....	233
<b>Anexo</b> .....	249
<b>About the author</b> .....	301



# Abstract

Intensification of Cellulose  
Hydrolysis Process by Supercritical  
Water. Obtaining of Added Value  
Products



In the last years a general tendency has been developed towards a society supported in bioeconomy. This term refers to the sustainable production and conversion of biomass into a range of food, health, fiber, industrial products and energy. Biobased industries, based in renewable materials and energy, still have to be developed in order to support a decentralized production as an alternative to the well supported centralized petrochemical production plants. In order to accomplish this challenge, the research must be focused on achieving the development of environmental compatible processes, the efficient handling of energy and on reducing the equipment costs. Environmental friendly processes are characterized by high yield and high selectivity. This is achieved by simplifying the number of processes steps, by searching opportunities among new raw materials and by using clean solvents as water or carbon dioxide. Equipment's cost reduction involves the development of compact apparatus with short operation times: changing the residence time from minutes to milliseconds allows a reactor volume reduction from  $\text{m}^3$  to  $\text{cm}^3$ .

The use of pressurized fluids has been proposed as an environmentally compatible process to integrate the depolymerization-reaction-separation processes. Particularly, high-temperature pressurized water has proved to be a good solvent for clean, safe and environmentally benign organic reactions.

The aim of this PhD Thesis is to develop a process capable of converting cellulose (biomass streams) into valuable products such as chemicals and fuels using supercritical water as reaction medium.

To do so an experimental facility that works with temperatures up to  $400^\circ\text{C}$ , pressures of up to 25 MPa and residence times of between 0.004s and 10s was used for the experimental study. The main achievements of the experimental setup are: (a) the reactor can be considered isothermal due to the instantaneous heating and cooling; (b), products are not diluted in the cooling process; (c) the residence time is varied from 0.004 s to 40 s using Ni-alloy tubular reactors of different lengths.

In Chapter 1, a new reactor was developed for the selective hydrolysis of cellulose. In this study, the glucose selectivity obtained from cellulose was improved by using ultra-fast reactions in which a selective medium was combined with an effective residence time control. A selective production of glucose, fructose and cellobiose (50%  $\text{w}\cdot\text{w}^{-1}$ ) or total mono-oligo saccharides ( $>96\% \text{w}\cdot\text{w}^{-1}$ ) was obtained from the cellulose in a reaction time of 0.03 s. Total cellulose conversion was achieved with a 5-hydroxymethylfural concentration lower than 5

ppm in a novel micro-reactor. Reducing the residence time from minutes to milliseconds opens the possibility of moving from the conventional  $\text{m}^3$  to  $\text{cm}^3$  reactor volumes.

In Chapter 2, a kinetic analysis of cellulose depolymerization in hot pressurized water is presented. A mathematical model was developed in order to predict the evolution of the cellulose concentration and its derivatives. To do so, a reaction scheme was proposed, and kinetics parameters currently unavailable in literature were adjusted, using the experimental data obtained with the same experimental device used in chapter 1. The kinetics for cellulose hydrolysis showed a change around the critical point of water, the activation energy being  $154.4 \pm 9.5$  kJ/mol and  $430.3 \pm 6.3$  kJ/mol below and above the critical point, respectively. The activation energy for oligosaccharide hydrolysis was  $135.2 \pm 9.2$  kJ/mol and  $111.5 \pm 9.1$  kJ/mol for the glucose to fructose reaction. The kinetics of 5-hydroxyl-methyl-furfural formation showed a drastic change at  $330^\circ\text{C}$ . The activation energy for 5-HMF formation is  $285 \pm 34$  kJ/mol and  $-61.3 \pm 15.7$  kJ/mol at temperatures below and above  $330^\circ\text{C}$  respectively. Above  $330^\circ\text{C}$  the low density and ionic product of the medium would disfavor the 5-HMF formation.

In Chapter 3, the role of reaction medium in the hydrolysis selectivity is presented. It is known that, at extremely low residence times (0.02 s), the sugars selectivity of cellulose hydrolysis was higher than  $98\% \text{ w}\cdot\text{w}^{-1}$  while 5-HMF concentration was lower than 5 ppm at  $400^\circ\text{C}$  and 23 MPa. When residence time is increased to 1 s, the selectivity of glycolaldehyde was  $60\% \text{ w}\cdot\text{w}^{-1}$  at  $400^\circ\text{C}$  and 23 MPa. The residence time was found to be a selectivity factor in the production of sugars or glycolaldehyde. In this study, the effect of temperature, pressure and residence time on cellulose hydrolysis in a hydrothermal media was analyzed. Experimental data up to  $400^\circ\text{C}$ , 27 MPa and residence times between 0.004 s and 40 s were obtained. A novel kinetic model was developed in order to evaluate the kinetics of glucose reactions. It was found that the hydroxide anion concentration in the medium due water dissociation is the determining factor in the selectivity of the process. The reaction of glucose isomerization to fructose and its further dehydration to produce 5-hydroxymethylfurfural are highly dependent on  $\text{OH}^-$  ion concentration. By increasing pOH, these reactions were minimized allowing the control of 5-HMF production. At this condition, the retro-aldol condensation pathway was enhanced instead of isomerization/dehydration pathway.

In Chapter 4, the effect of temperature and pressure on cellulose and glucose hydrolysis in a hydrothermal media is analyzed. Cellulose hydrolysis produced oligosaccharides, cellobiose, glucose and fructose. In general, concentration profiles of each component were similar for

the same temperature and different pressures. Nevertheless, glucose and fructose hydrolysis reaction to give decomposition products were strongly affected by changing the pressure, which is equivalent to changing the density. When increasing temperature and pressure, the reaction of glucose isomerization to fructose was inhibited, and the production of 5-hydroxymethylfurfural (5-HMF) obtained through fructose dehydration was also inhibited. On the other hand, 5-HMF production was favored by high hydroxide anion concentrations. Thus, at a constant temperature, the production of 5-HMF was increased by rising density (increasing pressure). On the other hand, the production of glycolaldehyde (retro-aldol condensation of glucose) was increased by increasing pressure and temperature. The kinetic constants of cellulose hydrolysis were fitted using the experimental data. Pressure seems to have no effect on the cellulose hydrolysis kinetic to simple sugars, and at subcritical temperatures the kinetic of glucose hydrolysis reactions did not show significant changes by increasing pressure. However, at 400°C glucose isomerization and dehydration reactions were diminished by increasing pressure while glucose retro-aldol condensation were enhanced.

In Chapter 5, the reactions of fructose in sub- and supercritical water were analyzed changing the properties of the reaction medium (pH and free radical kidnapers). The reactions were performed at 260°C, 330°C and 400°C; and 23 MPa. The pH of the medium was changed using oxalic acid and sodium hydroxide. Also, scavengers (TEMPO and BHT) were tested in order to determine its influences in the radical reactions. The main product of fructose hydrolysis in supercritical water was pyruvaldehyde (>80% carbon basis) at 400°C and 23 MPa with a residence time of 0.7 s. Furthermore, the reactions of fructose were analyzed in combination with glucose. It was determined that different retro-aldol condensation products can be obtained depending on the starting material. Fructose produces mainly C-3 molecules (pyruvaldehyde) and glucose produces mainly C-2 molecules (glycolaldehyde). The isomerization of fructose to glucose is negligible and so is the production of C-2 when the starting material is fructose. The yield of 5-HMF was negligible when the starting material was glucose.

In Chapter 6, the chemical transformation of glucose into added value products (lactic acid and 5-hydroxymethylfurfural) was analyzed using a hydrothermal reaction medium. The reactions of glucose in hot pressurized water were analyzed at 300°C, 350°C, 385°C and 400°C; the pressure was fixed at 23 MPa and 27 MPa for the experiments. No lactic acid was found at those conditions. A high concentration of glycolaldehyde (80% carbon basis) was

found operating at 400°C and 27 MPa with residence times of 20 s. Two homogeneous catalysts ( $\text{H}_2\text{O}_2$  and NaOH) were added in different experiments to improve the lactic acid production. The maximum concentration of lactic acid was 57% carbon basis using NaOH (0.5M) as catalyst at 27 MPa and 400°C with 20 s of residence time. It was observed that the pH of the medium plays an important role in the selectivity of the process. A model of the process kinetic was developed in order to identify the main influential factors on the selectivity.

In Chapter 7, the conversion of wheat bran into soluble oligosaccharides and monosaccharide such as glucose, xylose and arabinose was analyzed in a supercritical water medium. The hydrolysis reactions were performed in a continuous pilot plant at 400 °C, 25 MPa and residence times between 0.1 and 0.7 seconds. The yield of the process was evaluated for different products, such as C-6 (glucose derived from cellulose) and C-5 sugars (saccharide derived from hemicellulose hydrolysis). The production of glycolaldehyde and 5-hydroxymethylfural (5-HMF) was analyzed as byproducts formation. Operating under supercritical conditions a biomass liquefaction of 84%  $\text{w}\cdot\text{w}^{-1}$  was achieved at 0.3 s of residence time. The obtained solid after the hydrolysis is composed of 86%  $\text{w}\cdot\text{w}^{-1}$  of lignin. The highest recovery of cellulose (C-6) and hemicellulose (C-5) as soluble sugars (76%  $\text{w}\cdot\text{w}^{-1}$ ) was achieved at 0.19 s of residence time. An increase in the residence time decreased the yield of C-6 and C-5. A total recovery of C-5 was achieved at 0.19 s, however at longer residence times, the yield of C-5 decreased. On the other hand, the highest yield (65%  $\text{w}\cdot\text{w}^{-1}$ ) of C-6 was achieved at 0.22 s of residence time. The main hydrolysis product of C-6 and C-5 was glycolaldehyde yielding the 20%  $\text{w}\cdot\text{w}^{-1}$  at 0.22 s of residence time. The 5-HMF production was highly inhibited in the experimented conditions obtaining yields lower than 0.5 %  $\text{w}\cdot\text{w}^{-1}$ .

In Chapter 8, Production of glucose through hydrolysis from vegetal biomass is of interest because it can be used as starting point in the production of chemicals, materials and bio-fuels. Cellulose hydrolysis can be performed in supercritical water with a high selectivity of soluble sugars. This reaction yield can be achieved using a continuous reactor with instantaneous heating and cooling methods that allow the precise control of the residence time. Operation can be carried out by adding a stream of supercritical water to the cellulose stream and by cooling the reactor outlet by sudden decompression. With this technology it is possible to greatly decrease the temperature in a fraction of a second. The process produces a high pressure steam that can be integrated, from an energy point of view, with the global biomass treating process. This work investigate the integration of biomass hydrolysis reactors

with commercial Combined Heat and Power (CHP) schemes, with special attention to reactor outlet streams. Temperature of the flue gases from CHP around 500 °C and the use of direct shaft work in the process offer adequate energy integration possibilities for feed preheating and compression. The integration of biomass hydrolysis with a CHP process allow the selective conversion of biomass into sugars without any extra heat requirements. The wide range of commercially available GT sizes allows widespread process scaling.



# Symbols

A	Pre-exponential factor of Arrhenius equation
$E_a$	Activation energy of Arrhenius equation ( $\text{kJ}\cdot\text{mol}^{-1}$ )
k	Reaction constant rate of cellulose hydrolysis ( $\text{s}^{-1}$ )
$k_1$	Reaction constant rate of cellobiose reaction to glucosyl erythrose ( $\text{s}^{-1}$ )
$k_2$	Reaction constant rate of cellobiose reaction to glucosylglycoaldehyde ( $\text{s}^{-1}$ )
$k_a$	Reaction constant rate of glucose to organics acids ( $\text{s}^{-1}$ )
$k_{\text{cello}}$	Reaction constant rate of cellobiose decomposition ( $\text{s}^{-1}$ )
$k_{\text{dgly}}$	Reaction constant rate of dihydroxyacetone to glycoaldehyde ( $\text{s}^{-1}$ )
$k_{\text{dp}}$	Reaction constant rate of dihydroxyacetone to pyruvaldehyde ( $\text{s}^{-1}$ )
$k_{\text{ge}}$	Reaction constant rate of glucose to erythrose ( $\text{s}^{-1}$ )
$k_{\text{glyd}}$	Reaction constant rate of glycoaldehyde to dihydroxyacetone ( $\text{s}^{-1}$ )
$k_{\text{glyp}}$	Reaction constant rate of glycoaldehyde to pyruvaldehyde ( $\text{s}^{-1}$ )
$k_e$	Reaction constant rate of erythrose to organics acids ( $\text{s}^{-1}$ )
$k_f$	Reaction constant rate of fructose decomposition ( $\text{s}^{-1}$ )
$k_{\text{fa}}$	Reaction constant rate of fructose to organics acids ( $\text{s}^{-1}$ )
$k_{\text{fe}}$	Reaction constant rate of fructose to erythrose ( $\text{s}^{-1}$ )
$k_{\text{fgl}}$	Reaction constant rate of fructose to glycoaldehyde ( $\text{s}^{-1}$ )
$k_{\text{fgh}}$	Reaction constant rate of fructose to 5-HMF ( $\text{L}\cdot\text{mol}^{-1}\cdot\text{s}^{-1}/\text{s}^{-1}$ )
$k_g$	Reaction constant rate of glucose decomposition ( $\text{s}^{-1}$ )
$k_{\text{ga}}$	Reaction constant rate of glucose to 1,6 anhydroglucose ( $\text{s}^{-1}$ )
$k_{\text{gf}}$	Reaction constant rate of glucose to fructose ( $\text{L}\cdot\text{mol}^{-1}\cdot\text{s}^{-1}/\text{s}^{-1}$ )
$k_{\text{ggg}}$	Reaction constant rate of glucosyl glycoaldehyde to glucose ( $\text{s}^{-1}$ )
$k_{\text{geg}}$	Reaction constant rate of glucosyl erythrose to glucose ( $\text{s}^{-1}$ )
$k_h$	Reaction constant rate of cellobiose hydrolysis ( $\text{s}^{-1}$ )
$k_p$	Reaction constant rate of pyruvaldehyde to organics acids ( $\text{s}^{-1}$ )
$k_s$	Reaction constant rate of superficial decrease ( $\text{s}^{-1}$ )
$K_w$	Ionic product of water
S	Area of cellulose grain ( $\text{m}^2$ )
t	Time (s)
T	Temperature (K)

$T_c$	Critical temperature (K)
$t_R$	residence time (s)
$V$	Volume ( $m^3$ )
$W$	Mass (g)
$X$	Conversion
$\Delta v^\ddagger$	Activation volume ( $cm^3 \cdot mol^{-1}$ )
$\epsilon$	Dielectric constant
$\varphi$	Mass factor for cellobiose formation

# State of the Art: Biomass refining processes intensification by supercritical water

## Abstract

Status reports from public and private organizations make a roadmap for achieving a society based bioeconomy. Biobased industries, based on renewable materials and energy, are still in development to success in supporting a decentralized production that can be an alternative to the well supported centralized petrochemical production plants. The use of pressurized water has been proposed as an environmentally compatible process to integrate the depolymerization-reaction-separation biomass supported processes. The supercritical water is emerging as a solvent and reaction medium capable of providing selective processes while significantly reducing the reaction time, leading to the possibility of developing compact equipment for the use in biomass decentralized production plants. The main ways of biomass upgrading in a hydrothermal medium are reviewed in this work: hydrolysis, fractionation, gasification and reaction. In the last years, a significant progress was achieved in the obtaining of added value products from biomass by hydrothermal technologies. However, some challenges must still be overcome before a sustainable and efficient decentralized production is achieved.

**Keywords:** Biorefinery • Hydrolysis • Fractionation • Gasification • Reaction  
• Decentralized production.



## 1. Introduction

In the last years there is a general tendency towards a society supported in bioeconomy. This term refers to the sustainable production and conversion of biomass into a range of food, health, fiber, industrial products and energy as it is referred in "The European bioeconomy in 2030 Delivering Sustainable Growth by addressing the Grand Societal Challenges" presented by BECOTEPS [1] and in the "The Bioeconomy to 2030 Designing a policy agenda" report presented by OECD [2]. What it is more, achieving a European society supported in bioeconomy is one of the challenges of the European Strategy Horizon 2020.

The petrochemical industry has been an engine of rapid economic development in the 20<sup>th</sup> century. The large-scale centralized production has achieved rapid marketing from chemicals and energy. Biobased industries however, based on renewable materials and energy, are still in development to success in supporting a decentralized production that can be an alternative to the well supported centralized petrochemical production plants [3].

In order to accomplish this challenge, the research must be focused on achieving the development of environmental compatible processes, the efficient handling of energy and on reducing the equipment costs. Environmental friendly processes are characterized by high yield and high selectivity. This is achieved by simplifying the number of processes steps, by searching opportunities among new raw materials and by using clean solvents as water or carbon dioxide. Equipment's cost reduction involves the development of compact apparatus with short operation times: changing the residence time from minutes to milliseconds allows a reactor volume reduction from m<sup>3</sup> to cm<sup>3</sup>.

The use of pressurized fluids has been proposed as an environmentally compatible process to integrate the depolymerization-reaction-separation processes. Particularly, high-temperature pressurized water has proved to be a good solvent for clean, safe and environmentally benign organic reactions [4]. Main advantages that make hydrothermal media a promising alternative for biomass processing are: (1) it is not necessary to reduce the water content in the raw material, what implies an important energy saving; (2) the same reaction medium is suitable for the transformation of the different biomass fractions; (3) mass transfer limitations are reduced or avoided, thus reaction rates are faster [5-9]. Furthermore, tunable properties of the reaction medium act as a control factor for the reaction selectivity, avoiding the generation of by-products. The change in the dielectric constant is proportional to the density and inversely proportional to the temperature. Hydrogen bonds behavior is

analogous to that of the dielectric constant [4]. Another important property of the aqueous reaction media is the ionic product of water ( $K_w$ ). The maximum value of the ionic product of water is presented at a temperature around 300°C ( $10^{-11}$ ). This creates a medium with high  $H^+$  and  $OH^-$  concentrations, favoring in this way acid/basis catalyzed reactions. Above the critical temperature of water (374°C),  $K_w$  decreases drastically ( $10^{-25}$ ) [10] as shown in Figure 1. At higher pressures ( $P > 60$  MPa) the  $K_w$  again presents values similar to those of ambient water.

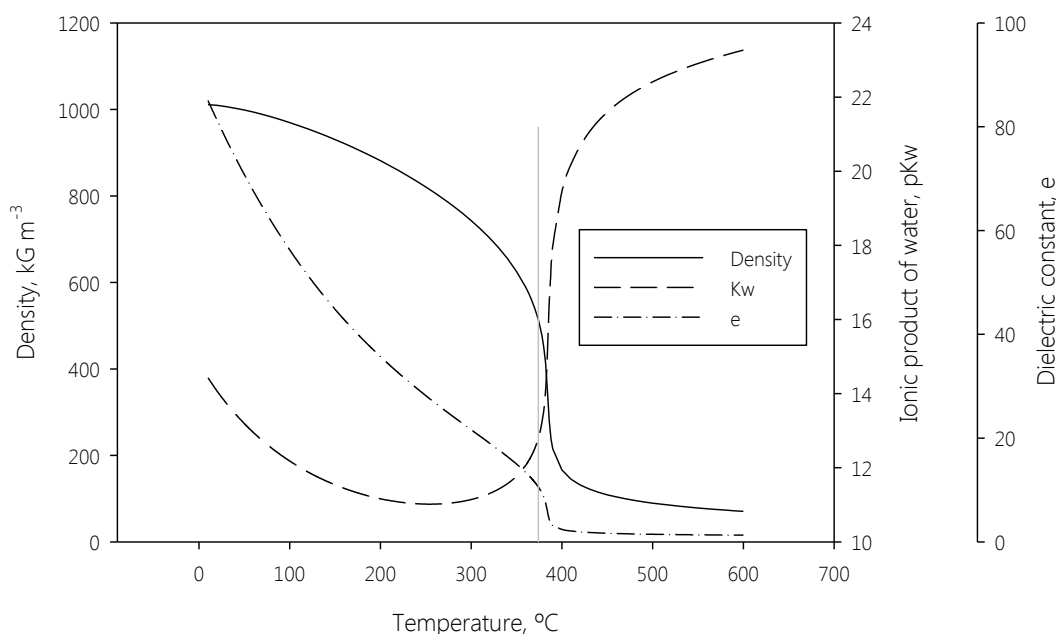


**Fig. 1.** Properties of pressurized water below and above critical point. Continuous line Density (kG/m<sup>3</sup>); dashed line represents ionic product of water (pKw) and dashed-dotted line represents the dielectric constant.

The combination of this properties and the high temperature that allow high reaction rates associated to the high temperature makes that water at high pressure and temperature accomplish all the conditions above exposed for the development of environmentally compatible processes such as efficient handling of energy and equipment's cost reduction by minimizing the operation time.

The sub/supercritical water hydrolysis, gasification, fractionation, and transformation in high added value compounds will be reviewed in this manuscript to evidence that sub/supercritical water can contribute to the decentralized development of industries based on the use of renewable raw materials and energy.

## 2.1. Hydrolysis

Hydrolysis is defined as the process in which a molecule is split into other two molecules by adding a molecule of water. The general equation for a hydrolysis reaction is shown in equation 1.



The hydrolysis of non-human food biomass have been extensively studied in the last decades due to the possibility of producing chemical compounds from natural polymers. The biomass is mainly composed by three polymers: cellulose, hemicellulose and lignin. Cellulose is the major component of vegetal biomass, representing in general the 50% in mass [11]. Cellulose is a polymer formed by the repeating  $\beta$ -D-gluco-pyranose (Figure 2) molecule linked through acetal functions of the OH group of C-4 and C-1 carbon atom [12]. This bond is called  $\beta$ -1,4-glucan. The hydrolysis of cellulose produces glucose molecules.

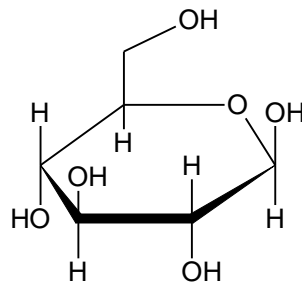


Fig. 2.  $\beta$ -D-Glucose. Constituent monomer of cellulose.

Hemicellulose is the second major component of biomass, being in general, the 25% in mass of vegetal biomass [11]. This compound is a hetero-polymer formed by pentoses: xylose and arabinose; and hexoses: glucose, galactose and mannose (Figure 3). In addition, glucuronic, acetic and ferulic acid are present in the polymer structure [13]. The composition of hemicellulose varies from one resource to another and it is generally classified by its main sugar component as: xylans ( $\beta$ -1,4-D-xylopyranose as backbone with a variety of side chains), mannans (linear polymer of  $\beta$ -1,4-mannopyranosyl) and glucans ( $\beta$ -glucan: alternate  $\beta$ -1,4 and  $\beta$ -1,3 glucose links; and xyloglucan: straight  $\beta$ -1,4-glucopyranose polymer with linked  $\alpha$ -1,6-xylose) [13, 14]. Therefore, the hydrolysis of hemicellulose would produce mainly, glucose, galactose, mannose, xylose, arabinose and organic acids. Lignin is another polymer being around the 20% in mass of the biomass [11]. This fraction is a highly amorphous polymer formed basically by phenolic units. The structure of lignin is complex due to the random polymerization reaction when it is produced in nature. However, the frequency of the internal

bonds is well known [15]. This compound is mainly formed by three monomers: p-coumaryl, coniferyl and sinapyl alcohols (Figure 4) [16, 17]. From the hydrolysis of lignin several kind of compounds can be obtained, such as phenols, catechol, alcohols, aldehydes and acids among others [18]. Depending on the biomass, sometimes proteins and oils can be present in biomass. Proteins can be hydrolyzed into amino acids and oils can be hydrolyzed into free fatty acids and glycerol [19-23].

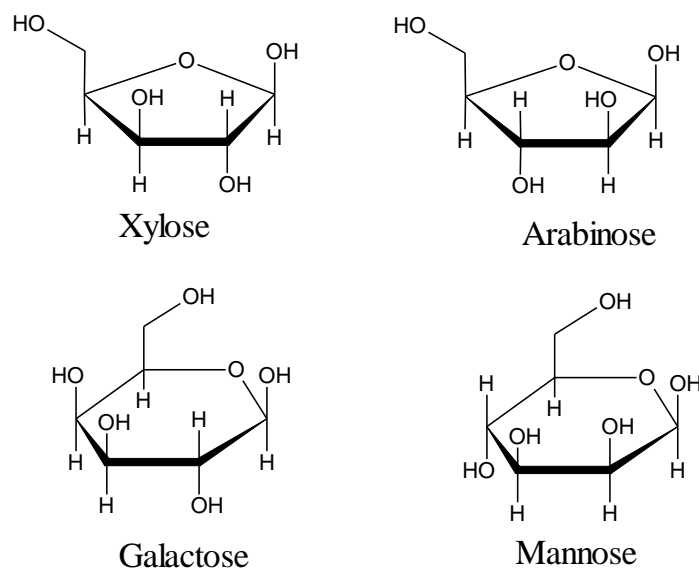


Fig. 3. Main constituent monomers of hemicellulose.

Another important compound found in some vegetal biomass is starch. This polymer is composed of glucose linked via  $\alpha$ -1,4-glucopyranosyl bonds. The hydrolysis of this polymer has been extensively studied in food industrial processes for the production of glucose [19]. The main use of starch is the human consumption as food, therefore its hydrolysis was not considered in this review as a starting material for the production of fuel and chemicals.

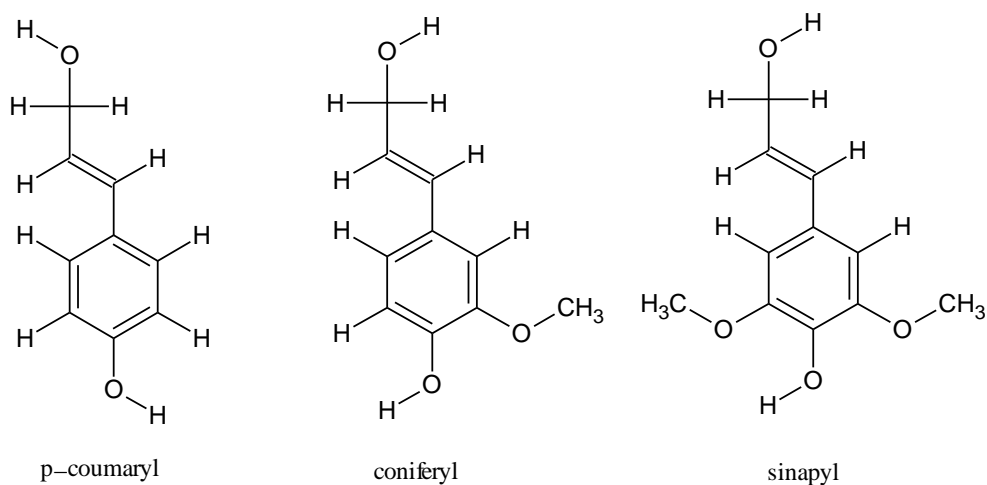
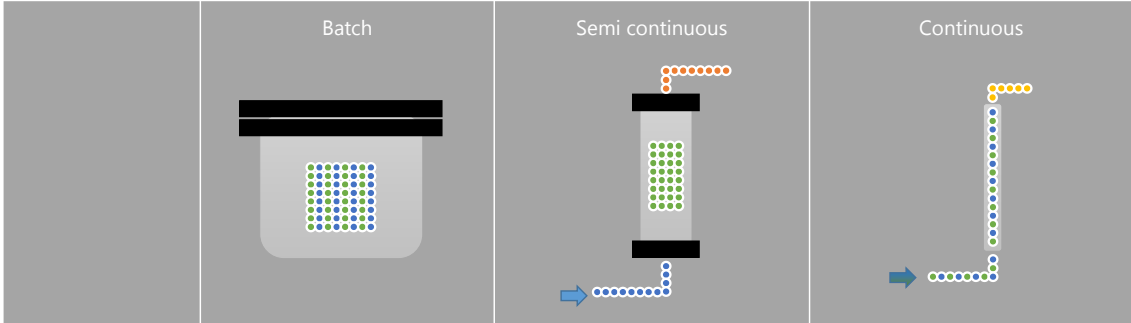


Fig. 4. Main constituent monomers of lignin.

## 2.1. Cellulose

Development of efficient and selective cellulose hydrolysis is a key aspect in the sustainable use of biomass as chemical and fuels resource [3, 24]. In this way, the hydrolysis of cellulose in pressurized water has been intensively studied using different ways of operation modes, such as batch [25-42], semi continuous [43-46] or continuous reactors [47-55]. The characteristics of each reactor are summarized in Figure 5. These characteristics are considered together with the hydrolysis yields in the analysis below. From the reaction medium point of view, the hydrolysis of cellulose was also analyzed in subcritical water [26, 27, 36, 43, 53], subcritical water plus catalysts [33-35, 38, 42, 47, 56] and supercritical water [25-27, 39, 48-54].



	Batch	Semi continuous	Continuous
Residence time	Minutes - hours	Minutes	Milliseconds – seconds
Temperature	100 – 380 °C	170 – 310 °C	250 – 450 °C
Pressure	0.1 – 22 MPa	10 – 20 MPa	23 – 100 MPa
Process control	Low	Medium	High
Equipment requirements	Low	Medium	High

Fig. 5. Main characteristics of batch, semi continuous and continuous hydrothermal reactors.

The main hydrolysis methods of cellulose hydrolysis under hydrothermal conditions are shown in Table 1. The decision of the operation type of reactor lies in the compromise between equipment requirements and selectivity – precision in the results. Batch type reactors allow the cellulose hydrolysis with quite simple equipment obtaining “non-expensive” results. However, the process control ( $t_r$ ,  $T$ ,  $P$ ) is poor, which will make difficult to obtain products with high selectivity. In general, the reaction temperature is achieved by immersing the reactor into a sand bath or into a furnace [25]. This heating method is simple to set, but the increment of temperature in ramp would start the hydrolysis reactions before the set point is reached. As a result, the determination of the residence time is not trivial. There are at least three different manners of residence time counting. One way is to start counting the residence time when

the target temperature is achieved [35]. In this case, the reaction time starts when the cellulose would be already degraded. Another way is to count the residence time considering the heating ramp and cooling time [25]. Contrary to the previous analysis, in this case, the residence time is overestimated. Another method to take into account the residence time is considering the time and temperature at the same time. This method is more precise than the others and can be applied by using the severity factor [57]. What it is more, these reactors normally consist of a tubing with two end caps in which the pressure measurement and control is not possible [25]. However, sometimes batch reactors consists of autoclave reactors that are provided of several outlets, so, in this case, pressure can be thoroughly measured and controlled. Therefore, the obtained products after batch hydrothermal hydrolysis of cellulose are usually divided and analyzed into fractions: bio-oils; water soluble; solids and; gases. Typical residence time for this batch reactors is around 60 s for supercritical temperatures [27] and between 15 and 30 min for subcritical temperatures [29, 33]. In addition, the discontinuous reactors constituted a simple option for rapidly testing of different kind of catalysts to improve the yield and reduce the residence time. The maximum yields of soluble sugars obtained with a batch reactor is around 40% w·w<sup>-1</sup> and 50% w·w<sup>-1</sup> [27, 29, 30].

Semi continuous processes represent an intermediate step between batch and continuous reactors. In general this kind of reactors permits a more adequate control of the pressure and residence time than the batch processes. The main advantage of these reactors is that it is possible to keep the solid in the reactor while the soluble products of cellulose leave the reactor through a filter. So, there are two important residence times, the solid residence time which depends on the kinetics of cellulose depolymerization and; the residence time of the liquid which depends on the reactor volume and the flow [43, 44]. However, if the degradation kinetics of the soluble products is fast, the only way to avoid their degradation is by reducing the residence time of the liquid phase. This means: reducing the reactor volume (low amounts of treated material) or increasing the flow (more diluted products). Although several temperatures and pressure can be applied to this kind of processes, in general, the hydrolysis in semi continuous reactor takes place at subcritical conditions [44-46]. Typical residence times for cellulose hydrolysis in a semi continuous reactor is between 60 and 90 min. However, the liquid residence time would vary between 1 and 20 s [39, 43-45]. The selectivity of soluble sugars that could be achieved in these processes is around 40% w·w<sup>-1</sup> of the initial cellulose [43, 44]. In some cases, a re-polymerization is observed after the hydrolysis treatment [44].

**Table 1.** Main processes of cellulose hydrolysis in a hydrothermal medium. \*Methyl glucosides. \*2 Reducing sugars. n.d. not determined.

Reactor	Solvent	Catalyst	T (°C)	P (MPa)	tr	Y <sub>sugars</sub>	Ref.
Batch	Water	-	280 - 380	22	15 – 50 s	0.51	[26]
Batch	Water	AC-SO <sub>3</sub> H	120 - 180	n.d.	30 min	0.40	[29]
Batch	Water	H <sub>3</sub> PO <sub>4</sub> /CaP <sub>2</sub> O <sub>6</sub> / α-Sr(PO <sub>3</sub> ) <sub>2</sub>	230	2.5	5 min	0.22	[30]
Batch	Methanol	Sulfonated carbon	275	n.d.	15 min	0.92*	[33]
Batch	Water	Hydrotalcite nanoparticles activated with Ca(OH) <sub>2</sub>	150	n.d.	1500 min	0.39	[34]
Batch	Water / ethanol	-	260	5.75	35 s	0.98* <sup>2</sup>	[36]
Batch	Water	-	355	n.d.	15 s	0.40	[39]
Batch	Water	-	380	22	20 s	0.65	[25]
Semi- continuous	Water	-	230 - 280	10	60 min / 1-4 s	0.34	[44]
Semi- continuous	Water	-	250 - 310	10	12 min	0.40	[43]
Semi- continuous	Water	-	270	10	15	0.50	[46]
Continuous	Water	CO <sub>2</sub>	230	25	4 min	0.60	[47]
Continuous	Water	-	400	25	0.02s	0.98	[49]
Continuous	Water	-	400	25	0.05s	0.70	[50, 52]
Continuous	Water	-	360	25	0.5 s	0.22	[53]
Continuous	Water	-	400 - 280	40	30.1 s	0.67	[55]
Continuous	Water	-	350	27.6	3.5 s	0.65	[54]

This can cause a problem when fractionating biomass, because dissolved lignin can re-precipitate over cellulose and create a layer that make difficult cellulose dissolution [58].

One of the main difficulties of the continuous hydrolysis reactors would be the steady supply of cellulose (solid, non-soluble in water) to the reactor due to the possible pump clogging. However, this problem can be overcome in lab scale by modifying the check valve system of low flow pumps. Also, this kind of problems would be solved in the scaling-up using higher flows [5]. The continuous hydrolysis of cellulose in a hydrothermal medium allows a major control over the process. The heating may be achieved instantaneously by mixing the cellulose stream with hot water at the reactor inlet [49, 50]. Moreover, the cooling of the reactor outlet stream could be suddenly cooled by the injection of cool water [50] or by depressurization [49]. These heating and cooling methods make possible the operation with isothermal reactors in which the cellulose is instantaneously heated and cooled. As a result, the considered residence time can be precisely determined. In addition, the residence time can be easily changed by modifying the reactor volume and the flow [48]. In this way, the reactions can be controlled in a continuous reactor by simply varying  $T$ ,  $P$  and  $t_r$ . Hence, the continuous process allows higher selectivity than the batch processes. So far, the maximum selectivity achieved by continuous cellulose hydrolysis was almost 70%  $w \cdot w^{-1}$  and less than 20%  $w \cdot w^{-1}$  for soluble sugars and monomers respectively [25, 51, 54, 55]. In a previous work of our research group [49] the selectivity of cellulose hydrolysis was improved by working at high temperatures at extremely low residence times (0.03 s). The experimental set up used in this work was specifically designed with the aim of controlling the residence time with accuracy. This was achieved by instantaneous heating and cooling methods (see Figure 6). With this process it is possible to obtain sugars or pyruvaldehyde selectivity of 98%  $w \cdot w^{-1}$  and 40%  $w \cdot w^{-1}$  respectively by using a novel reactor (see Figure 7). In general, the reaction temperature of cellulose hydrolysis is between 300°C and 400°C, at supercritical pressures. The residence time would vary between 0.02 s and 20 s depending on the temperature of the reaction medium [5, 49, 50].

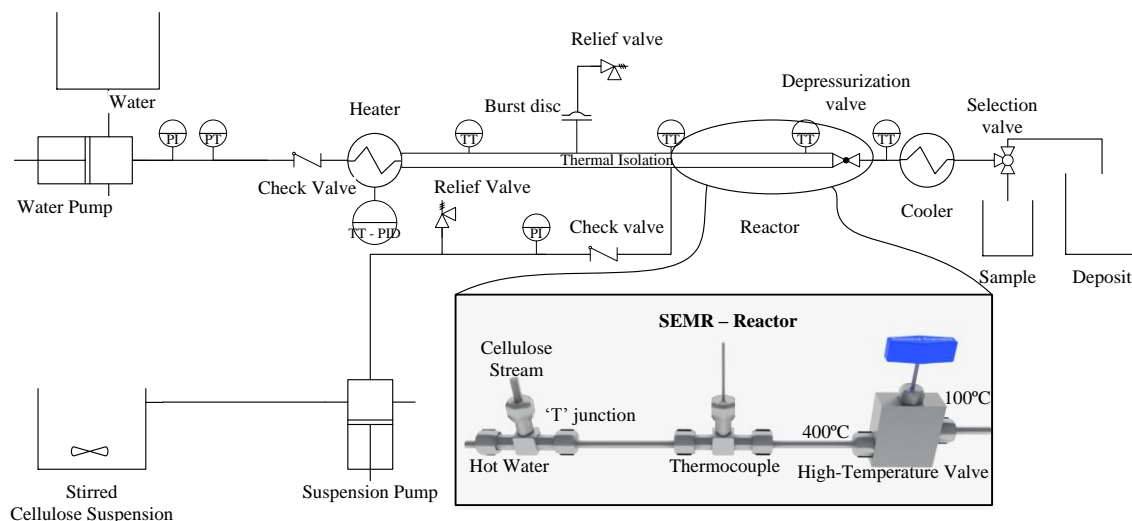


Fig. 6. Experimental setup. Schema of the pilot plant and Sudden Expansion Micro-Reactor (SEMR). Instantaneous heating of cellulose suspension is achieved by mixing with hot water. Instantaneous cooling from 400°C to 100°C is achieved by sudden decompression. Re-published from bibliography with permission [49].

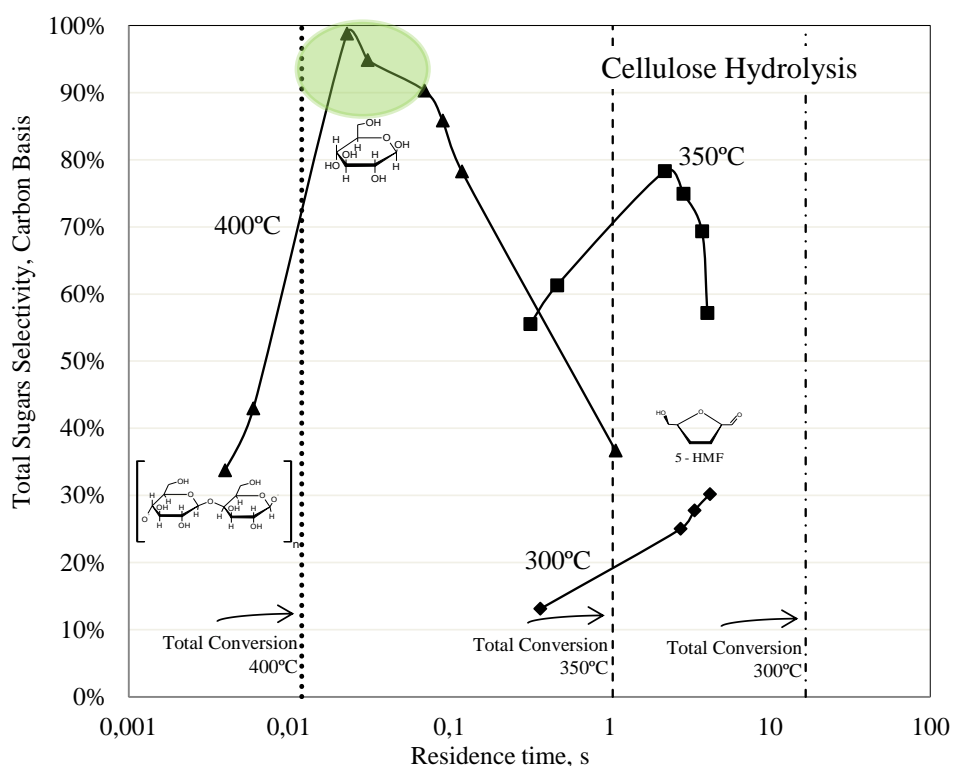


Fig. 7. Selectivity of the hydrolysis at different temperatures and residence times. A, selectivity of soluble oligosaccharides at: (◆) 300°C, (■) 350°C and (▲) 400°C depending on residence time. Dotted, dashed and dash-dotted vertical lines are the residence times for total conversion at 300°C, 350°C and 400°C respectively.

Re-published from bibliography with permission [49].

## 2.2. Hemicellulose

The study of hydrothermal hydrolysis of hemicellulose has not been so intensively investigated as cellulose hydrolysis. Maybe, this is because this polymer has a similar composition than cellulose (carbohydrates) and it is more difficult obtain it as an isolated material than in the case of cellulose. However, the acid hydrolysis of hemicelluloses in biomass has been extensively studied [59]. Typical temperatures of acid hydrolysis are between 100°C and 200°C with residence time between 1 and 400 min [13, 60]. In general, after applying this kind of hydrolysis to biomass, around 80% of hemicellulose is recovered as monomers [59]. Hemicellulose hydrolysis was mainly studied using batch reactors [61-64] at temperatures below 230°C and residence times around 10 min (Table 2). The yield of monomer recovery without catalyst is near 30% w·w<sup>-1</sup>, however, this yield can be enhanced to 93% w·w<sup>-1</sup> by using catalysts [64]. Examples of continuous hemicellulose hydrothermal processing are scarce in literature, it can be highlighted the continuous pilot plant built by Malishima and coworkers in order to obtain hemicellulose monomers from corncob [65]. Using this experimental setup it was possible to recover 82% w·w<sup>-1</sup> of hemicellulose (as monomers) by hydrothermal hydrolysis at 200°C, 2 MPa and 10 minutes of residence time.

The recovery of hemicellulose as well as cellulose and lignin from vegetal biomass will be discussed in Section 4 (*Biomass fractionation*).

**Table 2.** Main processes of hemicellulose hydrolysis in a hydrothermal medium. n.d. not determined

Reactor	Solvent	Catalyst	T (°C)	P (MPa)	tr	Y <sub>sugars</sub>	Ref.
Batch	Water	-	235	n.d.	Heating ramp	0.36	[61]
Batch	Water	CaCl <sub>2</sub>	190	n.d.	10 min	0.20	[62]
Batch	Water	-	190	n.d.	5 min	0.17	[63]
Batch	Water	Fe(NO <sub>3</sub> ) <sub>3</sub>	150	n.d.	10 min	0.93	[64]
Continuous	Water	-	200	1.5 - 2	10 min	0.82	[65]

## 2.3. Lignin

The nature of lignin as polymer makes difficult the analysis of selective production of a compound from it. In general, the hydrolysis of lignin produces a mixture of numerous phenolic compounds like catechol, phenol, and aromatic hydrocarbons. The main processes of ligning hydrolysis is presented in Table 3. In order to understand the reaction pathway of lignin depolymerization and hydrolysis, several investigations were done analyzing the hydrolysis reactions of lignin derivatives as guaiacol or other phenolic compounds [66-70]. Also,

the treatment of lignin at conditions close to the critical point of water produces high quantities of volatile compounds ( $\approx 15\%$ ) [71, 72]. In addition, lignin seems to follow a first depolymerization step that is favored at high temperatures. However, the residence time is very important at this point because the formed products (mainly guaiacol) can react with higher molecular weight compounds to form new polymers, called phenolic char [18, 72, 73].

**Table 3.** Main processes of lignin hydrolysis in a hydrothermal medium. \*Fraction of liquefaction products.  
\*2Diamond anvil cell. \*3Bio oil. n.d. not determined.

Reactor	Solvent	Catalyst	T (°C)	P (MPa)	tr	Y <sub>monomers</sub>	Ref.
Batch	Water	-	374	22	10 min	0.40 – 0.80*	[74]
Batch	Water	-	400	30	30 min	0.50	[75]
Batch	Water	-	400	37	60 min	0.22	[76]
Batch	Water	-	280	n.d.	Heating ramp	0.11	[77]
Batch	Water/phenol	-	400	n.d.	60 min	0.20	[73]
DAC*2	Water/phenol	-	400-600	93 - 1000	5 min	0.25	[18]
Batch	Water/CO <sub>2</sub> /Acetone	-	300	10	210 min	0.12	[78]
Batch	Water/p-cresol	-	400	n.d.	30 min	0.70	[79]
Batch	Ethanol/Hydrogen	5 Ru/γ-Al <sub>2</sub> O <sub>3</sub>	300	2	1200 min	0.92*3	[80]
Continuous	Water	-	390 - 450	25	0.5-10 s	0.20	[72]
Continuous	Water	-	300 - 370	25	0.5-10 s	0.30	[71]

This undesired repolymerization process can be avoided by adding to the reactor alcohol molecules such as methanol, phenol and p-cresol. The reactions between these alcohols and the produced monomers by lignin hydrolysis would be faster than the monomers repolymerization [18, 70, 73, 79, 81]. Also, the repolymerization process has been avoided by the addition of hydrogen and a Ni based catalyst to the medium [82]. The effect of residence time would change depending on the reaction medium. If the reaction medium is dosed with molecules that avoid the repolymerization of phenolic molecules, the residence time will favor the yield of monomers. However, if the reaction medium is just water, high residence time would favor repolymerization, thus, lowering the yield of monomers [77, 79]. This problem would be solved using continuous reactors capable of controlling the residence

times with accuracy [49]. This kind of reactor would allow to stop the reaction before monomers repolymerization.

The density of the medium is other important factor in lignin depolymerization. An increase in density would promote lignin conversion to low molecular weight compounds. However, an increase on density also enhances the repolymerization [73].

The depolymerization of lignin is also possible in a non aqueous medium. Supercritical ethanol was tested as reaction medium for the hydrolysis of lignin over 5Ru/ $\gamma$ -Al<sub>2</sub>O<sub>3</sub> catalyst. However, in this case the liquid products (80% w-w<sup>-1</sup>) was a bio-oil with a low oxygen composition [80]. The low oxygen composition and high heating value of the bio oil can be obtained by adding a hydrogen atmosphere in the batch reactor [80].

Like previous analyses for cellulose and hemicellulose, there is a high dependence between the type of reactor (batch, semi-continuous or continuous), the temperature/time treatment and the obtained yields of liquefied lignin. Batch reactors usually operate at temperatures up to 400°C with residence times between 10 and 30 min. In this cases, the selectivity of monomers is low obtaining a dispersed composition of phenolic compounds in the liquid products [18, 74, 75]. Continuous reactor can operate until 450°C with residence times between 0.2 s and 10 s [71, 72].

### 3. Hydrothermal Fractionation

The biopolymers that form vegetal biomass (mainly cellulose, hemicellulose and lignin) are present in nature in an associated way (see Figure 8). The interactions between them would occur by covalent bonds (hemicellulose – lignin), Van der Waals interactions (hemicellulose – cellulose) or hydrogen bond interactions (cellulose – cellulose) [15]. Biomass fractionation is the process in which the biomass is separated into its constitutive biopolymers. The hydrothermal processing of biomass allows the breaking of the interaction between the biopolymers as well as the monomers bonds between them to form the polymer structure. Therefore, the main products of biomass fractionation would be: (1) a liquid product enriched on hemicellulose oligomers and monomers; (2) a liquid product enriched on cellulose oligomers and monomers and; (3) in general, a solid enriched in lignin (small amount of lignin could also be dissolved in liquid phase) [83]. The extractives and protein fractions are generally separated from the vegetal matrix in a previous pre-treatment. The hydrothermal medium is a promising reaction atmosphere to make the fractionation of biomass because the medium can adopt different identities by changing temperature and pressure. For instance, at 300°C

and 25 MPa the reaction medium is highly ionic, favoring this autohydrolysis reactions (sometimes called autohydrolysis). However, at 400°C and 25 MPa the medium is highly non-ionic, favoring radical reactions. These differences can be used to set the desired media focused on each biomass fraction. Furthermore, the hydrolysis kinetics of cellulose and hemicellulose are different, so the temperature of the process would be an important parameter to control in order to start the hydrolysis/extraction of hemicellulose without hydrolyzing the cellulose.

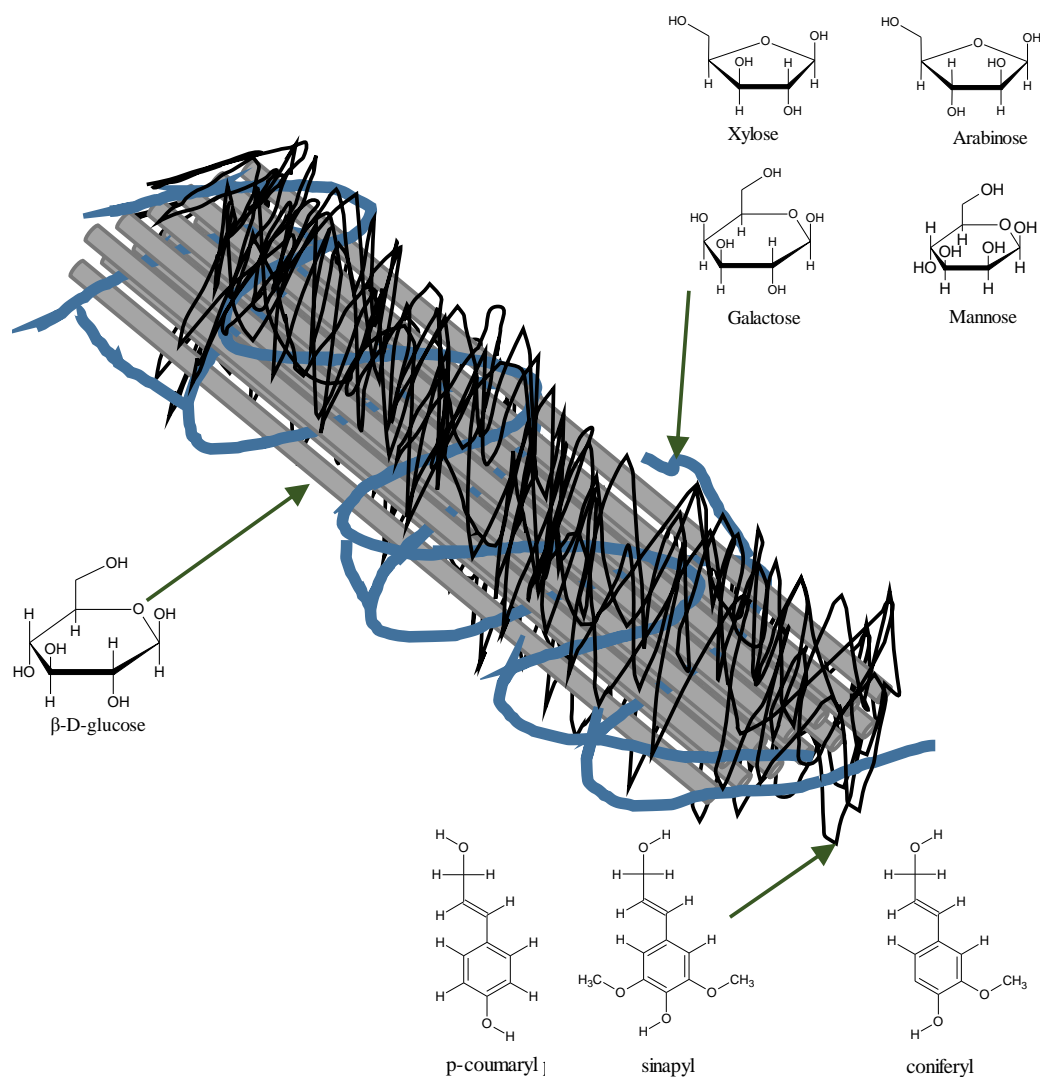


Fig. 8. Schematic representation of biomass composition.

Although the vegetal biomass composition is similar for diverse species, the processing of different raw materials would produce different products. In this section it will be discussed the main accomplishments and challenges of the technology. The hydrothermal fractionation of biomass was studied using batch [28, 84-95], semi continuous [87, 96-104] and continuous

reactors [21, 57, 105]. Typical processes for biomass fractionation using a hydrothermal medium are enlisted in Table 4.

**Table 4.** Main processes of biomass fractionation in a hydrothermal medium. \* Water soluble fraction. \*2 Solid fraction. n.d.: not determined.  $R_0$ : Severity factor.  $Y_{cel}$ : yield of cellulose in liquid phase.  $Y_{hemi}$ : yield of hemicellulose in liquid phase.  $Y_{lignin|sol}$ : yield of lignin in solid phase.

Reactor	Solvent	Catalyst	T (°C)	P (MPa)	tr	$Y_{cel}$	$Y_{hemi}$	$Y_{lignin sol}$	Ref.
Batch	Water/ethanol – water/NaOH	-	165°C – 195°C	-	30 – 165 min	0.03	0.97	0.53	[84]
Batch	Water	H <sub>2</sub> SO <sub>4</sub>	150°C – 180°C	n.d.	3 – 30 min	0.15	0.85	0.44	[86]
Batch	Water	-	150°C – 240°C	n.d.	1 < log( $R_0$ ) < 5	n.d.	0.53	0.31	[88]
Batch	Water	-	250°C – 350°C	25	0 – 20 min	0.30*	0.30*	0.60* <sup>2</sup>	[89]
Batch	Water	CO <sub>2</sub>	100°C – 250°C	27.5	90 min	0.77*	n.d.	0.23* <sup>2</sup>	[90]
Batch	Water	-	175°C – 215°C	n.d.	1 < log( $R_0$ ) < 5	n.d.	0.17	0.45	[91]
Batch	Water	-	190°C	n.d.	15 min	0.05	0.19	0.20	[87]
Semi- continuous	Water	-	230°C – 270°C	10	15 min	0.16	0.18	0.10	[87]
Semi- continuous	Water	-	170°C – 230°C	10	10 min	0.08	0.98	0.20	[96]
Semi- continuous	Water	-	200°C – 230°C	34.5	0 – 15 min	0.18	0.95	0.20	[98]
Semi- continuous	Water	-	115°C	n.d.	47 min	0.21	n.d.	n.d.	[99]
Semi- continuous	Water	KOH	190°C – 200°C	1.2 – 1.55	15 – 20 min	0.02	0.53	0.29	[10 0]
Semi- continuous	Water	-	200°C – 290°C	20	30 – 50 min	0.02* <sub>3</sub>	0.03* <sub>3</sub>	-	[10 1]
Semi- continuous	Water	-	165°C	11	60 min	0.09	0.80	0.50	[10 2, 103 ]
Semi- continuous	Water	-	150°C – 320°C	15	150 min	0.60*	n.d.	n.d.	[83]
Continuous	Water	-	170°C – 200°C	-	5 – 20 min	0.02	0.92	n.d.	[10 5]
Continuous	Water	CO <sub>2</sub>	240°C – 310°C	15 – 25	0 – 3 min	0.05	0.25	n.d.	[57]

In some cases, the available feedstock is a biomass with high value extractable oils such as polyphenols. In these cases a pre-treatment is sometimes necessary to recover the essential oils before hydrothermal hydrolysis/fractionation. The hemicellulose fraction is generally recovered by working at temperature ranges between 160°C – 220°C and pressures above the saturation pressure to ensure the liquid phase [11, 85, 96, 98, 106]. At these conditions, water is more dissociated than at room temperature resulting in higher concentration of hydroxide anions. Sometimes this phenomenon is called auto-hydrolysis because no catalyst is added to the medium. In addition, the hydrolysis of hemicellulose releases acetic acid to medium, which also favor acid catalysis of the hydrolysis reactions [85, 107]. Another advantage of working below 220°C is that cellulose or lignin hydrolysis is slow enough to avoid their degradation. So, after hydrothermal fractionation below 220°C a solid composed of cellulose and lignin would be recovered in the solid phase. This solid phase seems to be unaltered between 220°C and 250°C [83]. The cellulose fraction would start to depolymerize at temperature above 250°C [11, 85, 96]. Furthermore, at temperatures between 250°C and 320°C in liquid phase, the addition of CO<sub>2</sub> will enhance the kinetic of hemicellulose and cellulose hydrolysis [57]. A scheme of temperature, residence time and fractions extracted/hydrolyzed is shown in Figure 9. An alternative fractionation process is the fast hydrolysis in supercritical medium [49]. This technology would admit the simultaneous hydrolysis of hemicellulose and cellulose without degradation of the sugar monomers because of the extremely low residence times applied. In general, fractionation of biomass is carried out at temperatures below 320°C. At those conditions, lignin is slightly degraded. In fact, the lignin hydrolysis would occur in the sites where lignin interacts with hemicellulose [85]. Lignin remain in the solid as the main component after fractionation [88].

As it was discussed in section 2, the used reactor (batch, semi continuous or continuous) to perform the biomass fractionation is decisive in the process control. For instance, the determining and control of residence time in a batch reactor is poor due to unavoidable heating and cooling ramps. One way to overcome this problem is the use of the severity factor ( $R_0$ ). The severity factor is a mathematical expression that takes into account the residence time together with the temperature of the reactor [88, 91, 93]. A poor process control would lead to unselective products. These products are increased when the feedstock is a real biomass instead of its isolated fractions. One way to analyze these kind of products is by dividing them into water soluble fraction, bio-oils and remaining solid [108]. Therefore, this

kind of fractionation must be followed by an intensive analytical study of the products, such as sugars determination, lignin quantification, lignin quality, solid composition analysis, bio oils production and composition, molecular weight distribution, degraded product composition and quantification, and fatty extractable fractions quantification [88, 100, 109-111]. One of the challenges of biomass fractionation is the coordination between high selectivity processes together with adequate analytical methods.

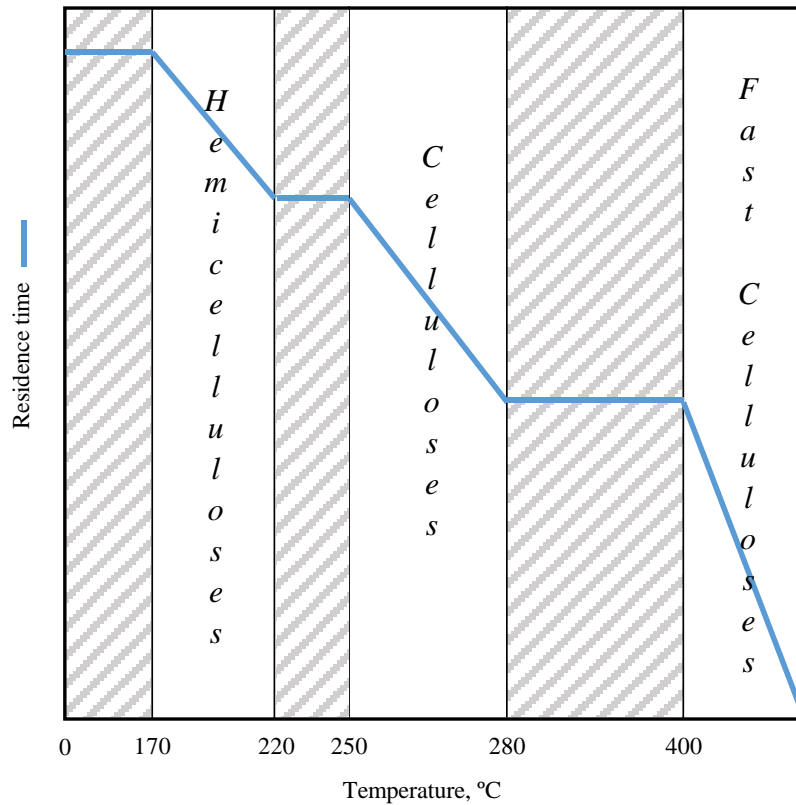


Fig. 9. Temperature dependence of biomass extraction in a hydrothermal treatment. The residence time decreased as temperature in increased.

Hydrothermal fractionation of biomass is already present in an industrial scale. Renmatix is a North American company proprietary of the Plantrose™ Process. This process produces the cellulosic sugars by using supercritical hydrolysis. Although the available information of the process is scarce, the company informs that they use very fast reaction times and small equipment sizes, reducing the capital and operating expenses. Furthermore, since it uses water as a solvent, the technology also avoids both the low utilization of infrastructure that occurs with traditional enzymatic batch processing and the high costs implied by the significant waste and expensive recovery systems associated with acid hydrolysis methods

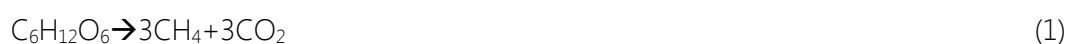
[112]. The main purpose of Renmatix is the production of sugars to further conversion into chemicals and fuels [112].

#### 4. Hydrothermal Gasification

The hydrothermal gasification of biomass is the process in which biomass is converted into gas molecules such as CH<sub>4</sub>, H<sub>2</sub>, CO and CO<sub>2</sub> in a hydrothermal reaction media. Depending on the gasification temperature, the process can be classified into three categories: aqueous phase reforming (APR) under 265°C; catalyzed near critical gasification around 350°C and supercritical water gasification above the critical point of water [113].

Supercritical water gasification presents some advantages compared to dry gasification process. First of all, biomass should not be dried before processing it. Biomass, with high compositions (90% w.w<sup>-1</sup>) of water can be gasified in this process [114-116]. Although the energy needed to heat water up to the gasification temperature (≈600°C) is high, this heat can be recovered in a heat exchanger. This is an important requirement in the design of the supercritical water gasification processes. Fortunately, efficient heat exchanger is available to work at high pressure, making possible the recovery of heat while the involved energy in biomass drying processes cannot be recovered [113]. Another advantage of this process is that the reactor operates at high pressure, therefore the gas phase should not be pressurized afterwards. In addition, the compressed medium allows the gasification in small reactors with low heat losses [116, 117]. Also, the reaction intermediates can be dissolved in the reaction medium which inhibits the formation of tar and coke [113]. The product selectivity towards either methane or hydrogen can be controlled with temperature, pressure and the application of catalysts [116, 118]. The main problems of biomass gasification in supercritical water are the technical difficulties of the process: high pressure reactors, solids accumulation and corrosion [119].

A simplified reaction of biomass gasification to produce methane and carbon dioxide is shown in equation 1 considering glucose as starting biomass. For hydrogen production, the reaction of gasification is shown in equation 2 [120]. Equation 3, 4 and 5 represent the reactions of steam reforming, water gas shift reaction and methanation reaction respectively.





Supercritical water gasification was studied in batch [121-128], semi continuous [129, 130] and continuous reactors [114, 115, 118, 122, 123, 131-142]. As it was discussed in section 1, batch reactors allow the easy testing of heterogeneous catalysts, concentration and heating rates effects. On the other hand, continuous reactor facilitates the analysis of temperature, pressure and residence time effect.

#### *4.1. Temperature, pressure and residence time*

In supercritical water gasification, the methane production is maximized by working at temperatures around 400°C [143]. An increase in temperature from 400°C to 600°C (and higher) would benefit the production of hydrogen [114]. This is because high temperatures and low pressures favor the free radical reactions in which the gas is produced [132]. Thus, in general, an increase in temperature would rise the hydrogen production and an increase in pressure (favoring ionic reaction medium) would reduce it [132]. The gases produced in supercritical water gasification are products of free radical reactions, therefore, high pressure would inhibit these reactions [115, 132]. In general, according to Le Chatelier's principle high pressure is shifting chemical equilibrium to the side where there is lower amount of molecules. As in gasification reactions the products are formed by more molecules than the reagents, high pressure disfavors gasification process [132]. However, the effect of pressure in the gas yield is negligible in comparison to the temperature effect [132]. If the gasification temperature is above 600°C the production of hydrogen and carbon monoxide would be increased by using a continuous reactor [133, 134, 144, 145]. Also, the carbon monoxide yield increases as the temperature does, with a maximum production around 650°C [134]. However, the yield of CO would be decreased if temperature is increased above 650°C [133, 134]. In addition, by working at temperatures above 600°C, the conversion of biomass to gasified products is benefited. At lower temperatures, the production of char is favored [115].

The reaction time is again highly influenced by the reactor type in supercritical water gasification. Working with continuous reactors, residence time seems to have no effect on the gas yields after total conversion of biomass into gases (less than 1 minute of residence time) [117, 133]. Although the reactions of supercritical water gasification are fast, at low residence times the yield of gas and hydrogen will be improved by increasing residence time (10 s → 40 s) [115]. On the other hand, the effect of residence time is highly influential when batch

reactor are used [124]. In this case, when the reaction time is increased from 30 minutes to 120 minutes, the yield of gas and hydrogen is decreased. Another important parameter to take into account in batch reactor is the time taken in the heating. High hydrogen, methane and carbon dioxide yields can be reached with high heating rate [125].

#### *4.2. Reaction Medium*

The concentration of inflow biomass to the reactor would have a negative effect on gas and hydrogen yields [114, 115, 146]. In addition, higher reaction temperatures are necessary for higher biomass concentration streams to complete the gasification process [146]. The biomass concentration in the reactor would also affect the product composition. Low biomass concentration would favor a gas product composed basically of H<sub>2</sub> and CO<sub>2</sub>. However, the CH<sub>4</sub> yield increase with the biomass concentration [114].

One of the main disadvantages of supercritical water gasification are the heat requirements [113, 120]. Partial oxidation of the biomass in the reactor would be a good alternative to generate heat in the reactor. This heat is used to rapidly heat up the reaction fluid preventing in this way char or tar formations and favoring the process of hydrogen production. Partial oxidation of the biomass can be achieved by feeding the reactor with hydrogen peroxide in amount lower than the stoichiometric (25%) in order to avoid total oxidation [144]. If oxygen is added to the system, two competing pathways would take place: gasification and oxidation reactions. In these cases it should be taken into account that the hydrogen yields will be lower due to the oxidation of biomass to produce CO<sub>2</sub> and H<sub>2</sub>O [114]. This self-heating system will reduce the heat requirements but increasing the proportion of oxidation reaction to obtain total heat independence can be not beneficial due to the high level of oxidation reactions that would decrease hydrogen yields substantially.

The use of catalysts in supercritical water gasification is used to improve the yield as well as decrease the process temperature. At temperatures above 500°C activated carbon is used to avoid char formation and alkali catalysts are used to promote water-shift reactions and methane reformation [123, 143]. Some typical catalyst used in supercritical water gasification are Na<sub>2</sub>CO<sub>3</sub>, KHCO<sub>3</sub> and KOH [135-137]. At temperatures between the 374°C and 500°C metals and noble metal catalysts such as Ru, Rh and Pt favor the gasification [5, 118, 140, 141, 147-150]. At temperatures below the critical temperature of water, the use of catalysts is necessary to produce gases [143].

The continuous catalytic supercritical water gasification process has been commercialized by the Swiss company Hydromethan that is a spin-off company from Paul Scherrer Institute focused in the production of synthetic natural gas (SNG) from organic waste fractions [151]. This process is based on a catalytic high pressure gasification and methanation in a hydrothermal phase at approx. 300 bar and 400°C. The efficiency of the biomass to methane conversion is around 60-70% [151].

### 5. Hydrothermal upgrading of biomass: Reactions

The main advances on biomass conversion into sugars were analyzed in sections 2 and 3. Almost 70% of biomass is composed of sugars, such as glucose, fructose, xylose, arabinose, mannose and galactose. The purpose of this sugars production is their further conversion into fuels (ethanol) or chemicals (lactic acid, 5-HMF, glycolaldehyde, poly-alcohols, etc.). In this section, the main alternatives of sugars conversion into chemicals in a hydrothermal medium are discussed. There are three main groups of reactions to transform carbohydrates in a hydrothermal medium: hydrolysis reactions, hydrogenation reactions and oxidation reactions.

The main hydrolysis reactions of carbohydrates in a hydrothermal medium are: dehydration, retro-aldol condensation and isomerization [152, 153]. A general reaction pathway for glucose and fructose hydrolysis in a hydrothermal medium is shown in Figure 10. It is observed that glucose can follow an isomerization reaction to produce fructose, however, the reverse reaction, fructose isomerization to glucose is almost inhibited at same conditions [153-157]. Glucose can also be transformed into 1,6 anhydroglucose *via* dehydration [158]. The other alternative of glucose conversion is the retro-aldol condensation reaction that produces glycolaldehyde and erythrose [153]. Erythrose is further transformed into glycolaldehyde by the same reaction mechanism [152]. On the other hand, fructose can be transformed into 5-hydroxymethylfurfural through a dehydration reaction [159]. The other important reaction of fructose is the retro-aldol condensation to produce glyceraldehyde and dihydroxyacetone. These molecules are further isomerized into pyruvaldehyde [160] that is considered as a lactic acid precursor [153, 161, 162].

Retro-aldol condensation is the reaction in which a sugar is split into two molecules. An aldose, like glucose, produce one molecule of two carbons (C-2) and one molecule of four carbons (C-4). On the other hand, a ketose like fructose produces two molecules of three carbons (C-3) after retro-aldol condensation [153]. Additionally, the C-4 molecule produced from glucose can be further split into two C-2 molecules. So, a six carbon aldose can be

divided into three C-2 molecules while a six carbon ketose can be divided into two C-3 molecules. In general, the molecules of two carbon generated from sugar, such as glycolaldehyde, are products of interest for the production of glycolaldehyde or ethylene glycol, while the molecules of three carbons, such as pyruvaldehyde are interesting for the production of lactic acid.

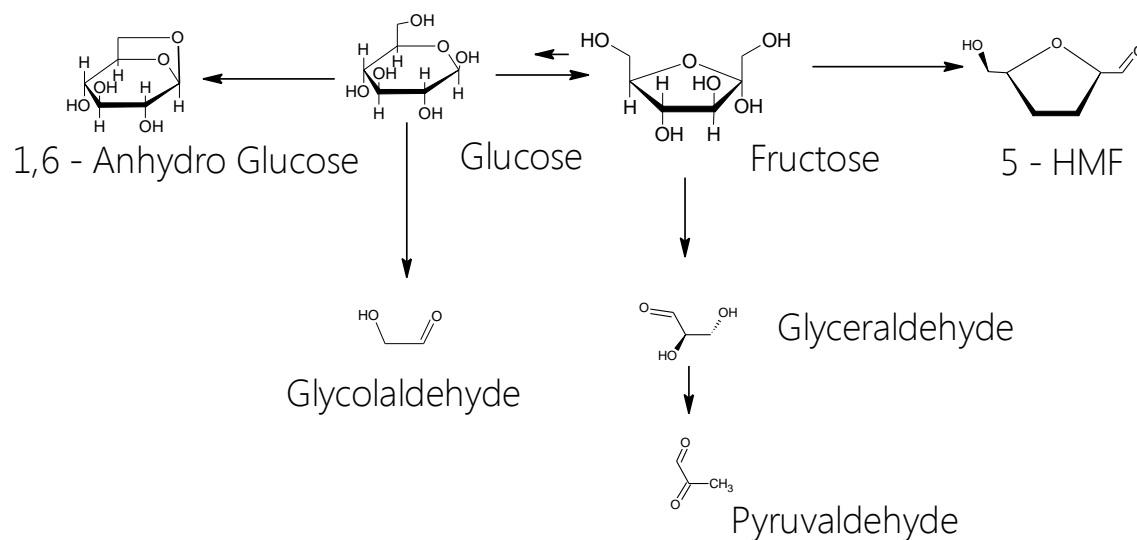


**Fig. 10.** Reaction pathway of glucose and fructose hydrolysis in a hydrothermal medium.

Retro-aldol condensation reactions is benefited over dehydration and isomerization reactions in a neutral medium. Dehydration as well as isomerization (*via* ring-opening and tautomerization) reactions are favored in acid mediums [153]. The density and the ionic product of water are two influential factors in the reactions of glucose and fructose. Retro-aldol condensation reactions are favored at low densities. On the other hand, 5-HMF formation is enhanced at high densities and ionic products [162, 163]. Thus, the reactions of glucose and fructose would be influenced by the reaction medium at near critical conditions due to the drastic changes in the ionic product of water. In some studies, these variations were quantified by changing the reaction order of glucose in the kinetic analysis [164].

The use of supercritical water as reaction medium allows the intensification of the process by reducing the required residence time of the reactions. Typical residence times of glucose and fructose reactions at temperatures above the critical point of water are between 0 s and 5 s [162, 165]. These residence times are three order of magnitude lower those required in low temperature catalyzed processes and up to five orders of magnituded lower than those needed in microorganism processes..

Other important reaction of aldoses and ketoses is their hydrogenation to produce poly-ols such as sorbitol or manitol among others [166]. These reactions are achieved by adding a catalyst to the medium and using hydrogen as reagent [166, 167]. These reactions are not reviewed in this work.

### *5.1. Glucose conversion*

The main product of glucose conversion in a hydrothermal medium without adding any catalyst is glycolaldehyde [152, 155, 163]. An increase in the reaction temperature above the critical point of water favors the retro-aldol condensation reactions, while the isomerization and dehydration reactions are highly inhibited. Thus, at 450°C and 35 MPa, it is possible to obtain glycolaldehyde yields as high as 70% w·w<sup>-1</sup> [152, 163, 168]. Glucose dehydration would be favored by performing the reaction in heated steam at atmospheric pressure. Using this process, a yield of 50% w·w<sup>-1</sup> of 1,6 anhydroglucose was obtained at 400°C and 0.1 MPa [158].

The production of lactic acid from glucose can be achieved by the addition of a base catalyst to the reaction medium. The catalyst would favor the isomerization of glucose into fructose as well as the conversion of pyruvaldehyde into lactic acid [165, 169, 170]. Sodium and calcium hydroxides showed to be promising catalysts for the conversion of glucose into lactic acid [171]. The obtained yields of lactic acid production from glucose using base catalyst in batch reactors are between 20 – 30% w·w<sup>-1</sup> [171]. These yields can be improved up to 50% w·w<sup>-1</sup> using a continuous reactor and working at supercritical temperatures. The time required for lactic acid production depends on the reaction temperature. Reaction temperatures around 300°C will require residence times of 60 s [171] while at 400°C, the residence time ranges between 10 s and 20 s [165].

The production of 5-HMF using glucose as starting material was also studied [172, 173]. The processes of 5-HMF production involved the use of acid catalyst in order to favor glucose isomerization to fructose and further dehydration [174, 175]. Therefore, the main processes to produce 5-HMF are analyzed using fructose as starting biomass.

### *5.2. Fructose conversion*

As it is observed in Figure 9, the main products of fructose reaction are 5-HMF and pyruvaldehyde. A further isomerization of pyruvaldehyde into lactic acid is favored by high pressure and temperature treatments [162]. This reaction is favored by the addition of catalysts

to medium. For instance, pyruvaldehyde can be converted into lactic acid by using  $\text{ZnSO}_4$  as catalyst [176].

The production of 5-HMF was studied using: biphasic reactors with solid catalyst [177] and; hydrothermal reactor with acid catalyst [56, 173, 175, 178-182]. The 5-HMF production from fructose dehydration was maximized by working at temperatures between 175°C and 250°C [181-183]. The residence times ranges between 1 min to 10 min depending on the reaction temperature. The maximum yield achieved for hydrothermal production of 5-HMF was around 50%  $\text{w}\cdot\text{w}^{-1}$  [173, 183].

### *5.3. C-5 conversion*

Xylose is an aldose composed of five carbon atoms (C-5). The reaction of xylose in a hydrothermal medium can produce its isomer, xylulose [156]. In this case, the retro-aldol condensation reaction produces a molecule of C-3 and C-2 independently of the aldose-ketose molecule nature. Therefore, the yield and selectivity of retro-aldol condensation products from C-5 to obtain exclusively C-2 and C-3 molecules would be lower than the products produced from C-6 molecules. As it was discussed above, a C-6 aldose or ketose can be selectively transformed into C-2 or C-3 molecules. This would be the main reason because of xylose was mostly studied for dehydration reactions. The product of xylose dehydration is furfural, a C-5 molecule [184].

The maximum yields of furfural production for xylose without adding any catalyst are around 50%  $\text{w}\cdot\text{w}^{-1}$  [184-188]. The xylose yield can be enhanced by adding acid catalysts to the reaction medium which catalyze the dehydration reactions [185, 186, 189, 190]. Several acid catalysts were tested for xylose conversion. For example: inorganic acids [191], zeolites [190, 192-194], zirconium-tungsten oxides [195], and sulfonic [185, 189, 196] and phosphate [197] groups supported in different porous materials. In general, the use of these catalyst enhance the yield of furfural production up to 75%. Once again, the use of batch reactor implies the operation at low temperatures (150°C – 200°C) and long residence times (0.5 h – 20 h) [185-187, 189, 195]. This residence time can be reduced to seconds by using continuous reactors at supercritical temperatures [184].

## **6. Research needs and challenges**

It has been presented that the hydrolysis of cellulose to sugars and sugars to C-2 or C-3 molecules can be completed residence times of milliseconds and seconds, respectively. That

implies that future research of the mechanism of these reactions must be carried out in continuous reactors in order to obtain accurate data.

Even when batch reactors can be easy and convenient to use in the case of fast testing of several catalysts or when solid handling is required, the comparable heating and cooling residence time will make that the results obtained in this way would be considered limited and insignificant for future continuous operation processes.

In the same way, pressure view cells used in solubility and phase behavior studies on biomass hydrothermal reaction requires avoiding the preheating time, since the dissolution/hydrolysis step could be extremely fast and take place during the preheating. Thus, continuous flow cells or those provided with a system for solid injection will be the most widely used.

The development of a continuous industrial process for biomass depolymerization requires continuous pumping of the biomass. Commercial suspension pumps are available for pilot/demonstration scale, but it is difficult to find commercial equipment for lab scale operation. One issue is that the pump valves could be plugged by the suspension particles. The development of high-pressure extruders that can operate with biomass chips would reduce the cost of the biomass pretreatment grinding step.

In addition, operating with solid biomass requires the development of reactors that allow the solid separation and the pressure reduction by commercial valves in order to improve the pressure control.

Other issues, such as work and heat recovery have a key relevance, due to the high temperatures involved in the process and the high energetic consumptions of these processes without an appropriate heat integration scheme. In its design an accurate knowledge of the reaction kinetics at different pressures and temperatures is of utmost importance.

This implies that the knowledge of the reaction mechanism in SCW should be improved. More research is needed to understand the reaction mechanisms that could explain and improve the high selectivity achieved in these processes.

In addition, even when the components of biomass are alike, each biomass presents its own peculiarities. Thus, study new local biomass sources to achieve specific chemicals and energy.

Finally, our knowledge in organic chemistry allows the elimination and rearrangement of functional groups from the building blocks produced. Whereas our expertise in chemical engineering enables the development of simplified and compact processes, contributing altogether to development of the Bioeconomy.

## Acknowledgements

The authors thank the Spanish Ministry of Economy and Competitiveness for the Project CTQ2011-23293 and ENE2012-33613. Also, thank Repsol for its technical support. D.A.C. thanks the Spanish Ministry of Education for the FPU fellowship (AP2009-0402).

## References

1. BECOTEPS. *European Technology Platforms for the FP7. The European Bioeconomy 2030. Delivering Sustainable Growth by addressing the Grand Societal Challenges* 2013 - 10/04/2014 10/04/2014].
2. OECD. *The Bioeconomy to 2030: designing a policy agenda*.
3. Arai, K., Smith Jr, R.L., and Aida, T.M., *Decentralized chemical processes with supercritical fluid technology for sustainable society*. The Journal of Supercritical Fluids, 2009. 47(3): p. 628-636.
4. Akiya, N. and Savage, P.E., *Roles of Water for Chemical Reactions in High-Temperature Water*. Chemical Reviews, 2002. 102(8): p. 2725-2750.
5. Peterson, A.A., Vogel, F., Lachance, R.P., Fröling, M., Michael J. Antal, Jr., and Tester, J.W., *Thermochemical biofuel production in hydrothermal media: A review of sub- and supercritical water technologies*. Energy & Environmental Science, 2008. 1(1): p. 32-65.
6. Bröll, D., Kaul, C., Krämer, A., Krammer, P., Richter, T., Jung, M., Vogel, H., and Zehner, P., *Chemistry in Supercritical Water*. Angewandte Chemie International Edition, 1999. 38(20): p. 2998–3014.
7. Loppinet-Serani, A., Aymonier, C., and Cansell, F., *Supercritical water for environmental technologies*. Journal of Chemical Technology & Biotechnology, 2010. 85(5): p. 583–589.
8. Akizuki, M., Fujii, T., Hayashi, R., and Oshima, Y., *Effects of water on reactions for waste treatment, organic synthesis, and bio-refinery in sub- and supercritical water*. Journal of Bioscience and Bioengineering, 2014. 117(1): p. 10-18.
9. Machida, H., Takesue, M., and Smith Jr, R.L., *Green chemical processes with supercritical fluids: Properties, materials, separations and energy*. The Journal of Supercritical Fluids, 2011. 60(0): p. 2-15.
10. Marshall, W.L. and Franck, E.U., *Ion Product of Water Substance, 0-1000°C, 1-10,000 Bars. New International Formulation and Its Background*. Journal of Physical and Chemical Reference Data, 1981. 10(2): p. 295-304.
11. Bobleter, O., *Hydrothermal degradation of polymers derived from plants*. Progress in polymer science, 1994. 19(5): p. 797-841.

12. Klemm, D., Heublein, B., Fink, H.P., and Bohn, A., *Cellulose: Fascinating Biopolymer and Sustainable Raw Material*. Angewandte Chemie International Edition, 2005. 44(22): p. 3358-3393.
13. Wyman, C.E., Decker, S.R., Himmel, M.E., Brady, J.W., Skopec, C.E., and Viikari, L., *Hydrolysis of cellulose and hemicellulose*, in *Polysaccharides: Structural Diversity and Functional Versatility*, S. Dumitriu, Editor. 2004, Marcel Dekker, Inc., New York. p. 995–1033.
14. Wyman, C.E., Dale, B.E., Elander, R.T., Holtzapple, M., Ladisch, M.R., and Lee, Y.Y., *Coordinated development of leading biomass pretreatment technologies*. Bioresource Technology, 2005. 96(18): p. 1959-1966.
15. Hill, C.A.S., *Wood Modification: Chemical, Thermal and Other Processes*. 2006.
16. Davin, L.B. and Lewis, N.G., *Lignin primary structures and dirigent sites*. Current Opinion in Biotechnology, 2005. 16(4): p. 407-415.
17. Pavlovič, I., Knez, Ž., and Škerget, M., *Hydrothermal Reactions of Agricultural and Food Processing Wastes in Sub- and Supercritical Water: A Review of Fundamentals, Mechanisms, and State of Research*. Journal of Agricultural and Food Chemistry, 2013. 61(34): p. 8003-8025.
18. Fang, Z., Sato, T., Smith Jr, R.L., Inomata, H., Arai, K., and Kozinski, J.A., *Reaction chemistry and phase behavior of lignin in high-temperature and supercritical water*. Bioresource Technology, 2008. 99(9): p. 3424-3430.
19. Brunner, G., *Near critical and supercritical water. Part I. Hydrolytic and hydrothermal processes*. The Journal of Supercritical Fluids, 2009. 47(3): p. 373-381.
20. Alenezi, R., Leeke, G.A., Santos, R.C.D., and Khan, A.R., *Hydrolysis kinetics of sunflower oil under subcritical water conditions*. Chemical Engineering Research and Design, 2009. 87(6): p. 867-873.
21. Rogalinski, T., Herrmann, S., and Brunner, G., *Production of amino acids from bovine serum albumin by continuous sub-critical water hydrolysis*. The Journal of Supercritical Fluids, 2005. 36(1): p. 49-58.
22. Esteban, M.B., García, A.J., Ramos, P., and Márquez, M.C., *Kinetics of amino acid production from hog hair by hydrolysis in sub-critical water*. The Journal of Supercritical Fluids, 2008. 46(2): p. 137-141.

23. Cheng, H., Zhu, X., Zhu, C., Qian, J., Zhu, N., Zhao, L., and Chen, J., *Hydrolysis technology of biomass waste to produce amino acids in sub-critical water*. *Bioresource Technology*, 2008. 99(9): p. 3337-3341.
24. Tollefson, J., *Energy: Not your father's biofuels*. *Nature News*, 2008. 451(7181): p. 880-883.
25. Zhao, Y., Lu, W.-J., and Wang, H.-T., *Supercritical hydrolysis of cellulose for oligosaccharide production in combined technology*. *Chemical Engineering Journal*, 2009. 150(2-3): p. 411-417.
26. Zhao, Y., Lu, W.-J., Wang, H.-T., and Li, D., *Combined Supercritical and Subcritical Process for Cellulose Hydrolysis to Fermentable Hexoses*. *Environmental Science Technology*, 2009. 43(5): p. 1565-1570.
27. Zhao, Y., Wang, H.-T., Lu, W.-J., and Wang, H., *Combined supercritical and subcritical conversion of cellulose for fermentable hexose production in a flow reaction system*. *Chemical Engineering Journal*, 2011. 166(3): p. 868-872.
28. Zhao, Y., Lu, W.-J., Wang, H.-T., and Yang, J.-L., *Fermentable hexose production from corn stalks and wheat straw with combined supercritical and subcritical hydrothermal technology*. *Bioresource Technology*, 2009. 100(23): p. 5884-5889.
29. Onda, A., Ochi, T., and Yanagisawa, K., *Hydrolysis of Cellulose Selectively into Glucose Over Sulfonated Activated-Carbon Catalyst Under Hydrothermal Conditions*. *Topics in Catalysis*, 2009. 52(6-7): p. 801-807.
30. Daorattanachai, P., Khemthong, P., Viriya-Empikul, N., Laosiripojana, N., and Faungnawakij, K., *Conversion of fructose, glucose, and cellulose to 5-hydroxymethylfurfural by alkaline earth phosphate catalysts in hot compressed water*. *Carbohydrate Research*, 2012. 363: p. 58-61.
31. Amarasekara, A.S. and Owereh, O.S., *Hydrolysis and Decomposition of Cellulose in Brønsted Acidic Ionic Liquids Under Mild Conditions*. *Ind. Eng. Chem. Res.*, 2009. 48(22): p. 10152-10155.
32. Amarasekara, A.S. and Wiredu, B., *Degradation of Cellulose in Dilute Aqueous Solutions of Acidic Ionic Liquid 1-(1-Propylsulfonic)-3-methylimidazolium Chloride, and p-Toluenesulfonic Acid at Moderate Temperatures and Pressures*. *Ind. Eng. Chem. Res.*, 2011. 50(21): p. 12276-12280.

33. Dora, S., Bhaskar, T., Singh, R., Naik, D.V., and Adhikari, D.K., *Effective catalytic conversion of cellulose into high yields of methyl glucosides over sulfonated carbon based catalyst*. *Bioresource Technology*, 2012. 120(0): p. 318-321.
34. Fang, Z., Zhang, F., Zeng, H.-Y., and Guo, F., *Production of glucose by hydrolysis of cellulose at 423 K in the presence of activated hydrotalcite nanoparticles*. *Bioresource Technology*, 2011. 102(17): p. 8017-8021.
35. Minowa, T., Zhen, F., and Ogi, T., *Cellulose decomposition in hot-compressed water with alkali or nickel catalyst*. *The Journal of Supercritical Fluids*, 1998. 13(1-3): p. 253-259.
36. Wang, C., Zhou, F., Yang, Z., Wang, W., Yu, F., Wu, Y., and Chi, R.a., *Hydrolysis of cellulose into reducing sugar via hot-compressed ethanol/water mixture*. *Biomass and Bioenergy*, 2012. 42: p. 143-150
37. Xiong, Y., Zhang, Z., Wang, X., Liu, B., and Lin, J., *Hydrolysis of cellulose in ionic liquids catalyzed by a magnetically-recoverable solid acid catalyst*. *Chemical Engineering Journal*, 2014. 235: p. 349-355.
38. Yang, M., Zhang, A., Liu, B., Li, W., and Xing, J., *Improvement of cellulose conversion caused by the protection of Tween-80 on the adsorbed cellulase*. *Biochemical Engineering Journal*, 2011. 56(3): p. 125-129.
39. Sakaki, T., Shibata, M., Miki, T., Hirose, H., and Hayashi, N., *Decomposition of Cellulose in Near-Critical Water and Fermentability of the Products*. *Energy & Fuels*, 1996. 10(3): p. 684-688.
40. Morales-delaRosa, S., Campos-Martin, J.M., and Fierro, J.L.G., *High glucose yields from the hydrolysis of cellulose dissolved in ionic liquids*. *Chemical Engineering Journal*, 2012. 181-182: p. 538-541.
41. Rinaldi, R., Palkovits, R., and Schüth, F., *Depolymerization of Cellulose Using Solid Catalysts in Ionic Liquids*. *Angewandte Chemie International Edition*, 2008. 47(42): p. 8047-8050.
42. Chareonlimkun, A., Champreda, V., Shotipruk, A., and Laosiripojana, N., *Reactions of C5 and C6-sugars, cellulose, and lignocellulose under hot compressed water (HCW) in the presence of heterogeneous acid catalysts*. *Fuel*, 2010. 89(10): p. 2873-2880.

43. Sakaki, T., Shibata, M., Sumi, T., and Yasuda, S., *Saccharification of Cellulose Using a Hot-Compressed Water-Flow Reactor*. Industrial & Engineering Chemistry Research, 2002. 41(4): p. 661-665.
44. Yu, Y. and Wu, H., *Understanding the Primary Liquid Products of Cellulose Hydrolysis in Hot-Compressed Water at Various Reaction Temperatures*. Energy & Fuels, 2010. 24(3): p. 1963-1971.
45. Yu, Y. and Wu, H., *Characteristics and precipitation of glucose oligomers in the fresh liquid products obtained from the hydrolysis of cellulose in hot-compressed water*. Industrial and Engineering Chemistry Research, 2009. 48(23): p. 10682-10690.
46. Abdullah, R., Ueda, K., and Saka, S., *Decomposition behaviors of various crystalline celluloses as treated by semi-flow hot-compressed water*. Cellulose, 2013. 20(5): p. 2321-2333.
47. Rogalinski, T., Liu, K., Albrecht, T., and Brunner, G., *Hydrolysis kinetics of biopolymers in subcritical water*. The Journal of Supercritical Fluids, 2008. 46(3): p. 335-341.
48. Cantero, D.A., Bermejo, M.D., and Cocero, M.J., *Kinetic analysis of cellulose depolymerization reactions in near critical water*. The Journal of Supercritical Fluids, 2013. 75: p. 48-57.
49. Cantero, D.A., Bermejo, M.D., and Cocero, M.J., *High glucose selectivity in pressurized water hydrolysis of cellulose using ultra-fast reactors*. Bioresource Technology, 2013. 135: p. 697-703.
50. Sasaki, M., Adschiri, T., and Arai, K., *Kinetics of cellulose conversion at 25 MPa in sub- and supercritical water*. AIChE Journal, 2004. 50(1): p. 192-202.
51. Sasaki, M., Fang, Z., Fukushima, Y., Adschiri, T., and Arai, K., *Dissolution and Hydrolysis of Cellulose in Subcritical and Supercritical Water*. Industrial & Engineering Chemistry Research, 2000. 39(8): p. 2883-2890.
52. Sasaki, M., Kabyemela, B., Malaluan, R., Hirose, S., Takeda, N., Adschiri, T., and Arai, K., *Cellulose hydrolysis in subcritical and supercritical water*. The Journal of Supercritical Fluids, 1998. 13(1-3): p. 261-268.
53. Tolonen, L.K., Penttilä, P.A., Serimaa, R., Kruse, A., and Sixta, H., *The swelling and dissolution of cellulose crystallites in subcritical and supercritical water*. Cellulose, 2013. 20(6): p. 2731-2744.

54. Kumar, S. and Gupta, R.B., *Hydrolysis of Microcrystalline Cellulose in Subcritical and Supercritical Water in a Continuous Flow Reactor*. Industrial & Engineering Chemistry Research, 2008. 47(23): p. 9321-9329.
55. Ehara, K. and Saka, S., *Decomposition behavior of cellulose in supercritical water, subcritical water, and their combined treatments*. Journal of Wood Science, 2005. 51(2): p. 148-153.
56. Hu, X., Wu, L., Wang, Y., Song, Y., Mourant, D., Gunawan, R., Gholizadeh, M., and Li, C.-Z., *Acid-catalyzed conversion of mono- and poly-sugars into platform chemicals: Effects of molecular structure of sugar substrate*. Bioresource Technology, 2013. 133: p. 469-474.
57. Schacht, C., Zetzl, C., and Brunner, G., *From plant materials to ethanol by means of supercritical fluid technology*. The Journal of Supercritical Fluids, 2008. 46(3): p. 299-321.
58. Li, H., Pu, Y., Kumar, R., Ragauskas, A.J., and Wyman, C.E., *Investigation of lignin deposition on cellulose during hydrothermal pretreatment, its effect on cellulose hydrolysis, and underlying mechanisms*. Biotechnology and Bioengineering, 2014. 111(3): p. 485-492.
59. Mäki-Arvela, P.i., Salmi, T., Holmbom, B., Willför, S., and Murzin, D.Y., *Synthesis of Sugars by Hydrolysis of Hemicelluloses- A Review*. Chemical Reviews, 2011. 111(9): p. 5638-5666.
60. Lu, X., Zhang, Y., Liang, Y., Yang, J., Zhang, S., and Suzuki, E., *Kinetic studies of hemicellulose hydrolysis of corn stover at atmospheric pressure*. Korean Journal of Chemical Engineering, 2008. 25(2): p. 302-307.
61. Pińkowska, H., Wolak, P., and Złocińska, A., *Hydrothermal decomposition of xylan as a model substance for plant biomass waste – Hydrothermolysis in subcritical water*. Biomass and Bioenergy, 2011. 35(9): p. 3902-3912.
62. Aoyama, M. and Seki, K., *Acid catalysed steaming for solubilization of bamboo grass xylan*. Bioresource Technology, 1999. 69(1): p. 91-94.
63. Carvalho, F., *Production of oligosaccharides by autohydrolysis of brewery's spent grain*. Bioresource Technology, 2004. 91(1): p. 93-100.

64. Sun, Y., Lu, X., Zhang, S., Zhang, R., and Wang, X., *Kinetic study for Fe(NO<sub>3</sub>)<sub>3</sub> catalyzed hemicellulose hydrolysis of different corn stover silages*. *Bioresource Technology*, 2011. 102(3): p. 2936-2942.
65. Makishima, S., Mizuno, M., Sato, N., Shinji, K., Suzuki, M., Nozaki, K., Takahashi, F., Kanda, T., and Amano, Y., *Development of continuous flow type hydrothermal reactor for hemicellulose fraction recovery from corncob*. *Bioresource Technology*, 2009. 100(11): p. 2842-2848.
66. Yong, T.L.-K. and Matsumura, Y., *Kinetics analysis of phenol and benzene decomposition in supercritical water*. *The Journal of Supercritical Fluids*, 2014. 87: p. 73-82.
67. Wahyudiono, Kanetake, T., Sasaki, M., and Goto, M., *Decomposition of a lignin model compound under hydrothermal conditions*. *Chemical Engineering and Technology*, 2007. 30(8): p. 1113-1122.
68. Yong, T.L.K. and Yukihiro, M., *Kinetic analysis of guaiacol conversion in sub- and supercritical water*. *Industrial and Engineering Chemistry Research*, 2013. 52(26): p. 9048-9059.
69. Yong, T.L.K. and Matsumura, Y., *Reaction pathways of phenol and benzene decomposition in supercritical water gasification*. *Journal of the Japan Petroleum Institute*, 2013. 56(5): p. 331-343.
70. Okuda, K., Ohara, S., Umetsu, M., Takami, S., and Adschiri, T., *Disassembly of lignin and chemical recovery in supercritical water and p-cresol mixture. Studies on lignin model compounds*. *Bioresource Technology*, 2008. 99(6): p. 1846-1852.
71. Yong, T.L.K. and Matsumura, Y., *Kinetic analysis of lignin hydrothermal conversion in sub- and supercritical water*. *Industrial and Engineering Chemistry Research*, 2013. 52(16): p. 5626-5639.
72. Yong, T.L.K. and Matsumura, Y., *Reaction kinetics of the lignin conversion in supercritical water*. *Industrial and Engineering Chemistry Research*, 2012. 51(37): p. 11975-11988.
73. Saisu, M., Sato, T., Watanabe, M., Adschiri, T., and Arai, K., *Conversion of lignin with supercritical water-phenol mixtures*. *Energy and Fuels*, 2003. 17(4): p. 922-928.

74. Zhang, B., Huang, H.J., and Ramaswamy, S., *Reaction kinetics of the hydrothermal treatment of lignin*. Applied Biochemistry and Biotechnology, 2008. 147(1-3): p. 119-131.
75. Wahyudiono, Sasaki, M., and Goto, M., *Recovery of phenolic compounds through the decomposition of lignin in near and supercritical water*. Chemical Engineering and Processing: Process Intensification, 2008. 47(9-10): p. 1609-1619.
76. Okuda, K., Umetsu, M., Takami, S., and Adschiri, T., *Disassembly of lignin and chemical recovery - Rapid depolymerization of lignin without char formation in water-phenol mixtures*. Fuel Processing Technology, 2004. 85(8-10): p. 803-813.
77. Pińkowska, H., Wolak, P., and Złocińska, A., *Hydrothermal decomposition of alkali lignin in sub- and supercritical water*. Chemical Engineering Journal, 2012. 187: p. 410-414.
78. Gosselink, R.J.A., Teunissen, W., van Dam, J.E.G., de Jong, E., Gellerstedt, G., Scott, E.L., and Sanders, J.P.M., *Lignin depolymerisation in supercritical carbon dioxide/acetone/water fluid for the production of aromatic chemicals*. Bioresource Technology, 2012. 106: p. 173-177.
79. Takami, S., Okuda, K., Man, X., Umetsu, M., Ohara, S., and Adschiri, T., *Kinetic study on the selective production of 2-(Hydroxybenzyl)-4- methylphenol from organosolv lignin in a mixture of supercritical water and p -cresol*. Industrial and Engineering Chemistry Research, 2012. 51(13): p. 4804-4808.
80. Patil, P.T., Armbruster, U., Richter, M., and Martin, A., *Heterogeneously catalyzed hydroprocessing of organosolv lignin in sub- and supercritical solvents*. Energy and Fuels, 2011. 25(10): p. 4713-4722.
81. Man, X., Okuda, K., Ohara, S., Umetsu, M., Takami, S., and Adschiri, T., *Disassembly of organosolv lignin in supercritical fluid - Phenol as a suppressor for repolymerization*. Nihon Enerugi Gakkaishi/Journal of the Japan Institute of Energy, 2005. 84(6): p. 486-490.
82. Forchheim, D., Hornung, U., Kempe, P., Kruse, A., and Steinbach, D., *Influence of RANEY Nickel on the formation of intermediates in the degradation of lignin*. International Journal of Chemical Engineering, 2012.
83. Sasaki, M., Adschiri, T., and Arai, K., *Fractionation of sugarcane bagasse by hydrothermal treatment*. Bioresource Technology, 2003. 86(3): p. 301-304.

84. Alfaro, A., López, F., Pérez, A., García, J.C., and Rodríguez, A., *Integral valorization of tagasaste (Chamaecytisus proliferus) under hydrothermal and pulp processing*. Bioresource Technology, 2010. 101(19): p. 7635-7640.
85. Gullón, P., Romaní, A., Vila, C., Garrote, G., and Parajó, J.C., *Potential of hydrothermal treatments in lignocellulose biorefineries*. Biofuels, Bioproducts and Biorefining, 2012. 6(2): p. 219-232.
86. Lee, J.Y., Ryu, H.J., and Oh, K.K., *Acid-catalyzed hydrothermal severity on the fractionation of agricultural residues for xylose-rich hydrolyzates*. Bioresource Technology, 2013. 132: p. 84-90.
87. Lü, X. and Saka, S., *Hydrolysis of Japanese beech by batch and semi-flow water under subcritical temperatures and pressures*. Biomass and Bioenergy, 2010. 34(8): p. 1089-1097.
88. Moniz, P., Pereira, H., Quilhó, T., and Carvalheiro, F., *Characterisation and hydrothermal processing of corn straw towards the selective fractionation of hemicelluloses*. Industrial Crops and Products, 2013. 50: p. 145-153.
89. Mosteiro-Romero, M., Vogel, F., and Wokaun, A., *Liquefaction of wood in hot compressed water: Part 1 – Experimental results*. Chemical Engineering Science.
90. Öztürk, İ., Irmak, S., Hesenov, A., and Erbatur, O., *Hydrolysis of kenaf (Hibiscus cannabinus L.) stems by catalytical thermal treatment in subcritical water*. Biomass and Bioenergy, 2010. 34(11): p. 1578-1585.
91. Requejo, A., Peleteiro, S., Rodríguez, A., Garrote, G., and Parajó, J.C., *Valorization of residual woody biomass (Olea europaea trimmings) based on aqueous fractionation*. Journal of Chemical Technology & Biotechnology, 2012. 87(1): p. 87-94.
92. Yáñez, R., Garrote, G., and Díaz, M.J., *Valorisation of a leguminous specie, Sesbania grandiflora, by means of hydrothermal fractionation*. Bioresource Technology, 2009. 100(24): p. 6514-6523.
93. Vegas, R., Kabel, M., Schols, H.A., Alonso, J.L., and Parajó, J.C., *Hydrothermal processing of rice husks: effects of severity on product distribution*. Journal of Chemical Technology & Biotechnology, 2008. 83(7): p. 965-972.
94. Rodríguez, A., Moral, A., Sánchez, R., Requejo, A., and Jiménez, L., *Influence of variables in the hydrothermal treatment of rice straw on the composition of the resulting fractions*. Bioresource Technology, 2009. 100(20): p. 4863-4866.

95. Luterbacher, J.S., Tester, J.W., and Walker, L.P., *High-solids biphasic CO<sub>2</sub>-H<sub>2</sub>O pretreatment of lignocellulosic biomass*. *Biotechnology and Bioengineering*, 2010. 107(3): p. 451-460.
96. Ingram, T., Rogalinski, T., Bockemühl, V., Antranikian, G., and Brunner, G., *Semi-continuous liquid hot water pretreatment of rye straw*. *Journal of Supercritical Fluids*, 2009. 48(3): p. 238-246.
97. Rogalinski, T., Ingram, T., and Brunner, G., *Hydrolysis of lignocellulosic biomass in water under elevated temperatures and pressures*. *The Journal of Supercritical Fluids*, 2008. 47(1): p. 54-63.
98. Mok, W.S.L. and Antal Jr, M.J., *Uncatalyzed solvolysis of whole biomass hemicellulose by hot compressed liquid water*. *Industrial and Engineering Chemistry Research*, 1992. 31(4): p. 1157-1161.
99. Kim, J.K., Um, B.-H., and Kim, T.H., *Bioethanol production from micro-algae, Schizocytrium sp., using hydrothermal treatment and biological conversion*. *Korean Journal of Chemical Engineering*, 2012. 29(2): p. 209-214.
100. Merali, Z., Ho, J.D., Collins, S.R.A., Gall, G.L., Elliston, A., Käsper, A., and Waldron, K.W., *Characterization of cell wall components of wheat straw following hydrothermal pretreatment and fractionation*. *Bioresource Technology*, 2013. 131: p. 226-234.
101. Prado, J.M., Follegatti-Romero, L.A., Forster-Carneiro, T., Rostagno, M.A., Maugeri Filho, F., and Meireles, M.A.A., *Hydrolysis of sugarcane bagasse in subcritical water*. *The Journal of Supercritical Fluids*, 2014. 86: p. 15-22.
102. Pronyk, C. and Mazza, G., *Fractionation of triticale, wheat, barley, oats, canola, and mustard straws for the production of carbohydrates and lignins*. *Bioresource Technology*, 2012. 106: p. 117-124.
103. Pronyk, C. and Mazza, G., *Optimization of processing conditions for the fractionation of triticale straw using pressurized low polarity water*. *Bioresource Technology*, 2011. 102(2): p. 2016-2025.
104. Liu, C. and Wyman, C.E., *Partial flow of compressed-hot water through corn stover to enhance hemicellulose sugar recovery and enzymatic digestibility of cellulose*. *Bioresource Technology*, 2005. 96(18): p. 1978-1985.

105. Mosier, N., Hendrickson, R., Ho, N., Sedlak, M., and Ladisch, M.R., *Optimization of pH controlled liquid hot water pretreatment of corn stover*. *Bioresource Technology*, 2005. 96(18): p. 1986-1993.
106. Jacobsen, S.E. and Wyman, C.E., *Cellulose and hemicellulose hydrolysis models for application to current and novel pretreatment processes*. *Applied Biochemistry and Biotechnology - Part A Enzyme Engineering and Biotechnology*, 2000. 84-86: p. 81-96.
107. Mosier, N., Wyman, C., Dale, B., Elander, R., Lee, Y.Y., Holtzapfle, M., and Ladisch, M., *Features of promising technologies for pretreatment of lignocellulosic biomass*. *Bioresource Technology*, 2005. 96(6): p. 673-686.
108. Wang, Y., Chen, G., Li, Y., Yan, B., and Pan, D., *Experimental study of the bio-oil production from sewage sludge by supercritical conversion process*. *Waste Management*, 2013. 33(11): p. 2408-2415.
109. Sluiter, J.B., Ruiz, R.O., Scarlata, C.J., Sluiter, A.D., and Templeton, D.W., *Compositional Analysis of Lignocellulosic Feedstocks. 1. Review and Description of Methods*. *J. Agric. Food Chem.*, 2010. 58(16): p. 9043-9053.
110. Templeton, D.W., Scarlata, C.J., Sluiter, J.B., and Wolfrum, E.J., *Compositional Analysis of Lignocellulosic Feedstocks. 2. Method Uncertainties*. *J. Agric. Food Chem.*, 2010. 58(16): p. 9054-9062.
111. Sun, X.F., Jing, Z., Fowler, P., Wu, Y., and Rajaratnam, M., *Structural characterization and isolation of lignin and hemicelluloses from barley straw*. *Industrial Crops and Products*, 2011. 33(3): p. 588-598.
112. Renmatix. 2013 - 10/04/2014 10/04/2014].
113. Kruse, A., *Hydrothermal biomass gasification*. *The Journal of Supercritical Fluids*, 2009. 47(3): p. 391-399.
114. Lu, Y., Guo, L., Zhang, X., and Yan, Q., *Thermodynamic modeling and analysis of biomass gasification for hydrogen production in supercritical water*. *Chemical Engineering Journal*, 2007. 131(1-3): p. 233-244.
115. Lu, Y., Guo, L., Ji, C., Zhang, X., Hao, X., and Yan, Q., *Hydrogen production by biomass gasification in supercritical water: A parametric study*. *International Journal of Hydrogen Energy*, 2006. 31(7): p. 822-831.

116. van Rossum, G., Potic, B., Kersten, S.R.A., and van Swaaij, W.P.M., *Catalytic gasification of dry and wet biomass*. Catalysis Today, 2009. 145(1-2): p. 10-18.
117. Williams, P.T. and Onwudili, J., *Composition of Products from the Supercritical Water Gasification of Glucose: A Model Biomass Compound*. Industrial & Engineering Chemistry Research, 2005. 44(23): p. 8739-8749.
118. Bagnoud-Velásquez, M., Brandenberger, M., Vogel, F., and Ludwig, C., *Continuous catalytic hydrothermal gasification of algal biomass and case study on toxicity of aluminum as a step toward effluents recycling*. Catalysis Today, 2014. 223: p. 35-43.
119. Marrone, P.A. and Hong, G.T., *Corrosion control methods in supercritical water oxidation and gasification processes*. Journal of Supercritical Fluids, 2009. 51(2): p. 83-103.
120. Kruse, A., *Supercritical water gasification*. Biofuels, Bioproducts and Biorefining, 2008. 2(5): p. 415-437.
121. Azadi, P., Khodadadi, A.A., Mortazavi, Y., and Farnood, R., *Hydrothermal gasification of glucose using Raney nickel and homogeneous organometallic catalysts*. Fuel Processing Technology, 2009. 90(1): p. 145-151.
122. Fang, Z., Minowa, T., Fang, C., Smith, J.R.L., Inomata, H., and Kozinski, J.A., *Catalytic hydrothermal gasification of cellulose and glucose*. International Journal of Hydrogen Energy, 2008. 33(3): p. 981-990.
123. Matsumura, Y., Minowa, T., Potic, B., Kersten, S.R.A., Prins, W., van Swaaij, W.P.M., van de Beld, B., Elliott, D.C., Neuenschwander, G.G., Kruse, A., and Jerry Antal Jr, M., *Biomass gasification in near- and super-critical water: Status and prospects*. Biomass and Bioenergy, 2005. 29(4): p. 269-292.
124. Guo, Y., Wang, S., Gong, Y., Xu, D., Tang, X., and Ma, H., *Partial oxidation of municipal sludge with activated carbon catalyst in supercritical water*. Journal of Hazardous Materials, 2010. 180(1-3): p. 137-144.
125. Sinač, A., Kruse, A., and Rathert, J., *Influence of the Heating Rate and the Type of Catalyst on the Formation of Key Intermediates and on the Generation of Gases during Hydrolysis of Glucose in Supercritical Water in a Batch Reactor*. Industrial and Engineering Chemistry Research, 2004. 43(2): p. 502-508.

126. Modell, M., *Gasification and Liquefaction of Forest Products in Supercritical Water*, in *Fundamentals of Thermochemical Biomass Conversion*, R.P. Overend, T.A. Milne, and L.K. Mudge, Editors. 1985, Springer Netherlands. p. 95-119.
127. Yanik, J., Ebale, S., Kruse, A., Saglam, M., and Yüksel, M., *Biomass gasification in supercritical water: Part 1. Effect of the nature of biomass*. *Fuel*, 2007. 86(15): p. 2410-2415.
128. Yanik, J., Ebale, S., Kruse, A., Saglam, M., and Yüksel, M., *Biomass gasification in supercritical water: II. Effect of catalyst*. *International Journal of Hydrogen Energy*, 2008. 33(17): p. 4520-4526.
129. Elliott, D.C., Hart, T.R., and Neuenschwander, G.G., *Chemical Processing in High-Pressure Aqueous Environments. 8. Improved Catalysts for Hydrothermal Gasification*. *Industrial & Engineering Chemistry Research*, 2006. 45(11): p. 3776-3781.
130. Elliott, D.C., Neuenschwander, G.G., Hart, T.R., Butner, R.S., Zacher, A.H., Engelhard, M.H., Young, J.S., and McCready, D.E., *Chemical Processing in High-Pressure Aqueous Environments. 7. Process Development for Catalytic Gasification of Wet Biomass Feedstocks*. *Industrial & Engineering Chemistry Research*, 2004. 43(9): p. 1999-2004.
131. Luterbacher, J.S., Fröling, M., Vogel, F.d.r., Maréchal, F.o., and Tester, J.W., *Hydrothermal Gasification of Waste Biomass: Process Design and Life Cycle Assessment*. *Environmental Science Technology*, 2009. 43(5): p. 1578-1583.
132. Bühler, W., Dinjus, E., Ederer, H.J., Kruse, A., and Mas, C., *Ionic reactions and pyrolysis of glycerol as competing reaction pathways in near- and supercritical water*. *The Journal of Supercritical Fluids*, 2002. 22(1): p. 37-53.
133. Lee, I.G., Kim, M.S., and Ihm, S.K., *Gasification of glucose in supercritical water*. *Industrial and Engineering Chemistry Research*, 2002. 41(5): p. 1182-1188.
134. Yan, Q., Guo, L., and Lu, Y., *Thermodynamic analysis of hydrogen production from biomass gasification in supercritical water*. *Energy Conversion and Management*, 2006. 47(11-12): p. 1515-1528.
135. Xu, D., Wang, S., Hu, X., Chen, C., Zhang, Q., and Gong, Y., *Catalytic gasification of glycine and glycerol in supercritical water*. *International Journal of Hydrogen Energy*, 2009. 34(13): p. 5357-5364.

136. Schmieder, H., Abeln, J., Boukis, N., Dinjus, E., Kruse, A., Kluth, M., Petrich, G., Sadri, E., and Schacht, M., *Hydrothermal gasification of biomass and organic wastes*. The Journal of Supercritical Fluids, 2000. 17(2): p. 145-153.
137. D'Jesús, P., Boukis, N., Kraushaar-Czarnetzki, B., and Dinjus, E., *Gasification of corn and clover grass in supercritical water*. Fuel, 2006. 85(7-8): p. 1032-1038.
138. Antal Jr, M.J., Allen, S.G., Schulman, D., Xu, X., and Divilio, R.J., *Biomass gasification in supercritical water*. Industrial and Engineering Chemistry Research, 2000. 39(11): p. 4040-4053.
139. Elliott, D.C., Hart, T.R., Neuenschwander, G.G., Rotness, L.J., Olarte, M.V., and Zacher, A.H., *Chemical Processing in High-Pressure Aqueous Environments. 9. Process Development for Catalytic Gasification of Algae Feedstocks*. Industrial & Engineering Chemistry Research, 2012. 51(33): p. 10768-10777.
140. Zöhrer, H. and Vogel, F., *Hydrothermal catalytic gasification of fermentation residues from a biogas plant*. Biomass and Bioenergy, 2013. 53: p. 138-148.
141. Waldner, M.H., Krumeich, F., and Vogel, F., *Synthetic natural gas by hydrothermal gasification of biomass*. The Journal of Supercritical Fluids, 2007. 43(1): p. 91-105.
142. Gassner, M., Vogel, F., Heyen, G., and Maréchal, F., *Optimal process design for the polygeneration of SNG, power and heat by hydrothermal gasification of waste biomass: Thermo-economic process modelling and integration*. Energy Environ. Sci., 2011. 4(5): p. 1726-1741.
143. Elliott, D.C., *Catalytic hydrothermal gasification of biomass*. Biofuels, Bioproducts and Biorefining, 2008. 2(3): p. 254-265.
144. Jin, H., Lu, Y., Guo, L., Cao, C., and Zhang, X., *Hydrogen production by partial oxidative gasification of biomass and its model compounds in supercritical water*. International Journal of Hydrogen Energy, 2010. 35(7): p. 3001-3010.
145. Hao, X.H., Guo, L.J., Mao, X., Zhang, X.M., and Chen, X.J., *Hydrogen production from glucose used as a model compound of biomass gasified in supercritical water*. International Journal of Hydrogen Energy, 2003. 28(1): p. 55-64.
146. Guo, L.J., Lu, Y.J., Zhang, X.M., Ji, C.M., Guan, Y., and Pei, A.X., *Hydrogen production by biomass gasification in supercritical water: A systematic experimental and analytical study*. Catalysis Today, 2007. 129(3-4): p. 275-286.

147. Peterson, A.A., Dreher, M., Wambach, J., Nachtegaal, M., Dahl, S., Nørskov, J.K., and Vogel, F., *Evidence of Scrambling over Ruthenium-based Catalysts in Supercritical-water Gasification*. ChemCatChem, 2012. 4(8): p. 1185-1189.
148. Wambach, J., Schubert, M., Döbeli, M., and Vogel, F., *Characterization of a spent Ru/C catalyst after gasification of biomass in supercritical water*. Chimia, 2012. 66(9): p. 706-711.
149. Waldner, M.H. and Vogel, F., *Renewable production of methane from woody biomass by catalytic hydrothermal gasification*. Industrial and Engineering Chemistry Research, 2005. 44(13): p. 4543-4551.
150. Stucki, S., Vogel, F., Ludwig, C., Haiduc, A.G., and Brandenberger, M., *Catalytic gasification of algae in supercritical water for biofuel production and carbon capture*. Energy and Environmental Science, 2009. 2(5): p. 535-541.
151. Hydromethan-AG.
152. Sasaki, M., Goto, K., Tajima, K., Adschiri, T., and Arai, K., *Rapid and selective retro-aldol condensation of glucose to glycolaldehyde in supercritical water*. Green Chem., 2002. 4(3): p. 285-287.
153. Assary, R.S., Kim, T., Low, J.J., Greeley, J., and Curtiss, L.A., *Glucose and fructose to platform chemicals: understanding the thermodynamic landscapes of acid-catalysed reactions using high-level ab initio methods*. Physical Chemistry Chemical Physics, 2012. 14(48): p. 16603-16611.
154. Kabyemela, B.M., Adschiri, T., Malaluan, R.M., and Arai, K., *Kinetics of Glucose Epimerization and Decomposition in Subcritical and Supercritical Water*. Industrial and Engineering Chemistry Research, 1997. 36(5): p. 1552-1558.
155. Kabyemela, B.M., Adschiri, T., Malaluan, R.M., and Arai, K., *Glucose and Fructose Decomposition in Subcritical and Supercritical Water: Detailed Reaction Pathway, Mechanisms, and Kinetics*. Industrial & Engineering Chemistry Research, 1999. 38(8): p. 2888-2895.
156. Lü, X. and Saka, S., *New insights on monosaccharides' isomerization, dehydration and fragmentation in hot-compressed water*. The Journal of Supercritical Fluids, 2012. 61(0): p. 146-156.
157. Usuki, C., Kimura, Y., and Adachi, S., *Isomerization of Hexoses in Subcritical Water*. Food Science and Technology Research, 2007. 13(3): p. 205-209.

158. Sasaki, M., Takahashi, K., Haneda, Y., Satoh, H., Sasaki, A., Narumi, A., Satoh, T., Kakuchi, T., and Kaga, H., *Thermochemical transformation of glucose to 1,6-anhydroglucose in high-temperature steam*. Carbohydrate Research, 2008. 343(5): p. 848-854.
159. Kimura, H., Nakahara, M., and Matubayasi, N., *In Situ Kinetic Study on Hydrothermal Transformation of d -Glucose into 5-Hydroxymethylfurfural through d -Fructose with <sup>13</sup>C NMR*. The Journal of Physical Chemistry A, 2011. 115(48): p. 14013-14021.
160. Kabyemela, B.M., Adschiri, T., Malaluan, R., and Arai, K., *Degradation Kinetics of Dihydroxyacetone and Glyceraldehyde in Subcritical and Supercritical Water*. Industrial & Engineering Chemistry Research, 1997. 36(6): p. 2025-2030.
161. Aida, T.M., Ikarashi, A., Saito, Y., Watanabe, M., Smith Jr, R.L., and Arai, K., *Dehydration of lactic acid to acrylic acid in high temperature water at high pressures*. The Journal of Supercritical Fluids, 2009. 50(3): p. 257-264.
162. Aida, T.M., Tajima, K., Watanabe, M., Saito, Y., Kuroda, K., Nonaka, T., Hattori, H., Smith Jr, R.L., and Arai, K., *Reactions of D-fructose in water at temperatures up to 400 °C and pressures up to 100 MPa*. The Journal of Supercritical Fluids, 2007. 42(1): p. 110-119.
163. Aida, T.M., Sato, Y., Watanabe, M., Tajima, K., Nonaka, T., Hattori, H., and Arai, K., *Dehydration of D-glucose in high temperature water at pressures up to 80 MPa*. The Journal of Supercritical Fluids, 2007. 40(3): p. 381-388.
164. Matsumura, Y., Yanachi, S., and Yoshida, T., *Glucose Decomposition Kinetics in Water at 25 MPa in the Temperature Range of 448–673 K*. Ind. Eng. Chem. Res., 2006. 45(6): p. 1875-1879.
165. Cantero, D.A., Álvarez, A., Bermejo, M.D., and Cocero, M.J., *Transformation of glucose in high added value compounds in a hydrothermal reaction media*. III Iberoamerican Conference on Supercritical Fluids, 2013.
166. Gallezot, P., *Conversion of biomass to selected chemical products*. Chem. Soc. Rev., 2012. 41(4): p. 1538-1558.
167. Ruppert, A.M., Weinberg, K., and Palkovits, R., *Hydrogenolysis Goes Bio: From Carbohydrates and Sugar Alcohols to Platform Chemicals*. Angewandte Chemie International Edition, 2012. 51(11): p. 2564-2601.

168. Kabyemela, B.M., Adschiri, T., Malaluan, R.M., Arai, K., and Ohzeki, H., *Rapid and Selective Conversion of Glucose to Erythrose in Supercritical Water*. Industrial & Engineering Chemical Research, 1997. 36(12): p. 5063-5067.
169. Wang, Y., Jin, F., Sasaki, M., Wahyudiono, Wang, F., Jing, Z., and Goto, M., *Selective conversion of glucose into lactic acid and acetic acid with copper oxide under hydrothermal conditions*. AIChE Journal, 2013. 59(6): p. 2096–2104.
170. Watanabe, M., Aizawa, Y., Iida, T., Aida, T.M., Levy, C., Sue, K., and Inomata, H., *Glucose reactions with acid and base catalysts in hot compressed water at 473K*. Carbohydrate Research, 2005. 340(12): p. 1925-1930.
171. Yan, X., Jin, F., Tohji, K., Moriya, T., and Enomoto, H., *Production of lactic acid from glucose by alkaline hydrothermal reaction*. Journal of Materials Science, 2007. 42(24): p. 9995-9999.
172. Qi, X., Watanabe, M., Aida, T.M., and Smith, R.L., *Synergistic conversion of glucose into 5-hydroxymethylfurfural in ionic liquid–water mixtures*. Bioresource Technology, 2012. 109: p. 224-228.
173. Khajavi, S.H., Kimura, Y., Oomori, T., Matsuno, R., and Adachi, S., *Degradation kinetics of monosaccharides in subcritical water*. Journal of Food Engineering, 2005. 68(3): p. 309-313.
174. Román-Leshkov, Y., Moliner, M., Labinger, J.A., and Davis, M.E., *Mechanism of Glucose Isomerization Using a Solid Lewis Acid Catalyst in Water*. Angewandte Chemie International Edition, 2010. 49(47): p. 8954–8957.
175. Srokol, Z., Bouche, A.-G., van Estrik, A., Strik, R.C.J., Maschmeyer, T., and Peters, J.A., *Hydrothermal upgrading of biomass to biofuel; studies on some monosaccharide model compounds*. Carbohydrate Research, 2004. 339(10): p. 1717-1726.
176. Bicker, M., Endres, S., Ott, L., and Vogel, H., *Catalytical conversion of carbohydrates in subcritical water: A new chemical process for lactic acid production*. Journal of Molecular Catalysis A: Chemical, 2005. 239(1–2): p. 151-157.
177. Yang, F., Liu, Q., Bai, X., and Du, Y., *Conversion of biomass into 5-hydroxymethylfurfural using solid acid catalyst*. Bioresource Technology, 2011. 102(3): p. 3424-3429.
178. Wu, X., Fu, J., and Lu, X., *Hydrothermal decomposition of glucose and fructose with inorganic and organic potassium salts*. Bioresource Technology, 2012. 119: p. 48-54.

179. Asghari, F.S. and Yoshida, H., *Kinetics of the Decomposition of Fructose Catalyzed by Hydrochloric Acid in Subcritical Water: Formation of 5-Hydroxymethylfurfural, Levulinic, and Formic Acids*. Ind. Eng. Chem. Res., 2007. 46(23): p. 7703-7710.
180. Asghari, F.S. and Yoshida, H., *Dehydration of fructose to 5-hydroxymethylfurfural in sub-critical water over heterogeneous zirconium phosphate catalysts*. Carbohydrate Research, 2006. 341(14): p. 2379-2387.
181. Bicker, M., Hirth, J., and Vogel, H., *Dehydration of fructose to 5-hydroxymethylfurfural in sub- and supercritical acetone*. Green Chemistry, 2003. 5(2): p. 280-284.
182. Bicker, M., Kaiser, D., Ott, L., and Vogel, H., *Dehydration of d-fructose to hydroxymethylfurfural in sub- and supercritical fluids*. The Journal of Supercritical Fluids, 2005. 36(2): p. 118-126.
183. Hu, L., Zhao, G., Tang, X., Wu, Z., Xu, J., Lin, L., and Liu, S., *Catalytic conversion of carbohydrates into 5-hydroxymethylfurfural over cellulose-derived carbonaceous catalyst in ionic liquid*. Bioresource Technology, 2013. 148: p. 501-507.
184. Aida, T.M., Shiraishi, N., Kubo, M., Watanabe, M., and Smith, R.L., *Reaction kinetics of d-xylose in sub- and supercritical water*. The Journal of Supercritical Fluids, 2010. 55(1): p. 208-216.
185. Lam, E., Chong, J.H., Majid, E., Liu, Y., Hrapovic, S., Leung, A.C.W., and Luong, J.H.T., *Carbocatalytic dehydration of xylose to furfural in water*. Carbon, 2012. 50(3): p. 1033-1043.
186. Lam, E., Majid, E., Leung, A.C.W., Chong, J.H., Mahmoud, K.A., and Luong, J.H.T., *Synthesis of Furfural from Xylose by Heterogeneous and Reusable Nafion Catalysts*. ChemSusChem, 2011. 4(4): p. 535-541.
187. Kim, S.B., Lee, M.R., Park, E.D., Lee, S.M., Lee, H., Park, K.H., and Park, M.-J., *Kinetic study of the dehydration of d-xylose in high temperature water*. Reaction Kinetics, Mechanisms and Catalysis, 2011. 103(2): p. 267-277.
188. Gairola, K. and Smirnova, I., *Hydrothermal pentose to furfural conversion and simultaneous extraction with SC-CO<sub>2</sub> – Kinetics and application to biomass hydrolysates*. Bioresource Technology, 2012. 123: p. 592-598.
189. Agirrezabal-Telleria, I., Larreategui, A., Requies, J., Güemez, M.B., and Arias, P.L., *Furfural production from xylose using sulfonic ion-exchange resins (Amberlyst) and*

- simultaneous stripping with nitrogen*. *Bioresource Technology*, 2011. 102(16): p. 7478-7485.
190. Dias, A.S., Lima, S., Brandão, P., Pillinger, M., Rocha, J., and Valente, A.A., *Liquid-phase Dehydration of d-xylose over Microporous and Mesoporous Niobium Silicates*. *Catalysis Letters*, 2006. 108(3-4): p. 179-186.
191. Yemiş, O. and Mazza, G., *Acid-catalyzed conversion of xylose, xylan and straw into furfural by microwave-assisted reaction*. *Bioresource Technology*, 2011. 102(15): p. 7371-7378.
192. Lima, S., Antunes, M.M., Fernandes, A., Pillinger, M., Ribeiro, M.F., and Valente, A.A., *Catalytic cyclodehydration of xylose to furfural in the presence of zeolite H-Beta and a micro/mesoporous Beta/TUD-1 composite material*. *Applied Catalysis A: General*, 2010. 388(1-2): p. 141-148.
193. Ferreira, L.R., Lima, S., Neves, P., Antunes, M.M., Rocha, S.M., Pillinger, M., Portugal, I., and Valente, A.A., *Aqueous phase reactions of pentoses in the presence of nanocrystalline zeolite beta: Identification of by-products and kinetic modelling*. *Chemical Engineering Journal*, 2013. 215-216: p. 772-783.
194. Antunes, M.M., Lima, S., Fernandes, A., Pillinger, M., Ribeiro, M.F., and Valente, A.A., *Aqueous-phase dehydration of xylose to furfural in the presence of MCM-22 and ITQ-2 solid acid catalysts*. *Applied Catalysis A: General*, 2012. 417-418: p. 243-252.
195. Antunes, M.M., Lima, S., Fernandes, A., Candeias, J., Pillinger, M., Rocha, S.M., Ribeiro, M.F., and Valente, A.A., *Catalytic dehydration of d-xylose to 2-furfuraldehyde in the presence of Zr-(W,Al) mixed oxides. Tracing by-products using two-dimensional gas chromatography-time-of-flight mass spectrometry*. *Catalysis Today*, 2012. 195(1): p. 127-135.
196. Agirrezabal-Telleria, I., Requies, J., Güemez, M.B., and Arias, P.L., *Dehydration of d-xylose to furfural using selective and hydrothermally stable arenesulfonic SBA-15 catalysts*. *Applied Catalysis B: Environmental*, 2014. 145: p. 34-42.
197. Lima, S., Fernandes, A., Antunes, M.M., Pillinger, M., Ribeiro, F., and Valente, A.A., *Dehydration of Xylose into Furfural in the Presence of Crystalline Microporous Silicoaluminophosphates*. *Catalysis Letters*, 2010. 135(1-2): p. 41-47.

# Aims and Contents

Process Intensification of  
Cellulose Hydrolysis by  
Supercritical Water. Obtaining  
of Added Value Products



## Outlook

In the last century, the production of chemical compounds has been founded on the availability of high amount of petroleum at low prices. These processes are developed in large chemical plants that allow the reduction of the products prices. This production concept allowed the big development of the economy in the 20<sup>th</sup> century. Nowadays, new environmental friendly processes capable of producing chemicals from renewable and "inexhaustible" raw materials are searched. In addition, this new way of production looks for a reduction in CO<sub>2</sub> emissions, a challenging goal that should be accomplished by the productive sector.

As it was analyzed in State of the Art, the use of biomass as alternative carbon resource for the production of chemicals and fuels has been extensively studied in the last years. The use of biomass as raw material makes necessary to change the concept of big and centralized chemical plants (petrochemical industry) into decentralized and efficient processes in small and versatile plants that can be placed near to the source of biomass. The accomplishment of this goal was analyzed by using supercritical water as reaction medium. This technology allows the process intensification of cellulose hydrolysis using low residence times, which will result in small and easy scalable reactors.

The **AIM OF THIS WORK** is to develop a process capable of converting cellulose (biomass streams) into valuable products such as chemicals and fuels using supercritical water as reaction medium.

In order to accomplish the general aim of this thesis, the following partial objectives were established;

- Design and construction of an experimental setup in order to study the cellulose hydrolysis in a hydrothermal medium. The main requirements of the pilot plant are:
  - Maximum temperature of operation: 425°C.
  - Maximum pressure of operation: 30 MPa.
  - Residence time versatility.
  - Instantaneous heating and cooling of cellulose.
  - Feeder: pump capable of impelling suspension with solids concentration of up to 20% w-w<sup>-1</sup>.

- Kinetic modelling of cellulose hydrolysis;
  - Develop a mathematical model to estimate the cellulose conversion as well as its derived product formation along residence time at different temperatures and pressures.
  - Activation energy and pre-exponential factor determination of the kinetic constants.
  - Activation volume determination of the kinetic constants.
  - Analysis of the process kinetic with the properties of the reaction medium.
- Study of cellulose hydrolysis;
  - Study of the residence time, temperature and pressure effect on the reaction of cellulose and glucose hydrolysis.
- Study of Fructose hydrolysis
  - Determination of the main reaction pathway of fructose reactions in a hydrothermal medium.
  - Effect of medium modifiers in the reactions of fructose hydrolysis.
- Study of glucose hydrolysis
  - Determination of the main reaction pathway of glucose reactions in a hydrothermal medium.
  - Production of lactic acid from glucose.
- Study of vegetal biomass hydrolysis: Wheat Bran
  - Study of the behavior of the develop reactor using natural biomass as feed.
- Study of the energetic aspects of the hydrolysis in supercritical water process
  - Analysis of different energetic alternatives for the production of added valued products in supercritical water.

In order to achieve the objectives of this thesis, the work was structured in: six chapters. In each of them, the partial objectives and challenges are presented. In each chapter, a literature review was done in order to know the main achievements and challenges of the analyzed study. The main content of the chapters are described below.

In Chapter 1, “**High glucose selectivity in pressurized water hydrolysis of cellulose using ultra-fast reactors**”, the development of the designed experimental setup is presented as well as the effect of residence time and temperature on the selectivity of cellulose hydrolysis. The main

advantages of the heating and cooling mechanism are analyzed and discussed. The instantaneous methods of heating and cooling make possible to work with extremely low residence times in micro-reactors.

In Chapter 2, "**Kinetics analysis of cellulose depolymerization reactions in near critical water**", a kinetic model of cellulose hydrolysis is proposed and tested. Cellulose hydrolysis was experimented at temperatures between 275°C and 400°C at 25 MPa. The residence time was varied between 0.004 s and 10 s. Reaction pathway of cellulose hydrolysis was supposed in three main steps. In the first stage, cellulose is hydrolyzed into oligosaccharides. Then, these oligosaccharides are hydrolyzed into glucose. Finally glucose can be converted *via* isomerization, dehydration or retro-aldol condensation. The model was used to fit the involved kinetic constants of cellulose hydrolysis. The effect of the reaction medium on 5-HMF production is analyzed. The reaction medium (density) would be determining in the reactions of glucose and fructose hydrolysis. In order to evaluate the model, it was tested for the modelling of cellulose and fructose. Also, the reaction pathway was elucidated by analyzing the reaction of fructose and glucose/fructose mixtures in pressurized water.

In Chapter 3, "**Tunable Selectivity on Cellulose Hydrolysis in Supercritical Water**", the analysis of the residence time and reaction medium effect is presented. The influence of the reaction medium was analyzed in the reaction kinetic. It was observed that the concentration of protons and hydroxide ions in the medium due to water dissociation is decisive in the reaction of glucose and fructose.

In Chapter 4, "**Pressure and Temperature Effect on Cellulose Hydrolysis Kinetic in Pressurized Water**", a kinetic study of pressure and temperature effect on cellulose and glucose hydrolysis is presented. Cellulose hydrolysis was experimented between 300°C and 400°C, at pressures between 10 and 30 MPa. The activation volumes of the reaction kinetics were calculated at pressures between 10 MPa and 27 MPa. Moreover, a general equation that reproduces the behavior of the kinetic constants with pressure and temperature at the same time was obtained.

In Chapter 5, "**Selective Transformation of Fructose into Pyruvaldehyde in Supercritical Water. Reaction Pathway Development**", the analysis of the reaction pathway of fructose in a hydrothermal medium is presented. Fructose reactions in a hydrothermal medium were analyzed using reaction medium modifiers, such as: oxalic acid, sodium hydroxide and scavengers. The reaction was also tested using glucose as starting material resulting in high

yields of glucose. Glucose and fructose were tested together yielding both products, glycolaldehyde and pyruvaldehyde.

In Chapter 6, **"Transformation of Glucose in Added Value Compounds in Supercritical Water"**, the analysis of the reaction pathway of glucose and the production of lactic acid in a hydrothermal medium is presented. The main product of glucose hydrolysis was glycolaldehyde.

In Chapter 7, **"Simultaneous and Selective Recovery of Cellulose and Hemicellulose Fractions from Wheat Bran by Supercritical Water Hydrolysis"**, the conversion of wheat bran into soluble oligosaccharides and monosaccharide such as glucose, xylose and arabinose was analyzed in a supercritical water medium using the developed reactor in Chapter 1. The hydrolysis reactions were performed in a continuous pilot plant at 400 °C, 25 MPa and residence times between 0.1 and 0.7 seconds.

In Chapter 8, **"On the Energetic Approach of Biomass Hydrolysis in Supercritical Water"**, the integration of biomass hydrolysis reactors with commercial Combined Heat and Power (CHP) schemes was investigated, with special attention to reactor outlet streams. Temperature of the flue gases from CHP around 500 °C and the use of direct shaft work in the process offer adequate energy integration possibilities for feed preheating and compression.

In the Annex (Anexo, written in Spanish) it is shown operation manual of the constructed pilot plant.

# Chapter 1. High glucose selectivity in pressurized water hydrolysis of cellulose using ultra-fast reactors.

## Abstract

A new reactor was developed for the selective hydrolysis of cellulose. In this study, the glucose selectivity obtained from cellulose was improved by using ultra-fast reactions in which a selective medium was combined with an effective residence time control. A selective production of glucose, fructose and cellobiose (50%) or total mono-oligo saccharides (>96%) was obtained from the cellulose in a reaction time of 0.03 s. Total cellulose conversion was achieved with a 5-hydroxymethylfural concentration lower than 5 ppm in a novel micro-reactor. Reducing the residence time from minutes to milliseconds opens the possibility of moving from the conventional m<sup>3</sup> to cm<sup>3</sup> reactor volumes.

**Keywords:** Biorefinery • Hydrothermal medium • Cellulose • Glucose



## 1. Introduction

Vegetal biomass grows globally in different climates and types of soils providing an alternative renewable source for the sustainable production of chemicals and fuels. The average production of biomass energy crops in the world [1, 2] is  $\sim 10$  dry tons  $\text{ha}^{-1}$  year $^{-1}$ . Biomass is composed of 34-50% cellulose, 16-34% hemi-cellulose and 11-29% of lignin [3]. The challenging step in the processing of cellulose is the production of glucose. Glucose is a target product because it can be used as a raw material in the production of chemicals, materials and bio-fuels.

Although traditional methods for the hydrolysis of cellulose have been remarkably improved in recent years, they still present limitations in carrying out the hydrolysis to provide high yield and selectivity through energetically efficient and environmentally friendly processes. Acid hydrolysis can be done with sulfuric acid (0.5 – 10% w-w $^{-1}$ ) at temperatures between 150°C and 220°C, obtaining 52% in mass basis (w-w $^{-1}$ ) of glucose in 10 h of treatment [4]. This acid catalysis can be improved using solid catalysts [5, 6]. This hydrolysis procedure using chloromethyl polystyrene resin as catalyst support, with sulfonic acid groups as catalyst yields 93% w-w $^{-1}$  of glucose in 10 h of hydrolysis time at 120°C [4]. The typical yield for enzymatic hydrolysis is 60% w-w $^{-1}$  of glucose in 1 – 60 minutes of pre-treatment time and 24 – 72 h of hydrolysis time [7]. Enzymatic hydrolysis was also studied in combination with additives (Tween 20/80), reporting glucose selectivity of 45% w-w $^{-1}$  at 50°C with an experimental time of 22 h [8]. The enzymatic hydrolysis of cellulose has been enhanced by a cellulose pre-treatment, of the cellulose achieving a glucose selectivity of 92% w-w $^{-1}$  in 48 h [9] or 92% w-w $^{-1}$  in 6 h [10], without considering the pre-treatment time. It is also possible to hydrolyze cellulose through dissolution and hydrolysis in ionic liquids, with or without acid catalyst. It takes about 3 h, achieving 25% - 27% w-w $^{-1}$  of oligosaccharides [11, 12]. A high concentration of derived products such as 5-hydroxymethylfurfural (5-HMF) has been reported in the experiments with ionic liquids without acid catalyst [12]. Cellulose hydrolysis in ionic liquids was improved by adding small quantities of water along the course of the reaction, obtaining a glucose and cellobiose selectivity of 99% w-w $^{-1}$  in 3 h of treatment, at temperatures between 105 – 135°C [13].

The use of pressurized fluids has been proposed as a clean technology to integrate the depolymerization-reaction-separation processes. Particularly, high temperature pressurized water has proved to be a good solvent for clean, safe and environmentally benign organic

reactions [1, 14-20]. The main reasons that make the hydrothermal media a promising alternative for biomass processing are as follows [20]: (1) it is not necessary to reduce the water content in the raw material, thus avoiding energy losses; (2) the reaction media permits the transformation of the different biomass fractions; (3) the mass transfer limitations are reduced or avoided, thus allowing faster reaction rates. Furthermore, the adjustable properties of the reaction media work as a control factor for the reaction selectivity, avoiding the generation of by-products. The density ( $\rho$ ), dielectric constant ( $\epsilon$ ) and ionic product of water ( $K_w$ ) from 0°C to 600°C at a pressure of 25 MPa are plotted in Fig. 1. The properties were calculated according to the equations developed in literature [21, 22]. The change in the dielectric constant is proportional to the density and inversely proportional to the temperature. Hydrogen bonds present a behavior analogous to that of the dielectric constant [14]. Another important property of the organic reaction media is the ionic product of water. Around 300°C the value of the ionic product of water reaches its maximum ( $1.10^{-11}$ ), which creates a medium with high  $H^+$  and  $OH^-$  concentrations, thus favoring in this way acid/basis catalyzed reactions. Above the critical temperature of water (374°C), the  $K_w$  decreases drastically ( $1.10^{-25}$ ) [14]. At higher pressures ( $P > 60\text{MPa}$ ) the  $K_w$  again presents values similar to those of ambient water.

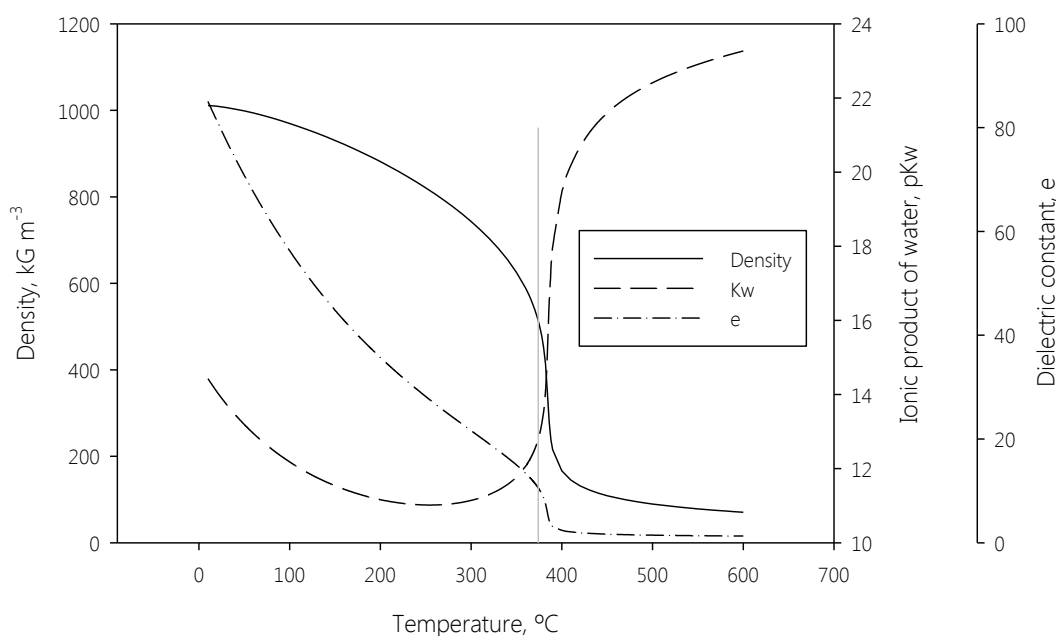


**Fig. 1.** Properties of pressurized water below and above critical point. Continuous line Density ( $\text{kG/m}^3$ ); dashed line represents ionic product of water ( $\text{pKw}$ ) and dashed-dotted line represents the dielectric constant [21, 22].

Sugar selectivity (glucose, fructose and oligomers of glucose up to 6 units) of between 20

and 77% was achieved in residence times ( $\tau$ ) from 0.01 s to 30 s when cellulose was hydrolyzed in a supercritical water medium. The reactions of cellulose hydrolysis under supercritical conditions are fast, but, if the reactions are not controlled, a high quantity of derived products are yielded [16, 23]. The hydrolysis of cellulose is completed at subcritical temperatures, obtaining a high concentration of glucose and oligosaccharides, but the reaction has a low selectivity and needs bigger reactors and higher residence times [24]. Using subcritical water hydrolysis in the presence of a catalyst, the process can take place at a low temperature (150°C), but the residence time is increased up to 24 or 48 h [25].

In this work, a novel reactor capable of operating under supercritical conditions with an effective control of the residence time was developed. In the facility described here, high selectivity of glucose and oligosaccharides of up to six units of glucose (98% carbon basis - c.b.-) can be achieved.

## 2. Materials and Methods

### 2.1. Materials

The cellulose used in the experiments was micro-crystalline cellulose with a particle size of between 20 and 137  $\mu\text{m}$ , purchased from VWR. Distilled water was used in the experiments. The reagents used in HPLC analysis were: cellobiose (+98%), glucose (+99%), fructose (+99%), glyceraldehyde (95%), pyruvaldehyde (40%), erythrose (+75%) and 5-hydroxymethylfurfural (99%), purchased from Sigma. The reagents used in the enzymatic analysis were:  $\beta$ -glucosidase (glucose oxidase plus peroxidase and 4-aminoantipyrine) and GOPOD reagent (buffer, pH 7.4, p-hydroxybenzoic acid and sodium azide -0.4%w/v-).

### 2.2. Methods

The residence time was evaluated as shown in equation 1, where  $V$  is the volume of the reactor ( $\text{m}^3$ ),  $\rho$  ( $\text{kg}\cdot\text{m}^{-3}$ ) is the density of water [26] at working temperature and pressure (it is considered as water, due to the low concentration of cellulose) and  $F_m$  is the mass flow ( $\text{kg}\cdot\text{s}^{-1}$ ).

$$\tau = \frac{V\rho}{F_m} \quad (1)$$

The conversion of cellulose was determined by equation 2.

$$X = \frac{W_0 - W}{W_0} \quad (2)$$

Where  $W_0$  is the inlet mass of cellulose to the reactor and  $W$  is the mass of cellulose after the hydrolysis. The carbon content of the liquid products was determined by total organic carbon analysis with Shimadzu TOC-VCSH equipment. The composition of the liquid products was determined using an HPLC. The HPLC column used for the separation of the compounds was SUGAR KS-802 Shodex at 80°C and a flow of 0.8 mL/min using water milli-q as the mobile phase. The selectivity ( $S_i$ ) of each compound was calculated according to equation 3.

$$S_i = \frac{C_{i,p}}{TC_{input}} 100 \quad (3)$$

Where  $C_{i,p}$  is the carbon of 'i' in the products,  $TC_{input}$  is the total carbon input. The selectivity of total sugars ( $S_{TS}$ ) was calculated with equation 4, using carbon balance taking into account all the degradation products ( $C_{dp}$ ).

$$S_{TS} = \frac{TC_{input} - C_{dp}}{TC_{input}} 100 \quad (4)$$

In order to validate our method of calculating sugar selectivity, the oligosaccharide concentration was determined by the enzymatic hydrolysis of the products. The sugar selectivity was calculated by using the concentration of the oligosaccharides, glucose, fructose and cellobiose. The enzymatic method is described as follows. One hundred  $\mu$ L of product solution were hydrolyzed with 100  $\mu$ L of  $\beta$ -glucosidase (2 U/mL) for 15 min at 40°C. After that, 3 mL of GOPOD reactant was added, and the sample was incubated at 40°C for 20 min. The glucose concentrations of the samples were measured by the spectrophotometer Hitachi U-2000 using glucose as a standard. The oligosaccharide concentration was measured, taking into account the initial glucose and cellobiose concentration of the solutions. The enzymatic determination differed by less than 5% with respect to the original determination for the experiments, except for one of them where the difference was 9%.

### 2.3. Experimental setup design

A sudden expansion micro-reactor (SEMR) was designed and built (Fig. 2). The reaction was started and stopped by sharp temperature changes, in order to avoid heating and cooling slopes that could lead to uncontrolled reactions. Heating was achieved by mixing the compressed room temperature suspension of cellulose with a stream of hot pressurized water in a "T" junction, in order to reach the target temperature of the reaction. Instantaneous cooling was achieved by sudden decompression using a high temperature valve. This cooling

method is more effective than the conventional heat transfer methods because the temperature change is instantaneous. After the decompression valve, a jacket cooler was set up in order to get the sample to room temperature.

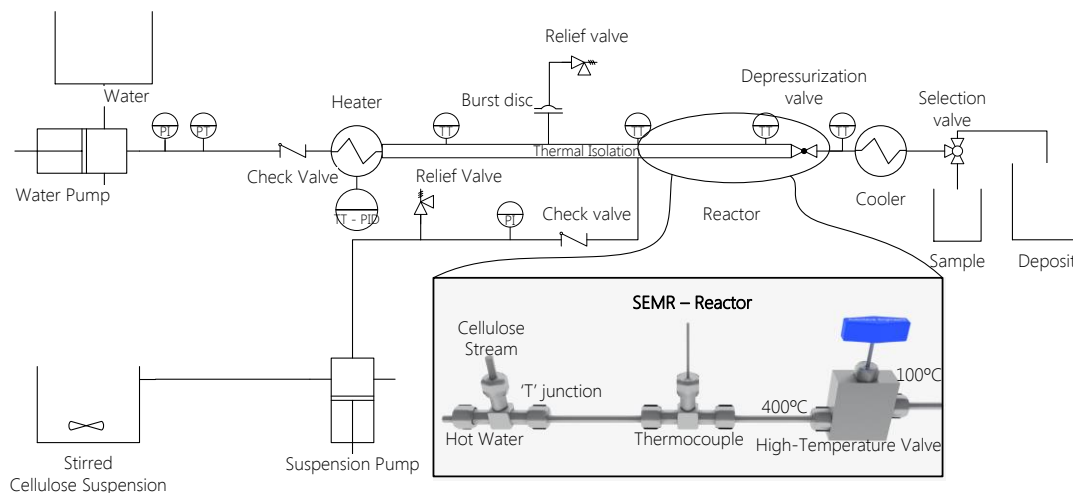


**Fig. 2.** Experimental setup. Schema of the pilot plant and Sudden Expansion Micro-Reactor (SEMR). Instantaneous heating of cellulose suspension is achieved by mixing with hot water. Instantaneous cooling from 400°C to 100°C is achieved by sudden decompression.

The cellulose-water suspension ( $7.5\% \text{ w}\cdot\text{w}^{-1}$ ) was continuously stirred during the experiments in order to obtain homogeneity. The suspension was fed to the reactor by a Gilson 305 pump at a flow rate of 17-24 mL/min. The rate of mixing was kept constant during the experiments in order to set the same inlet concentration of cellulose to the reactor ( $1.6\% \text{ w}\cdot\text{w}^{-1}$ ). The reactor used for the experiments comprises tubing of 1/4" and 1/16" of different lengths, depending on the residence times. The reactor was thermally isolated. The pressure of the system was controlled manually using the high temperature valve Autoclave Engineers 30VRMM4812. The pressure stability of the reactor is shown in Fig. 3. A schema of the SEMR is shown in Fig. 2. The short time needed to start and stop the reaction, along with the small reactor volume, made the micro-reactor isothermal, allowing a constant and homogenous reaction rate through the whole reactor. Another advantage of the reactor design is that reaction rates could be directly evaluated as a function of residence time, avoiding the use of the traditional severity factor [24]. Several experiments were performed to evaluate the selectivity of glucose and oligosaccharides as a function of reaction temperature and residence times. Different residence times were achieved by changing the inlet flow to the reactor, and the reactor volume. It was not possible to analyze all the residence times only by changing the inlet flow. Therefore, the reactor volume was changed using different reactors of various lengths and

diameters. The total inlet flows to the reactor varied from 3 kg/h to 6 kg/h. The reactor volumes varied from 50  $\mu\text{L}$  to 8 mL. The residence times ranged from 0.004 s to 5 s. The pressure in the reactor was fixed at 25 MPa for all the experiments.

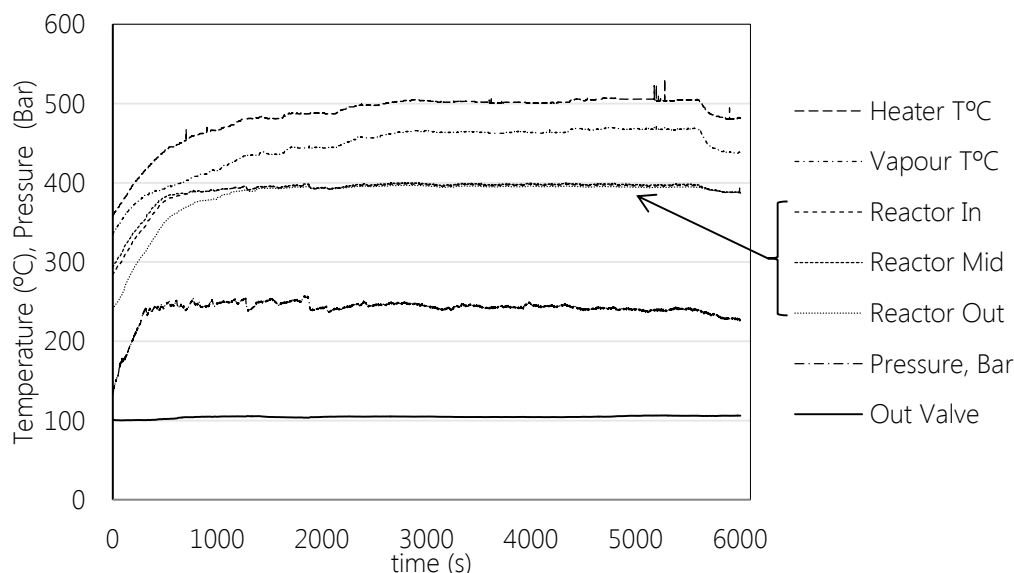


**Fig. 3.** Temperature and pressure profiles for an experiment at 400°C and 25 MPa. Heater T°C: temperature measured in the center of the Heater. Vapor T°C: temperature measured for inlet hot water. Reactor In: temperature measured 2 cm after the 'T' junction. Reactor Mid: temperature measured in the middle of the reactor. Reactor Out: temperature measured 2 cm before the high temperature valve. Out Valve: temperature measured after the high temperature valve. Pressure: pressure inside the reactor, Bar. The reactor length is 1 m and the reactor diameter is 0.0034 m.

### 3. Results and Discussion

Three sets of experiments were performed in the SEMR for reaction temperatures of 300°C, 350°C and 400°C. The typical temperature and pressure profile for an experiment is shown in Fig. 3. Figure 4A shows the selectivity of sugars for the three temperatures investigated. Total cellulose conversion was obtained at  $t_r=0.015$  s (vertical dotted line) and 1 s  $t_r$  (vertical dashed line) for temperatures of 400°C and 350°C respectively. At 300°C total cellulose conversion was not achieved in the investigated residence time range but it was estimated mathematically by determining the hydrolysis kinetic constant from the experimental data. Calculation predicted that total cellulose conversion at 300°C would be reached at  $t_r=16$  s (vertical dash-dotted line). Conversion curves for 400°C and 350°C show clear maxima, while the curve for 300°C did not reach a maximum at the latest time reported. For the data set corresponding to 300°C, the concentration of derived products in the final experiment was high; suggesting

that at the maximum selectivity would be in the range from 30 to 40% c.b. The highest selectivity of sugars in the SEMR was achieved for 400°C at  $t_r = 0.023$  s with a value of 98% c.b. The highest sugar selectivity values reported in literature for SCW cellulose hydrolysis, where the reaction was stopped by injecting cool water were lower than 65-77% c.b. [16]. Figure 4B shows the carbon balance for the data set of experiments at 400°C. The carbon balance was almost 100%, except in two cases which still reported high values of 96% and 95%. No char formation was observed at residence times lower than 1 s. Glucose production at 400°C reached its maximum at  $t_r$  between 0.03 s and 0.07 s. Total cellulose conversion happened at  $t_r = 0.015$  s. This indicates that the cellulose was hydrolyzed, producing oligosaccharides that became soluble oligomer and finally glucose.

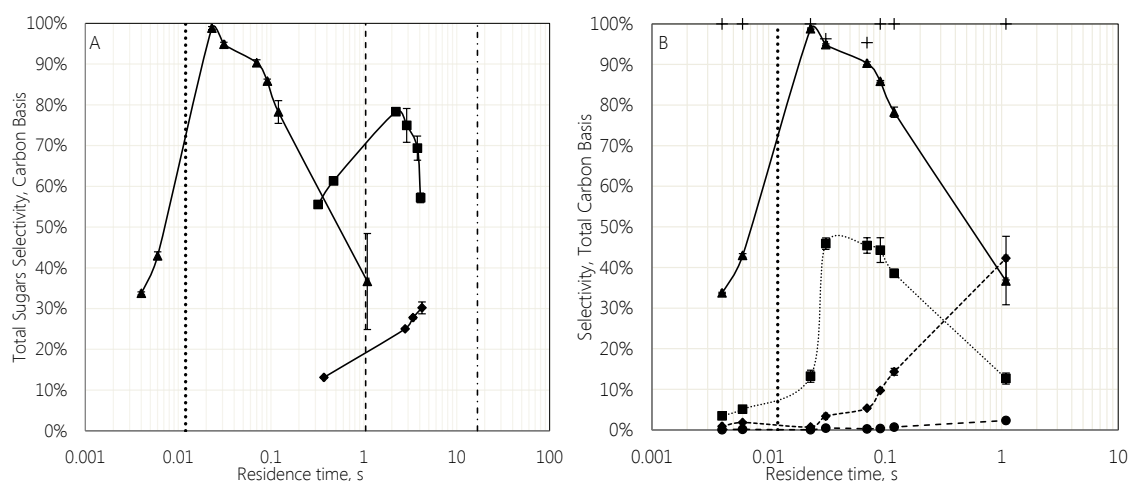


**Fig. 4.** Selectivity of the hydrolysis at different temperatures and residence times. A, selectivity of soluble oligosaccharides at: (◆) 300°C, (■) 350°C and (▲) 400°C depending on residence time. Dotted, dashed and dash-dotted vertical lines are the residence times for total conversion at 300°C, 350°C and 400°C respectively. B, selectivity at 400°C for: (▲) total soluble sugar, (■) glucose-fructose-cellobiose, (◆) pyruvaldehyde, (●) 5-hydroxy methyl furfural, (+) Carbon Balance. Cellulose concentration fed into the reactor is 1.6% w-w<sup>-1</sup> for these experiments. Error bars  $\pm$ (s.d.).

All the reactions involved in this process were shown to accelerate with an increase in temperature. Figure 4A shows that cellulose hydrolysis accelerates with increasing temperature (vertical lines). Above 375°C, the cellulose hydrolysis reaction accelerated more than was predicted by the Arrhenius parameters of the reaction for subcritical temperature. Under these conditions, Sasaki *et al.* [27] concluded that the hydrolysis would occur in a homogenous phase between water and cellulose, and that the mass transfer limitations would be avoided (Medium Effect 1). Glucose in hot pressurized water can follow two reaction paths: 1) degradation to glyceraldehyde, dihydroxyacetone and pyruvaldehyde via retro-aldol

condensation, or 2) dehydration to 5-HMF via fructose [28, 29]. With high water density and a large concentration of  $H^+$ , glucose can be degraded through ionic reactions (reaction path 1)[14, 30, 31]. These reactions might be disfavored in SCW medium due to the decrease in the ionic product of water, water density and dielectric constant (Medium Effect 2). For example, at 25MPa, water density is reduced from  $743 \text{ kg m}^{-3}$  to  $167 \text{ kg m}^{-3}$ ,  $K_w$  is reduced from  $10^{-11}$  to  $10^{-20}$ , and  $\epsilon$  is reduced from 21 to 2.4 when temperature is increased from 300°C to 400°C (See Fig. 1). On the other hand, glucose degradation through radical reactions (reaction path 2) [32] might be favored by the ability of SCW to generate free radicals (Medium Effect 3). The formation of free radicals is the initial stage of the radical reactions; this stage is the slowest one in this kind of reaction.

The higher values of the selectivity shown in Fig. 4A for 400°C, compared to those at 300°C and 350°C, also show that the rate of cellulose hydrolysis is increases faster than the rate of glucose degradation. That is consistent with the Medium Effects 1, 2 and 3. Between  $t_r$  0.015 s and 0.03 s, sugar selectivity was higher than 90% c.b. at 400°C. Therefore, in this interval of residence time, high concentrations of oligosaccharides and glucose can be obtained, with only a low degradation of the glucose formed. As explained above, glucose degradation in SCW may occur through radical reactions. The existence of this interval of residence time and the ability of the SEMR to rapidly stop the reaction allows the radical glucose degradation reaction to be stopped in the slow initiation stage, avoiding the fast propagation stage.

The composition of the products for different residence times at 400°C may be observed in Figure 5. The selectivity evolution of glucose, fructose and cellobiose are analogous along the residence time. An increase in residence time from 0.023 to 0.03s presents the advantage of an increase in glucose, fructose and cellobiose selectivity from 12 to 47% c.b., albeit at the expense of a decrease in sugar selectivity from 98 to 96% c.b. The quantity of 5-HMF remains lower than 0.4% c.b. up to  $t_r=0.1$  s. At residence times between 0.03 and 0.09 s the concentration of glucose, fructose and cellobiose remains almost constant, but the concentration of oligosaccharides is reduced, and the concentration of derived products such as pyruvaldehyde and organic acids is increased.

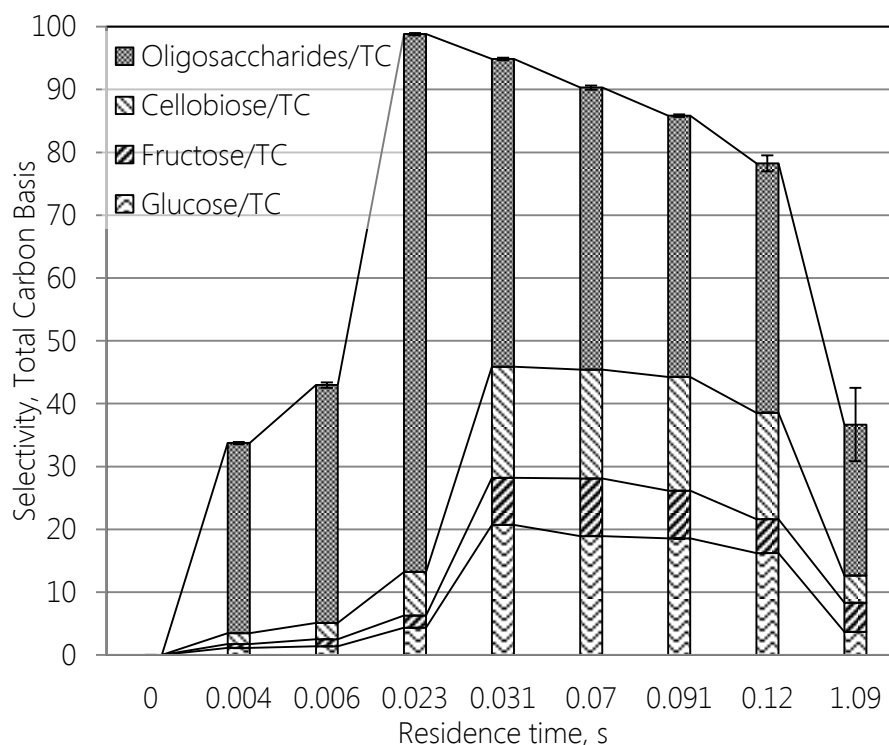


**Fig. 5.** Composition of the hydrolysis products. Fraction of Glucose (^), fructose (/), cellobiose (\) and oligosaccharides up to 6 glucose units (::) in the products at different residence times at 400°C. Error bars  $\pm$ (s.d.).

A comparison of the cellulose hydrolysis method developed in work and the processes discussed in section 1 is presented in table 1. The behavior of cellulose and glucose degradation kinetics found in this work is analogous to that presented by Sasaki *et al.*[16, 23]. Cellulose hydrolysis in supercritical water is a promising process, due to the fact that cellulose hydrolysis occurs faster than glucose degradation above the critical point [20]. This fact makes it possible to work in this field to improve the yields of glucose. This kinetic behavior, along with the development of the SEMR, makes it possible to work with short residence times and sugar yields of up to 98% c.b. This selectivity value is 21% higher than that reached by Sasaki *et al.* working with a residence time of 0.05s [16, 23]. The selectivity is increased by lowering the residence time while avoiding the degradation reactions of glucose.

The sugar concentration in the product stream depends on the inlet cellulose concentration. In this work, the sugar concentration in the products is about 17 g/L and the inlet cellulose concentration is 7.5% w-w<sup>-1</sup>. One way to increase the sugar concentration is by increasing the cellulose concentration in the feed. Another important point to take into account is the potential of the cooling system. In the cooling stage of the reaction, the pressure drop is 25 MPa with a temperature drop of 300°C. This kind of cooling generates 2 phases after the

reactor (vapor, with low sugar concentration and liquid, with high sugar concentration) which could be separated by installing a flash chamber after the decompression valve. Additionally, the generated vapor phase could be used for energy purposes.

**Table 1.** Comparison of hydrolysis methods for cellulose. Gl: glucose; fr: fructose; cello: cellobiose.

Method	Reactor	Temperature	Hydrolysis Time	Selectivity to sugars (%w-w <sup>-1</sup> )	Reference
Hydrothermal	Continuous	400°C	0.01 – 0.03 s	>96% 50%(gl+fr+cello)	This chapter
Hydrothermal	Continuous	400°C 350°C 320°C	0.01– 0.05 s 1 – 4 s 1 – 10 s	65-77% 27 – 50% 20 – 50%	[16]
Hydrothermal	Continuous	(400°C + 250°C)	30 s	66.8%	[17, 18]
	Batch	380°C	5 s	40%	
Hydrothermal	Batch	380°C	16 s	63% 36%(gl+fr+cello)	[33]
Hydrothermal + Catalyst	Batch Sulf. activated carbon	150°C	24 – 48 h pretreatment 24 h hydrolysis	20 – 39% (gl)	[25, 34]
Acid / Acid +Catalyst	Batch / Batch	150°C – 220°C / 120°C	10 h / 10 h	52% (gl) / 93% (gl)	[4]
Enzymatic	Batch	50°C	24 – 72 h	60% (gl)	[7]
Enzymatic + Tween-80	Batch Enzymes	50°C	22h	45% X≈0.45	[8]
Enzymatic + Pretreatment	Batch Acid pretreat. + TiO <sub>2</sub>	50°C	72 h pretreat. 48 h hydrolysis	92% (gl) X≈0.9	[9]
Acidic Ionic liquid	Batch Acid catalyst	170°C	3h	27% 21.6% (gl)	[11]
Ionic liquid	Batch	120°C	3.5h	25% X ≈0.5; 21% (HMF)	[12]
Ionic liquid	Batch	105°C - 130°C	3h	99% (cello+glu)	[13]

The activation energy of the cellulose hydrolysis reaction in supercritical water is 547.9 kJ/mol.[27] This value is one order of magnitude higher than the activation energy of cellulose hydrolysis with enzymes or acid catalyst (50 – 90 kJ/mol) [4], and this is why higher temperatures are required. However, the hydrolysis of cellulose in supercritical water is completed in residence times 6 or 7 orders of magnitude lower than in the enzymatic and acid catalyst methods. This short residence time can reduce the size of the facility and the energy requirements significantly.

Many studies in literature evaluate the fractionation of biomass for obtaining cellulose,

hemi-cellulose and lignin in semi-continuous processes using hot pressurized water as a solvent [35]. The cellulose fraction of the biomass could be hydrolyzed with the method proposed in this work for obtaining glucose from biomass. The integration of the fractionation and hydrolysis processes would be an interesting study in obtaining sugars from biomass in a one step process.

The procedure proposed here was developed for cellulose hydrolysis, but it could be extended to other processes where ionic and radical reactions are involved. For example, in the gasification processes, where the target reactions for avoiding undesired products are radical reactions [31]. The instantaneous heating and cooling method set out in this work offers a solution for immediately creating the media conditions that favor radical reactions, thus minimizing the ionic reactions and leading to a more selective gasification process.

#### 4. Conclusions

This work proves that the hydrolysis of cellulose to glucose and oligomers of glucose can be performed in residence times between 0.02 – 0.03 s in SCW with high selectivity of sugars (up to 98%). The keys to reducing the production of derived products when SCW is the reaction medium are: (a) effective control of the residence time, in order to stop the reaction after the total hydrolysis of cellulose and before the glucose degradation reactions; and (b) setting the conditions of the media to favor the hydrolysis reactions and disfavor the degradation reactions. Reducing the residence time from minutes to milliseconds allows for a reactor volume reduction from  $\text{m}^3$  to  $\text{cm}^3$ .

## References

1. Ragauskas, A.J., Williams, C.K., Davison, B.H., Britovsek, G., Cairney, J., Eckert, C.A., Frederick, W.J., Hallett, J.P., Leak, D.J., Liotta, C.L., Mielenz, J.R., Murphy, R., Templer, R., and Tschaplinski, T., *The Path Forward for Biofuels and Biomaterials*. Science, 2006. 311(5760): p. 484 -489.
2. Klemm, D., Heublein, B., Fink, H.P., and Bohn, A., *Cellulose: Fascinating Biopolymer and Sustainable Raw Material*. Angewandte Chemie International Edition, 2005. 44(22): p. 3358-3393.
3. Bobleter, O., *Hydrothermal degradation of polymers derived from plants*. Progress in polymer science, 1994. 19(5): p. 797-841.
4. Shuai, L. and Pan, X., *Hydrolysis of cellulose by cellulase-mimetic solid catalyst* Energy & Environmental Science, 2012.
5. Dora, S., Bhaskar, T., Singh, R., Naik, D.V., and Adhikari, D.K., *Effective catalytic conversion of cellulose into high yields of methyl glucosides over sulfonated carbon based catalyst*. Bioresource Technology, 2012. 120(0): p. 318-321.
6. Guo, F., Fang, Z., Xu, C.C., and Smith Jr, R.L., *Solid acid mediated hydrolysis of biomass for producing biofuels*. Progress in Energy and Combustion Science, 2012. 38(5): p. 672-690.
7. Wyman, C.E., Dale, B.E., Elander, R.T., Holtzapple, M., Ladisch, M.R., and Lee, Y.Y., *Comparative sugar recovery data from laboratory scale application of leading pretreatment technologies to corn stover*. Bioresource Technology, 2005. 96(18): p. 2026-2032.
8. Yang, M., Zhang, A., Liu, B., Li, W., and Xing, J., *Improvement of cellulose conversion caused by the protection of Tween-80 on the adsorbed cellulase*. Biochemical Engineering Journal, 2011. 56(3): p. 125-129.
9. Abushammala, H. and Hashaikh, R., *Enzymatic hydrolysis of cellulose and the use of TiO<sub>2</sub> nanoparticles to open up the cellulose structure*. Biomass and Bioenergy, 2011. 35(9): p. 3970-3975.
10. Khodaverdi, M., Jeihanipour, A., Karimi, K., and Taherzadeh, M., *Kinetic modeling of rapid enzymatic hydrolysis of crystalline cellulose after pretreatment by NMMO*. Journal of Industrial Microbiology & Biotechnology, 2012. 39(3): p. 429-438.

11. Amarasekara, A.S. and Wiredu, B., *Degradation of Cellulose in Dilute Aqueous Solutions of Acidic Ionic Liquid 1-(1-Propylsulfonic)-3-methylimidazolium Chloride, and p-Toluenesulfonic Acid at Moderate Temperatures and Pressures*. Ind. Eng. Chem. Res., 2011. 50(21): p. 12276-12280.
12. Hsu, W.-H., Lee, Y.-Y., Peng, W.-H., and Wu, K.C.W., *Cellulosic conversion in ionic liquids (ILs): Effects of H<sub>2</sub>O/cellulose molar ratios, temperatures, times, and different ILs on the production of monosaccharides and 5-hydroxymethylfurfural (HMF)*. Catalysis Today, 2011. 174(1): p. 65-69.
13. Morales-delaRosa, S., Campos-Martin, J.M., and Fierro, J.L.G., *High glucose yields from the hydrolysis of cellulose dissolved in ionic liquids*. Chemical Engineering Journal, 2012. 181-182: p. 538-541.
14. Akiya, N. and Savage, P.E., *Roles of Water for Chemical Reactions in High-Temperature Water*. Chemical Reviews, 2002. 102(8): p. 2725-2750.
15. Arai, K., Smith Jr, R.L., and Aida, T.M., *Decentralized chemical processes with supercritical fluid technology for sustainable society*. The Journal of Supercritical Fluids, 2009. 47(3): p. 628-636.
16. Sasaki, M., Fang, Z., Fukushima, Y., Adschiri, T., and Arai, K., *Dissolution and Hydrolysis of Cellulose in Subcritical and Supercritical Water*. Industrial & Engineering Chemistry Research, 2000. 39(8): p. 2883-2890.
17. Ehara, K. and Saka, S., *A comparative study on chemical conversion of cellulose between the batch-type and flow-type systems in supercritical water*. Cellulose, 2002. 9(3): p. 301-311.
18. Ehara, K. and Saka, S., *Decomposition behavior of cellulose in supercritical water, subcritical water, and their combined treatments*. Journal of Wood Science, 2005. 51(2): p. 148-153.
19. Zhao, Y., Lu, W.-J., Wang, H.-T., and Li, D., *Combined Supercritical and Subcritical Process for Cellulose Hydrolysis to Fermentable Hexoses*. Environmental Science Technology, 2009. 43(5): p. 1565-1570.
20. Peterson, A.A., Vogel, F., Lachance, R.P., Fröling, M., Michael J. Antal, Jr., and Tester, J.W., *Thermochemical biofuel production in hydrothermal media: A review of sub- and supercritical water technologies*. Energy & Environmental Science, 2008. 1(1): p. 32-65.

21. Marshall, W.L. and Franck, E.U., *Ion Product of Water Substance, 0-1000°C, 1-10,000 Bars. New International Formulation and Its Background*. Journal of Physical and Chemical Reference Data, 1981. 10(2): p. 295-304.
22. Uematsu, M. and Franck, E.U., *Static Dielectric Constant of Water and Steam*. Journal of Physical and Chemical Reference Data, 1980. 9(4): p. 1291-1306.
23. Sasaki, M., Kabyemela, B., Malaluan, R., Hirose, S., Takeda, N., Adschiri, T., and Arai, K., *Cellulose hydrolysis in subcritical and supercritical water*. The Journal of Supercritical Fluids, 1998. 13(1-3): p. 261-268.
24. Rogalinski, T., Ingram, T., and Brunner, G., *Hydrolysis of lignocellulosic biomass in water under elevated temperatures and pressures*. The Journal of Supercritical Fluids, 2008. 47(1): p. 54-63.
25. Fang, Z., Zhang, F., Zeng, H.-Y., and Guo, F., *Production of glucose by hydrolysis of cellulose at 423 K in the presence of activated hydrotalcite nanoparticles*. Bioresource Technology, 2011. 102(17): p. 8017-8021.
26. Wagner, W, Cooper, J, R., Dittmann, et al., *The IAPWS industrial formulation 1997 for the thermodynamic properties of water and steam*. 2000, American Society of Mechanical Engineers: New York, N, ETATS-UNIS.
27. Sasaki, M., Adschiri, T., and Arai, K., *Kinetics of cellulose conversion at 25 MPa in sub- and supercritical water*. AIChE Journal, 2004. 50(1): p. 192-202.
28. Sasaki, M., Goto, K., Tajima, K., Adschiri, T., and Arai, K., *Rapid and selective retro-aldol condensation of glucose to glycolaldehyde in supercritical water*. Green Chem., 2002. 4(3): p. 285-287.
29. Holm, M.S., Saravanamurugan, S., and Taarning, E., *Conversion of Sugars to Lactic Acid Derivatives Using Heterogeneous Zeotype Catalysts*. Science, 2010. 328(5978): p. 602 -605.
30. Aida, T.M., Sato, Y., Watanabe, M., Tajima, K., Nonaka, T., Hattori, H., and Arai, K., *Dehydration of D-glucose in high temperature water at pressures up to 80 MPa*. The Journal of Supercritical Fluids, 2007. 40(3): p. 381-388.
31. Kruse, A. and Gawlik, A., *Biomass Conversion in Water at 330–410 °C and 30–50 MPa. Identification of Key Compounds for Indicating Different Chemical Reaction Pathways*. Industrial & Engineering Chemistry Research, 2002. 42(2): p. 267-279.

32. Promdej, C. and Matsumura, Y., *Temperature Effect on Hydrothermal Decomposition of Glucose in Sub- And Supercritical Water*. Industrial & Engineering Chemistry Research, 2011. 50(14): p. 8492-8497.
33. Zhao, Y., Lu, W.-J., and Wang, H.-T., *Supercritical hydrolysis of cellulose for oligosaccharide production in combined technology*. Chemical Engineering Journal, 2009. 150(2-3): p. 411-417.
34. Onda, A., Ochi, T., and Yanagisawa, K., *Hydrolysis of Cellulose Selectively into Glucose Over Sulfonated Activated-Carbon Catalyst Under Hydrothermal Conditions*. Topics in Catalysis, 2009. 52: p. 801-807.
35. Sasaki, M., Adschiri, T., and Arai, K., *Fractionation of sugarcane bagasse by hydrothermal treatment*. Bioresource Technology, 2003. 86(3): p. 301-304.



# Chapter 2. Kinetics analysis of cellulose depolymerization reactions in near critical water

## Abstract

In this work, a kinetic analysis of cellulose depolymerization in hot pressurized water is presented. An experimental facility that works with temperatures up to 400°C, pressures of up to 25 MPa and residence times of between 0.004s and 10s was used for the experimental study. A mathematical model was developed in order to predict the evolution of the cellulose concentration and its derivatives. To do so, a reaction scheme was proposed, and kinetics parameters currently unavailable in literature were adjusted, using the experimental data obtained in this work. The kinetics for cellulose hydrolysis showed a change around the critical point of water, the activation energy being  $154.4 \pm 9.5$  kJ/mol and  $430.3 \pm 6.3$  kJ/mol below and above the critical point, respectively. The activation energy for oligosaccharide hydrolysis was  $135.2 \pm 9.2$  kJ/mol and  $111.5 \pm 9.1$  kJ/mol for the glucose to fructose reaction. The kinetics of 5-hydroxyl-methyl-furfural formation showed a drastic change at 330°C. The activation energy for 5-HMF formation is  $285 \pm 34$  kJ/mol and  $-61.3 \pm 15.7$  kJ/mol at temperatures below and above 330°C respectively. Above 330°C the low density and ionic product of the medium would disfavor the 5-HMF formation.

**Keywords:** Biorefinery • Hydrothermal medium • Supercritical water •  
Cellulose Hydrolysis kinetics • 5-HMF



## 1. Introduction

Biomass unfit for human consumption is a viable alternative as a renewable source of chemicals and energy. Cellulose is one of the principal components of this biomass. In order to reach an appropriate sustainability level, new policies have been initiated to promote the use of renewable energy and the rational use of raw materials. This environmental philosophy imposes substantial changes in production, moving from centralized large scale plants to decentralized plants on a scale according to the biomass availability in each neighborhood [1]. To fit this new conception, the development of energy efficient processes using renewable raw materials is highly necessary.

The main goals for achieving a decentralized production may be the reduction of the equipment cost and the development of environmental friendly processes. The reduction in equipment cost can be achieved by using compact apparatus, simplified production steps and reactions in one step. These kinds of processes can be achieved by using ultra-fast processes with high yield and selectivity from alternative raw materials. The environmental compatibility can be achieved using 'green solvents' like water or carbon dioxide.

The supercritical fluids are a promising media for obtaining biofuels and useful chemicals from biomass. Supercritical water (SCW) presents a low dielectric constants and few, weak hydrogen bonds, making it a good solvent for organic components [2]. The properties of water may vary considerably when changing the conditions from subcritical to supercritical. Just by changing pressure and temperature, the identity of the medium may be altered to favor different kinds of reactions. Pressurized water (e.g. 25 MPa) has a density of between  $800 \text{ kg/m}^3$  and  $1000 \text{ kg/m}^3$  and an ionic product between 11 and 14; at temperatures below  $300^\circ\text{C}$ . In these conditions, the media may favor ionic reactions, and reactions favored by high densities [2-4]. If the temperature is increased up to  $400^\circ\text{C}$ , the density is almost  $150 \text{ kg/m}^3$  and the ionic product is near 21. Under these conditions, the media favors radical reactions [5], but the reactions enhanced by high densities will be disfavored.

In literature, the hydrolysis and processing of biomass in hot pressurized water for the production of glucose and its derivatives has been analyzed [1-3, 6-9]. Water at temperatures between  $327^\circ\text{C}$  and  $387^\circ\text{C}$  was used to separate cellulose from lignin[10]. Under these conditions, secondary components were degraded and cellulose with a high purity (89.5 to 100%) was obtained with residence times in the reactor between 0.35 s and 0.5 s. Cellulose

hydrolysis was completed in pressurized water at subcritical temperatures, obtaining a high concentration of glucose and oligosaccharides. Nevertheless, the reaction presented a low selectivity, and indicated the need for bigger reactors and higher residence times than those achieved at higher temperatures. Rogalinski et al. [11] analyzed the cellulose hydrolysis between 240°C and 310°C obtaining Arrhenius parameters of  $\ln A = 32$  (pre-exponential factor) and  $E_a = 163.9$  kJ/mol (activation energy). The influence of the  $\text{CO}_2$  catalysis was analyzed using a temperature range of 240 – 280°C. It was observed that the use of  $\text{CO}_2$  as a catalyst enhanced the reaction rate of cellulose hydrolysis at subcritical temperatures. At temperatures above 260°C the catalysis effect is negligible [12]. Cellulose hydrolysis in Supercritical Water (SCW) was investigated, reporting 100% conversions at 400°C and 25 MPa with 0.5 s of residence time [13]. Up to 370°C the activation energy and pre-exponential factor of cellulose hydrolysis were found to be 145.9 kJ/mol and 27.4 respectively. At temperatures higher than 370°C the reaction rate of cellulose hydrolysis was found to increase; the activation energy and pre-exponential factor being 547.9 and 102.7 respectively [9]. The change in the properties of the medium around the critical point of water is expected to modify the mechanism of the hydrolysis and thus increase the reaction rate. The authors explained that near critical water would be able to swell or dissolve the cellulose, since the hydrolysis reaction took place in an homogeneous phase [9].

The objective of the present work is to identify the kinetic pathway of cellulose hydrolysis, and its intermediate production and decomposition reactions in both, sub and supercritical water media, as well as adjusting the kinetic parameters of these reactions. To do so, a novel facility was designed and built for the study of cellulose hydrolysis. A mathematical model of an isothermal tubular reactor was developed. The kinetic reaction parameters of cellulose hydrolysis, oligosaccharides degradation, glucose to fructose reaction and 5-hydroxymethylfurfural (5-HMF) production were fitted.

## **2. Material and Methods**

### **2.1. Materials**

The cellulose used in the experiments was micro-crystalline cellulose with a particle size between 20 – 130  $\mu\text{M}$ , purchased from VWR chemical company. Distilled water was used in the experiments. The reagents used in HPLC (High Performance Liquid Chromatography) analysis were: cellobiose (+98%), glucose (+99%), fructose (+99%), glyceraldehyde (95%),

pyruvaldehyde (40%), erythrose (+75%), 5-hydroxymethylfurfural (99%) purchased from Sigma.

## 2.2. Analysis

The solids in the products were separated by centrifugation and filtration, and dried at 60°C for 24 hours. The conversion of cellulose (X) was determined by equation 1, where 'W<sub>0</sub>' is the concentration of cellulose at the inlet of the reactor and 'W' is the concentration of cellulose after the hydrolysis, at the outlet of the reactor.

$$X = \frac{W_0 - W}{W_0} \quad (1)$$

The carbon content of the liquid products was determined by total organic carbon (TOC) analysis with Shimadzu TOC-VCSH equipment. The composition of the liquid products was determined with an HPLC. The HPLC column used for the separation of the compounds was SUGAR KS-802 Shodex at 80°C and a flow of 0.8mL/min using water milli-Q as mobile phase. A Waters IR detector 2414 was used to identify the sugars and their derivatives.

## 2.3. Pilot Plant Concept

To analyze the kinetics of cellulose hydrolysis, it is necessary to know the residence times of the reactions with accuracy, that is, to know when the reaction starts and ends. At temperatures higher than 350°C, the hydrothermal reactions are extremely fast, so heating and cooling ramps can lead to inaccurate results. In order to avoid this problem, instantaneous heating and cooling systems were designed and installed. A schematic diagram of the experimental setup is shown in Fig. 1.

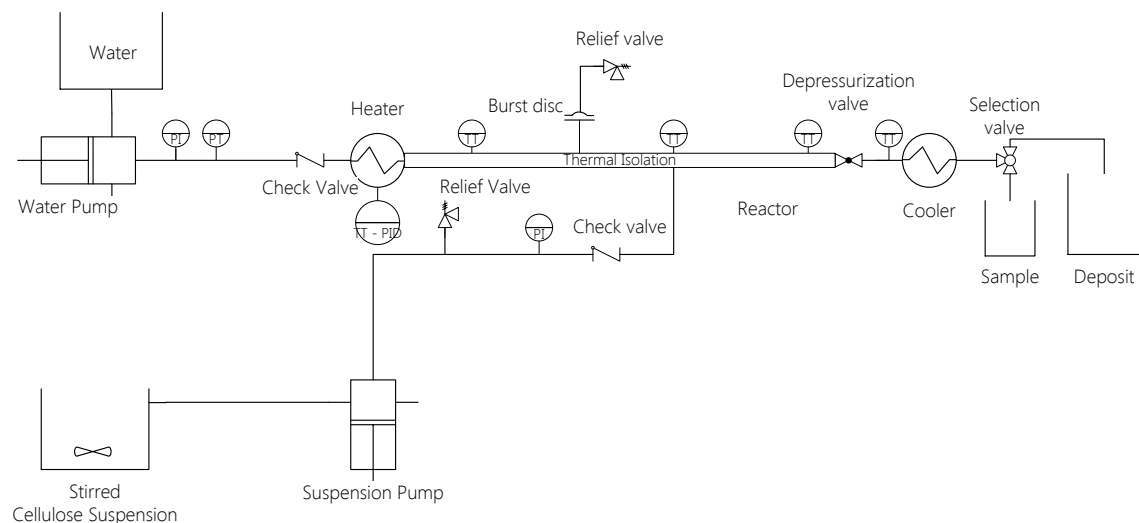


Fig. 1. Plan of the experimental setup.

A cellulose-water suspension ( $7.5\% \text{ w}\cdot\text{w}^{-1}$ ) was continuously stirred during the experiments in order to ensure the homogeneity of the slurry. The cellulose suspension was fed into the reactor by a HPLC pump with a maximum flow rate of  $1.5 \text{ kg/h}$ . The heating of the process was achieved by the injection of supercritical water into a tee junction working as the reactor's inlet. This stream was generated by an electric heater which provided adjustable power of up to  $10\text{kW}$ , in order to control the temperature of the stream. Supercritical water was supplied up to a maximum flow rate of  $5 \text{ kg/h}$ . A plan of the reactor is shown in Fig. 2. The disposition of the streams in the tee junction (hot water / cellulose slurry) was set according to the best arrangement in terms of mixing efficiency [14, 15]. Cellulose concentration at the inlet of the reactor was  $1.5\% \text{ w}\cdot\text{w}^{-1}$  due to the dilution in the heating. The different temperatures in each experiment were achieved by mixing the slurry stream with streams of supercritical water at different temperatures. The reactors used for the experiments were Ni-alloy tubing of  $1/4$  inches and  $1/16$  inches in diameter.

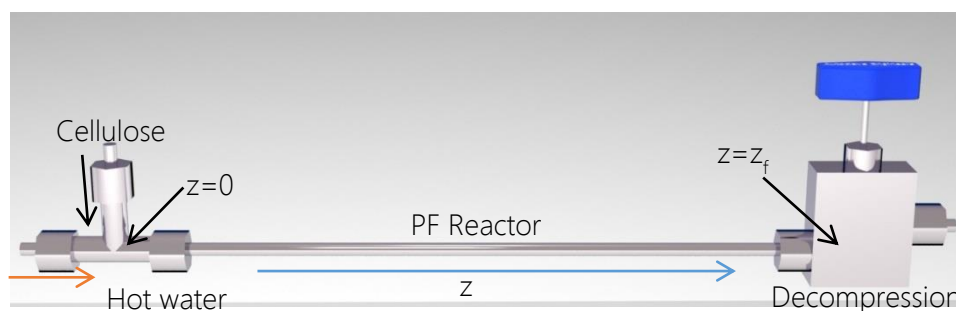


Fig. 2. Plan of the reactor.

The cooling method is an important part of the process, because it is the mechanism used to stop the reactions. In order to avoid uncontrolled reactions, instantaneous cooling by sudden decompression was set up after the reactor stage. The high temperature valve Autoclave Engineers 30VRMM4812 was used to carry out the decompression. With this isenthalpic expansion, the temperature was lowered down to  $100 \pm 10^\circ\text{C}$ . It can be considered that at  $100^\circ\text{C}$  the reactions of cellulose degradation are stopped. After the valve stage, a jacket cooler was set up to get the sample to room temperature. The described system is capable of instantaneously cooling the products, while simultaneously avoiding their dilution of the products, which would occur if they were cooled down by quenching.

The kinetics of cellulose hydrolysis and glucose decomposition are highly influenced by temperature. The residence times necessary for completing the reaction ranged from  $16 \text{ s}$  at  $300^\circ\text{C}$  to  $0.015 \text{ s}$  at  $400^\circ\text{C}$ . Therefore a wide range of residence times ( $t_R$ ) should be reached

in order to analyze the reactions at subcritical and supercritical water. Just by varying the flow in a single reactor, it is not possible to achieve residence times between 0.004 s and 30 s. Hence, both, the length of the reactor and the flow of the pumps were varied in order to obtain residence times in the whole range. The reactor length varied from 0.1 – 6 meters. In order to avoid heat losses and keep a constant temperature throughout the reactor, all the hot elements of the facility were thermally isolated using rock-wool. The residence times in the reactor were calculated as the ratio of reactor volume / volumetric flow in the reactor. The volume of the reactor was calculated using the dimensions of the reactor (diameter, length) and the flow was calculated using the mass flow and the density in the reactor considering the fluid as pure water, at the measured temperature and pressure [16]. As mentioned above, rapid heating and cooling systems were used at the beginning and at the end of the reactor stage, respectively. Since the reactor was thermally isolated it can be considered that the temperature along it was constant. Therefore, the density can be considered constant and  $t_R$  can be calculated by equation 2.

$$t_R = \frac{V}{F_v} = \frac{\pi D^2}{4} L \frac{\rho_h}{F_{v,0} \rho_0} \quad (2)$$

Where 'V' is the reactor volume in m<sup>3</sup>, 'F<sub>v</sub>' is the volumetric flow occurring at reaction temperature and pressure, measured in m<sup>3</sup>s<sup>-1</sup>, 'D' is the reactor diameter in m, 'L' is the reactor length, measured in m, 'ρ<sub>h</sub>' is the density of the medium at the reaction temperature and pressure, measured in kg m<sup>-3</sup>, 'F<sub>v,0</sub>' is the volumetric flow at room temperature, measured in m<sup>3</sup>s<sup>-1</sup>, 'ρ<sub>0</sub>' is the density of the medium at room temperature, measured in kg m<sup>-3</sup>.

The conditions experimented in this work are resumed in table 1. Reynolds number (Re) and the volumetric concentration (C<sub>v</sub>) of the cellulose particles were calculated in order to analyze the flow regime in the reactor. The Re was between 7600 and 120000. The volumetric concentration of cellulose particles is lower than 0.8%. The low particle concentration along with the turbulent flow regime in the reactor (Re>7600) would make a homogeneous particle distribution. This supposition will be corroborated in section 4, where different samples of one experimental condition are analyzed.

**Table 1.** Experimental conditions investigated in this work. Volumetric concentration of the cellulose particles in the reactor and; Reynolds number developed in the reactor.

Conditions	Temperature	Reactor Diameter	Density	Reynolds Number	$\rho_{\text{fluid}} / \rho_{\text{particle}}$	Particle Concentration
	°C	m	kg/m <sup>3</sup>			% volume
Slurry	40		1002.9		0.67	1.01
A	400	0.0007	166.5	121237	0.11	0.17
B	400	0.0032	166.5	26520	0.11	0.17
C	375	0.0032	505.6	13280	0.34	0.51
D	350	0.0032	625.5	10632	0.42	0.63
E	325	0.0032	692.4	9368	0.46	0.70
F	300	0.0032	743.0	8442	0.50	0.75
G	275	0.0032	784.8	7655	0.52	0.79

## 2.4. Operation Procedure

The electrical heater was turned on before starting the experiment in order to achieve the target temperature. After that, the water pumping of water was started and the flow was kept constant until the reactor reached the reaction temperature. The pressure of the system was set manually by tightening and loosening the high temperature decompression valve. Before pumping the cellulose suspension, the pressure was set at a fixed value to ensure the liquid or supercritical phase. The cellulose suspension was heated to 40°C and stirred before the experiment to ensure the homogeneity of the suspension. Pumping of the cellulose suspension was started when the reactor reached the desired temperature. When cellulose pumping was stable, the temperature and pressure were adjusted to the target values. The first sample was taken 30 minutes after the steady state was achieved. For each experiment, at least 3 samples were taken every 30 minutes. When the experiment had finished, the cellulose feed was replaced by distilled water and the heater was turned off. In order to clean the pilot plant, water was pumped through continuously until clear water was obtained in the sampling pipe. Once clear water was obtained and the pipes were cooled, acetone was pumped through, in order to dissolve the non-polar compounds than might be present in the

system. Acetone was pumped through until clear acetone was obtained in the sample pipe. When the pilot plant was clean, the pumps were turned off.

### 3. Model

A mathematical model was developed in order to predict the concentration profiles of cellulose depolymerization products in hot pressurized water as a function of the residence time and reaction temperature. The model was performed to describe the results of the experimental device. Thus, the model reproduces an isothermal tubular reactor, considering plug flow in steady state. In Fig. 2 a plan of the reactor is shown. The heating is achieved instantaneously by supercritical water injection. The cooling is reached by sudden decompression at the end of the reactor. The diameters of the reactor are 6.35 mm (1/4") in outer diameter and 1.57 mm in thickness. The model was solved along the reactor length.

It is considered that the cellulose instantaneously reaches the reaction temperature when it mixes with hot water at the inlet of the reactor. The inlet concentration of cellulose for the model was the same that obtained in the experimental device; 1.5 % w-w<sup>-1</sup>. Due to the low cellulose concentration at the inlet of the reactor, the properties of the mixture were estimated as those of pure water at the same pressure and temperature [16]. In order to know the progress of the reactions through the reactor, a group of differential equations was solved for creation/disappearance of each component. These equations are solved using the function *ode45* of Matlab®. The reaction simulations were conducted at: 275°C, 300°C, 325°C, 350°C, 375°C and 400°C. The pressure of the system was fixed at 25 MPa.

The reaction rate of cellulose hydrolysis was analyzed considering a superficial consumption of the grain of cellulose, in the same way as Sasaki *et al* 2004. Equation 2 represents the conversion of cellulose at different residence times.

$$\frac{dx}{dt} = 2k(1-x)^{1/2} \quad (3)$$

Where 'x' is the conversion, 't' is the time (s) and 'k' is the kinetic constant of cellulose hydrolysis (s<sup>-1</sup>). An equation that relates the conversion with the reactor length ( $dx/dz$ ) is needed to solve the model. The residence time can be represented as function of volume and volumetric flow as it is shown in equation 4.

$$dt = \frac{dV}{Q_v} = \frac{Sdz}{\frac{\dot{M}}{\rho}} \quad (4)$$

Where 'V' is the volume of the reactor (m<sup>3</sup>), 'Q<sub>v</sub>' is the volumetric flow (m<sup>3</sup>/s), 'S' is the cross-sectional area (m<sup>2</sup>), 'z' is the length of the reactor (m), 'M' is the mass flow (kg/s) and 'ρ' is density (kg/m<sup>3</sup>) of water in the reactor. Combining equation 3 and 4, equation 5 is obtained.

$$\frac{dx}{dz} = \frac{\rho S}{\dot{M}} 2k(1-x)^{1/2} \quad (5)$$

The reaction pathway of cellulose depolymerization shown in Fig. 3 was proposed according to literature [9, 17-19]. The system of equations that represents the cellulose reactions in pressurized water was developed following the reaction pathway shown in Fig. 3 and the kinetic reaction constants presented in table 2. The reaction pathway shown in Fig. 3 can be divided into three main steps: 1<sup>st</sup> step in which cellulose is hydrolyzed to oligosaccharides; 2<sup>nd</sup> step in which the saccharides are hydrolyzed to glucose and; 3<sup>rd</sup> step in which glucose is degraded. The products of cellulose hydrolysis, in the first step, are oligosaccharides and small saccharides like cellobiose. The model considers separately the fraction of cellulose that is hydrolyzed to oligosaccharides (F) and the fraction that is hydrolyzed to cellobiose (1-F). Equation 6 represents the concentration of oligosaccharides (n<sub>2</sub>) along the reactor.

$$\frac{dn_2}{dz} = \frac{\rho S}{\dot{M}} \left[ FM_c 2k(1-x)^{1/2} - k_{og}n_2 \right] \quad (6)$$

Where 'M<sub>c</sub>' is the cellulose flow in the reactor, 'k<sub>og</sub>' is the kinetic constant of oligosaccharide hydrolysis. In the reaction of hydrolysis, a molecule of H<sub>2</sub>O is added to the glucose units per cleavage bond, thus the total mass of glucose is increased. A mass correction is needed to calculate the production of cellobiose. This correction can be calculated as a fraction of carbon in each molecule as is described in equation 7.

$$\phi = \frac{\varphi_{cellulose}}{\varphi_{cellobiose}} = \frac{\frac{CW_{cellulose}}{MW_{cellulose}}}{\frac{CW_{cellobiose}}{MW_{cellobiose}}} = 1.055 \quad (7)$$

Where 'CW<sub>cellulose</sub>' is the mass of carbon per unit of cellulose; 'MW<sub>cellulose</sub>' is the molecular weight per unit of cellulose; 'CW<sub>cellobiose</sub>' is the mass of carbon per molecule of cellobiose and 'MW<sub>cellobiose</sub>' is the molecular weight of cellobiose. Thus, the cellobiose (n<sub>3</sub>) molar flow [mol/h] is calculated by equation 8.

$$\frac{dn_3}{dz} = \frac{\rho S}{M} \left[ \frac{(1-F)\phi M_c}{MW_{cello}} 2k(1-x)^{1/2} - (k_1 + k_2 + k_h)n_3 \right] \quad (8)$$

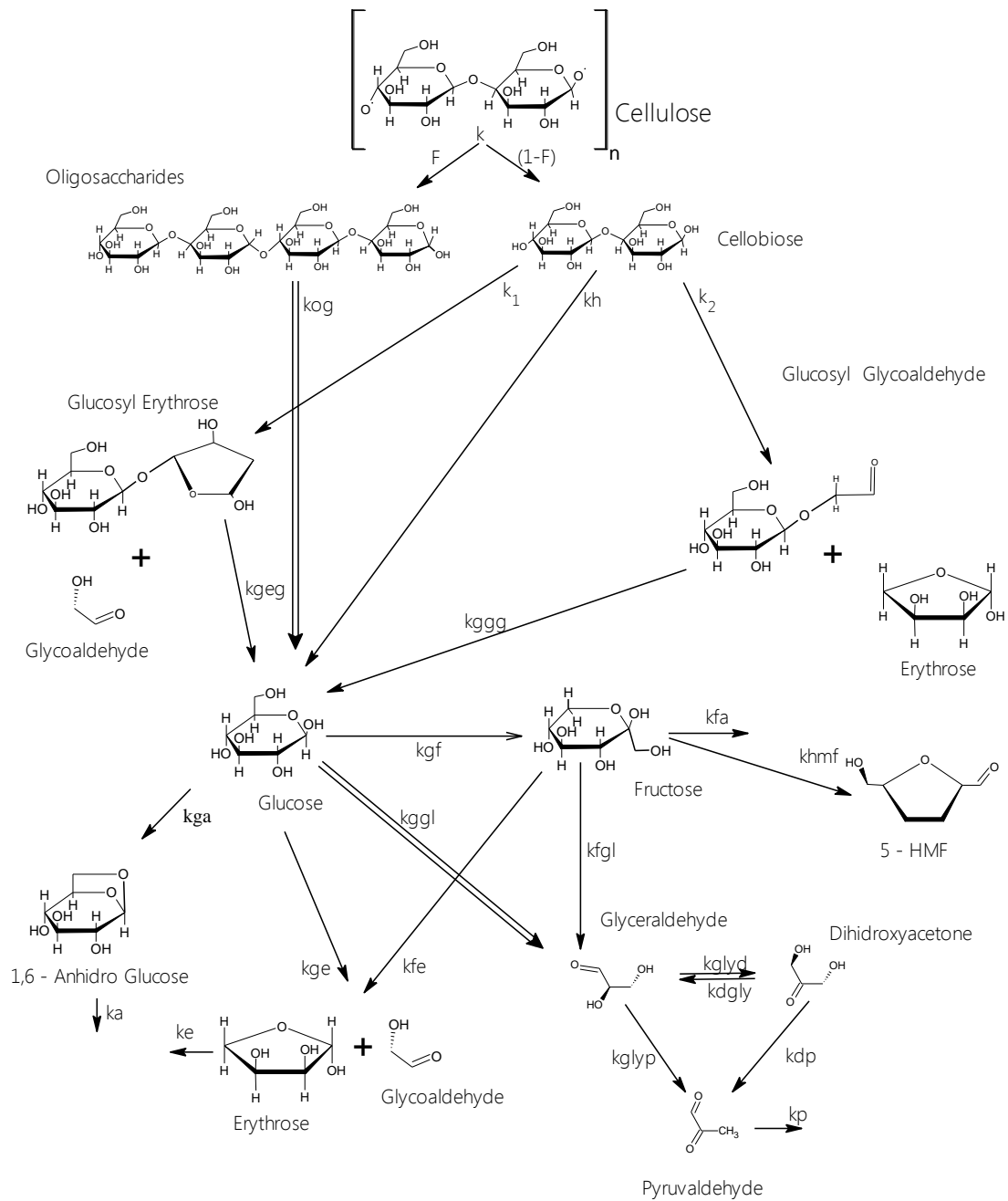


**Fig. 3.** Reaction rate pathway for cellulose hydrolysis and glucose reactions in hot pressurized water [9, 17-19].

The double arrow is not a different reaction, it was drawn double in order to avoid confusion with the other reaction steps.

**Table 2.** Arrhenius parameters for the reaction of cellulose hydrolysis and degradation in hot pressurized water.

Kinetic Constants, Reference	Ea (kJ/mol)	Ln A	Observation	Symbol
Cellulose Hydrolysis, [9]	145.9	27.4	T (320-370)	k
	547.9	102.7	T (370-400)	k
Cellobiose Hydrolysis, [19]	66.89	10.34		k1
	69.3	11.27		k2
	108.6	21.09		kh
	106.1	19.71		kgeg
	110.5	18.74		kggg
Glucose → Fructose, [18]	112.69	21.81		kgf
Glucose → Erythrose, [18]	141.34	27.83		kge
Glucose → 1,6 Anhydroglucose, [18]	65.93	9.11		kga
Glucose → Gliceraldehyde, [18]	95.65	17.02		kgly
Fructose → Erythrose, [18]	140.44	26.99		kfe
Fructose → Acids, [18]	128.63	25.03		kfa
Fructose → Gliceraldehyde, [18]	133.04	25.48		kfgly
Gliceraldehyde → DHA, [17]	154.36	30.37		kglyd
Gliceraldehyde ← DHA, [17]	77.32	13.04		kdgly
DHA → Pyruvaldehyde, [17]	88.65	16.71		kdp
Gliceraldehyde → Pyruvaldehyde, [17]	82.56	15.84		kglyp
Pyruvaldehyde → Acids, [17]	94	18.004		kpl
Erythrose → Acids, [20]	124.72	23.754		ke
1,6 Anhydroglucose → Acids, [18]	109.29	18.194		ka

The molar flow (mol/h) profiles of glucosyl erythrose ( $n_4$ ); glucosyl glycolaldehyde ( $n_5$ ); glucose ( $n_6$ ); fructose ( $n_7$ ); glycolaldehyde ( $n_8$ ); 1,6 anhydroglucose ( $n_9$ ); erythrose ( $n_{10}$ ); glycerinaldehyde ( $n_{11}$ ); dihydroxyacetone ( $n_{12}$ ); pyruvaldehyde ( $n_{13}$ ); organic acids ( $n_{14}$ ); 5-HMF ( $n_{15}$ ) were

calculated using the equations 9 to 20 respectively. The organic acid profiles were calculated assuming that the acids formed have 3 carbons. The residence time was calculated according to equation 21.

$$\frac{dn_4}{dz} = \frac{\rho S}{M} (k_1 n_3 - k_{geg} n_4) \quad (9)$$

$$\frac{dn_5}{dz} = \frac{\rho S}{M} (k_2 n_4 - k_{ggg} n_5) \quad (10)$$

$$\frac{dn_6}{dz} = \frac{\rho S}{M} \left[ \left( k_{og} n_2 \frac{CW_{cellulose}}{MW_{glucose} CW_{glucose}} + 2k_h n_3 + k_{geg} n_4 + k_{ggg} n_5 \right) - (k_{gf} + k_{ge} + k_{ga} + k_{ggl}) n_6 \right] \quad (11)$$

$$\frac{dn_7}{dz} = \frac{\rho S}{M} [(k_{gf} n_6) - (k_{fe} + k_{fa} + k_{fgl}) n_7] \quad (12)$$

$$\frac{dn_8}{dz} = \frac{\rho S}{M} [k_1 n_3 + k_{ge} n_6 + k_{fe} n_7] \quad (13)$$

$$\frac{dn_9}{dz} = \frac{\rho S}{M} [k_{ga} n_6 - k_a n_9] \quad (14)$$

$$\frac{dn_{10}}{dz} = \frac{\rho S}{M} [k_{ge} n_6 + k_{fe} n_7 + k_2 n_3 - k_e n_{10}] \quad (15)$$

$$\frac{dn_{11}}{dz} = \frac{\rho S}{M} [2k_{fgl} n_7 + 2k_{ggl} n_6 + k_{dgl} n_{12} - (k_{glyd} + k_{glyp}) n_{11}] \quad (16)$$

$$\frac{dn_{12}}{dz} = \frac{\rho S}{M} [k_{glyd} n_{11} - (k_{dp} + k_{dgl}) n_{12}] \quad (17)$$

$$\frac{dn_{13}}{dz} = \frac{\rho S}{M} [k_{glyp} n_{11} + k_{dp} n_{12} - k_p n_{13}] \quad (18)$$

$$\frac{dn_{14}}{dz} = \frac{\rho S}{M} \left[ 2k_{fa} n_7 + \frac{4}{3} k_e n_{10} + k_p n_{13} + k_p n_{13} + 2k_a n_9 \right] \quad (19)$$

$$\frac{dn_{15}}{dz} = \frac{\rho S}{M} [k_{hmf} n_6] \quad (20)$$

$$\frac{dt}{dz} = \frac{\rho S}{M} \quad (21)$$

With equations 5 – 21 and the experimental data obtained (cellulose conversion and cellobiose, glucose, fructose, 5-HMF and pyruvaldehyde molar flows) obtained experimentally,

four main parameters of the model were fitted:  $F$ ,  $k_{og}$ ,  $k_{gf}$  and  $k_{hmf}$ . The fitting process was performed with the Matlab® function *lsqcurvefit*.

#### 4. Results and Discussion

Experiments for cellulose depolymerization were carried out between 275°C and 400°C, at 25 MPa. The residence times were fixed between 0.004s and 30s. The carbon balance was between 90% - 100%. The lower values of carbon balance were achieved at 400°C with residence times higher than 1 s. No char formation was observed at residence times lower than 1 s.

The analysis of three samples taken at different time of pumping under similar temperature, pressure and reagents flow rate is shown in table 3. The errors of the data are lower than 7% in mass. Due to the low deviation of the data shown in table 3, it can be concluded that the particles distribution is homogeneous (assumption made in section 2.3). The main reaction intermediates identified were cellobiose, glucose, fructose, glyceraldehyde, 5 hydroxy-methyl-furfural (5-HMF), pyruvaldehyde and erythrose. The uncertainties of the reaction rates and Arrhenius parameters were calculated following the EA-4/02 document [21].

**Table 3.** Analysis of three samples at same conditions at different moments of the steady state. Mean and standard deviation.

	bar	°C	s		%	ppm	ppm	ppm	ppm	ppm
	P	T	tr	X	Carbon Balance	Cellobiose	Glucose	Fructose	Pyruvaldehyde	HMF
Exp. 1	250	350	0.44	0.71	95	2190	1683	960	880	203
Exp. 2	250	350	0.49	0.66	96	2151	1660	930	884	192
Exp. 3	250	350	0.49	0.62	96	1978	1543	872	788	187
Average			0.47	0.66	95.7	2107	1629	920	851	194
Standard Deviation			0.03	0.04	0.6	113	75	45	54	8

##### 4.1. Cellulose hydrolysis

The logarithms of cellulose hydrolysis kinetic constants at different temperatures (diamond dots) were plotted versus the reciprocal temperature in Fig. 4. Up to 375°C, the kinetic constants of cellulose hydrolysis were seen to increase as the temperature increased, according to the Arrhenius law, the activation energy ( $E_a$ ) and pre-exponential factor ( $\ln A$ ) being  $154.4 \pm 9.5$  kJ/mol and  $29.6 \pm 1.9$  respectively.

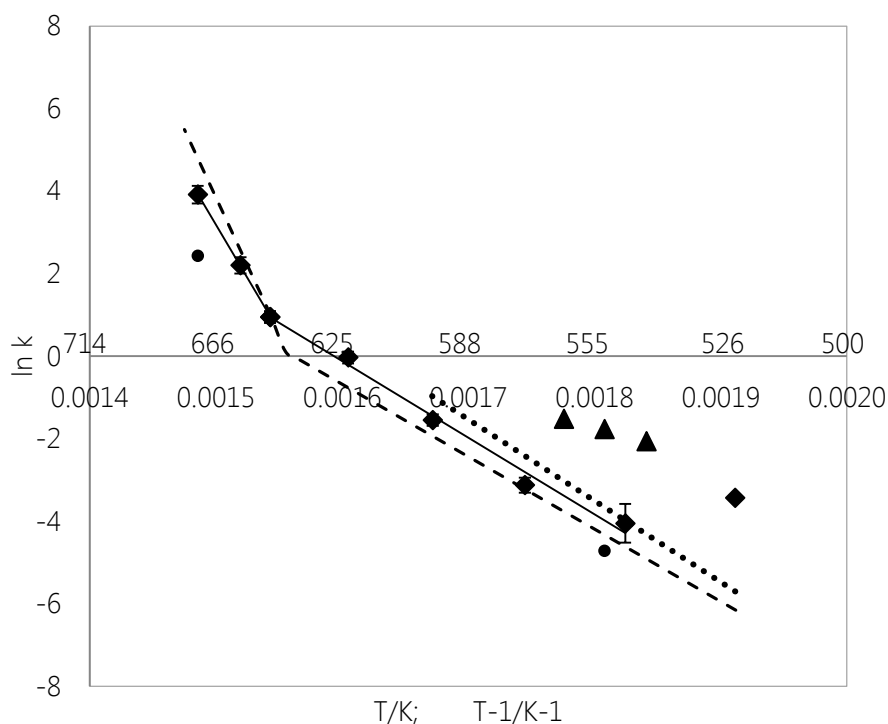


**Fig. 4.** Kinetic constant for cellulose hydrolysis in hot pressurized water obtained in this work (◆). Error bars  $\pm$  uncertainty. Continuous line represents the linear fit ( $\ln k$  vs  $1/T$ ). Dashed line represents the kinetics developed by Sasaki et al [9]. Dotted line represents the kinetic developed by Rogalinski et al. [11]. Filled dots (●) are the kinetics constant obtained by Ehara et al.[22]. Triangles (▲) are the kinetic values obtained by Lü et al.[23].

At temperatures above the critical point of water, the kinetic constants still correlated with temperature, following the Arrhenius equation, but the activation energy and the pre-exponential factor of the cellulose hydrolysis were higher than at subcritical temperatures, being  $430.3 \pm 6.3$  kJ/mol and  $80.8 \pm 1.2$  respectively. This can be explained because, at temperatures higher than  $350^{\circ}\text{C}$ , the medium may dissolve the cellulose, and thus the mass transfer limitation of a heterogeneous reaction is avoided. The hydrolysis reaction may occur in a homogeneous phase, thus increasing the reaction rate. In this work, the change in the behavior seen in the cellulose hydrolysis in hot pressurized water is less drastic than the one found in literature [9]. A comparison between the data developed in this work and literature data is shown in Fig. 4 [9, 11, 22, 23]. The kinetics developed by Sasaki et al [9] (dashed line) were determined using a similar device and conditions to this work. At subcritical temperatures, the kinetics developed in this work seem to be faster than those found by Sasaki et al, but at supercritical temperatures the kinetics developed in this work are slower than determined by Sasaki et al[9]. The change in the hydrolysis kinetics near the critical point is less drastic than that found in literature [9], the main differences lies in the cooling method

used in the devices. Although the literature kinetic constants in literature, shown in Fig. 4 [11, 22, 23], were developed using a smaller range of temperature than in this work, they present a similar behavior to that of the kinetics determined here.

## 4.2. Kinetic adjustment

### 4.2.1. Oligosaccharide production fraction (F)

The fitted values for the oligosaccharide production fraction (F) at different temperatures are shown in Fig. 5. F is increased by increasing the reaction temperature up to a value of 0.8. Three different zones can be analyzed in Fig.5. At temperatures below 300°C, F is 0.5, indicating that half of the cellulose is hydrolyzed to small molecules like cellobiose and the other 50% is hydrolyzed to bigger oligosaccharides. At temperatures above 350°C the factor is 0.8, indicating that 80% of the cellulose is hydrolyzed to large oligosaccharides. In the temperature range between 300°C and 350°C, the factor presents a transition between the other two values. Fig.5 also shows the change in the density of the medium and the dielectric constant of water. According the discussion in 4.1, the cellulose hydrolysis at supercritical temperature occurs when the cellulose is in solution. Bigger oligosaccharides would be formed at higher temperatures, rather than at lower temperatures, since the reaction occurs in a heterogeneous phase. At low temperatures (not dissolved cellulose) the reaction would take place on the surface of the cellulose grain, generating small molecules.

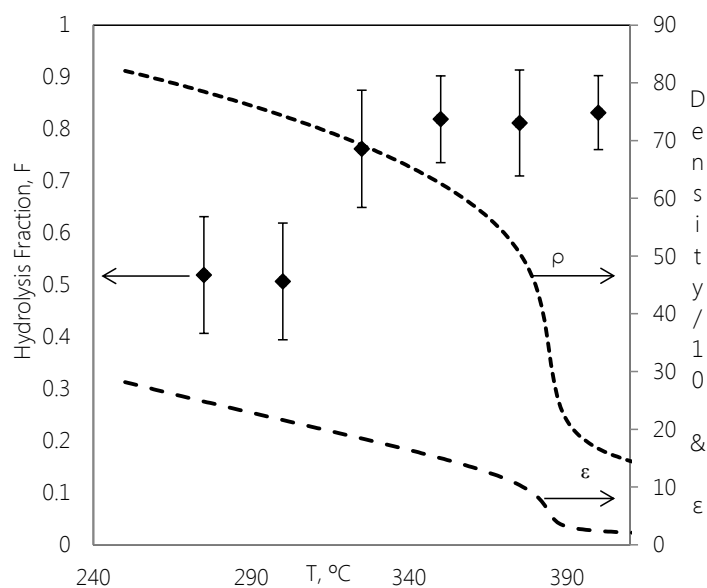


**Fig. 5.** Oligosaccharide production factor, F, (♦). Error bars  $\pm$  uncertainty. The dashed line is the value of the density (divided by 10) along the temperature ( $\text{kg}/\text{m}^3$ ). The spaced dashed line is the evolution of the dielectric constant ( $\epsilon$ ) over temperature.

#### 4.2.2. Oligosaccharide hydrolysis kinetic constant ( $k_{og}$ )

The kinetic constants for oligosaccharide hydrolysis versus the reciprocal of temperature are shown in Fig. 6. The kinetics follow the Arrhenius law with  $R^2=0.99$ . The activation energy of the reaction,  $E_a$ , and pre-exponential factor,  $\ln A$ , are  $135.2\pm 9.2$  kJ/mol and  $26.4\pm 1.2$  respectively.

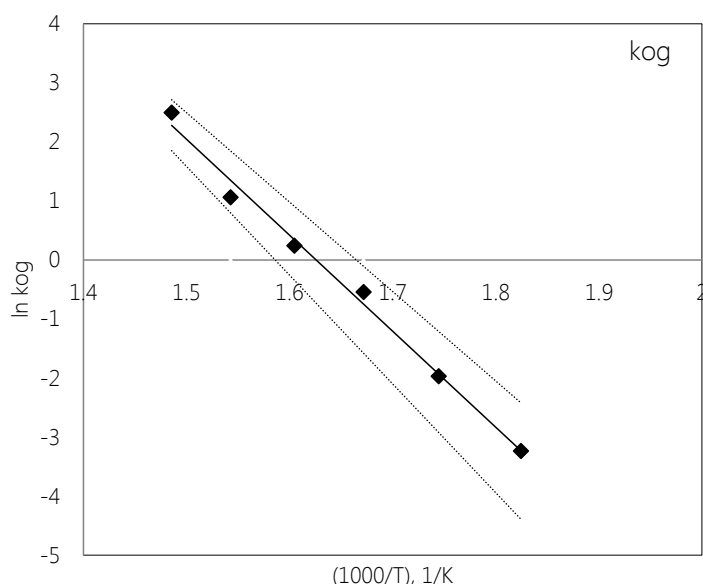
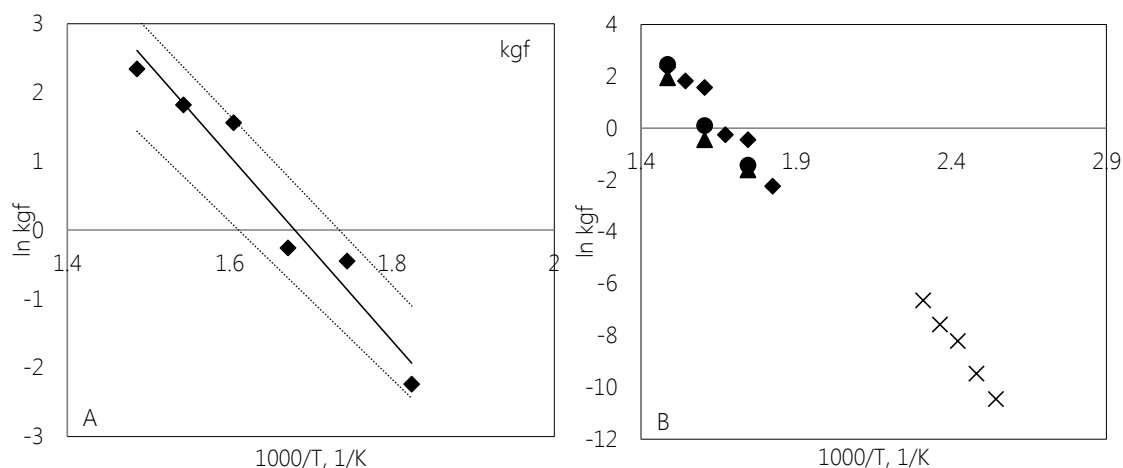


Fig. 6. Oligosaccharide hydrolysis kinetic constants, kog, versus reciprocal temperature (◆). The upper and lower dotted lines show the error margin of the linear fit (uncertainty).

#### 4.2.3. Glucose to fructose kinetic constant ( $k_{gf}$ )

The kinetic constants for glucose to fructose reaction are plotted versus the reciprocal temperature in Fig. 7A. The kinetics follow the Arrhenius law with  $R^2=0.95$ . The activation energy of the reaction,  $E_a$ , and pre-exponential factor,  $\ln A$ , are  $111.5\pm 10.2$  kJ/mol and  $22.5\pm 1.1$  respectively. A comparison of the  $k_{gf}$  obtained in this work with the  $k_{gf}$  reported in literature is shown in Fig. 7B [17-19, 24]. The literature's kinetic constants are consistent to those obtained in this work. In this work  $k_{gf}$  was fitted, using cellulose as the starting material and taking into account the reaction pathway. The values presented in literature for  $k_{gf}$  were developed using glucose as the starting material[20]. The kinetic concordance between the two different kinetic methods may be taken as a qualitative parameter of the correct functioning of the model presented in this article.



**Fig. 7. (A)** Glucose to fructose kinetic constants,  $kgf$ , versus the reciprocal temperature ( $\blacklozenge$ ). The upper and lower dotted lines show the error margin of the linear fit (uncertainty). **(B)** Comparison between the kinetics obtained in this work ( $\blacklozenge$ ) and kinetics from literature. The triangles ( $\blacktriangle$ ) are the kinetic values obtained by Kabyemela et al. [18]. The filled dots ( $\bullet$ ) are the kinetic values from Kabyemela et al. [20]. The crosses are the kinetics from Kimura et al. [24].

#### 4.2.4. 5-HMF formation kinetic constant ( $k_{hmf}$ )

The reaction rate constants of the 5-HMF formation were fitted using the concentrations at low residence times in order to avoid the interference of subsequent reactions. The fitted kinetic constants of 5-HMF formation ( $k_{hmf}$ ) versus the reciprocal temperature are presented in Fig. 8. This kinetic can be analyzed in two zones. At temperatures below 330°C the kinetic constants increase at higher temperatures. The kinetic follows the Arrhenius law with  $R^2=0.99$ . The activation energy of the reaction,  $E_a$ , and pre-exponential factor,  $\ln A$ , are  $285\pm 34$  kJ/mol and  $57.6\pm 6.5$  respectively. However, at temperatures above 330°C the kinetic constants seem to decrease with increasing temperature. The reaction follows the Arrhenius law with  $R^2=0.99$ , presenting a negative activation energy and pre-exponential factor with values  $-61.3\pm 15.7$  kJ/mol and  $-11.3\pm 4.3$  respectively. Fig. 9 shows the values of the ionic product of water, density and  $k_{hmf}$  against temperature. At temperatures higher than 330°C the ionic product of water varies from  $10^{-12}$  to  $10^{-20}$  at 400°C. This change in the polarity and ionic product affects the kinetics of glucose/fructose degradation, avoiding the ionic degradation reaction and favoring the radical degradation reactions. The radical reaction of fructose dehydration producing 5-HMF could be favored by the ability of supercritical water to generate free radicals [5]. The low concentration of 5-HMF at 400°C would be a reason of a fast further

hydrolysis to produce levulinic acid and formic acid. However, at low residence time, any concentration of 5-HMF should have been detected.

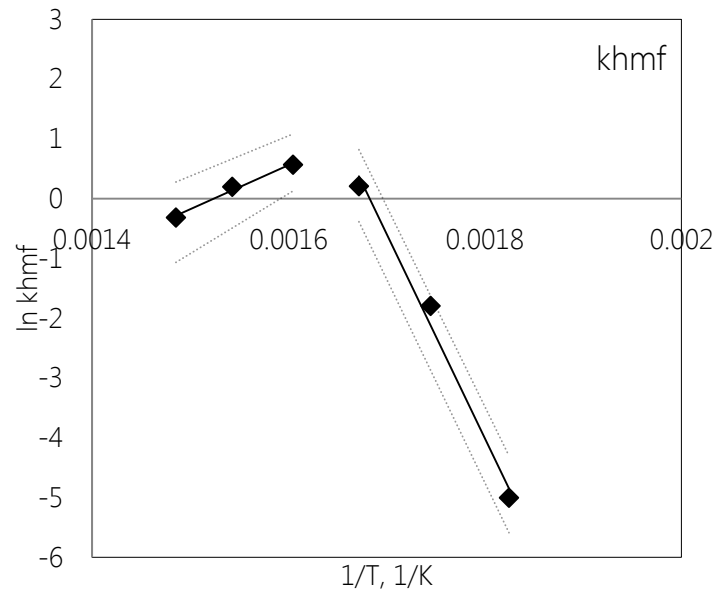


**Fig 8.** 5-HMF formation kinetic constant, khmf, (◆). The upper and lower dotted lines show the error margin of the linear fit (uncertainty).

In addition, the fructose dehydration producing 5-HMF would be also affected by the density of the medium, as determined by Aida et al [3, 25]. They found that the effect of density would be the dominating effect due to the low yield of 5-HMF found in the experiments when the temperature was increased to values higher than 350°C. The 5-HMF yield is decreased when the density is decreased; the lowest value obtained was almost 1% when the density was 0.5 g/cm<sup>3</sup>. In our work, the yield of 5-HMF was lower than 0.5%, the mean density being around 0.17 g/cm<sup>3</sup>. To explain this behavior, they proposed a reaction mechanism in which water molecules would participate in a transition state in the reaction of fructose dehydration. If the reaction occurs using this mechanism, a low water density would disfavor the reaction of fructose dehydration because the population of water molecules near the fructose would be low, and thus also the possibility of reaching the intermediate transition state. The kinetic of 5-HMF formation calculated using equation 20 was recalculated ( $k_{hmf,w}$ ) considering the water concentration in the reaction using equation 22.

$$\frac{dn_{15}}{dz} = \frac{\rho S}{\dot{M}} [k_{hmf,w} n_w n_6] \quad (22)$$

Where 'n<sub>w</sub>' is the concentration of water in mol/L. At temperatures below 330°C the kinetic ( $k_{hmf,w}$ ) follows the Arrhenius law with R<sup>2</sup>=0.99. The activation energy of the reaction and pre-

exponential factor are  $291.8 \pm 34$  kJ/mol and  $62.3 \pm 6.5$  respectively. At temperatures above 330°C the kinetic constants follows the Arrhenius law with  $R^2=0.80$ , presenting an activation energy and pre-exponential factor with values  $34.1 \pm 3.7$  kJ/mol and  $10.4 \pm 4.3$  respectively.

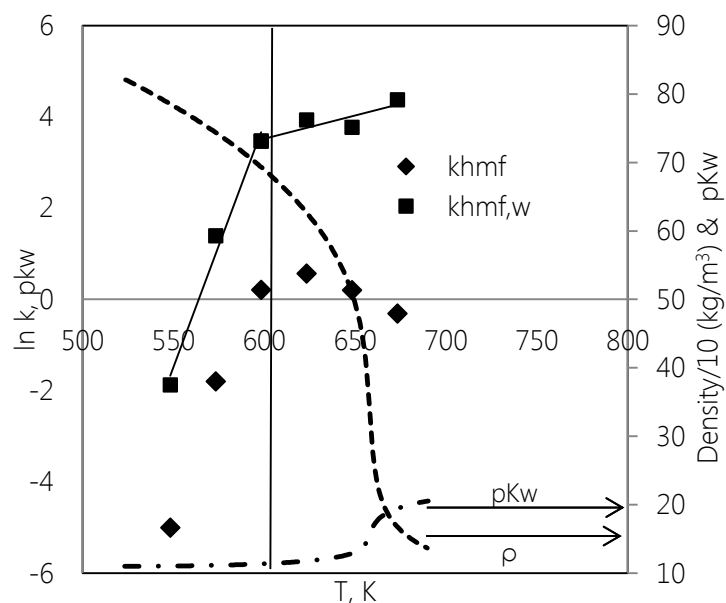


**Fig. 9.** 5-HMF formation kinetic constant,  $k_{hmf}$  (◆). 5-HMF formation kinetic constant considering water concentration,  $k_{hmf,w}$  (■). The dashed-dotted line is the ionic product of water over temperature. The dashed line is the evolution of density with temperature (divided by 10) over the temperature ( $\text{kg}/\text{m}^3$ ).

The kinetic of 5-HMF formation is increased when temperature is increased if the water concentration is taken into account in the reaction. Thus, the changes in the properties of the medium, especially density (water concentration), would be responsible for the change in the kinetic of 5-HMF.

The hydrolysis of cellulose to glucose can be carried out avoiding 5-HMF formation by controlling the reaction media through pressure and temperature; and the residence time through an effective reactor [26].

#### 4.3. Model and Experimental Data

The comparison of some of the molar flow profiles and the experimental data is shown in Fig. 10. The graphics represent the profiles at 400°C, 375°C, 325°C and 300°C (from left to right) of cellulose conversion, glucose production, fructose production and pyruvaldehyde production (from top to bottom). The model correctly predicts the concentration of the cellulose, glucose and fructose. The experimental concentration of pyruvaldehyde appears to be higher than the model's prediction. The model calculates the pyruvaldehyde profile

considering the reaction pathway shown in Fig. 4 and the kinetic parameters shown in table 2. This difference between the model and the experimental data would be evidence of an unconsidered reaction pathway or higher reaction rates of pyruvaldehyde formation.

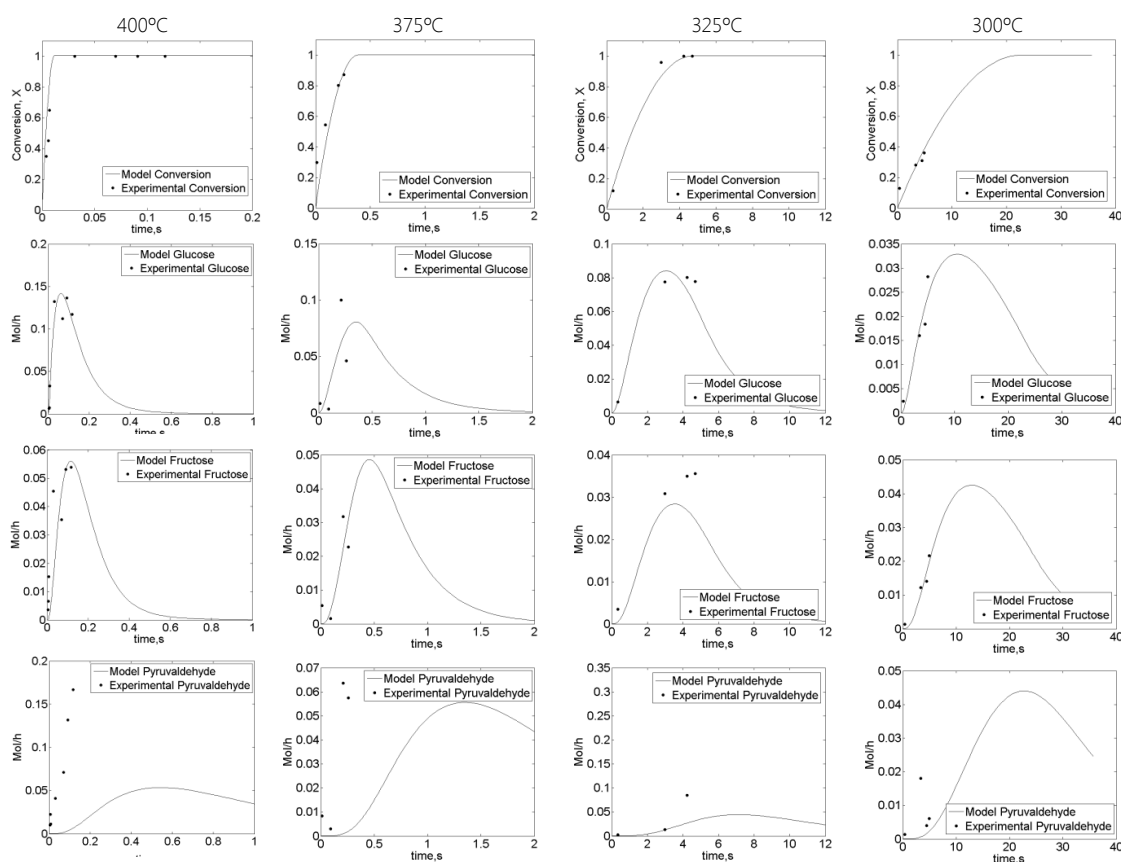


Fig. 10. Comparison between the model prediction and the experimental data of cellulose conversion, glucose, fructose and pyruvaldehyde at 400°C, 375°C, 325°C and 300°C. The pressure of the system was 25MPa.

## 5. Conclusions

Cellulose depolymerization in near critical water was analyzed experimentally. A mathematical model was developed using kinetic constants and reaction pathways from literature as well as the experimental data obtained in this work. Four main parameters of the cellulose reactions in pressurized water were fitted ( $F$ ,  $k_{og}$ ,  $k_{gf}$  and  $k_{hmf}$ ).

It was found that the cellulose hydrolysis kinetics depend strongly on temperature. At supercritical temperatures, cellulose would be dissolved in water, thus, hydrolysis in a homogeneous phase would be the main reason for the faster cellulose hydrolysis kinetics when approaching the critical point of water.

Cellulose hydrolysis produces bigger molecules as a first step hydrolysis at temperatures above 350°C.

The reaction rate of glucose to fructose isomerization fitted in this work is consistent with the values found in literature ( $E_a=111.5$  vs  $E_{a, \text{lit}}=112.7$ ).

The 5-HMF formation reaction rate will be highly influenced by the density (water concentration) of the reaction medium.

The experimental data and the model's predictions show good concordance in both the analyzed temperatures and residence times.

## References

1. Arai, K., Smith Jr, R.L., and Aida, T.M., *Decentralized chemical processes with supercritical fluid technology for sustainable society*. The Journal of Supercritical Fluids, 2009. 47(3): p. 628-636.
2. Akiya, N. and Savage, P.E., *Roles of Water for Chemical Reactions in High-Temperature Water*. Chemical Reviews, 2002. 102(8): p. 2725-2750.
3. Aida, T.M., Sato, Y., Watanabe, M., Tajima, K., Nonaka, T., Hattori, H., and Arai, K., *Dehydration of D-glucose in high temperature water at pressures up to 80 MPa*. The Journal of Supercritical Fluids, 2007. 40(3): p. 381-388.
4. Kruse, A. and Gawlik, A., *Biomass Conversion in Water at 330–410 °C and 30–50 MPa. Identification of Key Compounds for Indicating Different Chemical Reaction Pathways*. Industrial & Engineering Chemistry Research, 2002. 42(2): p. 267-279.
5. Promdej, C. and Matsumura, Y., *Temperature Effect on Hydrothermal Decomposition of Glucose in Sub- And Supercritical Water*. Industrial & Engineering Chemistry Research, 2011. 50(14): p. 8492-8497.
6. Peterson, A.A., Vogel, F., Lachance, R.P., Fröling, M., Michael J. Antal, Jr., and Tester, J.W., *Thermochemical biofuel production in hydrothermal media: A review of sub- and supercritical water technologies*. Energy & Environmental Science, 2008. 1(1): p. 32-65.
7. Ragauskas, A.J., Williams, C.K., Davison, B.H., Britovsek, G., Cairney, J., Eckert, C.A., Frederick, W.J., Hallett, J.P., Leak, D.J., Liotta, C.L., Mielenz, J.R., Murphy, R., Templer, R., and Tschaplinski, T., *The Path Forward for Biofuels and Biomaterials*. Science, 2006. 311(5760): p. 484 -489.
8. Zhao, Y., Lu, W.-J., Wang, H.-T., and Li, D., *Combined Supercritical and Subcritical Process for Cellulose Hydrolysis to Fermentable Hexoses*. Environmental Science Technology, 2009. 43(5): p. 1565-1570.
9. Sasaki, M., Adschiri, T., and Arai, K., *Kinetics of cellulose conversion at 25 MPa in sub- and supercritical water*. AIChE Journal, 2004. 50(1): p. 192-202.
10. McGinnis, G.D., Wilson, W.W., and Mullen, C.E., *Biomass pretreatment with water and high-pressure oxygen. The wet-oxidation process*. Industrial & Engineering Chemistry Product Research and Development, 1983. 22(2): p. 352-357.

11. Rogalinski, T., Ingram, T., and Brunner, G., *Hydrolysis of lignocellulosic biomass in water under elevated temperatures and pressures*. The Journal of Supercritical Fluids, 2008. 47(1): p. 54-63.
12. Brunner, G., *Near critical and supercritical water. Part I. Hydrolytic and hydrothermal processes*. The Journal of Supercritical Fluids, 2009. 47(3): p. 373-381.
13. Sasaki, M., Fang, Z., Fukushima, Y., Adschiri, T., and Arai, K., *Dissolution and Hydrolysis of Cellulose in Subcritical and Supercritical Water*. Industrial & Engineering Chemistry Research, 2000. 39(8): p. 2883-2890.
14. Sierra-Pallares, J., Marchisio, D.L., Alonso, E., Teresa Parra-Santos, M., Castro, F., and José Cocero, M., *Quantification of mixing efficiency in turbulent supercritical water hydrothermal reactors*. Chemical Engineering Science, 2011. 66(8): p. 1576-1589.
15. Takami, S., Sugioka, K.-i., Tsukada, T., Adschiri, T., Sugimoto, K., Takenaka, N., and Saito, Y., *Neutron radiography on tubular flow reactor for hydrothermal synthesis: In situ monitoring of mixing behavior of supercritical water and room-temperature water*. The Journal of Supercritical Fluids, 2012. 63(0): p. 46-51.
16. Wagner, W, Cooper, J, R., Dittmann, et al., *The IAPWS industrial formulation 1997 for the thermodynamic properties of water and steam*. 2000, American Society of Mechanical Engineers: New York, N, ETATS-UNIS.
17. Kabyemela, B.M., Adschiri, T., Malaluan, R., and Arai, K., *Degradation Kinetics of Dihydroxyacetone and Glyceraldehyde in Subcritical and Supercritical Water*. Industrial & Engineering Chemistry Research, 1997. 36(6): p. 2025-2030.
18. Kabyemela, B.M., Adschiri, T., Malaluan, R.M., and Arai, K., *Glucose and Fructose Decomposition in Subcritical and Supercritical Water: Detailed Reaction Pathway, Mechanisms, and Kinetics*. Industrial & Engineering Chemistry Research, 1999. 38(8): p. 2888-2895.
19. Kabyemela, B.M., Takigawa, M., Adschiri, T., Malaluan, R.M., and Arai, K., *Mechanism and Kinetics of Cellobiose Decomposition in Sub- and Supercritical Water*. Industrial & Engineering Chemistry Research, 1998. 37(2): p. 357-361.
20. Kabyemela, B.M., Adschiri, T., Malaluan, R.M., Arai, K., and Ohzeki, H., *Rapid and Selective Conversion of Glucose to Erythrose in Supercritical Water*. Industrial & Engineering Chemical Research, 1997. 36(12): p. 5063-5067.

21. *Expression of the Uncertainty of Measurement in Calibration, European Cooperation for Accreditation, EA-4/02*. 1999.
22. Ehara, K. and Saka, S., *Decomposition behavior of cellulose in supercritical water, subcritical water, and their combined treatments*. *Journal of Wood Science*, 2005. 51(2): p. 148-153.
23. Lü, X., Sakoda, A., and Suzuki, M., *Decomposition of Cellulose by Continuous Near-Critical Water Reactions*. *Chinese Journal of Chemical Engineering*, 2000. 8(4): p. 321-325.
24. Kimura, H., Nakahara, M., and Matubayasi, N., *In Situ Kinetic Study on Hydrothermal Transformation of d -Glucose into 5-Hydroxymethylfurfural through d -Fructose with  $^{13}C$  NMR*. *The Journal of Physical Chemistry A*, 2011. 115(48): p. 14013-14021.
25. Aida, T.M., Tajima, K., Watanabe, M., Saito, Y., Kuroda, K., Nonaka, T., Hattori, H., Smith Jr, R.L., and Arai, K., *Reactions of D-fructose in water at temperatures up to 400 °C and pressures up to 100 MPa*. *The Journal of Supercritical Fluids*, 2007. 42(1): p. 110-119.
26. Cantero, D.A., Bermejo, M.D., and Cocero, M.J., *High glucose selectivity in pressurized water hydrolysis of cellulose using ultra-fast reactors*. *Bioresource Technology*, 2013. 135: p. 697-703.



# Chapter 3. Tunable Selectivity on Cellulose Hydrolysis in Supercritical Water

## Abstract

At extremely low residence times (0.02 s), the sugars selectivity of cellulose hydrolysis was higher than 98% w/ w·w<sup>-1</sup> while 5-HMF concentration was lower than 5 ppm at 400°C and 23 MPa. At residence times of 1 s, the selectivity of glycolaldehyde was 60% w·w<sup>-1</sup> at 400°C and 23 MPa. The residence time was a selectivity factor in the production of sugars or glycolaldehyde. In this study, the effect of temperature, pressure and residence time on cellulose hydrolysis in a hydrothermal media was analyzed. The experiments were carried out in a continuous pilot plant capable of operating up to 400°C, 27 MPa and residence times between 0.004 s and 40 s. A novel kinetic model was developed in order to evaluate the kinetics of glucose reactions. It was found that the hydroxide anion concentration in the medium due water dissociation is the determining factor in the selectivity of the process. The reaction of glucose isomerization to fructose and its further dehydration to produce 5-hydroxy-methyl-furfural are highly dependent on OH<sup>-</sup> ion concentration. By increasing pOH, these reactions were minimized allowing the control of 5-HMF production. At this condition, the retro-aldol condensation pathway was enhanced instead of isomerization/dehydration pathway.

**Keywords:** Biomass • Ionic Product • Kinetics • Sugars • Water Chemistry



## 1. Introduction

The biomass exploitation as raw material is growing as an alternative for the sustainable production of fuels and chemicals [1]. Cellulose is one of the main compounds of biomass, representing the most abundant biopolymer [2]. An important challenge in the processing of cellulosic biomass is to hydrolyze the  $\beta$ 1-4 glucose-glucose bond producing a stream of sugars with low concentration of byproducts, by using an efficient process [3, 4]. This sugars streams could be further transformed in valuable chemical like pyruvaldehyde, glycolaldehyde [5-8], organic acids or poly-alcohols [9, 10]. Acid and enzymatic hydrolysis of cellulose are two conventional methods that need long treatment times (>3 h) to obtain a non-selective product (<60% w·w<sup>-1</sup>) [11, 12].

The use of ionic liquids as solvent and reaction medium has been intensively studied due to the possibility of dissolve cellulose making it more 'accessible' to the hydrolysis reaction [13, 14]. However, this kind of process take at least 3 h of hydrolysis to obtain a selectivity near to 30% w·w<sup>-1</sup> of reducing sugars [13]. Large residence times would require big reactors at the scaling up time. The use of pressurized water is an alternative as reaction medium for the processing of cellulosic biomass in a one-step fast process. Total hydrolysis of cellulose can be achieved in 0.02 s of residence time in a supercritical water medium producing a stream of water soluble sugars with low concentration of derived products (<2% w·w<sup>-1</sup>) [15, 16]. This kind of process represents an advantageous intensification that will reduce the energetic and equipment requirements in the scaling up.

## 2. Results and Discussion

Cellulose depolymerization in hot pressurized water can be done in different ways allowing the selective production of sugars or glycolaldehyde. The reactions of cellulose in hot pressurized water were analyzed at 300°C, 350°C and 400°C. The pressure of the experiments was varied between 10 and 27 MPa. The evolution of the selectivity along residence time can be seen in Figure 1 (see also Tables S.1 – S.10 in SI). The best conditions to obtain soluble sugars (up to six glucose units) from the hydrolysis of cellulose were achieved by working at 400°C with extremely short residence times (0.015 s). When residence time was increased, the sugars were hydrolyzed, so the selective decreased as it is shown in Figure 1. At 400°C, the

selectivity of soluble sugars was higher than 95% in carbon at the three experimented pressures (see Figure S.1 in SI).

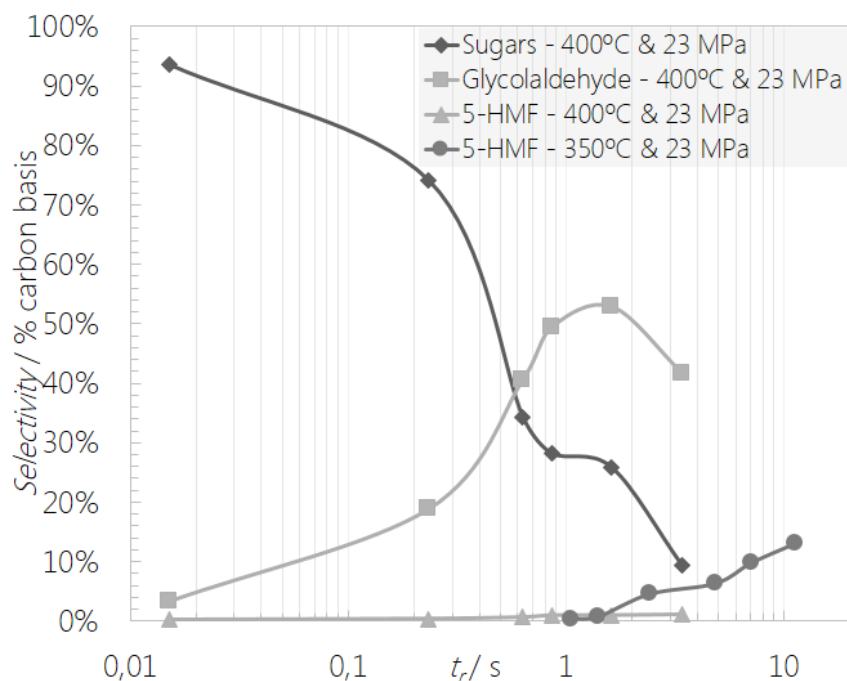


Fig. 1. Sugar, glycolaldehyde and 5-HMF selectivity in cellulose hydrolysis.

Similar methods of cellulose hydrolysis in pressurized water were developed in literature with selectivity of sugars lower than  $77\% \text{ w}\cdot\text{w}^{-1}$  [17-20]. The combination of supercritical water medium and the effective method of residence time control presented in this work allow cellulose hydrolysis with high selectivity to sugars. This is because, at those conditions, the cellulose hydrolysis kinetic is fast enough while the glucose hydrolysis kinetics are slow enough to allow our reactor to stop the reactions after total hydrolysis and before glucose degradation [16]. It was observed that the cellulose hydrolysis would have a sugars selectivity between  $80 - 98\% \text{ w}\cdot\text{w}^{-1}$  if the residence time is between  $0.015 - 0.2 \text{ s}$ .

The best analyzed combination of conditions to obtain high selectivity of glycolaldehyde can be achieved by working at  $400^\circ\text{C}$  and  $23 \text{ MPa}$  with a residence time of  $1 \text{ s}$ . In those conditions the selectivity of glycolaldehyde was around  $60\% \text{ w}\cdot\text{w}^{-1}$ . Sometimes, the production of 5-HMF is undesired, especially when a microorganism post process is needed [21]. At  $400^\circ\text{C}$ , the 5-HMF production was highly avoided for all the studied pressures. Independently of the residence time ( $0.015 \text{ s}$  for sugars or  $1 \text{ s}$  for glycolaldehyde) the concentration of 5-HMF was lower than  $0.1\% \text{ w}\cdot\text{w}^{-1}$ .

Supercritical water (SCW) is water at temperature and pressure values above its critical point ( $T_c=374^\circ\text{C}$  and  $P_c=22.1 \text{ MPa}$ ). In the surroundings of the critical point, the properties of water

can be highly influenced by changing pressure and temperature. So, the identity of the medium can be modified without changing the solvent. The medium density represents the quantity of water per volume unit ( $\text{kg}/\text{m}^3$ ); this is a measurement of water concentration, an important factor to take into account in the reactions where water participates as reagent or forming intermediate states [22]. Another important property of water as reaction medium is the ion product ( $\text{mol}^2/\text{kg}^2$ ), which represents how dissociated is water molecule (ion concentration). If the molal concentration of  $\text{H}^+/\text{OH}^-$  (square root of ionic product) is multiplied by density, the molar concentration of protons or hydroxide anions in the medium is obtained. This concentration parameter includes both, the variations in water volume and its dissociation. The concentration of  $\text{OH}^-$  (which is the same for  $\text{H}^+$ ) in the surroundings of the critical point of water is plotted in Figure 2.

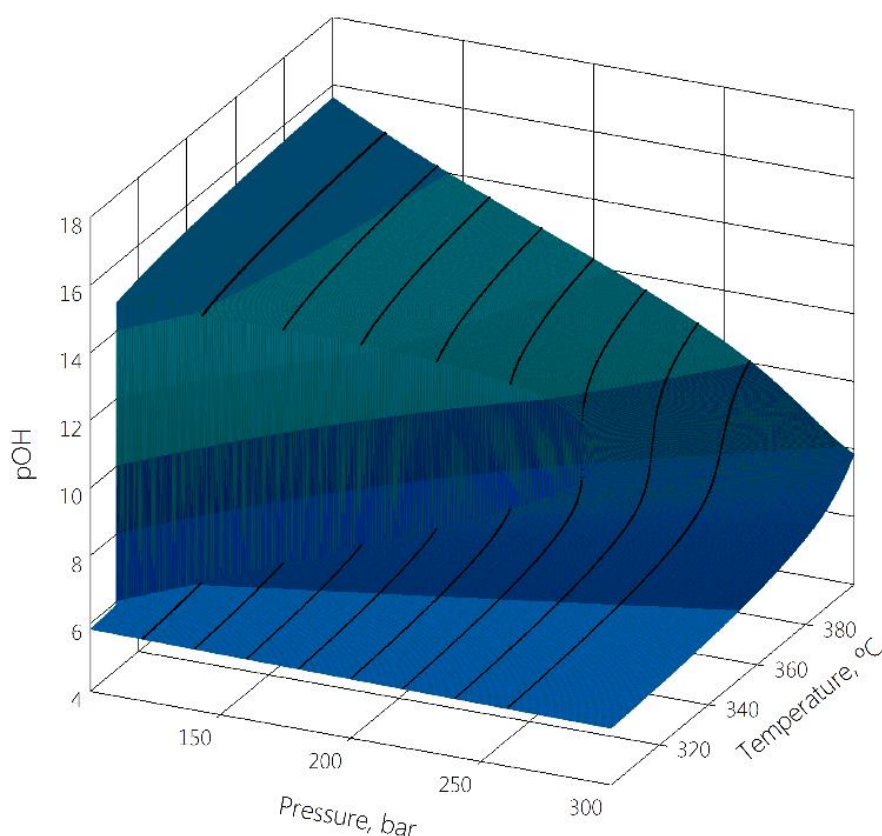
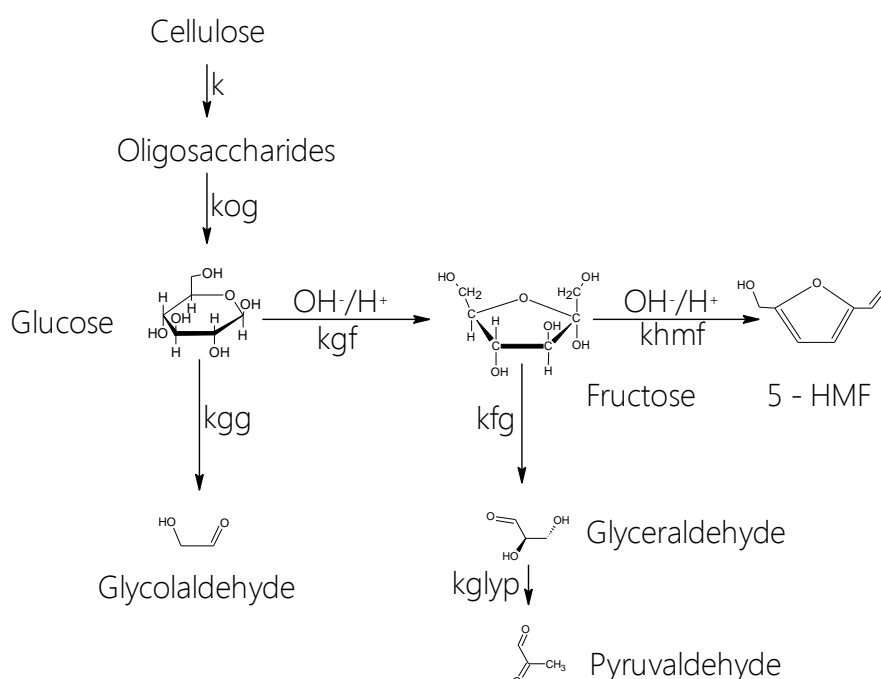


**Fig. 2.** Hydroxyl concentration ( $\text{mol}\cdot\text{L}^{-1}$ ) along temperature and pressure.  $\text{pOH}=-\log([\text{OH}^-])=\text{pH}$  [23, 24]. Water density was calculated according the IAPWS industrial formulation[23], while the molal ionic product of water was calculated following 'International Formulation of Ionic Product of Water Substance'[24].

Important changes in the identity of the medium can be obtained if temperature and pressure are changed at the same time. For example, the density of water at  $300^\circ\text{C}$  and  $27\text{MPa}$  is around  $750\text{ kg}/\text{m}^3$ ; this value can be decreased to  $130\text{ kg}/\text{m}^3$  if the conditions are modified to  $400^\circ\text{C}$  and  $23\text{MPa}$ . The  $\text{H}^+/\text{OH}^-$  concentration varies six orders of magnitude in

the neighborhood of the critical point allowing the possibility of working with markedly different reaction mediums. The  $H^+/OH^-$  concentration at 300°C and 23 MPa is around  $2 \cdot 10^{-6}$  mol/L which means that the medium has high concentration of ions favoring the ionic reactions [5, 25-27]. The  $H^+/OH^-$  concentration will take a value of  $5.5 \cdot 10^{-12}$  mol/L if the temperature and pressure are changed to 400°C and 23 MPa; this reaction medium would favor radical reactions [28].

The reactions were assumed to follow the reaction pathway shown in Schema 1. This reaction pathway was built following the schemas developed in literature[29]. The reaction of glucose isomerization occurs via ring-opening and keto-enol tautomerism. These reactions take place forming transition states with  $OH^-$  or  $H^+$ . Also, fructose dehydration takes place forming transition states incorporating  $H^+$  (one per  $H_2O$  molecule lost) [30]. In order to identify these reactions in Schema 1, the symbols  $OH^-/H^+$  were added above the reaction arrow. The production of glycolaldehyde was enhanced at supercritical conditions because the hydroxide/proton concentration is highly decreased ( $pH=pOH=13$ ) and so is the concentration of fructose and its derived products. Although the reaction of glucose isomerization is avoided at low concentration of ions, fructose selectivity near to 10% w·w<sup>-1</sup> was obtained at supercritical conditions.



**Schema 1.** Main reaction pathway of cellulose hydrolysis in pressurized water.

As it is shown in Schema 1, fructose can follow two main reaction pathways: fructose dehydration or retro aldol condensation. The second reaction was more benefited compared

to the first one obtaining, in this way, glyceraldehyde as main product from fructose. The maximum quantity of 5-HMF was obtained working at 350°C, 23 MPa (pOH=pH=6) at a residence time of 10 s. In those conditions the selectivity was around 15% w·w<sup>-1</sup>.

A reaction model was built considering cellulose as starting material. The concentration of each compound shown in Schema 1 was calculated along residence time. The difference between the calculated concentrations and the experimental ones was minimized obtaining the kinetic constant of the reactions. Equation 1 shows the evolution of compound *i* along residence time, where *n<sub>i</sub>* is the concentration of compound *i* (mol/L); *t* is time (s) and; *k<sub>ji</sub>* is the kinetic constant of the reaction in which *j* reacts producing *i*.

$$\frac{dn_i}{dt} = \sum_1^n k_{ji} n_j - \sum_1^n k_{io} n_i \quad (1)$$

In order to evaluate the medium effect in the selectivity, the model was solve in three ways; (1) considering only the concentration of cellulose and its derived products; (2) considering also the water concentration and; (3) considering the concentration of cellulose, its derived products and the proton or hydroxide anions concentration in the reactions of glucose isomerization and fructose dehydration. Therefore, as an example it is shown how is calculated the concentration of fructose according equation 2 or 3 in the resolution of model 2 or 3 respectively.

$$\frac{dn_f}{dt} = k_{gf} n_g n_w - k_{fh} n_f n_w - k_{fg} n_f \quad (2)$$

$$\frac{dn_f}{dt} = k_{gf} n_g n_{OH-H} - k_{fh} n_f n_{OH-H} - k_{fg} n_f \quad (3)$$

Where *n<sub>w</sub>* is the water concentration (mol/L) and *n<sub>OH-H</sub>* is the concentration of H<sup>+</sup> or OH<sup>-</sup> in the medium (mol/L) calculated as the square root of the ionic product (K<sub>w</sub><sup>0.5</sup>). The kinetic constants for the reaction rates *k<sub>og</sub>*, *k<sub>gg</sub>* and *k<sub>fg</sub>* obtained by the resolution of model 1 follow the Arrhenius Law. However, the kinetics of glucose isomerization and fructose dehydration showed a break point near the critical point of water (circles in Figure 3). This phenomenon would be predicted because of the low concentration of 5-HMF in the products. Moreover, the concentration profiles for 5-HMF obtained at 400°C were lower than the found at 350°C or 300°C.

The reactions of glucose and fructose in near critical water are usually analyzed together with the medium density in order to explain the selectivity of the process [4-6, 15]. Qualitatively,

the theory of water transition states works well; if density is low the concentration of 5-HMF is low. In order to quantify the participation of water in the reaction, water concentration was added as reagent in the reaction of glucose isomerization and fructose dehydration (model 2). Unfortunately, the kinetic constants obtained considering water concentration as reagent did not follow the Arrhenius Law (squares in Figure 3). Thus, from a quantitative point of view, the theory of water transition states would not explain the low concentration of 5-HMF at supercritical conditions.

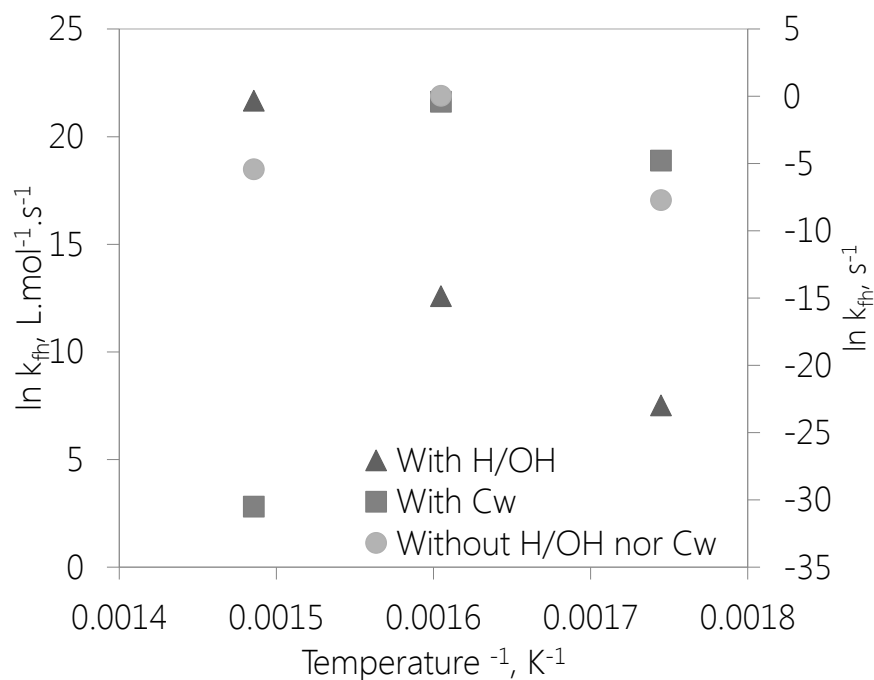


**Figure 3.** Kinetic constant of fructose dehydration considering H<sup>+</sup>/OH<sup>-</sup> concentration (▲), considering water concentration (■) and non-considering H<sup>+</sup>/OH<sup>-</sup> nor water concentration (●).

The kinetic constant of the whole reaction system followed the Arrhenius law when model 3 was resolved (triangles in Figure 3). The kinetic constants of fructose dehydration obtained for model 1, 2 and 3 are shown in Figure 3. Although the results shown in Figure 3 correspond to 27 MPa series, the results of Model 3 follow the Arrhenius Law for all the experimented pressures.

The reaction rates obtained from model 3 were used to calculate the Arrhenius parameter of each reaction. The activation energy (E<sub>a</sub>) and pre-exponential factor (Ln A<sub>0</sub>) are shown in Table 1. It can be seen that the values of Arrhenius parameters for k<sub>gf</sub> and k<sub>fh</sub> are higher than the values for the other kinetics. This is because the kinetics of k<sub>gf</sub> and k<sub>fh</sub> took higher values (left axis in Figure 3) when they were adjusted considering the H<sup>+</sup>/OH<sup>-</sup> concentration.

Furthermore, the units of these kinetic constants ( $L \cdot mol^{-1} \cdot s^{-1}$ ) are different than the units of kog, kgg and kfg ( $s^{-1}$ ).

**Table 1.** Activation energy (kJ/mol) and pre-exponential factor of the fitted kinetic constants for cellulose hydrolysis in pressurized water. P=27MPa.

Kinetic	Ea	Ea error	Ln Ao	Ln Ao error	R <sup>2</sup>
kog	182.2	30.3	35.7	5.9	0.97
kgg	151.4	32.7	28.4	6.4	0.96
kgf	403.6	97.0	94.4	18.8	0.95
kfh	449.6	95.2	101.1	18.5	0.96
kfg	180.6	36.0	35.8	7.0	0.96

### 3. Conclusions

The process presented in this work shows an efficient alternative to hydrolyze cellulose selectively. The control of the residence time is the key to obtain a selectivity higher than 95% w-w<sup>-1</sup> of soluble sugars or 60% w-w<sup>-1</sup> of glycolaldehyde. From the viewpoint of chemistry, the selectivity of the process would be governed by the hydroxide anion concentration.

### 4. Materials and Methods

#### 4.1. Materials

The cellulose (99%) used in the experiments was purchased from VWR. Distilled water was used as reaction medium in the experiments. The standards used in HPLC (High Performance Liquid Chromatography) analysis were: cellobiose (+98%), glucose (+99%), fructose (+99%), glyceraldehyde (95%), pyruvaldehyde (40%), glycolaldehyde dimer (99%), levulinic acid (+99%), (5-HMF) 5-hydroxymethylfurfural (99%) purchased from Sigma.

#### 4.2. Analysis

Each sample was centrifuged and filtered in order to recover solids and calculate the conversion. The carbon content of the liquid samples was determined by TOC analysis with Shimadzu TOC-VCSH equipment. The composition of the samples was analyzed by HPLC (IR-UV/Vis) with a sugar column Shodex SH1011, The oligosaccharides concentration was

determined following the 'Determination of Structural Carbohydrates and Lignin in Biomass' report [31].

The cellulose conversion was determined by equation S.1, where  $X$  is the cellulose conversion,  $W_0$  is the inlet cellulose concentration measured in g cellulose/g total,  $W$  is the outlet cellulose concentration measured in g cellulose/g total.

$$X = \frac{W_0 - W}{W_0} \quad (\text{S.1})$$

The carbon content of the liquid products was determined by total organic carbon (TOC) analysis with Shimadzu TOC-VCSH equipment. The composition of the liquid products was determined by High Performance Liquid Chromatography (HPLC) analysis. The HPLC column used for the separation of the compounds was Sugar SH-1011 Shodex at 50°C using H<sub>2</sub>SO<sub>4</sub> (0.01 N) as mobile phase with a flow rate of 0.8mL/min. A Waters IR detector 2414 was used to identify and quantify the sugars and their derivatives. An UV-Vis detector was used to determine the 5-hydroxy-methyl-furfural (5-HMF) concentration at a wavelength of 254nm.

The selectivity of each compound ( $S_i$ ) was calculated as the ratio of: compound carbon composition ( $X_c$ ) multiplied by compound concentration ( $C_i$ ) and total carbon at the reactor inlet (TC).  $S_i = C_i X_c / TC$ .

#### 4.3. Model

The model was solved using the Matlab®. The used function to solve the system of equation was ode45. The kinetic constants were fitted using the function lsqcurvefit. More detail of the mathematical resolution were published in a previous work [1].

#### 4.4. Experimental Setup

The pilot plant was continuously operated at temperatures of up to 400°C and pressures of up to 30 MPa. The cellulose suspension (7% w-w<sup>-1</sup>) was pumped to the reactor at room temperature. The heating of this stream was done at the reactor inlet by mixing it with a supercritical water stream (inlet concentration 1.5% w-w<sup>-1</sup>). The reaction was cooled by sudden expansion. A detailed description of the pilot plant and of the operation procedure were presented in a previous work [1]. The main working advantages of the pilot plat are: (a) the reactor can be considered isothermal due to the instantaneous heating and cooling; (b), products not diluted in the cooling process; (c) the residence time is varied from 0.004 s to 40 s using tubular reactors of different lengths.

## References

1. Ragauskas, A.J., Williams, C.K., Davison, B.H., Britovsek, G., Cairney, J., Eckert, C.A., Frederick, W.J., Hallett, J.P., Leak, D.J., Liotta, C.L., Mielenz, J.R., Murphy, R., Templer, R., and Tschaplinski, T., *The Path Forward for Biofuels and Biomaterials*. Science, 2006. 311(5760): p. 484 -489.
2. Klemm, D., Heublein, B., Fink, H.P., and Bohn, A., *Cellulose: Fascinating Biopolymer and Sustainable Raw Material*. Angewandte Chemie International Edition, 2005. 44(22): p. 3358-3393.
3. Tollefson, J., *Energy: Not your father's biofuels*. Nature News, 2008. 451(7181): p. 880-883.
4. Arai, K., Smith Jr, R.L., and Aida, T.M., *Decentralized chemical processes with supercritical fluid technology for sustainable society*. The Journal of Supercritical Fluids, 2009. 47(3): p. 628-636.
5. Aida, T.M., Sato, Y., Watanabe, M., Tajima, K., Nonaka, T., Hattori, H., and Arai, K., *Dehydration of D-glucose in high temperature water at pressures up to 80 MPa*. The Journal of Supercritical Fluids, 2007. 40(3): p. 381-388.
6. Aida, T.M., Tajima, K., Watanabe, M., Saito, Y., Kuroda, K., Nonaka, T., Hattori, H., Smith Jr, R.L., and Arai, K., *Reactions of D-fructose in water at temperatures up to 400 °C and pressures up to 100 MPa*. The Journal of Supercritical Fluids, 2007. 42(1): p. 110-119.
7. Kabyemela, B.M., Adschiri, T., Malaluan, R.M., and Arai, K., *Glucose and Fructose Decomposition in Subcritical and Supercritical Water: Detailed Reaction Pathway, Mechanisms, and Kinetics*. Industrial & Engineering Chemistry Research, 1999. 38(8): p. 2888-2895.
8. Kabyemela, B.M., Adschiri, T., Malaluan, R.M., Arai, K., and Ohzeki, H., *Rapid and Selective Conversion of Glucose to Erythrose in Supercritical Water*. Industrial & Engineering Chemical Research, 1997. 36(12): p. 5063-5067.
9. Ruppert, A.M., Weinberg, K., and Palkovits, R., *Hydrogenolysis Goes Bio: From Carbohydrates and Sugar Alcohols to Platform Chemicals*. Angewandte Chemie International Edition, 2012. 51(11): p. 2564-2601.

10. Luo, C., Wang, S., and Liu, H., *Cellulose Conversion into Polyols Catalyzed by Reversibly Formed Acids and Supported Ruthenium Clusters in Hot Water*. *Angewandte Chemie International Edition*, 2007. 46(40): p. 7636–7639.
11. Shuai, L. and Pan, X., *Hydrolysis of cellulose by cellulase-mimetic solid catalyst* *Energy & Environmental Science*, 2012.
12. Wyman, C.E., Dale, B.E., Elander, R.T., Holtzapple, M., Ladisch, M.R., and Lee, Y.Y., *Comparative sugar recovery data from laboratory scale application of leading pretreatment technologies to corn stover*. *Bioresource Technology*, 2005. 96(18): p. 2026-2032.
13. Rinaldi, R., Palkovits, R., and Schüth, F., *Depolymerization of Cellulose Using Solid Catalysts in Ionic Liquids*. *Angewandte Chemie International Edition*, 2008. 47(42): p. 8047–8050.
14. Morales-delaRosa, S., Campos-Martin, J.M., and Fierro, J.L.G., *High glucose yields from the hydrolysis of cellulose dissolved in ionic liquids*. *Chemical Engineering Journal*, 2012. 181-182: p. 538-541.
15. Cantero, D.A., Bermejo, M.D., and Cocero, M.J., *Kinetic analysis of cellulose depolymerization reactions in near critical water*. *The Journal of Supercritical Fluids*, 2013. 75: p. 48-57.
16. Cantero, D.A., Bermejo, M.D., and Cocero, M.J., *High glucose selectivity in pressurized water hydrolysis of cellulose using ultra-fast reactors*. *Bioresource Technology*, 2013. 135: p. 697-703.
17. Sasaki, M., Adschiri, T., and Arai, K., *Kinetics of cellulose conversion at 25 MPa in sub- and supercritical water*. *AIChE Journal*, 2004. 50(1): p. 192-202.
18. Ehara, K. and Saka, S., *Decomposition behavior of cellulose in supercritical water, subcritical water, and their combined treatments*. *Journal of Wood Science*, 2005. 51(2): p. 148-153.
19. Zhao, Y., Lu, W.-J., and Wang, H.-T., *Supercritical hydrolysis of cellulose for oligosaccharide production in combined technology*. *Chemical Engineering Journal*, 2009. 150(2–3): p. 411-417.
20. Kumar, S. and Gupta, R.B., *Hydrolysis of Microcrystalline Cellulose in Subcritical and Supercritical Water in a Continuous Flow Reactor*. *Industrial & Engineering Chemistry Research*, 2008. 47(23): p. 9321-9329.

21. Schacht, C., Zetzl, C., and Brunner, G., *From plant materials to ethanol by means of supercritical fluid technology*. *The Journal of Supercritical Fluids*, 2008. 46(3): p. 299-321.
22. Akizuki, M., Fujii, T., Hayashi, R., and Oshima, Y., *Effects of water on reactions for waste treatment, organic synthesis, and bio-refinery in sub- and supercritical water*. *Journal of Bioscience and Bioengineering*.
23. Wagner, W, Cooper, J, R., Dittmann, et al., *The IAPWS industrial formulation 1997 for the thermodynamic properties of water and steam*. 2000, American Society of Mechanical Engineers: New York, N, ETATS-UNIS.
24. Marshall, W.L. and Franck, E.U., *Ion Product of Water Substance, 0-1000°C, 1-10,000 Bars. New International Formulation and Its Background*. *Journal of Physical and Chemical Reference Data*, 1981. 10(2): p. 295-304.
25. Akiya, N. and Savage, P.E., *Roles of Water for Chemical Reactions in High-Temperature Water*. *Chemical Reviews*, 2002. 102(8): p. 2725-2750.
26. Kruse, A. and Gawlik, A., *Biomass Conversion in Water at 330–410 °C and 30–50 MPa. Identification of Key Compounds for Indicating Different Chemical Reaction Pathways*. *Industrial & Engineering Chemistry Research*, 2002. 42(2): p. 267-279.
27. Weingärtner, H. and Franck, E.U., *Supercritical Water as a Solvent*. *Angewandte Chemie International Edition*, 2005. 44(18): p. 2672–2692.
28. Promdej, C. and Matsumura, Y., *Temperature Effect on Hydrothermal Decomposition of Glucose in Sub- And Supercritical Water*. *Industrial & Engineering Chemistry Research*, 2011. 50(14): p. 8492-8497.
29. Sasaki, M., Goto, K., Tajima, K., Adschiri, T., and Arai, K., *Rapid and selective retro-aldol condensation of glucose to glycolaldehyde in supercritical water*. *Green Chem.*, 2002. 4(3): p. 285-287.
30. Assary, R.S., Kim, T., Low, J.J., Greeley, J., and Curtiss, L.A., *Glucose and fructose to platform chemicals: understanding the thermodynamic landscapes of acid-catalysed reactions using high-level ab initio methods*. *Physical Chemistry Chemical Physics*, 2012. 14(48): p. 16603-16611.
31. A. Sluiter, B.H., R. Ruiz, C. Scarlata, J. Sluiter, D. Templeton, and D. Crocker, *Determination of Structural Carbohydrates and Lignin in Biomass 2012*, National Renewable Energy Laboratory.



# Chapter 4. Pressure and Temperature Effect on Cellulose Hydrolysis Kinetic in Pressurized Water

## Abstract

In this study, the effect of temperature and pressure on cellulose and glucose hydrolysis in a hydrothermal media is analyzed. To do so, hydrolysis experiments were carried out in a continuous pilot plant capable of operating up to 400°C, 27 MPa and residence times between 0.004 s and 40 s. This is possible by using an instantaneous heating system consisting of supercritical water injection and cooling by sudden depressurization of the hot product stream. Cellulose hydrolysis produced oligosaccharides, cellobiose, glucose and fructose. In general, concentration profiles of each component were similar for the same temperature and different pressures. Nevertheless, glucose and fructose hydrolysis reaction to give decomposition products were strongly affected by changing the pressure, which is equivalent to changing the density. When increasing temperature, the reaction of glucose isomerization to fructose was inhibited, and the production of 5-hydroxymethylfurfural (5-HMF) obtained through fructose dehydration was also inhibited. On the other hand, 5-HMF production was favored by high hydroxide anion concentrations. Thus, at a constant temperature, the production of 5-HMF was increased by rising density (increasing pressure). The production of glycolaldehyde (retro-aldol condensation of glucose) was increased by increasing pressure and temperature. The kinetic constants of cellulose hydrolysis were fitted using the experimental data. Pressure seems to have no effect on the cellulose hydrolysis kinetic to simple

sugars, and at subcritical temperatures the kinetic of glucose hydrolysis reactions did not show significant changes by increasing pressure. However, at 400°C glucose isomerization and dehydration reactions were diminished by increasing pressure while glucose retro-aldol condensation were enhanced.

**Keywords:** Activation Volume • Biorefinery • Glycolaldehyde • Ionic Product • Selectivity • 5-HMF

## 1. Introduction

Vegetal biomass chemical transformations have been intensively studied in the last years looking for a renewable sources of chemicals and fuels [1]. Cellulose is generally the major compound of vegetal biomass representing the most abundant biopolymer in nature[2]. Cellulose depolymerization was studied following different methods in order to obtain valuable compounds like soluble sugars [3-6], lactic acid [7] or 5-hydroxymethylfurfural (5-HMF) [8, 9] among others.

Cellulose conversion into these kind of products depends on the reaction medium and the reactions conditions. The use of supercritical fluids as reaction medium is a promising alternative in the biomass upgrading due to the possibility of tuning medium properties by changing pressure and temperature. Supercritical water (SCW) is water at temperature and pressure above its critical point ( $T_c=374^\circ\text{C}$  and  $P_c=22.1\text{ MPa}$ ). The properties of water can be highly varied by changing pressure and temperature in the neighborhood of its critical point. The different identities that water could adopt by changing pressure and temperature will affect the reaction medium favoring some kind of reactions over others. Two important properties of water as reaction medium are density and ionic product. The density of the medium is a measurement of the water molecules population per volume. The water concentration is an important factor to take into account in the reactions where water participates, both as reagent or forming intermediate states[10]. The ionic product of water ( $K_w$ ) represents how dissociated are water molecules (ion concentration). This property could be modified in order to favor or disfavor the acid/basis catalysis. The variations of these two properties of water in the surroundings of the critical point are shown in Figure 1 [11, 12]. Significant variations in density and ionic product can be obtained at  $400^\circ\text{C}$  by increasing pressure in the range 150 – 300 bar. However, at subcritical temperatures changes in properties with pressure are softer than at  $400^\circ\text{C}$  (less than 10%). Important changes in the identity of the medium can be obtained if temperature and pressure are changed at the same time. For example, density of water at  $300^\circ\text{C}$  and 27 MPa is around  $750\text{ kg/m}^3$ ; this value can be decreased to  $130\text{ kg/m}^3$  if the conditions are modified to  $400^\circ\text{C}$  and 23MPa. Ion product of water at  $300^\circ\text{C}$  and 27 MPa is around  $10^{-11}\text{ mol}^2\cdot\text{l}^{-2}$  which means that medium has high concentration of ions ( $[\text{H}^+]$  and  $[\text{OH}^-]$ ) favoring the ionic reactions [13-15]. The ionic product

of water will take a value of  $10^{-21} \text{ mol}^2 \cdot \text{l}^{-2}$  if the temperature and pressure are changed to  $400^\circ\text{C}$  and  $23 \text{ MPa}$  favoring radical reactions [16].

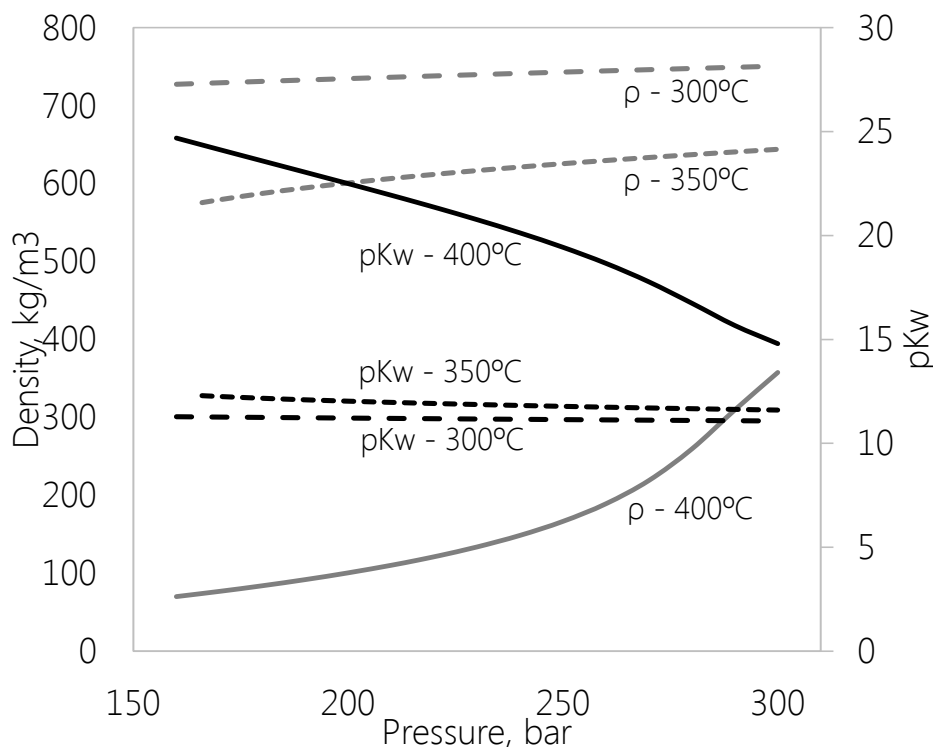


**Fig. 1.** Density and ionic product of water at different temperatures along pressure. Black lines: minus logarithmic of ionic product; grey lines: density. Continuous lines refer to  $400^\circ\text{C}$ ; dashed lines refer to  $350^\circ\text{C}$  and spaced dashed lines refer to  $300^\circ\text{C}$ .

Cellulose hydrolysis in pressurized water medium was studied in different kind of reactors; batch [17-19], semi-continuous [20] and continuous [3, 21-27]. Batch experiments of cellulose hydrolysis can be done with quite simple equipment allowing fast and non-expensive results. However, the process control ( $t_r$ ,  $T$ ) is poor, making difficult to obtain products with high selectivity. Therefore, the products of these kinds of processes are usually divided into fractions: bio-oils; water soluble; solids and; gases. The main difficulty of the continuous process is the steady supply of cellulose (solid, non-soluble in water) to the reactor due to the possible pump clogging. However, this problem can be overcome by scaling-up of the process using higher flows [1]. The hydrolysis and modification of cellulose in a hydrothermal medium can be controlled in a continuous reactor by simply varying  $T$ ,  $P$  and  $t_r$ . Hence, the continuous process allows higher selectivity than the batch processes. So far, the maximum selectivity achieved by continuous cellulose hydrolysis was almost  $70\% \text{ w} \cdot \text{w}^{-1}$  and less than  $20\% \text{ w} \cdot \text{w}^{-1}$  for soluble sugars or fragmented products respectively [21-23, 27]. Recently, our research group could improve the selectivity obtaining sugars or pyruvaldehyde selectivity of  $98\% \text{ w} \cdot \text{w}^{-1}$  and

40% w·w<sup>-1</sup> respectively by using a novel reactor [3]. The sugars obtained after biomass hydrolysis were susceptible to be further modified in a hot pressurized water medium in order to obtain high added value products like glycolaldehyde, poly-alcohols or 5-hydroxy-methyl-furfural (5-HMF) [13, 28-30].

In this work, the effect of pressure, temperature (medium properties) and residence time on cellulose hydrolysis in a hydrothermal medium were analyzed and the experimental data were used to fit kinetic parameters of the reactions involved.

## 2. Materials and Methods

### 2.1. Materials

Microcrystalline cellulose (99%) used in the experiments was purchased from VWR. Distilled water was used as reaction medium in the experiments. The standards used in HPLC (High Performance Liquid Chromatography) analysis were: cellobiose (+98%), glucose (+99%), fructose (+99%), glyceraldehyde (95%), pyruvaldehyde (40%), glycolaldehyde dimer (99%), levulinic acid (+99%), (5-HMF) 5-hydroxymethylfurfural (99%) purchased from Sigma.

### 2.2. Analysis

The cellulose conversion was determined by equation 1, where  $X$  is the cellulose conversion,  $W_0$  is the inlet cellulose concentration measured in g cellulose/g total,  $W$  is the outlet cellulose concentration measured in g cellulose/g total.

$$X = \frac{W_0 - W}{W_0} \quad (1)$$

The carbon content of the liquid products was determined by total organic carbon (TOC) analysis with Shimadzu TOC-VCSH equipment. The composition of the liquid products was determined by High Performance Liquid Chromatography (HPLC) analysis. The HPLC column used for the separation of the compounds was Sugar SH-1011 Shodex at 50°C using H<sub>2</sub>SO<sub>4</sub> (0.01 N) as mobile phase with a flow rate of 0.8mL/min. A Waters IR detector 2414 was used to identify and quantify the sugars and their derivatives. A Waters UV-Vis detector was used to determine the 5-hydroxy-methyl-furfural (5-HMF) concentration at a wavelength of 254nm.

### 2.3. Experimental set-up

A continuous pilot plant designed to operate at 400°C was used to perform the experiments. A scheme of the experimental set up is presented in Figure 2. The cellulose hydrolysis pilot plant could operate at temperatures up to 400°C and pressures of up to 30 MPa. A cellulose

suspension ( $7\% \text{ w}\cdot\text{w}^{-1}$ ) was continuously pumped up to the operation pressure and remains at room temperature up to the reactor's inlet. In that point it is instantaneously heated by mixing it with a supercritical water stream. In this way, heating of cellulose (start of the reactions) is achieved almost instantaneously [3]. Mixing ratio of cold and hot streams mixing was chosen in order to obtain a biomass concentration at the reactor inlet of approximately  $1.5\% \text{ w}\cdot\text{w}^{-1}$ . Reactor effluent was cooled (stopping the reaction) by sudden expansion obtaining an instantaneous cooling from the reaction temperature to  $100 \pm 10^\circ\text{C}$ . More detailed descriptions of the pilot plant and the operation procedure were presented in a previous work[3].

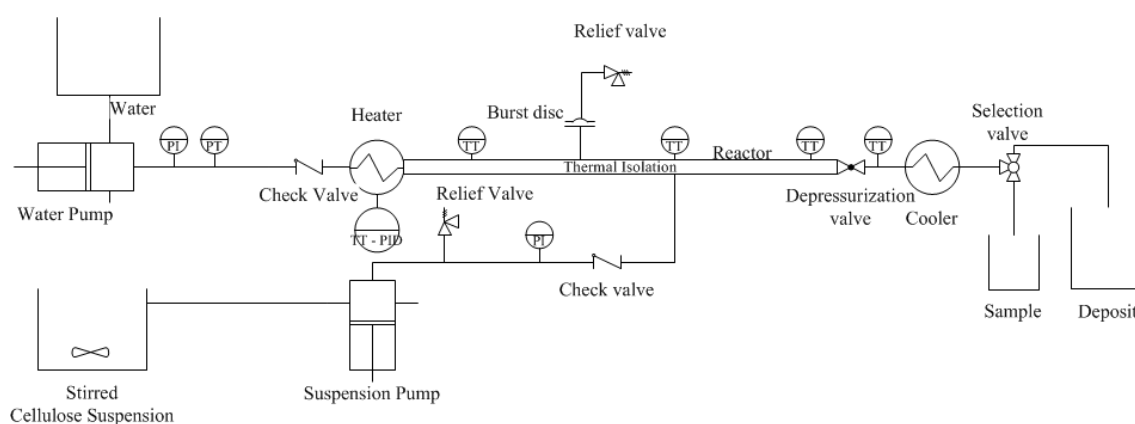


Fig. 2. Schema of the pilot plant.

The main achievements of the experimental setup are: (a) the reactor can be considered isothermal due to the instantaneous heating and cooling; (b), products are not diluted in the cooling process; (c) the residence time is varied from 0.004 s to 40 s using Ni-alloy tubular reactors of different lengths.

### 3. Reaction Modeling

The reaction pathway of cellulose hydrolysis can be analyzed by dividing it in three main steps: 1) cellulose hydrolysis to produce oligosaccharides; 2) hydrolysis of oligosaccharides to produce glucose and; 3) the different glucose degradation reactions (isomerization, dehydration or retro-aldol condensation). A scheme (Figure 3) of the supposed reaction pathway was built from reaction pathways found in literature [31, 32]. A detailed analysis of the two first steps of cellulose hydrolysis was presented in a previous work [33]. In this work, the kinetic analysis was focused in glucose hydrolysis reactions. In figure 3 it is shown that glucose could follow two main degradation pathways: 1) isomerization step to form fructose

or 2) retro-aldol condensation to produce glycolaldehyde and erythrose; erythrose also follows an additional retro-aldol condensation producing glycolaldehyde as final product. So, one glucose molecule produces three molecules of glycolaldehyde. Another minor reaction of glucose is its dehydration to produce 1,6-anhydroglucose.

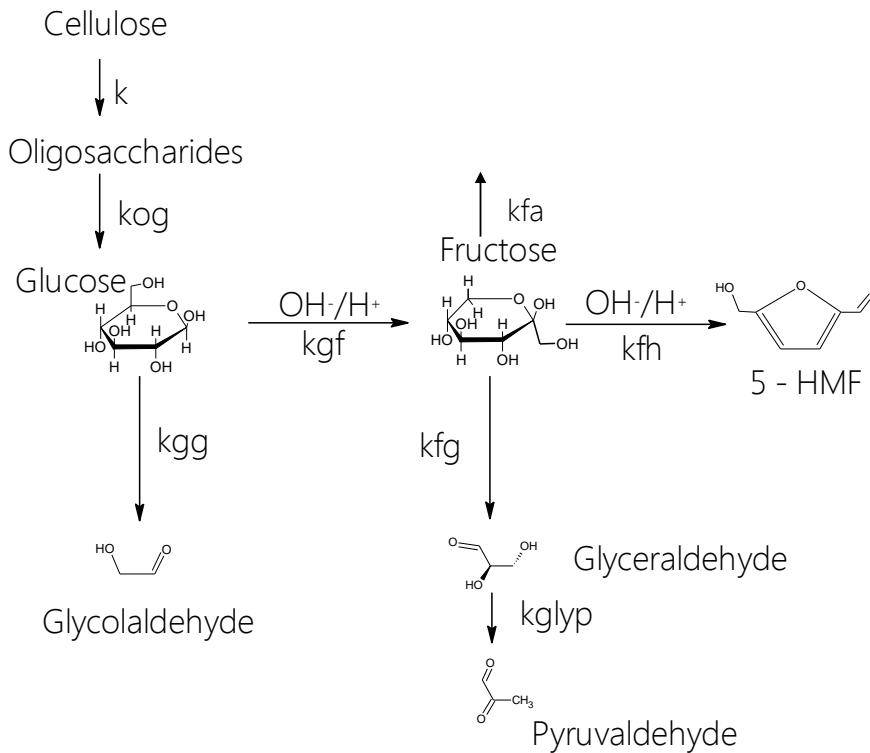


Figure 3. Reaction pathway for cellulose and glucose hydrolysis in pressurized water.

A mathematical model was developed in order to calculate concentrations profiles of the main derivatives of cellulose hydrolysis along the residence time at different conditions of pressure and temperature. The model was developed taking into account the  $\text{OH}^-$  concentration in the reactions of glucose isomerization and fructose dehydration. The role of hydroxide anion concentration was analyzed in Chapter 4. The concentration of glucose was calculated as shown in equation 2. Where  $n_g$  is the concentration of glucose in  $\text{mol}\cdot\text{L}^{-1}$  (M);  $z$  is the length of the reactor in m;  $\rho$  is the density of the reaction medium in  $\text{kg}\cdot\text{m}^{-3}$ ;  $S$  is the cross section of the tubular reactor in  $\text{m}^2$  and;  $M$  is the mass flow through the reactor in  $\text{kg}\cdot\text{s}^{-1}$ . The kinetic parameters used in equation 2 were obtained in a previous work [33]. The molar concentration of each component was represented as  $n$  (mol/L), where the subscripts:  $og$ ,  $cello$  and  $OH$  refer to oligosaccharides, cellobiose and hydroxide anions respectively.  $CW_{og}$  is the carbon weight of the oligosaccharide monomer molecule (g/mol).  $MW_{og}$  is the molecular weight of the oligosaccharide monomer molecule. The constants were represented as  $k$  ( $\text{s}^{-1}$ ),

where the subscripts: *og*, *h*, *gf*, *gg* and *ga* refer to oligosaccharide hydrolysis, cellobiose hydrolysis, glucose to fructose isomerization, glucose to glycolaldehyde and, glucose dehydration.

$$\frac{dn_g}{dz} = \frac{\rho S}{\dot{M}} \left[ k_{og} n_{og} \frac{CW_{og}}{CW_g MW_g} + 2k_h n_{cello} - (k_{gf} n_{OH} + k_{gg} + k_{ga}) n_g \right] \quad (2)$$

The concentration of fructose was determined as shown in equation 3, where  $n_f$  is the molar concentration of fructose (M). The subscripts *fh*, *fa* and *fg* refer to 5-HMF formation, fructose to acids and fructose retro-aldol condensation reactions. The units of the kinetic constants  $k_{gf}$  and  $k_{fh}$  were  $\text{L}\cdot\text{mol}^{-1}\cdot\text{s}^{-1}$ .

$$\frac{dn_f}{dl} = \frac{\rho S}{\dot{M}} \left[ k_{gf} n_g n_{OH} - (k_{fh} n_{OH} + k_{fa} + k_{fg}) n_f \right] \quad (3)$$

The concentration of 5-HMF was calculated as shown in equation 4, where  $n_h$  is the molar concentration of 5-HMF (M).

$$\frac{dn_h}{dl} = \frac{\rho S}{\dot{M}} \left[ k_{fh} n_{OH} n_f \right] \quad (4)$$

The concentrations of glycolaldehyde and glyceraldehyde were calculated by equation 5 and 6 respectively.

$$\frac{dn_{glyco}}{dl} = \frac{\rho S}{\dot{M}} \left[ 3k_{gg} n_g \right] \quad (5)$$

$$\frac{dn_{gly}}{dl} = \frac{\rho S}{\dot{M}} \left[ 2k_{fg} n_f - k_{glyp} n_{gly} \right] \quad (6)$$

Where  $n_{glyco}$  is the molar concentration of glycolaldehyde;  $n_{gly}$  is the molar concentration of glyceraldehyde and;  $k_{glyp}$  is the kinetic constant of the reaction of glyceraldehyde to pyruvaldehyde isomerization. Pyruvaldehyde concentration was calculated as in a previous work [33] by equation 7.

$$\frac{dn_{pyr}}{dl} = \frac{\rho S}{\dot{M}} \left[ k_{glyp} n_{gly} - k_p n_p \right] \quad (7)$$

The values of the kinetic constants  $k_{og}$ ,  $k_{gf}$ ,  $k_{fh}$ ,  $k_{gg}$  and  $k_{fg}$  were fitted by comparing the experimental concentration profiles to the profiles calculated by the model using the Matlab® function *lsqcurvefit*. Further information about model resolution can be found in a previous work [33].

## 4. Results and discussion

The reactions of cellulose hydrolysis in hot pressurized water were analyzed at 300°C (10 MPa, 18 MPa, 23 MPa and 27 MPa), 350°C (10 MPa, 18 MPa and 23 MPa) and 400°C (23 MPa, 25 MPa and 27 MPa). In this range of conditions, the density ( $\rho$ ) of the medium was varied from 150 to 750 kg·m<sup>-3</sup>; the ionic product ( $pK_w$ ) was varied from 11 to 21 mol<sup>2</sup>·kg<sup>2</sup> and the dielectric constant ( $\epsilon$ ) was varied from 2 to 22. The carbon balance between the inlet and outlet of the reactor were in the range 88 – 100% for all the experiments.

### 4.1. Experimental concentration profiles

#### 4.1.1. Cellulose hydrolysis kinetics

The results of cellulose conversion along residence time at 400°C, 350°C and 300°C are shown in figure 4-A, 4-B and 4-C respectively. The lowest residence times tested for 400°C were 15 ms, 13 ms and 17 ms for 23 MPa, 25 MPa and 27 MPa respectively. At those residence times no cellulose was found in the products and thus, the conversion was  $X=1$  for all the experimental conditions analyzed at 400°C. In a previous work, the residence time for total cellulose conversion at 25 MPa was determined to be 15 ms [3]. At 350°C and 300°C pressure seems to have no effect in the kinetics of cellulose depolymerization.

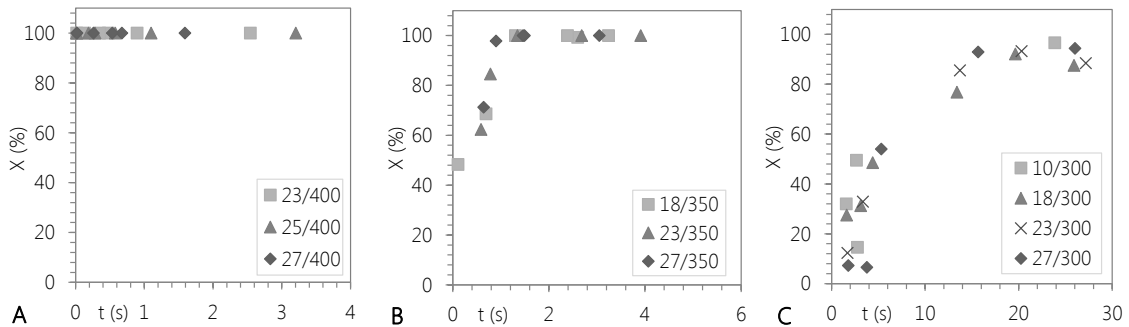


**Fig. 4.** (A) Cellulose conversion at 400°C; (■) P= 23 MPa; (▲) P=25 MPa and; (◆) P= 27 MPa. (B) Cellulose conversion at 350°C; (■) P= 18 MPa; (▲) P=23 MPa and; (◆) P= 27 MPa. (C) Cellulose conversion at 300°C; (■) P= 10 MPa; (▲) P=18 MPa; (x) P=23 MPa and; (◆) P= 27 MPa.

Experimental data shown in figure 4 were used to obtain the kinetics of cellulose hydrolysis according equation 8. Where  $X$  is the cellulose conversion (determined experimentally by equation 1);  $t$  is the residence time (s) and;  $k$  is the kinetic constant of cellulose hydrolysis (s<sup>-1</sup>) according the expression proposed by Sasaki et al [31].

$$\frac{dX}{dt} = 2k(1 - X)^{1/2} \quad (8)$$

The  $k$  values were plotted in Figure 5 along with the analogous values developed for a pressure of 25 MPa [33]. Similar values were obtained, showing that the pressure had no effect on the kinetics of cellulose hydrolysis in the studied range of pressure. If the kinetics of cellulose hydrolysis is analyzed along temperature, a break point around the critical point of water can be appreciated. At temperatures higher than 374°C the depolymerization reaction rate is increased faster than at lower temperatures. This phenomenon can be explained considering that cellulose could be dissolved in supercritical water due to the change of the reaction medium identity. Therefore, the reaction of hydrolysis would occur in a homogeneous phase, avoiding the mass transfer limitations [31, 33].

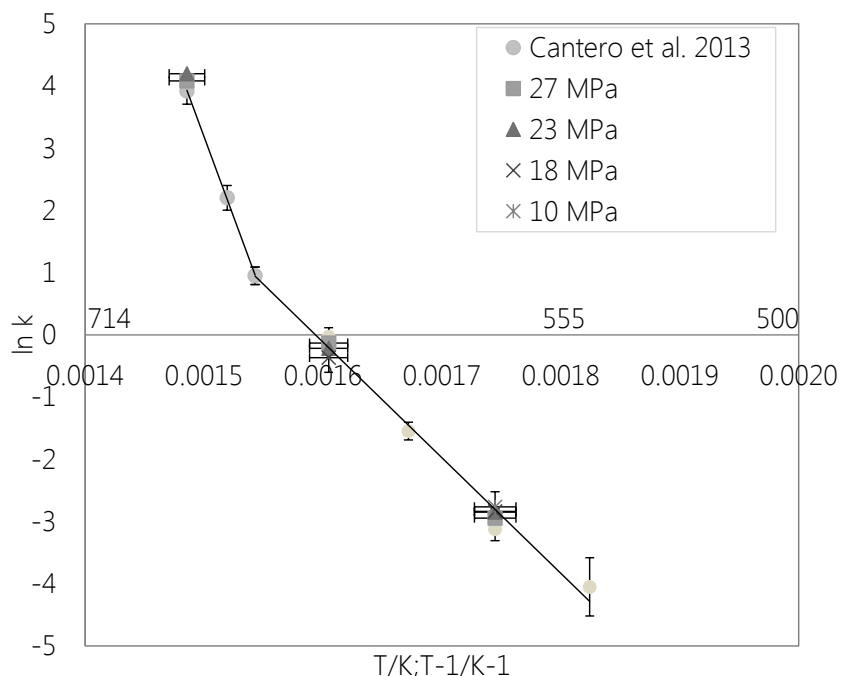


**Fig. 5.** Cellulose hydrolysis kinetic constant between 275°C and 400°C at (■) P= 27 MPa; (●) P=25 MPa; (▲) P=23 MPa and; (x) P= 18 MPa and; (\*) 10 MPa. The continuous line was taken from a previous work [33]. Error bars ( $\pm$  s.d.).

#### 4.1.2. Cellobiose

The concentration profiles of cellobiose (glucose disaccharide) at different pressures along residence time at 400°C, 350°C and 300°C are shown in Figure 6-A, 6-B and 6-C respectively. A maximum in the concentration of cellobiose was achieved at each considered temperature, at residence times of 0.016 s, 2 s and 15 s for 400°C, 350°C and 300°C respectively, being highest concentration at the maximum temperature investigated, 400°C and the lowest pressure (23MPa). Thus, the cellobiose production was reduced when the pressure was

increased and reaction temperature was reduced. These results agree with those found in literature [21], if it is had into account that, the maximum cellobiose selectivity is obtained at lower temperatures if the lowest analyzed residence time is higher than 1 second [27].

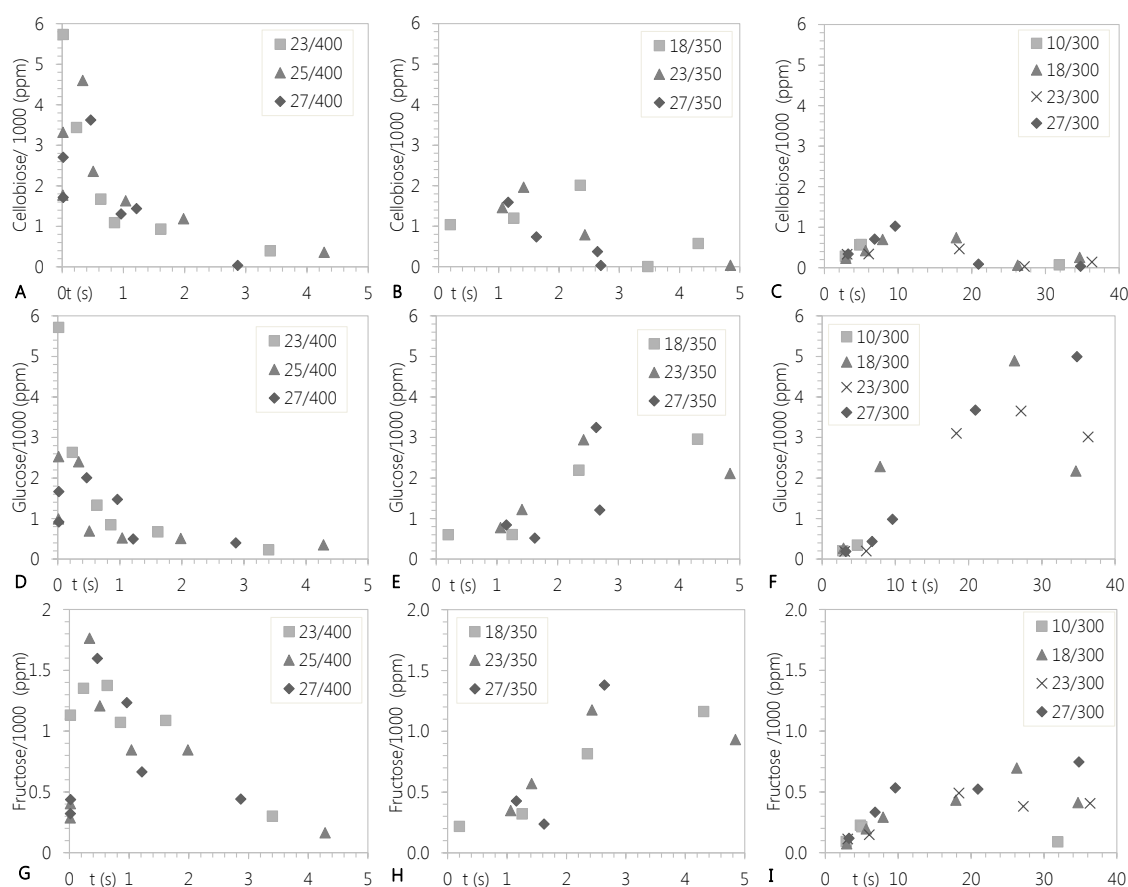


**Fig. 6.** (A) Cellobiose concentration at 400°C; (■) P= 23 MPa; (▲) P=25 MPa and; (◆) P= 27 MPa. (B) Cellobiose concentration at 350°C; (■) P= 18 MPa; (▲) P=23 MPa and; (◆) P= 27 MPa. (C) Cellobiose concentration at 300°C; (■) P= 10 MPa; (▲) P=18 MPa; (x) P=23 MPa and; (◆) P= 27 MPa. (D) Glucose concentration at 400°C; (■) P= 23 MPa; (▲) P=25 MPa and; (◆) P= 27 MPa. (E) Glucose concentration at 350°C; (■) P= 18 MPa; (▲) P=23 MPa and; (◆) P= 27 MPa. (F) Glucose concentration at 300°C; (■) P= 10 MPa; (▲) P=18 MPa; (x) P=23 MPa and; (◆) P= 27 MPa. (G) Fructose concentration at 400°C; (■) P= 23 MPa; (▲) P=25 MPa and; (◆) P= 27 MPa. (H) Fructose concentration at 350°C; (■) P= 18 MPa; (▲) P=23 MPa and; (◆) P= 27 MPa. (I) Fructose concentration at 300°C; (■) P= 10 MPa; (▲) P=18 MPa; (x) P=23 MPa and; (◆) P= 27 MPa.

#### 4.1.3. Glucose

The glucose concentration profiles along residence time at different pressures at 400°C, 350°C and 300°C were plotted in Figure 6-D, 6-E and 6-F respectively. The glucose production followed a similar behavior than that of cellobiose. Nevertheless, high quantities of glucose were found in all the experimented temperatures. The literature data show high glucose concentration (14 – 35 %  $w \cdot w^{-1}$ ) at 300°C [22, 23, 26, 27]. The disadvantage of working at

350°C or 300°C is that high residence times are needed which also favor the reactions of glucose hydrolysis, and favoring the apparition of other compounds.

#### **4.1.4. Fructose**

The fructose concentrations along residence time at different pressures at 400°C, 350°C and 300°C are shown in Figure 6-G, 6-H and 6-I respectively. The highest selectivity of fructose were achieved at 400°C and 350°C at a residence time around 0.3 s and 2 s respectively. The maximum concentrations of fructose were lower than the concentrations of cellobiose and glucose (almost 20% compared with glucose). Although the peak concentration of fructose at 400°C was found at 25 MPa and 27 MPa (one experimental point), for the other analyzed residence times the higher concentrations were achieved at a pressure of 23 MPa. The reaction of glucose isomerization to produce fructose takes place via ring-opening producing several transition states (keto-enol tautomerism). This reaction was slowed down when pressure was increased. Kabyemela et al [34] obtained a similar behavior working in glucose hydrolysis. They concluded that the reaction of glucose isomerization to produce fructose is retarded by increasing pressure when the working temperature is above the critical point of water.

#### **4.1.5. Glyceraldehyde**

The glyceraldehyde concentration along residence time at the experimented pressures and temperatures are shown in Figure 7-A, 7-B and 7-C. The maximum amount of glyceraldehyde was achieved at 400°C and 350°C with residence times of 0.5 s and 2 s respectively. In this case, the pressure seems to have no effect in the production of glyceraldehyde at 350°C or 300°C. However, at 400°C the concentration of glyceraldehyde was slightly increased by decreasing the pressure.

#### **4.1.6. Glycolaldehyde**

The values of glycolaldehyde concentration obtained at different pressures for 400°C, 350°C and 300°C are shown in Figure 7-D, 7-E and 7-F respectively. The maximum concentration of glycolaldehyde (around 8000 ppm) was achieved at 400°C, 27 MPa and 1 s of residence time. An increase in the pressure improved the production of glycolaldehyde for all the experimented temperatures. If the concentration profiles of glycolaldehyde are analyzed along temperature, it is observed that increasing temperature, the production of glycolaldehyde was highly increased in the studied range. Peak concentrations of glycolaldehyde at 300 and 350°C were around 3000 ppm and 4000 respectively.

#### 4.1.7. 5-HMF

The 5-HMF concentration profiles obtained at 400°C, 350°C and 300°C were plotted in Figure 7-G, 7-H and 7-I respectively. The production of 5-HMF was highly inhibited at temperatures higher than the critical temperature of water. The maximum concentration was obtained at the lowest experimented temperature with 25 s of residence time. For all the investigated temperatures, an increase in pressure increased the production of 5-HMF. Different data about the 5-HMF behavior can be found in literature. Sasaki et al. [21] and Ehara et al. [22] obtained low concentration of 5-HMF at supercritical conditions ( $\approx 0.1\% w-w^{-1}$ ). Nevertheless, Zhao et al [23] and Kumar et al [27] obtained similar values of 5-HMF selectivity at sub and supercritical conditions ( $\approx 8\% w-w^{-1}$ ).

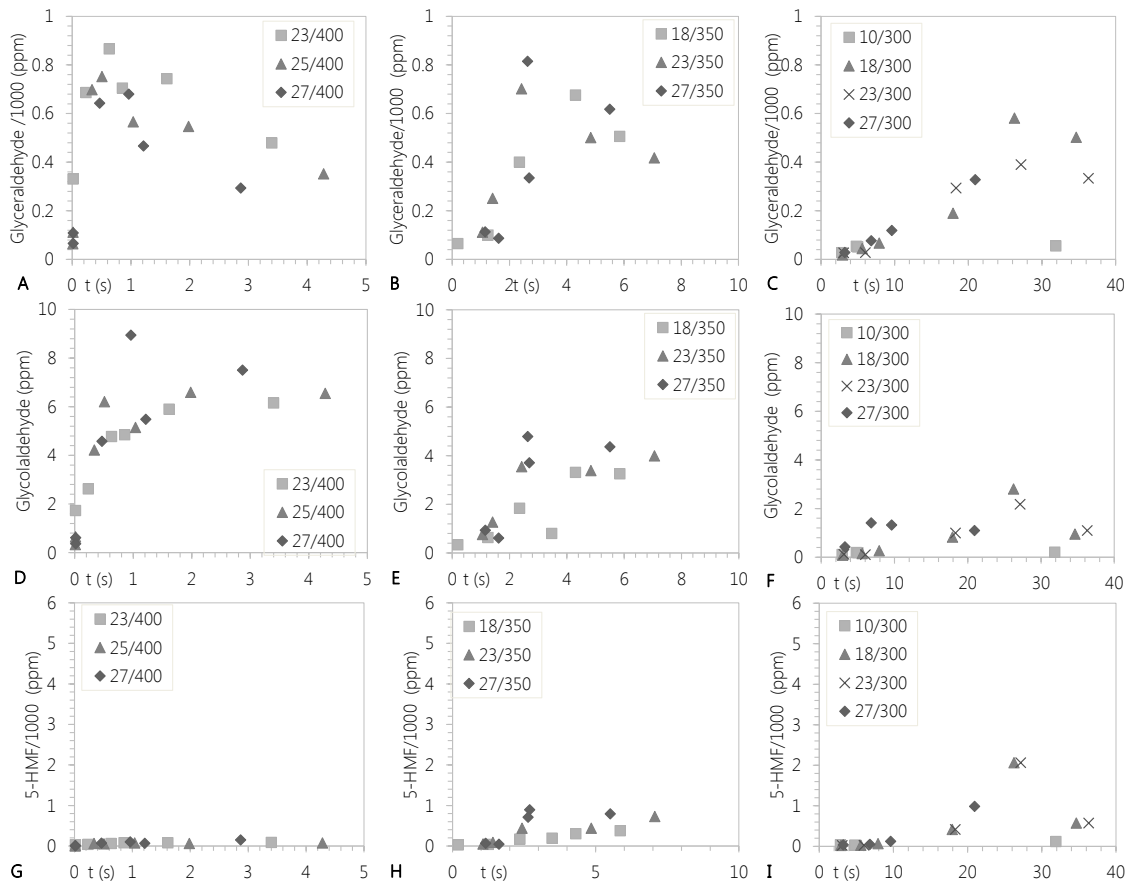


**Fig. 7.** (A) Glyceraldehyde concentration at 400°C; (■) P= 23 MPa; (▲) P=25 MPa and; (◆) P= 27 MPa. (B) Glyceraldehyde concentration at 350°C; (■) P= 18 MPa; (▲) P=23 MPa and; (◆) P= 27 MPa. (C) Glyceraldehyde concentration at 300°C; (■) P= 10 MPa; (▲) P=18 MPa; (x) P=23 MPa and; (◆) P= 27 MPa. (D) Glycolaldehyde concentration at 400°C; (■) P= 23 MPa; (▲) P=25 MPa and; (◆) P= 27 MPa. (E) Glycolaldehyde concentration at 350°C; (■) P= 18 MPa; (▲) P=23 MPa and; (◆) P= 27 MPa. (F) Glycolaldehyde concentration at 300°C; (■) P= 10 MPa; (▲) P=18 MPa; (x) P=23 MPa and; (◆) P= 27 MPa. (G) 5-HMF concentration at 400°C; (■) P= 23 MPa; (▲) P=25 MPa and; (◆) P= 27 MPa. (H) 5-HMF concentration at 350°C; (■) P= 18 MPa; (▲) P=23 MPa and; (◆) P= 27 MPa. (I) 5-HMF concentration at 300°C; (■) P= 10 MPa; (▲) P=18 MPa; (x) P=23 MPa and; (◆) P= 27 MPa.

## 4.2. Kinetic Model

The kinetic constants of glucose to fructose isomerization ( $k_{gf}$ ), fructose to 5-HMF dehydration ( $k_{fh}$ ), glucose to glycolaldehyde retro-aldol condensation ( $k_{gg}$ ) and fructose retro-aldol condensation ( $k_{fg}$ ) were fitted for all the experimental conditions using the concentration data profiles along residence time according the method explained in section 3. The activation energy ( $E_a$ ) and pre-exponential factor ( $\ln k_0$ ) for each kinetic was determined at 23 MPa and 27 MPa according equation 9 (Arrhenius relationship). Where  $k$  is the kinetic constant ( $s^{-1}$ );  $R$  is the gas constant ( $\text{kJ K}^{-1} \text{mol}^{-1}$ ) and;  $T$  is the temperature (K). The Arrhenius parameters are shown in table 1 and are analyzed in sections 4.2.1. to 4.2.5.

$$\ln k = \ln k_0 - \frac{E_a}{R} \frac{1}{T} \quad (9)$$

**Table 1.** Fitted Arrhenius parameters for the reactions of glucose in pressurized water.

	P=23 MPa			P=27MPa		
	Ea kJ·mol <sup>-1</sup>	Ln Ao	R <sup>2</sup>	Ea kJ·mol <sup>-1</sup>	Ln Ao	R <sup>2</sup>
kgf	516 ± 182	117 ± 35	0.88	403 ± 97	94 ± 18	0.95
kfh	463 ± 160	104 ± 31	0.89	449 ± 95	101 ± 18	0.96
kgg	150.7 ± 26	28.0 ± 5.0	0.97	151.4 ± 32.7	28.4 ± 6.4	0.96
kfg	115.3 ± 2.6	22.8 ± 0.5	0.99	180.6 ± 36.0	35.8 ± 7.0	0.96

The influence of pressure in the kinetic constants can be analyzed by using the concept of activation volume ( $\Delta V^\ddagger$ ) that is defined as the excess of the partial molar volume of the transition state over the partial molar volume of the initial species [35]. The relationship between the kinetics dependence with pressure and the activation volume is shown in equation 10. Where  $\Delta V^\ddagger$  is the activation volume in  $\text{cm}^3 \cdot \text{mol}^{-1}$ ;  $P$  is pressure in bar and;  $R$  is the gas constant ( $83.14 \text{ cm}^3 \cdot \text{bar} \cdot \text{mol}^{-1} \cdot \text{K}^{-1}$ ).

$$\left. \frac{\partial \ln k}{\partial P} \right|_T = - \frac{\Delta V^\ddagger}{RT} \quad (10)$$

Sometimes the activation volume can be divided into two terms as it is shown in equation 11 [36]. Where  $\Delta V_{2^\ddagger}$  represents the molar volume difference between the transition state and the reactants and;  $\Delta V_{2^\ddagger}$  represents the interactions between the reactants and solvent molecules. If a reactive system shows more attractive potential between solvent and transition state, than between solvent and reactant; the reaction rate would be enhanced by rising pressure [37].

$$\Delta V^\ddagger = \Delta V_1^\ddagger + \Delta V_2^\ddagger \quad (11)$$

The second term is usually the most important when the reactions occur in conditions near the critical point of the solvent. Although the typical values of  $\Delta V^\ddagger$  ranges between -60 and 30  $\text{cm}^3\cdot\text{mol}^{-1}$ ; in the surroundings of the critical point the volume of activation can reach values greater than  $\pm 1000 \text{ cm}^3\cdot\text{mol}^{-1}$  [38] because the phenomenon is amplified due to near divergence of the isothermal compressibility of the medium [37]. The fitted values of  $\Delta V^\ddagger$  for  $k_{gf}$ ,  $k_{fv}$ ,  $k_{gg}$  and  $k_{fg}$  are listed in table 2 and are analyzed in sections 4.2.2. to 4.2.5.

**Table 2.** Fitted volumes of activation for the reactions of glucose in pressurized water.

	400°C		350°C		300°C	
	$\Delta v^0$ $\text{cm}^3\cdot\text{mol}^{-1}$	$R^2$	$\Delta v^0$ $\text{cm}^3\cdot\text{mol}^{-1}$	$R^2$	$\Delta v^0$ $\text{cm}^3\cdot\text{mol}^{-1}$	$R^2$
<b>k<sub>gf</sub></b>	3226 ± 194	1.00	-82 ± 3	1.00	232 ± 34	0.96
<b>k<sub>fv</sub></b>	1385 ± 171	0.98	-578 ± 160	0.93	363 ± 57	0.95
<b>k<sub>gg</sub></b>	-201 ± 5	1.00	-229 ± 37	0.97	-28 ± 21	0.48
<b>k<sub>fg</sub></b>	-1403 ± 329	0.95	-14 ± 122	0.01	68 ± 49	0.50

#### 4.2.1. Glucose isomerization to fructose ( $k_{gf}$ )

The kinetic constants of glucose isomerization to produce fructose at different temperatures and pressures are shown in Figure 8. At 300°C and 350°C the pressure showed to have almost no effect in the reaction rate. However, when the temperature was increased until 400°C, the kinetic constants were reduced when pressure was increased. It is observed that by increasing the reaction temperature, the pressure has a negative effect in the reaction rate. At 23 MPa the  $E_a$  and  $\ln k_0$  were  $516 \pm 182 \text{ kJ}\cdot\text{mol}^{-1}$  and  $117 \pm 35$  respectively (see Table 1). The activation volume of  $k_{gf}$  took a value of  $3226 \pm 194 \text{ cm}^3\cdot\text{mol}^{-1}$  at 400°C (see Table 2). However, at subcritical temperatures the activation volume was small, being the pressure effect negligible. The activation volume was high and positive at 400°C, meaning that the reaction of glucose isomerization is inhibited when pressure is increased. This phenomenon would mean that the interaction between the transition state of glucose-fructose (ring opening and keto-enol tautomerism by hydroxide/proton transfer [39]) and the solvent is less attractive than the interaction of glucose with supercritical water (solvent).

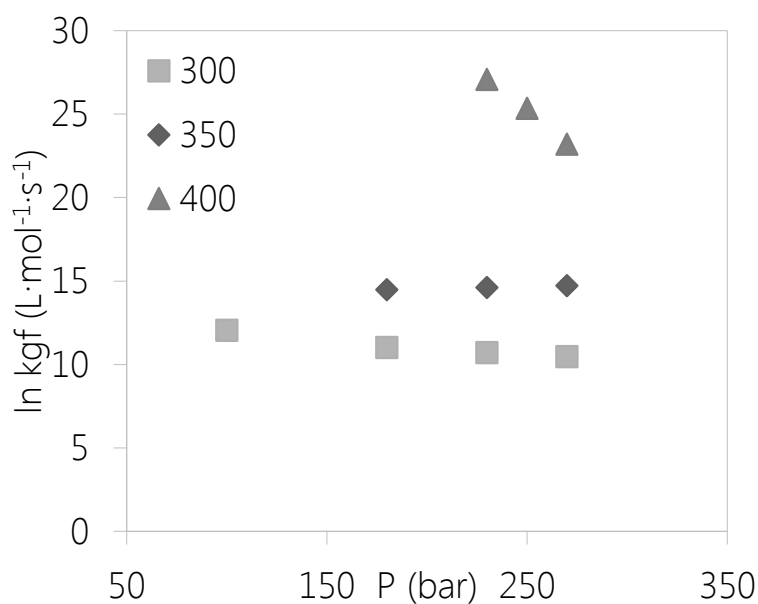


Fig. 8. Kinetic constant of glucose isomerization to fructose along pressure; (■) T= 300°C; (◆) T= 350°C and; (▲) T=400°C. ( $k_g$ ).

#### 4.2.2. Fructose dehydration to 5-HMF ( $k_{fh}$ )

The fitted kinetic constants at the studied temperatures and pressures were plotted in Figure 9. The activation energy and pre-exponential factor were slightly decreased ( $\approx 3\%$ ) by increasing pressure from 23 MPa to 27 MPa (see Table 1). The  $E_a$  and  $\ln k_0$  for  $k_{fh}$  took values of  $463.7 \pm 160.6 \text{ kJ}\cdot\text{mol}^{-1}$  and  $104.6 \pm 31.2$  respectively at 23 MPa. The kinetic constant is decreased by rising pressure at 400°C. However, the values of activation volume for 300°C and 350°C showed little variations. The fitted values of  $\Delta V^\ddagger$  are listed in Table 2.

#### 4.2.3. Glucose to glycolaldehyde reaction ( $k_{gg}$ )

The kinetic constants of glycolaldehyde production from glucose at different temperature are plotted against pressure in Figure 10. Contrary than the kinetic constant of glucose isomerization,  $k_{gg}$  was increased at 400°C when pressure was increased. At 300°C and 350°C, pressure showed to have almost no effect in the kinetic of glucose to glycolaldehyde reaction. The values of  $E_a$  and  $\ln k_0$  for the kinetic of glycolaldehyde production from glucose at 23 and 27 MPa are shown in Table 1. The activation energy and pre-exponential factor were almost the same when pressure was increased from 23 MPa to 27 MPa. The volumes of activation at 350°C and 400°C are shown in Table 2. The activation volume was  $-201 \pm 5 \text{ cm}^3\cdot\text{mol}^{-1}$  at

400°C. In this case the volumes of activation were negatives. Following with the discussion of section 4.2.2., the activation volume value of  $k_{gg}$  would mean that the interaction of the transition state of glucose-glyceraldehyde with the solvent is more attractive than the interaction between glucose and supercritical water (solvent). Accordingly, it can be concluded that at 400°C when pressure is increased from 23 MPa to 27 MPa, the reaction of glycolaldehyde production is improved while the reaction of glucose epimerization to give fructose is diminished.

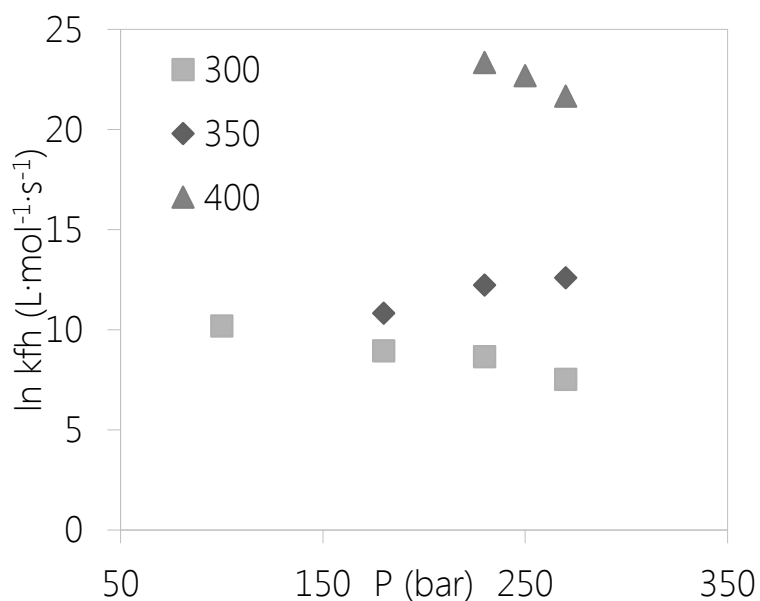


Fig. 9. Kinetic constant of 5-HMF formation along pressure ( $k_{fh}$ ); (■) T= 300°C; (◆) T= 350°C and; (▲) T=400°C.

#### 4.2.4. Fructose retro-aldol condensation ( $k_{fg}$ )

Glyceraldehyde production kinetic constants are plotted against pressure at different temperature in Figure 11. The pressure effect in this reaction was negligible at subcritical temperatures. The values of activation energy for this reaction rate at 23 MPa and 27 MPa were  $115.3 \pm 2.6 \text{ kJ}\cdot\text{mol}^{-1}$  and  $180.6 \pm 36.0 \text{ kJ}\cdot\text{mol}^{-1}$  respectively. The pre-exponential factors were  $22.8 \pm 0.5$  and  $35.8 \pm 7.0$  for 23 MPa and 27 MPa respectively. The activation volumes at subcritical temperatures were near to zero ( $k_{fg}$  do not change appreciable with pressure) and that is why the error of the linear fit was high. If the activation value of  $k_{fg}$  at 400°C is analyzed together with  $k_{fh}$ , it can be seen that  $k_{fg}$  is improved by increasing pressure while  $k_{fh}$  is decreased.

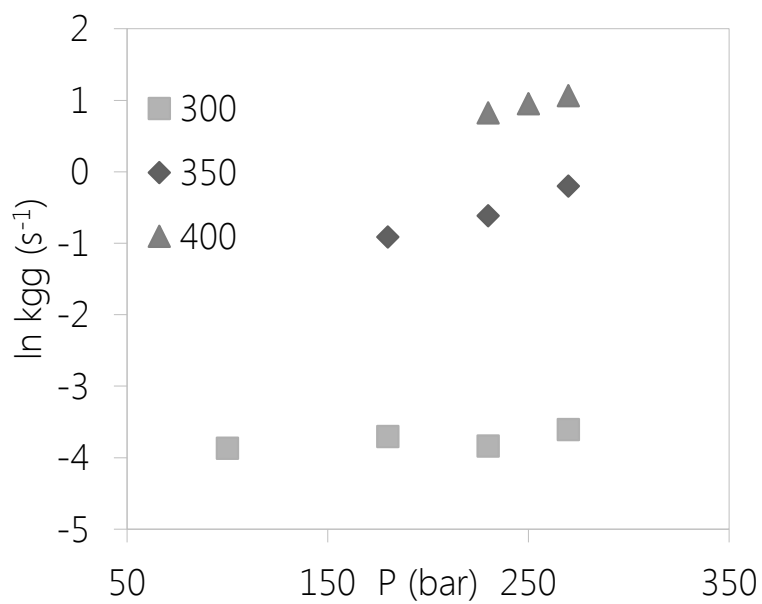


Fig. 10. Kinetic constant of glucose retro-aldol condensation along pressure; (■) T= 300°C; (◆) T= 350°C and; (▲) T=400°C. ( $k_{gg}$ ).

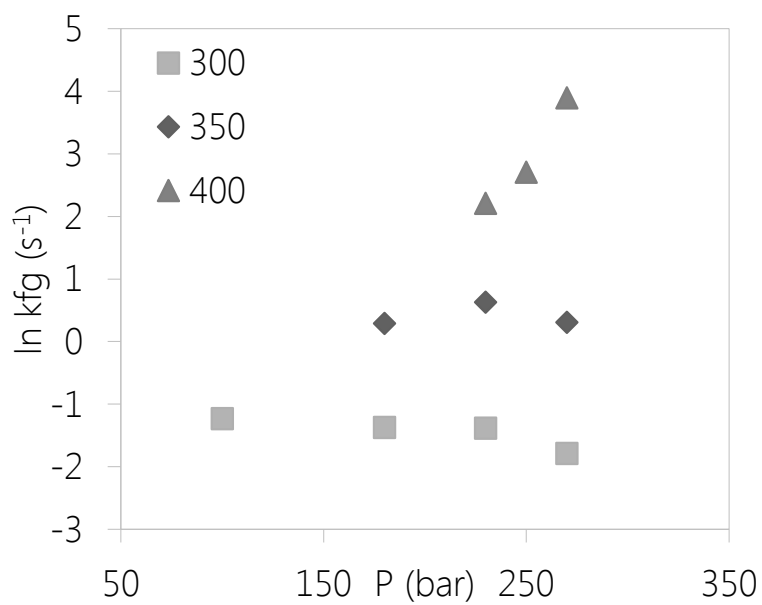


Fig. 11. Kinetic constant of fructose retro-aldol condensation along pressure; (■) T= 300°C; (◆) T= 350°C and; (▲) T=400°C. ( $k_{fg}$ ).

#### 4.2.5. Global parameters

For reactors design, it would be interesting to have an equation that relates the kinetic of the reactions with temperature and pressure at the same time. For this purpose equation 12 was proposed.

$$k = k_0 e^{\frac{-E_a}{RT}} e^{\frac{-\Delta v^\ddagger P}{RT}} \quad (12)$$

The global activation energy, pre-exponential factor ( $k_0$ ) and the activation volume were fitted for each reaction kinetic using the fitting tool *stool* of Matlab®. The fitted parameters are shown in Table 3. The adjusted parameters for the kinetic constants  $k_{gf}$  and  $k_{fh}$  were fitted using the kinetic constants at 300°C and 350°C. The kinetic values at 400°C were too high compared to the subcritical ones as it can be seen in Figures 8 and 9. So, it was not possible to fit values of  $E_a$ ,  $k_0$  and  $\Delta v^\ddagger$  that represent the behavior of the kinetic in the whole range of temperature. Using the parameters shown in Table 3 for  $k_{gg}$  and  $k_{fg}$ ; it is possible to calculate the kinetic constants over the entire analyzed range of pressure (10 – 27 MPa) and temperature (300 – 400°C).

**Table 3.** Global pre-exponential factors, activation energies and volumes of activation fitted for the reactions of glucose in pressurized water.

P=23 MPa				
	Ea kJ·mol <sup>-1</sup>	Ln k <sub>0</sub>	ΔV cm <sup>3</sup> ·mol <sup>-1</sup>	R <sup>2</sup>
kgf	87.8	30.8	-158.4	0.91
kfh	105.8	27.7	-1011	0.85
kgg	106.7	-353.8	18.4	1.00
kfg	184.4	-2802.0	23.3	0.96

In Figure 12 it is shown the evolution  $k_{gg}$  along pressure and temperature. The surface was calculated with the fitted parameters shown in Tables 3, the dots are the experimental data.

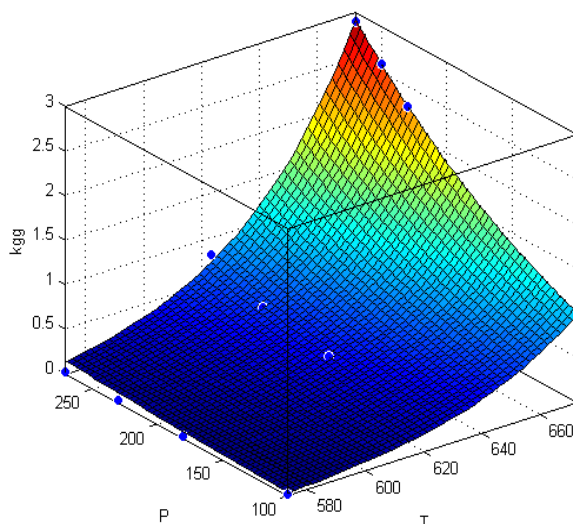


Fig. 12. Kinetic constant ( $s^{-1}$ ) of glucose retro-aldol condensation ( $k_{gg}$ ) along pressure (bar) and temperature (K).

## 5. Conclusions

Cellulose hydrolysis was studied experimentally in order to analyze the effect of pressure and temperature in the kinetics of cellulose and glucose in a hydrothermal medium. The experiments were carried out in the pressure range of 10 MPa – 27 MPa, at 300°C, 350°C and 400°C. A mathematical model was built in order to fit the main kinetic constants of glucose hydrolysis ( $k_{og}$ ,  $k_{gf}$ ,  $k_{gg}$ ,  $k_{fn}$  and  $k_{fg}$ ).

The reactions of glucose hydrolysis were found to be highly influenced by temperature. Nevertheless, in general, pressure has a slight effect on the kinetics at subcritical temperatures, while at temperatures higher than the critical temperature of water, that influence can be remarkable: i.e. at 400°C, the kinetic constant of glucose isomerization to fructose ( $k_{gf}$ ) would be decreased when pressure is increased. On the other hand, the reaction of glucose retro-aldol condensation ( $k_{gg}$ ) would be enhanced by raising pressure. The reaction of 5-HMF production ( $k_{fn}$ ) and oligosaccharides hydrolysis ( $k_{og}$ ) would be enhanced by decreasing pressure. The cellulose hydrolysis reaction rate was not affected by pressure in the studied range.

The Arrhenius parameters to calculate the kinetic constants of the main glucose reactions in a hydrothermal medium were calculated at 23 and 27 MPa. Also, the activation volume was calculated at 300°C, 350°C and 400°C. It was observed that the activation volume was small at subcritical temperatures, nevertheless, at supercritical temperatures the activation volume was high.

## **Acknowledgements**

The authors thank the Spanish Ministry of Economy and Competitiveness for the Project CTQ2011-23293 and ENE2012-33613. The authors thank Repsol for its technical support. D.A.C. thanks the Spanish Ministry of Education for the FPU fellowship (AP2009-0402).

## References

1. Peterson, A.A., Vogel, F., Lachance, R.P., Fröling, M., Michael J. Antal, Jr., and Tester, J.W., *Thermochemical biofuel production in hydrothermal media: A review of sub- and supercritical water technologies*. Energy & Environmental Science, 2008. 1(1): p. 32-65.
2. Klemm, D., Heublein, B., Fink, H.P., and Bohn, A., *Cellulose: Fascinating Biopolymer and Sustainable Raw Material*. Angewandte Chemie International Edition, 2005. 44(22): p. 3358-3393.
3. Cantero, D.A., Bermejo, M.D., and Cocero, M.J., *High glucose selectivity in pressurized water hydrolysis of cellulose using ultra-fast reactors*. Bioresource Technology, 2013. 135: p. 697-703.
4. Zhao, Y., Wang, H.-T., Lu, W.-J., and Wang, H., *Combined supercritical and subcritical conversion of cellulose for fermentable hexose production in a flow reaction system*. Chemical Engineering Journal, 2011. 166(3): p. 868-872.
5. Lenihan, P., Orozco, A., O'Neill, E., Ahmad, M.N.M., Rooney, D.W., and Walker, G.M., *Dilute acid hydrolysis of lignocellulosic biomass*. Chemical Engineering Journal, 2010. 156(2): p. 395-403.
6. Xiong, Y., Zhang, Z., Wang, X., Liu, B., and Lin, J., *Hydrolysis of cellulose in ionic liquids catalyzed by a magnetically-recoverable solid acid catalyst*. Chemical Engineering Journal, 2014. 235: p. 349-355.
7. Sánchez, C., Egüés, I., García, A., Llano-Ponte, R., and Labidi, J., *Lactic acid production by alkaline hydrothermal treatment of corn cobs*. Chemical Engineering Journal, 2012. 181-182: p. 655-660.
8. Liu, B., Zhang, Z., and Zhao, Z.K., *Microwave-assisted catalytic conversion of cellulose into 5-hydroxymethylfurfural in ionic liquids*. Chemical Engineering Journal, 2013. 215-216: p. 517-521.
9. Qi, X., Watanabe, M., Aida, T.M., and Jr, R.L.S., *Catalytic conversion of cellulose into 5-hydroxymethylfurfural in high yields via a two-step process*. Cellulose, 2011. 18(5): p. 1327-1333.

10. Akizuki, M., Fujii, T., Hayashi, R., and Oshima, Y., *Effects of water on reactions for waste treatment, organic synthesis, and bio-refinery in sub- and supercritical water*. Journal of Bioscience and Bioengineering.
11. Marshall, W.L. and Franck, E.U., *Ion Product of Water Substance, 0-1000°C, 1-10,000 Bars. New International Formulation and Its Background*. Journal of Physical and Chemical Reference Data, 1981. 10(2): p. 295-304.
12. Wagner, W, Cooper, J, R., Dittmann, et al., *The IAPWS industrial formulation 1997 for the thermodynamic properties of water and steam*. 2000, American Society of Mechanical Engineers: New York, N, ETATS-UNIS.
13. Aida, T.M., Sato, Y., Watanabe, M., Tajima, K., Nonaka, T., Hattori, H., and Arai, K., *Dehydration of D-glucose in high temperature water at pressures up to 80 MPa*. The Journal of Supercritical Fluids, 2007. 40(3): p. 381-388.
14. Akiya, N. and Savage, P.E., *Roles of Water for Chemical Reactions in High-Temperature Water*. Chemical Reviews, 2002. 102(8): p. 2725-2750.
15. Kruse, A. and Gawlik, A., *Biomass Conversion in Water at 330–410 °C and 30–50 MPa. Identification of Key Compounds for Indicating Different Chemical Reaction Pathways*. Industrial & Engineering Chemistry Research, 2002. 42(2): p. 267-279.
16. Promdej, C. and Matsumura, Y., *Temperature Effect on Hydrothermal Decomposition of Glucose in Sub- And Supercritical Water*. Industrial & Engineering Chemistry Research, 2011. 50(14): p. 8492-8497.
17. Yin, S. and Tan, Z., *Hydrothermal liquefaction of cellulose to bio-oil under acidic, neutral and alkaline conditions*. Applied Energy, 2012. 92(0): p. 234-239.
18. Sakanishi, K., Ikeyama, N., Sakaki, T., Shibata, M., and Miki, T., *Comparison of the Hydrothermal Decomposition Reactivities of Chitin and Cellulose*. Industrial & Engineering Chemistry Research, 1999. 38(6): p. 2177-2181.
19. Minowa, T., Zhen, F., and Ogi, T., *Cellulose decomposition in hot-compressed water with alkali or nickel catalyst*. The Journal of Supercritical Fluids, 1998. 13(1–3): p. 253-259.
20. Sakaki, T., Shibata, M., Sumi, T., and Yasuda, S., *Saccharification of Cellulose Using a Hot-Compressed Water-Flow Reactor*. Industrial & Engineering Chemistry Research, 2002. 41(4): p. 661-665.

21. Sasaki, M., Fang, Z., Fukushima, Y., Adschiri, T., and Arai, K., *Dissolution and Hydrolysis of Cellulose in Subcritical and Supercritical Water*. Industrial & Engineering Chemistry Research, 2000. 39(8): p. 2883-2890.
22. Ehara, K. and Saka, S., *Decomposition behavior of cellulose in supercritical water, subcritical water, and their combined treatments*. Journal of Wood Science, 2005. 51(2): p. 148-153.
23. Zhao, Y., Lu, W.-J., and Wang, H.-T., *Supercritical hydrolysis of cellulose for oligosaccharide production in combined technology*. Chemical Engineering Journal, 2009. 150(2-3): p. 411-417.
24. Fang, Z., Zhang, F., Zeng, H.-Y., and Guo, F., *Production of glucose by hydrolysis of cellulose at 423 K in the presence of activated hydrotalcite nanoparticles*. Bioresource Technology, 2011. 102(17): p. 8017-8021.
25. Onda, A., Ochi, T., and Yanagisawa, K., *Hydrolysis of Cellulose Selectively into Glucose Over Sulfonated Activated-Carbon Catalyst Under Hydrothermal Conditions*. Topics in Catalysis, 2009. 52(6-7): p. 801-807.
26. Brunner, G., *Near critical and supercritical water. Part I. Hydrolytic and hydrothermal processes*. The Journal of Supercritical Fluids, 2009. 47(3): p. 373-381.
27. Kumar, S. and Gupta, R.B., *Hydrolysis of Microcrystalline Cellulose in Subcritical and Supercritical Water in a Continuous Flow Reactor*. Industrial & Engineering Chemistry Research, 2008. 47(23): p. 9321-9329.
28. Aida, T.M., Tajima, K., Watanabe, M., Saito, Y., Kuroda, K., Nonaka, T., Hattori, H., Smith Jr, R.L., and Arai, K., *Reactions of D-fructose in water at temperatures up to 400 °C and pressures up to 100 MPa*. The Journal of Supercritical Fluids, 2007. 42(1): p. 110-119.
29. Kabyemela, B.M., Adschiri, T., Malaluan, R.M., and Arai, K., *Glucose and Fructose Decomposition in Subcritical and Supercritical Water: Detailed Reaction Pathway, Mechanisms, and Kinetics*. Industrial & Engineering Chemistry Research, 1999. 38(8): p. 2888-2895.
30. Kabyemela, B.M., Adschiri, T., Malaluan, R.M., Arai, K., and Ohzeki, H., *Rapid and Selective Conversion of Glucose to Erythrose in Supercritical Water*. Industrial & Engineering Chemical Research, 1997. 36(12): p. 5063-5067.

31. Sasaki, M., Adschiri, T., and Arai, K., *Kinetics of cellulose conversion at 25 MPa in sub- and supercritical water*. *AIChE Journal*, 2004. 50(1): p. 192-202.
32. Sasaki, M., Goto, K., Tajima, K., Adschiri, T., and Arai, K., *Rapid and selective retro-aldol condensation of glucose to glycolaldehyde in supercritical water*. *Green Chem.*, 2002. 4(3): p. 285-287.
33. Cantero, D.A., Bermejo, M.D., and Cocero, M.J., *Kinetic analysis of cellulose depolymerization reactions in near critical water*. *The Journal of Supercritical Fluids*, 2013. 75: p. 48-57.
34. Kabyemela, B.M., Adschiri, T., Malaluan, R., and Arai, K., *Degradation Kinetics of Dihydroxyacetone and Glyceraldehyde in Subcritical and Supercritical Water*. *Industrial & Engineering Chemistry Research*, 1997. 36(6): p. 2025-2030.
35. Luft, G., Recasens, F., and Velo, E., *Chapter 3 Kinetic properties at high pressure*, in *Industrial Chemistry Library*, A. Bertucco and G. Vetter, Editors. 2001, Elsevier. p. 65-140.
36. Bröll, D., Kaul, C., Krämer, A., Krammer, P., Richter, T., Jung, M., Vogel, H., and Zehner, P., *Chemistry in Supercritical Water*. *Angewandte Chemie International Edition*, 1999. 38(20): p. 2998-3014.
37. Rice, S.F., Steeper, R.R., and Aiken, J.D., *Water Density Effects on Homogeneous Water-Gas Shift Reaction Kinetics*. *The Journal of Physical Chemistry A*, 1998. 102(16): p. 2673-2678.
38. Savage, P.E., Gopalan, S., Mizan, T.I., Martino, C.J., and Brock, E.E., *Reactions at supercritical conditions: Applications and fundamentals*. *AIChE Journal*, 1995. 41(7): p. 1723-1778.
39. Román-Leshkov, Y., Moliner, M., Labinger, J.A., and Davis, M.E., *Mechanism of Glucose Isomerization Using a Solid Lewis Acid Catalyst in Water*. *Angewandte Chemie International Edition*, 2010. 49(47): p. 8954-8957.



# Chapter 5. Selective Transformation of Fructose into Pyruvaldehyde in Supercritical Water. Reaction Pathway Development

## Abstract

The reactions of fructose in sub- and supercritical water were analyzed changing the properties of the reaction medium (pH and free radical kidnapers). The reactions were performed in a continuous reactor at 260°C, 330°C and 400°C; and 23 MPa. The pH of the medium was changed using oxalic acid and sodium hydroxide. Also, scavengers (TEMPO and BHT) were tested in order to determine its influences in the radical reactions. The main product of fructose hydrolysis in supercritical water was pyruvaldehyde (>80% carbon basis) at 400°C and 23 MPa with a residence time of 0.7 s. Furthermore, the reactions of fructose were analyzed in combination with glucose. It was determined that different retro-aldol condensation products can be obtained depending on the starting material. Fructose produces mainly C-3 molecules (pyruvaldehyde) and glucose produces mainly C-2 molecules (glycolaldehyde). The isomerization of fructose to glucose is negligible and so is the production of C-2 when the starting material is fructose. The yield of 5-HMF was negligible when the starting material was glucose. Sugar cane molasses was used as raw material to analyze the behavior of a non-synthetic biomass in the production of added value products in pressurized water. Lactic acid was the main product of molasses hydrolysis.

**Keywords:** Biomass • Biorefinery • Lactic Acid • Pyruvaldehyde



## 1. Introduction

Processes that involve the use of biomass as raw material have been intensively studied in the near past looking for new processes capable of producing bio-chemicals and bio-energy using "green" solvents. One way to achieve these processes is by using selective and efficient reaction mediums. The vegetal biomass is an alternative as raw material, being cellulose (glucose resource) one of the main component of biomass [1, 2]. A method to break cellulose into sugars (mainly glucose and fructose) was developed in a previous work obtaining a solution with low degradation formation products, such as 5-hydroxymethylfurfural (5-HMF) in a supercritical water medium [3]. Another interesting raw materials for the production of chemicals are the by-products of the food and agriculture industry with high amounts of carbohydrates, such as the sugar cane molasses produced in the sugar manufacturing process. This by-product stream is composed mainly of sucrose, glucose and fructose.

Lactic acid is a product of interest of many industries; it is used in food, chemical, pharmaceutical and cosmetic industries. Nowadays, the most valuable alternative for the use of lactic acid would be the production of the biodegradable lactic acid polymer [4]. The lactic acid can be produced by chemical synthesis or by carbohydrates fermentation. However, lactic acid is industrially produced mainly by fermentation [4]. Glucose can be modified in a hot pressurized water medium in order to obtain high added value products like lactic acid [5-9]. The production of lactic acid was achieved in a previous work of our group by using NaOH as medium modifier [9]. The production of lactic acid was also studied using by-products streams like sugar cane molasses [10, 11]; paper sludge [12] or other cellulosic biomass [13, 14] as raw materials. Also the production of lactic acid was studied using fructose as raw material [15]. However, several works in literature attempt to produce 5-hydroxymethylfurfural (5-HMF) from fructose because this product is considered as a building block in the production of chemicals [16]. The production of 5-HMF was studied using ionic liquids with acid catalysts [17-19]; biphasic reactors with solid catalyst [20] and; hydrothermal reactor with catalyst [21, 22].

Pressurized water at temperature between 300°C and 400°C can adopt different identities depending on the temperature and pressure. This behavior of compressed water could be used to change the medium identity and chose the most appropriate to the desired reactions. Thus, a selective medium could be set only by using water. The density and the ionic product of water are the two key factors in the hydrolysis reactions of glucose and fructose, favoring

retro-aldol reactions at low densities (lactic acid formation pathway) and favoring 5-HMF formation at high densities and ionic products [5, 6, 23-25]. Additionally, the use of supercritical water as reaction medium allows the intensification of the process by reducing the required residence time of the reactions. Typical residence times of glucose and fructose reactions at supercritical conditions are between 0 s and 5 s [6, 9]. These residence times are substantially lower than the required for the low temperature catalyzed processes (from seconds to hours) or microorganism processes (from seconds to days).

In this study, the influence of the reaction medium in the chemical modification of fructose into pyruvaldehyde, considered as a lactic acid precursor [26, 27], was analyzed using a hydrothermal reaction medium. The reaction pathway was analyzed to understand the driving factors to obtain high selectivity of the desired products. The production of lactic acids in a hydrothermal medium was analyzed using sugar cane molasses as starting material.

## 2. Materials and methods

### 2.1. Materials

Glucose (99%), fructose (99%), sodium hydroxide (>98%) and oxalic acid (98%) used in the experiments was purchased from Sigma. 2,2,6,6-Tetramethyl-1-piperidinyloxy (TEMPO) and 2,6-Di-tert-butyl-4-methylphenol (BHT) were supplied by Sigma. Distilled water was used in the experiments. The chemicals used in HPLC (High Performance Liquid Chromatography) analysis were: cellobiose (+98%), glucose (+99%), fructose (+99%), glyceraldehyde (95%), pyruvaldehyde (40%), erythrose (+75%), glycolaldehyde dimer, 5-hydroxymethylfurfural (99%), lactic acid (85%), levulinic acid (98%), formic acid (96%) and acetic acid purchased from Sigma.

### 2.2. Analysis

The carbon content of the products was determined by total organic carbon (TOC) analysis with Shimadzu TOC-VCSH equipment. The pH of the samples was measured by a pH meter Nahita model 903. The composition of the liquid products was determined with an HPLC. The HPLC column used for the separation of the compounds was Sugar SH-1011 Shodex at 50°C and a flow of 0.8mL/min using H<sub>2</sub>SO<sub>4</sub> (0.01 N) as mobile phase. A Waters IR detector 2414 was used to identify the sugars and their derivatives. An UV-Vis detector was used to

determine the 5-hydroxy-methyl-furfural (5-HMF) concentration at a wavelength of 254nm. In order to identify the main peaks and calculate the areas of the complex mixture that we obtained during the experiments we have used a band-analysis via Fast Fourier Transform (fft) and band-adjustment by Gaussian functions. The adjustment was done by minimizing the quadratic error using a Nelder-Mead algorithm.

The yield of the determined compounds (fructose, glucose, glyceraldehyde, pyruvaldehyde, lactic acid, formic acid, acrylic acid and 5-HMF) was determined by equation 1, where  $Y_s$  is the yield of compound 's',  $C_s$  is the concentration of the compound 's' measured in ppm,  $F_{c,s}$  is the carbon composition of the component 's' with a value between 0 and 1; TOC is the total organic carbon content in the sample.

$$Y_s = \frac{C_s F_{c,s}}{TOC} \quad (1)$$

### 2.3. Experimental setup

To perform the experiments presented here a continuous sub- and supercritical continuous hydrolysis plant able to works at conditions up to 400°C and 30 MPa used. The solution/suspension of biomass is continuously pumped to the operation pressure and instantaneously heating by injecting a stream of supercritical water at the inlet of the reactor. The effluent is suddenly depressurized at the outlet of the reactor without previous cooling in order to instantaneously stop the reaction, reducing in this way its temperature down to 150°C. A scheme of the plant is shown in Figure 1. The main advantages of the pilot plat are: (a) the reactor can be considered isothermal due to the instantaneous heating and cooling; (b) the products are not diluted in the cooling water; (c) the residence time can be varied from 0.004 s to 50 s by using different reactors. A more detailed description of the facility and the operation procedure of the pilot plant was presented in a previous work [28]. The catalyst and/or medium modifier (if used) were fed in the system together with biomass stream.

## 3. Results and discussion

The experiments of fructose hydrolysis in pressurized water were carried out at 260°C, 330°C and 400°C, at 23 MPa and 27 MPa. The residence time was varied between 0.1 s and 6 s. In order to evaluate the effect of pH, oxalic acid [29] or NaOH [30] were added to the medium. The carbon balance between the inlet and outlet of the reactor was between 93% - 100%.

The reaction products identified were glucose, glycolaldehyde, glyceraldehyde, 5-HMF, pyruvaldehyde, lactic acid and acrylic acid. However, the acids concentration was low.

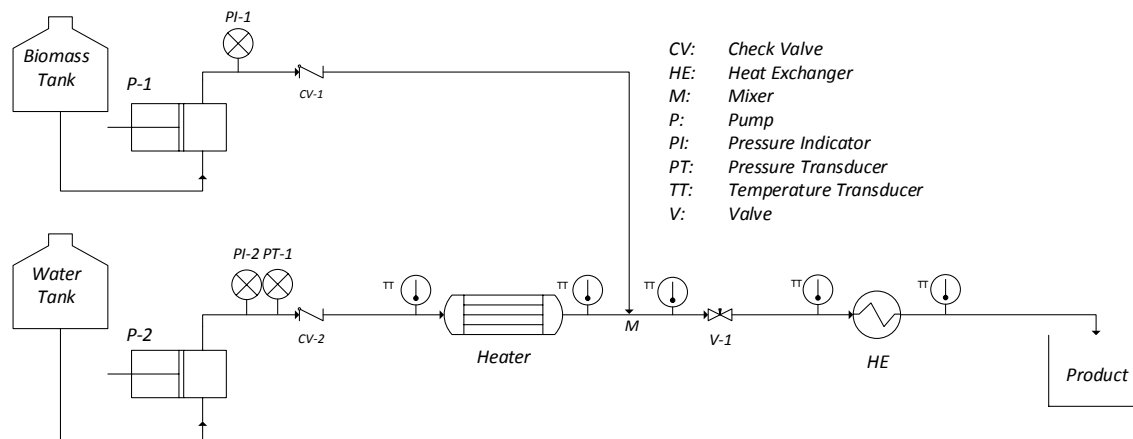


Fig. 1. Pilot plant diagram.

A reaction pathway of glucose degradation in hot pressurized water is shown in figure 2. The reaction pathways were constructed following the reaction pathways developed in literature [31]. Fructose can be degraded mainly by (1) retro-aldol reaction to produce glyceraldehyde or (2) via dehydration to 5-HMF, being the isomerization of fructose to glucose a minor reaction. Glucose can react following mainly three different pathways: (1) isomerization to produce fructose; (2) retro-aldol condensation producing glycolaldehyde; and (3) dehydration to 1,6-anhydroglucose. Experiments with glucose and mixtures of glucose and fructose were done in order to confirm the reaction pathway.

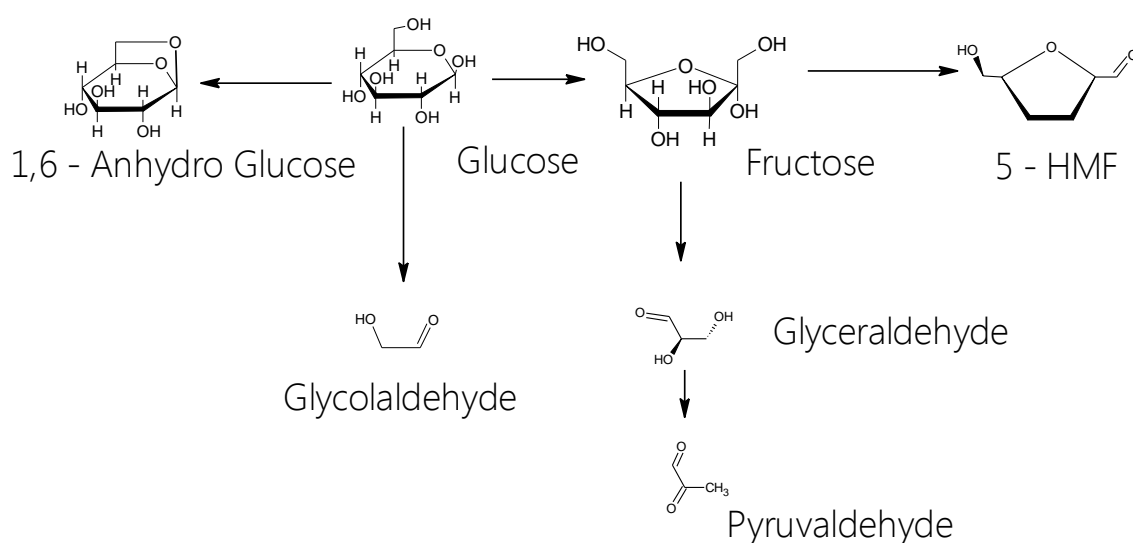


Fig. 2. Main reaction pathways of glucose and fructose hydrolysis.

### 3.1. Fructose reactions along residence time

The yield of the main products of fructose hydrolysis at 260°C and 330°C and 23 MPa are shown in figure 3-A and 3-B respectively. Fructose was not totally hydrolysed at 260°C in the experimented range of residence time (up to 6 s). However, at a reaction temperature of 330°C, it can be seen that at a residence time of 3 s the fructose conversion is 0.94. The reaction of isomerization to produce glucose was not significant. The higher glucose production (around 5% w-w<sup>-1</sup>) were achieved at 1.8 s and 4.2 s of residence time at a reaction temperature of 330°C and 260°C respectively. The reaction of glucose-fructose isomerization would take place via ring-opening and keto-enol tautomerism. This kind of reaction would be favoured by the association of the glucose or fructose with a proton or hydroxide anion. These transitions states are favoured by working at temperatures between 260°C and 330°C at 23 MPa due to the high ionic product of water at these conditions. For instance, at 23 MPa, the ionic product of water is around  $9 \cdot 10^{-12}$  and  $3 \cdot 10^{-12}$  when the temperature is 260°C and 330°C respectively. The main products of fructose hydrolysis were pyruvaldehyde and 5-HMF. The maximum pyruvaldehyde yield was 67% w-w<sup>-1</sup> in carbon basis at 3.5 s of residence time. At those conditions the amount of 5-HMF was around 10% w-w<sup>-1</sup> carbon basis.

The data for fructose hydrolysis at 400°C at 23MPa and 27 MPa is shown in Figure 3- C and 3-D respectively. For this set of experiments, fructose conversions of 90% were achieved around 1 s. glucose yields were lower than 1 % w-w<sup>-1</sup> for all the experimented residence times. In this case, the reaction medium is supercritical water. The ionic product of water at 400°C and 23 MPa is around  $2 \cdot 10^{-21}$ , therefore, the medium is poorly dissociated and the reactions of fructose isomerization would be disfavoured. The main products were also, pyruvaldehyde and 5-HMF, but in this case, the yield of pyruvaldehyde was higher reaching 89% w-w<sup>-1</sup> at 0.7 s of residence time. It was observed that increasing residence time, the concentration of pyruvaldehyde decreased being in this case the main product organic acids. It was observed that the production of organic acids was not selective, producing several organics acids with low concentration such as formic acid, acrylic acid and levulinic acid among others. The yield of 5-HMF was lower than 9% w-w<sup>-1</sup> carbon basis at 400°C. Pyruvaldehyde yield was higher at 400°C than at 330°C, however, when the pressure was increased up to 27 MPa at 400°C, the yield of 5-HMF was increased up to 20%.

The effective control of the residence time due to the sudden heating and cooling of the biomass stream (see Figure 1 – start and end of the reaction) allows the operation managing with precision when the reactions starts and ends. So, the reactions could be stopped before the degradation of pyruvaldehyde.

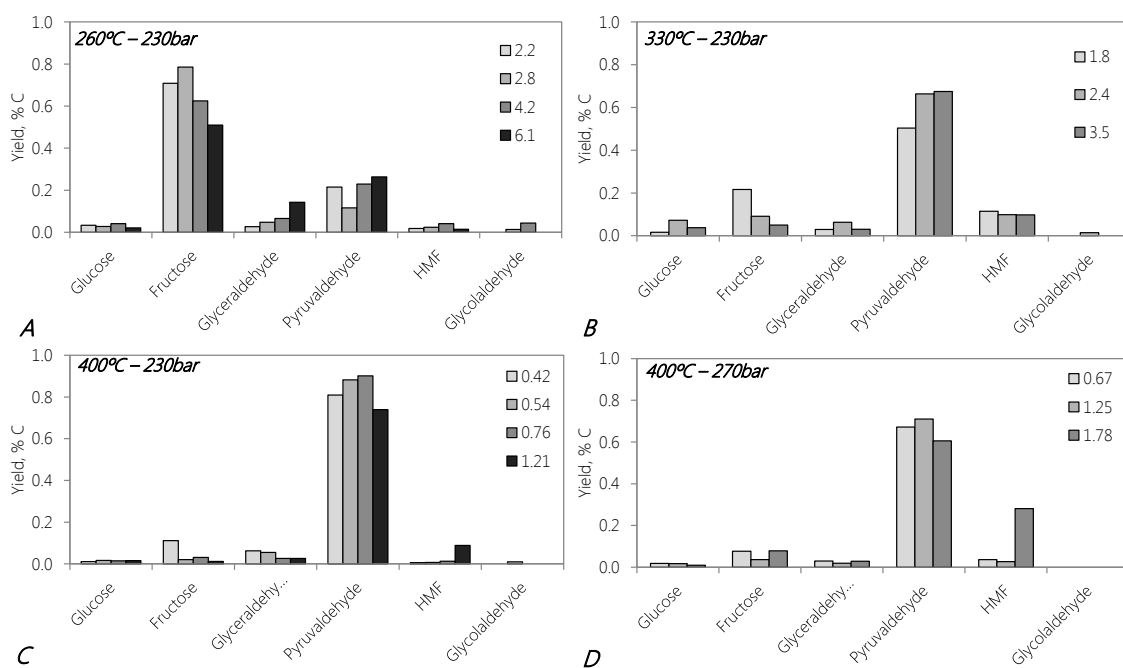


**Fig. 3.** Evolution of fructose hydrolysis products along residence time at: (A) 260°C – 23 MPa, (B) 330°C – 23 MPa, (C) 400°C – 23 MPa and (D) 400°C – 27 MPa. The residence time was varied between 0.4 s and 1.5 s at 400°C. For subcritical temperature the residence time was varied between 1 s and 6 s.

### 3.2. Fructose reactions with medium modifiers

In order to test the effect of ions concentration in the medium, pH was varied using NaOH (sample pH=11) and oxalic acid (sample pH=3). Radical reactions would be enhanced at supercritical conditions. This kind of reactions would be avoided by adding to the system a free radical kidnapper (scavenger). This effect was tested using two commercial scavengers: TEMPO and BHT.

The effect of medium modifiers in the reactions of fructose at 400°C at 23 MPa is shown in figure 4. The maximum pyruvaldehyde yield was 84% w·w<sup>-1</sup> using TEMPO as a medium modifier. Nevertheless, the maximum yield of pyruvaldehyde was similar for all the modifiers at the conditions tested. However, the pH shift, obtained by using NaOH, would affect the reaction of fructose dehydration to produce 5-HMF. The highest yield of 5-HMF was obtained using an acid medium (13% w·w<sup>-1</sup>).

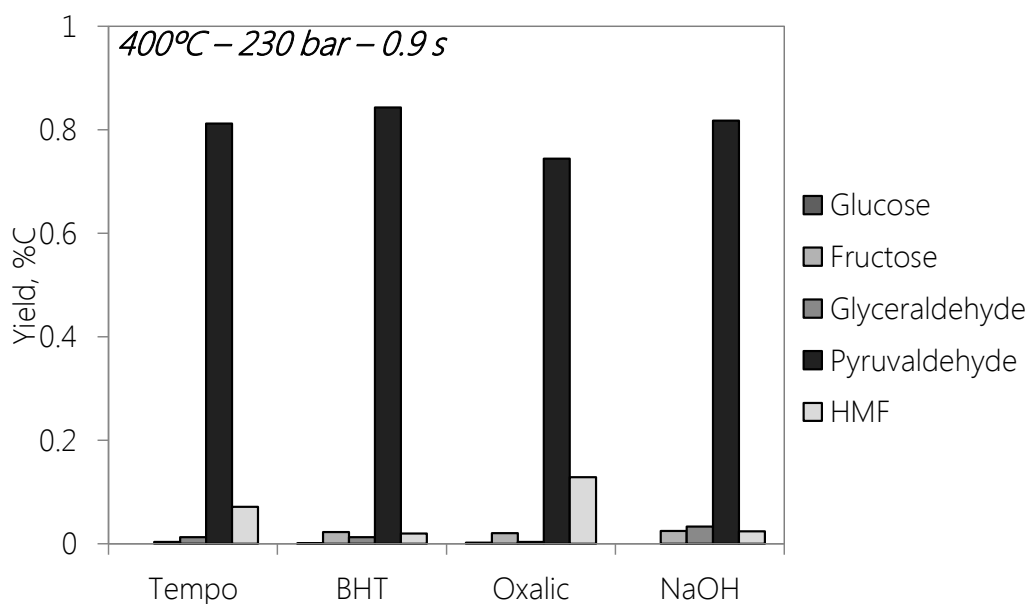


Fig. 4. Fructose hydrolysis products at 400°C and 23 MPa with a modified medium.

### 3.3. Reaction Pathway development. Mixture of Fructose – Glucose as biomass model compound

The reaction pathway was analysed following the reactions of fructose and different mixtures of fructose/glucose. The analysis was made using four different starting biomass depending on fructose/glucose concentrations. The starting solutions were prepared as: 25/75 w-w<sup>-1</sup>; 50/50 w-w<sup>-1</sup>; 75/25 w-w<sup>-1</sup> and 100/0 w-w<sup>-1</sup> of fructose/ glucose. The composition of the products obtained from the different starting materials are shown in figure 5. It can be seen that the main product of glucose and fructose hydrolysis with a residence time of 0.5 s are glycolaldehyde and pyruvaldehyde. Pyruvaldehyde concentration is higher with feeds richer in fructose while glycolaldehyde production is higher with feeds richer in glucose. The main reaction mechanism that proceeded in the analysed conditions was the retro-aldol condensation to give two molecules, an aldose and a ketose. If the reactions proceeded from an aldose (glucose), the products were a C-4 (erythrose) and C-2 (glycolaldehyde). Erythrose is also an aldose and it was also decomposed into two molecules of glycolaldehyde. The yield of glycolaldehyde at 400°C, 23 MPa with 0.5 s of residence time was 76% w-w<sup>-1</sup> carbon basis using the biomass with 25% of fructose. On the other hand, when the reactions proceeded from ketoses (fructose), two molecules of C-3 were produced. Glyceraldehyde was detected as retro-aldol condensation product of fructose, however the yield of glyceraldehyde was low for all the experiments, but the yield of pyruvaldehyde (further reaction of glyceraldehyde)

was high. The reaction of glyceraldehyde to produce pyruvaldehyde would be faster than glyceraldehyde production resulting in low yields of glyceraldehyde.

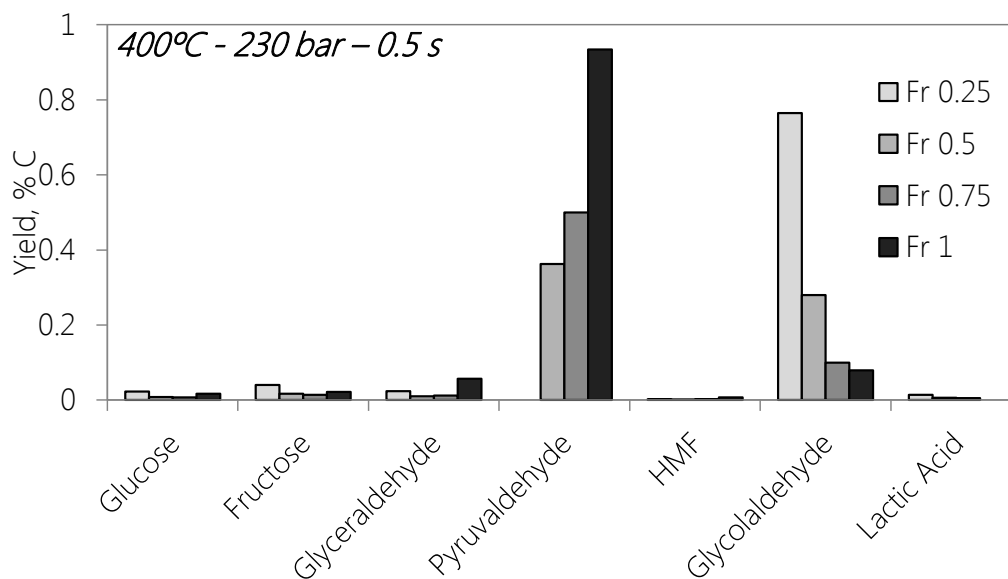


Fig. 5. Hydrolysis reactions of different mixtures of glucose and fructose at 400°C and 23 MPa.

When the feed stream was a mixture of fructose and glucose, the products were composed of a glycolaldehyde – pyruvaldehyde mix. This should be taken into account when the analysis of the samples are performed with and HPLC sugar method because glycolaldehyde and pyruvaldehyde have almost the same retention time. In this work, a mathematical treatment of the chromatograms was applied to each analysis in order to quantify the exact quantity of each component (as it was explained in section 2.2).

#### 4. Conclusions

In this study, the reactions of fructose and glucose as biomass model compounds in pressurized water were analyzed. Fructose can be selectively transformed into pyruvaldehyde (lactic acid precursor) with a yield of 89% without using any catalyst at 400°C and 23 MPa as reaction conditions and 0.7 s of residence time.

The main reaction products of glucose were molecules of two and four carbons, being the C-2 products the highest. In the other hand fructose retro-aldol condensation produced molecules of three carbons. The route of lactic acid production from sugars raw materials would be optimized if the used biomass are ketoses molecules (like fructose) favoring the C-3 molecules production (glyceraldehyde – pyruvaldehyde).

## Acknowledgements

The authors thank the Spanish Ministry of Science and 513 Innovation for the Project CTQ2011-23293 and ENE2012-33613. The authors thank Repsol for its technical support. D.A.C. thanks the Spanish Ministry of Education for the FPU fellowship (AP2009-0402).

## References

1. Bobleter, O., *Hydrothermal degradation of polymers derived from plants*. Progress in polymer science, 1994. 19(5): p. 797-841.
2. Tollefson, J., *Energy: Not your father's biofuels*. Nature News, 2008. 451(7181): p. 880-883.
3. Cantero, D.A., Bermejo, M.D., and Cocero, M.J., *High glucose selectivity in pressurized water hydrolysis of cellulose using ultra-fast reactors*. Bioresource Technology, 2013. 135: p. 697-703.
4. Corma, A., Iborra, S., and Velty, A., *Chemical Routes for the Transformation of Biomass into Chemicals*. Chemical Reviews, 2007. 107(6): p. 2411-2502.
5. Aida, T.M., Sato, Y., Watanabe, M., Tajima, K., Nonaka, T., Hattori, H., and Arai, K., *Dehydration of D-glucose in high temperature water at pressures up to 80 MPa*. The Journal of Supercritical Fluids, 2007. 40(3): p. 381-388.
6. Aida, T.M., Tajima, K., Watanabe, M., Saito, Y., Kuroda, K., Nonaka, T., Hattori, H., Smith Jr, R.L., and Arai, K., *Reactions of D-fructose in water at temperatures up to 400 °C and pressures up to 100 MPa*. The Journal of Supercritical Fluids, 2007. 42(1): p. 110-119.
7. Kabyemela, B.M., Adschiri, T., Malaluan, R.M., and Arai, K., *Glucose and Fructose Decomposition in Subcritical and Supercritical Water: Detailed Reaction Pathway, Mechanisms, and Kinetics*. Industrial & Engineering Chemistry Research, 1999. 38(8): p. 2888-2895.
8. Kabyemela, B.M., Adschiri, T., Malaluan, R.M., Arai, K., and Ohzeki, H., *Rapid and Selective Conversion of Glucose to Erythrose in Supercritical Water*. Industrial & Engineering Chemical Research, 1997. 36(12): p. 5063-5067.
9. Cantero, D.A., Álvarez, A., Bermejo, M.D., and Cocero, M.J., *Transformation of glucose in high added value compounds in a hydrothermal reaction media*. III Iberoamerican Conference on Supercritical Fluids, 2013.
10. Wang, L., Zhao, B., Liu, B., Yu, B., Ma, C., Su, F., Hua, D., Li, Q., Ma, Y., and Xu, P., *Efficient production of L-lactic acid from corncob molasses, a waste by-product in xylitol production, by a newly isolated xylose utilizing Bacillus sp. strain*. Bioresource Technology, 2010. 101(20): p. 7908-7915.

11. Dumbrepatil, A., Adsul, M., Chaudhari, S., Khire, J., and Gokhale, D., *Utilization of Molasses Sugar for Lactic Acid Production by Lactobacillus delbrueckii subsp. delbrueckii Mutant Uc-3 in Batch Fermentation*. Applied and Environmental Microbiology, 2008. 74(1): p. 333-335.
12. Budhavaram, N.K. and Fan, Z., *Production of lactic acid from paper sludge using acid-tolerant, thermophilic Bacillus coagulan strains*. Bioresource Technology, 2009. 100(23): p. 5966-5972.
13. Choi, H.-Y., Ryu, H.-K., Park, K.-M., Lee, E.G., Lee, H., Kim, S.-W., and Choi, E.-S., *Direct lactic acid fermentation of Jerusalem artichoke tuber extract using Lactobacillus paracasei without acidic or enzymatic inulin hydrolysis*. Bioresource Technology, 2012. 114: p. 745-747.
14. Wang, L., Zhao, B., Liu, B., Yang, C., Yu, B., Li, Q., Ma, C., Xu, P., and Ma, Y., *Efficient production of L-lactic acid from cassava powder by Lactobacillus rhamnosus*. Bioresource Technology, 2010. 101(20): p. 7895-7901.
15. Xu, K. and Xu, P., *Efficient production of L-lactic acid using co-feeding strategy based on cane molasses/glucose carbon sources*. Bioresource Technology, 2014. 153: p. 23-29.
16. van Putten, R.-J., van der Waal, J.C., de Jong, E., Rasrendra, C.B., Heeres, H.J., and de Vries, J.G., *Hydroxymethylfurfural, A Versatile Platform Chemical Made from Renewable Resources*. Chemical Reviews, 2013. 113(3): p. 1499-1597.
17. Li, Y., Liu, H., Song, C., Gu, X., Li, H., Zhu, W., Yin, S., and Han, C., *The dehydration of fructose to 5-hydroxymethylfurfural efficiently catalyzed by acidic ion-exchange resin in ionic liquid*. Bioresource Technology, 2013. 133: p. 347-353.
18. Hu, L., Zhao, G., Tang, X., Wu, Z., Xu, J., Lin, L., and Liu, S., *Catalytic conversion of carbohydrates into 5-hydroxymethylfurfural over cellulose-derived carbonaceous catalyst in ionic liquid*. Bioresource Technology, 2013. 148: p. 501-507.
19. Qu, Y., Huang, C., Zhang, J., and Chen, B., *Efficient dehydration of fructose to 5-hydroxymethylfurfural catalyzed by a recyclable sulfonated organic heteropolyacid salt*. Bioresource Technology, 2012. 106: p. 170-172.
20. Yang, F., Liu, Q., Bai, X., and Du, Y., *Conversion of biomass into 5-hydroxymethylfurfural using solid acid catalyst*. Bioresource Technology, 2011. 102(3): p. 3424-3429.

21. Hu, X., Wu, L., Wang, Y., Song, Y., Mourant, D., Gunawan, R., Gholizadeh, M., and Li, C.-Z., *Acid-catalyzed conversion of mono- and poly-sugars into platform chemicals: Effects of molecular structure of sugar substrate*. *Bioresource Technology*, 2013. 133: p. 469-474.
22. Wu, X., Fu, J., and Lu, X., *Hydrothermal decomposition of glucose and fructose with inorganic and organic potassium salts*. *Bioresource Technology*, 2012. 119: p. 48-54.
23. Akiya, N. and Savage, P.E., *Roles of Water for Chemical Reactions in High-Temperature Water*. *Chemical Reviews*, 2002. 102(8): p. 2725-2750.
24. Kruse, A. and Gawlik, A., *Biomass Conversion in Water at 330–410 °C and 30–50 MPa. Identification of Key Compounds for Indicating Different Chemical Reaction Pathways*. *Industrial & Engineering Chemistry Research*, 2002. 42(2): p. 267-279.
25. Kruse, A. and Dinjus, E., *Hot compressed water as reaction medium and reactant: 2. Degradation reactions*. *The Journal of Supercritical Fluids*, 2007. 41(3): p. 361-379.
26. Holm, M.S., Saravanamurugan, S., and Taarning, E., *Conversion of Sugars to Lactic Acid Derivatives Using Heterogeneous Zeotype Catalysts*. *Science*, 2010. 328(5978): p. 602 -605.
27. Aida, T.M., Ikarashi, A., Saito, Y., Watanabe, M., Smith Jr, R.L., and Arai, K., *Dehydration of lactic acid to acrylic acid in high temperature water at high pressures*. *The Journal of Supercritical Fluids*, 2009. 50(3): p. 257-264.
28. Cantero, D.A., Bermejo, M.D., and Cocero, M.J., *Kinetic analysis of cellulose depolymerization reactions in near critical water*. *The Journal of Supercritical Fluids*, 2013. 75: p. 48-57.
29. Stein, T.v., Grande, P.M., Kayser, H., Sibilla, F., Leitner, W., and María, P.D.d., *From biomass to feedstock: one-step fractionation of lignocellulose components by the selective organic acid-catalyzed depolymerization of hemicellulose in a biphasic system*. *Green Chemistry*, 2011. 13(7): p. 1772-1777.
30. Wang, Y., Jin, F., Sasaki, M., Wahyudiono, Wang, F., Jing, Z., and Goto, M., *Selective conversion of glucose into lactic acid and acetic acid with copper oxide under hydrothermal conditions*. *AIChE Journal*, 2013. 59(6): p. 2096–2104.
31. Sasaki, M., Goto, K., Tajima, K., Adschiri, T., and Arai, K., *Rapid and selective retro-aldol condensation of glucose to glycolaldehyde in supercritical water*. *Green Chem.*, 2002. 4(3): p. 285-287.

# Chapter 6. Transformation of Glucose in Added Value Compounds in a Hydrothermal Reaction Media

## Abstract

In this study, the chemical transformation of glucose into added value products (lactic acid and 5-hydroxymethylfurfural) was analyzed using a hydrothermal reaction medium. A continuous pilot plant that operates up to 400°C, 30 MPa and residence times between 0.004 s and 50 s was used in order to study the process. The reactions of glucose in hot pressurized water were analyzed at 300°C, 350°C, 385°C and 400°C; the pressure was fixed at 23 MPa and 27 MPa for the experiments. No lactic acid was found at those conditions. A high concentration of glycolaldehyde (80% carbon basis) was found operating at 400°C and 27 MPa with residence times of 20 s. Two homogeneous catalysts (H<sub>2</sub>O<sub>2</sub> and NaOH) were added in different experiments to improve the lactic acid production. The maximum concentration of lactic acid was 57% carbon basis using NaOH (0.5M) as catalyst at 27 MPa and 400°C with 20 s of residence time. It was observed that the pH of the medium plays an important role in the selectivity of the process. A model of the process kinetic was developed in order to identify the main influential factors on the selectivity.

**Keywords:** Biomass • Lactic Acid • Supercritical Water • Homogeneous Catalyst



## 1. Introduction

The processes that involve biomass valorization for the production of chemicals and fuels are growing in interest looking for sustainable production of these goods [1, 2]. This kind of developments can be achieved by the combination of selective and effective processes using renewable raw materials. The vegetal biomass unfit for human consumption is a massive alternative as a raw material for the production of chemicals, being cellulose (glucose resource) one of the main component of biomass [3]. In a previous work [4, 5], a method to selectively break cellulose into sugars was developed obtaining a solution with 98% w-w<sup>-1</sup> of sugars with a low concentration of degraded products in a supercritical water medium.

Glucose can be modified in a hot pressurized water medium in order to obtain valuable products like lactic acid or 5-hidroxy-methyl-furfural (5-HMF), among others [6-9]. Lactic acid is a product of interest for many industries such as food, chemical, pharmaceutical and cosmetic. Nowadays, the major use of lactic acid would be the production of the biodegradable lactic acid polymer [10]. So far, most lactic acid is produced by chemical synthesis or by carbohydrates fermentation. This last method being the most used in industry [10]. The 5-HMF can be used as starting material for a number of applications, including; polymer productions by monomer modification and polymerization, use as fine chemicals (pharmaceutical, agrochemical, etc.), and the production of fuels[11]. 5-HMF production is mainly achieved by carbohydrates dehydration. The different method of 5-HMF synthesis can be classified by the characteristics of the reaction medium as: single phase systems; biphasic systems and; ionic liquids systems[11].

The different properties that pressurized water medium can adopt depending of its pressure and temperature can be used to choose medium where highest selectivity of chosen compounds are obtained. Ion concentration of the medium seems to be a key factor in the glucose degradations reactions, favoring retro-aldol reactions at low ion concentrations (lactic acid formation pathway) and favoring 5-HMF formation at high ion concentrations (see Chapter 3). For example, the production of lactic acid was

maximized in a batch reactor using NaOH and Ca(OH)<sub>2</sub> as catalysts obtaining yields of between 20 – 30% at temperatures of 300°C and residence time of 60 s[12].

In this study, the influence of the reaction medium in the chemical modification of glucose into added value products (lactic acid) was analyzed using a hydrothermal reaction medium.

## 2. Materials and Methods

### 2.1. Materials

The glucose (99%) sodium hydroxide (>98%) and hydrogen peroxide (30%) used in the experiments was purchased from Sigma. Distilled water was used in the experiments. The patterns used in HPLC (High Performance Liquid Chromatography) analysis were: glucose (>99%), fructose (>99%), glyceraldehyde (95%), glycolaldehyde dimer (99%), pyruvaldehyde (40%), erythrose (>75%), 5-hydroxymethylfurfural (99%) purchased from Sigma.

### 2.2. Analysis

The carbon content of the products was determined by total organic carbon (TOC) analysis with Shimadzu TOC-VCSH equipment. The composition of the liquid products was determined by HPLC. The HPLC column used for the separation of the compounds was Sugar SH-1011 Shodex at 50°C and a flow of 0.8mL/min using H<sub>2</sub>SO<sub>4</sub> (0.01 N) as mobile phase. A Waters IR detector 2414 was used to identify the sugars and their derivatives. An UV-Vis detector was used to determine the 5-hydroxymethylfurfural (5-HMF) concentration at a wavelength of 254nm.

Glucose conversion was determined by equation 1, where  $X$  is the glucose conversion,  $C_i$  is the inlet glucose concentration measured in ppm,  $C_o$  is the outlet glucose concentration measured in ppm.

$$X = \frac{C_i - C_o}{C_i} \quad (1)$$

The selectivity of the determined compounds (fructose, glyceraldehyde, methyl glyoxal, lactic acid, formic acid, acrylic acid and 5-HMF) was determined by equation 2, where  $Y_s$  is the yield of compound 's',  $C_s$  is the concentration of the compound 's' measured in ppm,  $F_{C,s}$  is the carbon composition of the component 's' with a value between 0 and 1 (g carbon/ molecular weight); and 'TOC' is the total organic carbon composition of the sample.

$$Y_s = \frac{C_s F_{C,s}}{TOC} \quad (2)$$

### 2.3. Pilot plant

The continuous pilot plant used in this work is presented in Figure 1. The hydrolysis pilot plant could operate at temperatures up to 400°C and pressures of up to 30 MPa.

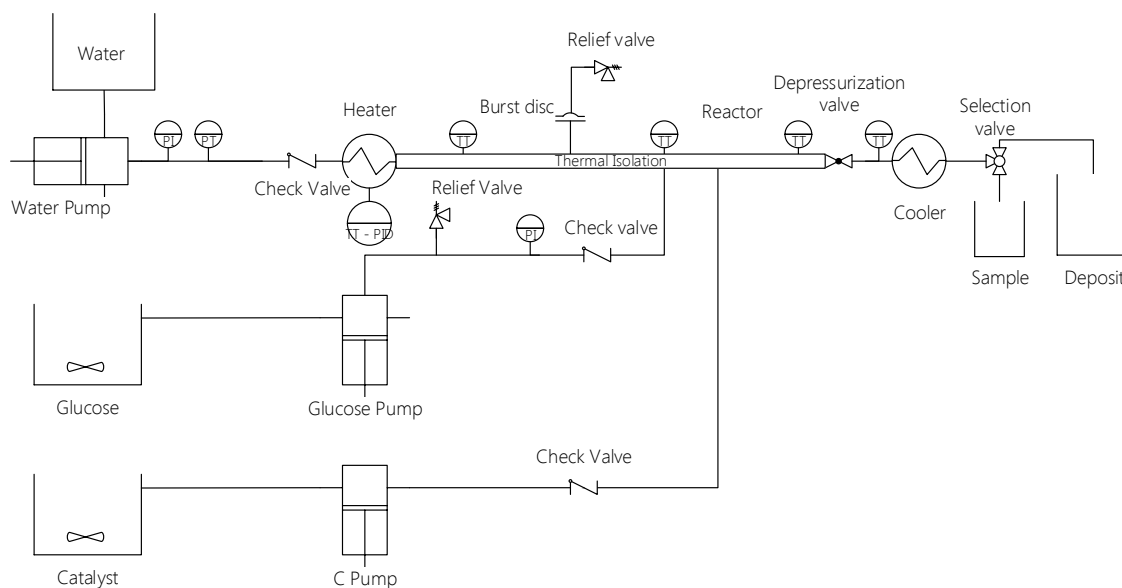


Fig. 1. Pilot plant diagram.

A biomass solution (7% w-w<sup>-1</sup>) was continuously pumped up to the operation pressure and remains at room temperature until the inlet of the reactor. In that point glucose is heated by mixing it with a supercritical water stream. In this way, heating of biomass (start of the reactions) is achieved almost instantaneously. The facility was developed in a previous work [4], however, it was modified in order to be possible of feeding the reactor 10 cm after the inlet. The reactor inlet was fed with a hot stream and the cold glucose stream. Also, the reactor could be fed 10 cm after the inlet. This option was

used to feed the catalyst. A more detailed description and the operation procedure of the pilot plant was presented in a previous work [13].

#### 2.4. Model

In order to evaluate the kinetic of glucose decomposition in pressurized water, the experimental results were fitted using the reaction pathway shown in Figure 2. The used model was developed in Chapter 3. This model takes into account the hydroxide anions concentration in the medium in the reactions where  $\text{OH}^-$  participates forming transition states. In this way the improvements or inhibition of these reactions when  $\text{OH}^-$  is increased or diminished in the reaction media due to the large variations of  $K_w$  (and so, hydroxyls concentration) around the critical point of water can be mathematically described. The fitted reaction rates corresponds to the following reactions: glucose isomerization to produce fructose ( $k_{gf}$ ); fructose dehydration to produce 5-HMF ( $k_{fh}$ ); glucose retro-aldol condensation to produce glycolaldehyde ( $k_{gg}$ ); fructose retro-aldol condensation to produce glyceraldehyde ( $k_{fg}$ ) and glyceraldehyde isomerization to produce pyruvaldehyde ( $k_{gp}$ ).

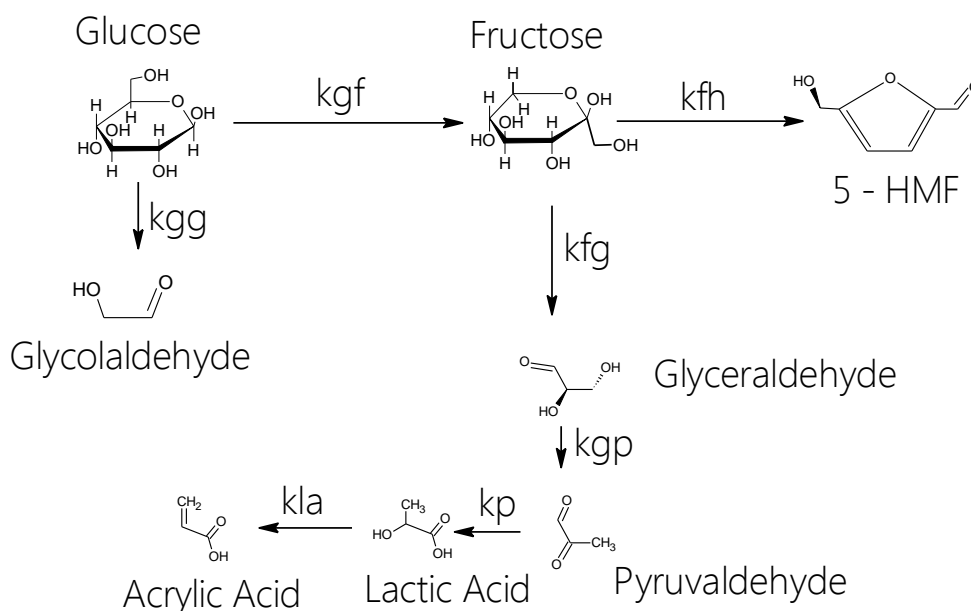


Fig. 2. Reaction pathway of glucose degradation in sub and supercritical water [6-8, 14].

### 3. Results and Discussion

Experiments for glucose reaction in pressurized water were carried out at the conditions shown in Table 1. The residence times were fixed between 0.4s and 50s. The carbon balance in reactor was between 87% - 100%. The lowest values of carbon balance were obtained at 400°C with residence times higher than 3 s. These low values of carbon balance may be obtained due to the gasification process that could take place at 400°C and high residence times. No char formation was observed in the effluent of the reactor. The main reaction products identified were glucose, fructose, glyceraldehyde, 5-HMF, glycolaldehyde, pyruvaldehyde, lactic acid and acrylic acid.

**Table 1.** Reaction medium properties at reactions conditions.

Temperature °C	Pressure MPa	Density kg/m <sup>3</sup>	Ionic Product pKw	Dielectric Constant ε
300	23	739	11.7	24.5
350	23	616	11.9	14.7
385	23	171	19.4	2.5
400	23	133	20.8	2.0
400	27	219	17.8	3.2

#### 3.1. Concentration Profiles

A reaction pathway of glucose hydrolysis in hot pressurized water is shown in figure 2. Glucose can be degraded mainly by a retro-aldol reaction to glycolaldehyde or via isomerization to fructose. Then, fructose can be dehydrated to 5-HMF [6, 15]. Also, fructose can follow a retro-aldol condensation reaction to produce glyceraldehyde, which is further isomerized to pyruvaldehyde. These three carbon molecules have similar chemical composition as pyruvaldehyde and they could be considered as lactic acids precursors [16]. In order to analyze the effect of the medium temperature and residence time in the reactions of glucose hydrolysis the experiments were analyzed

at a temperature of 300, 350, 385 and 400°C. The concentration evolution of the glucose, fructose, glyceraldehyde, glycolaldehyde and 5-HMF along residence time are shown in Figures 3, 4 and 5.

Total glucose conversion was achieved at residence time of 4 s, 4.5s, 8 s and 40 s for temperatures of 400°C, 385°C, 350°C and 300°C respectively at 23 MPa as it is shown in Figure 3-A, 3-B, 3-C and 3-D.

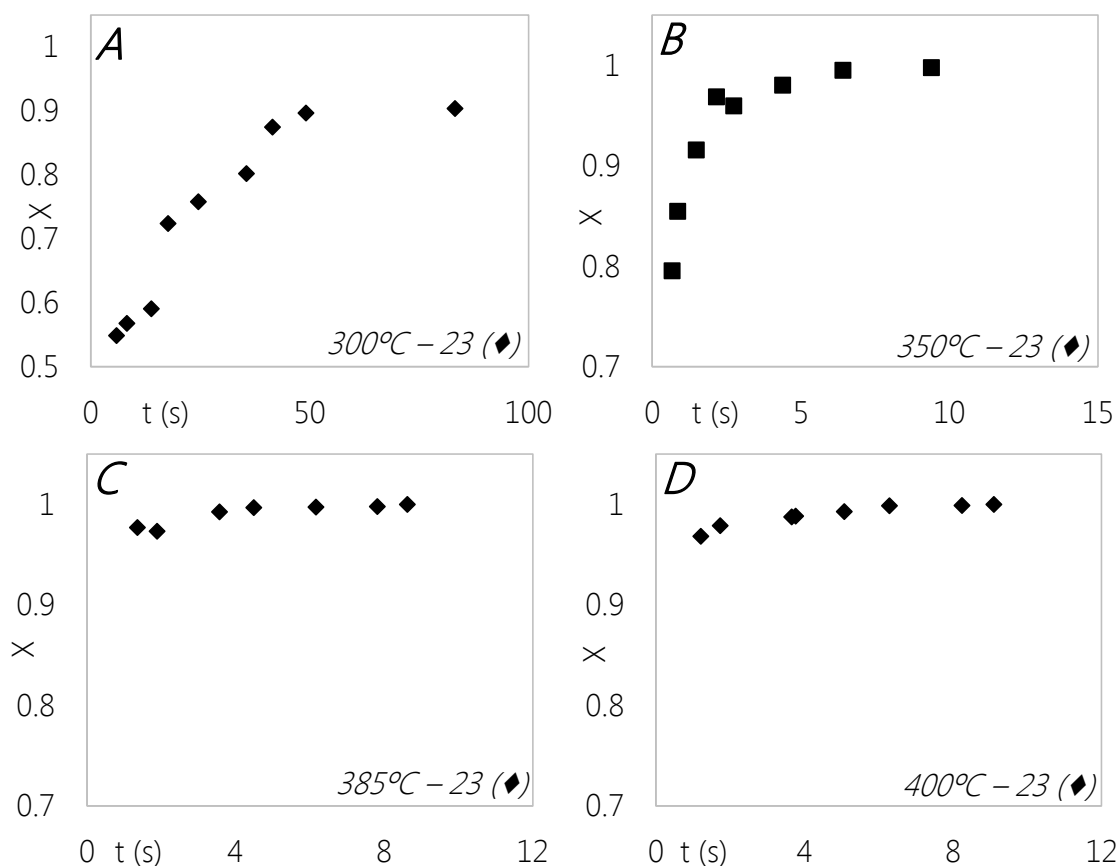


**Fig. 3.** Glucose conversion along residence time at 300°, 350°C, 385°C and 400°C. Selectivity evolution along residence time of fructose, glyceraldehyde, pyruvaldehyde and 5-HMF at 300°, 350°C, 385°C and 400°C.

The concentration evolution along residence time of fructose and glyceraldehyde are shown in Figure 4. These products had a similar behavior, so their evolutions are analyzed together. The maximum selectivity was achieved at 300°C and 23 MPa as it is shown in Figures 4-A and 4-E for fructose and glyceraldehyde respectively. About 20% of glucose was converted into fructose in a residence time of 5 s and about 15% of glucose is converted to glyceraldehyde (via fructose) at the same conditions.

The concentration profiles of glycolaldehyde along residence time are shown in Figures 5-A to 5-D. The maximum concentration of glycolaldehyde was achieved at 400°C and 23 MPa with a residence time of 3 s, glycolaldehyde selectivity at those conditions was 75% w·w<sup>-1</sup> as it can be seen in Figure 5-D. In the studied range of pressure, the density effect is not significant over glycolaldehyde selectivity. Thus, reaction temperature is the main factor to be considered to improve selectivity because the kinetic of glycolaldehyde production is increased more than others kinetics. From the chemical point of view, an increase in the temperature over the critical point of water will decrease the ionic product of water, and so the hydroxyl anion concentration. A low concentration of OH<sup>-</sup> in the medium would disfavor the reactions of glucose isomerization to fructose. Hence, retro-aldol condensation reaction of glucose would be enhanced instead glucose isomerization when temperature is increased above the critical point of water.

The maximum concentration of 5-HMF was achieved at the lowest temperature, 300°C. The maximum selectivity of 5-HMF was 30% at 50 s of residence time. By increasing the reaction temperature the production of 5-HMF was highly avoided. The reaction of fructose dehydration would take place forming transition states with OH<sup>-</sup> (1 transition state per water molecule lost). As it was analyzed for glucose isomerization, when temperature is increased, the OH<sup>-</sup> concentration would be determining in the selectivity of 5-HMF.

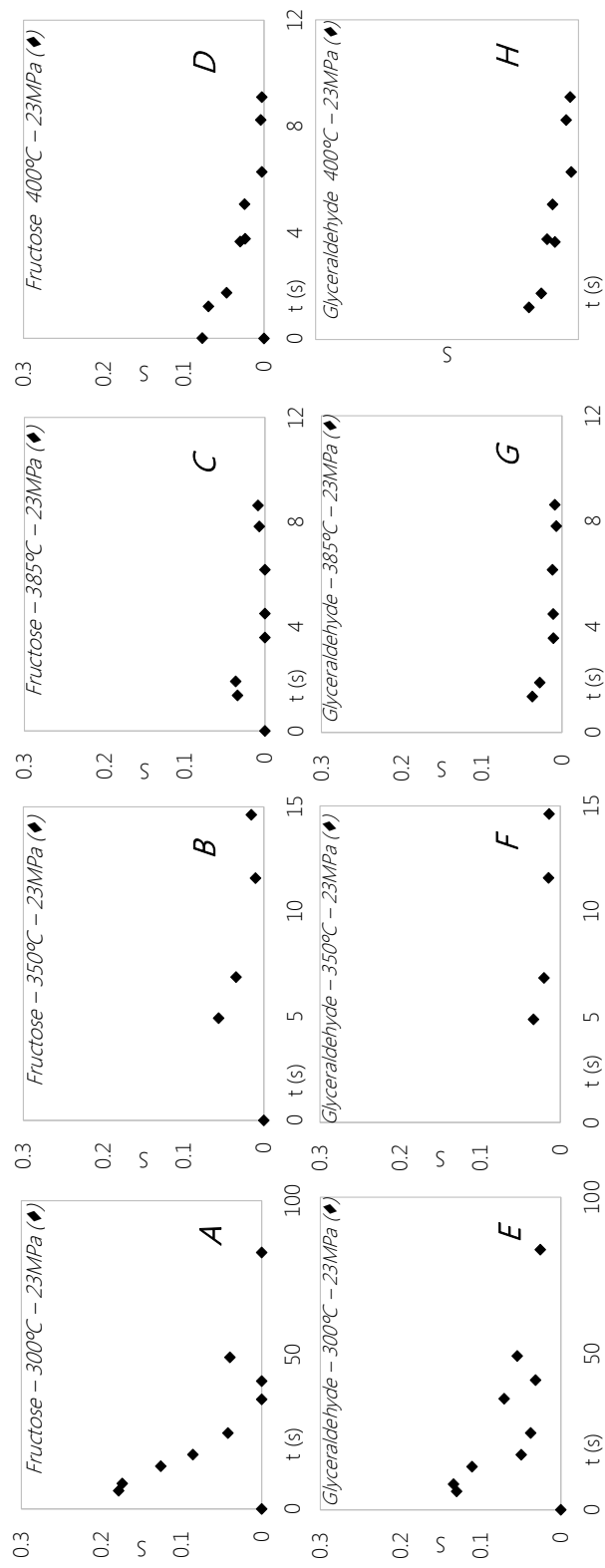


Fig. 4. Selectivity evolution along residence time of fructose (A, B, C, D) and glyceraldehyde (E, F, G, H) at 300°, 350°C, 385°C and 400°C

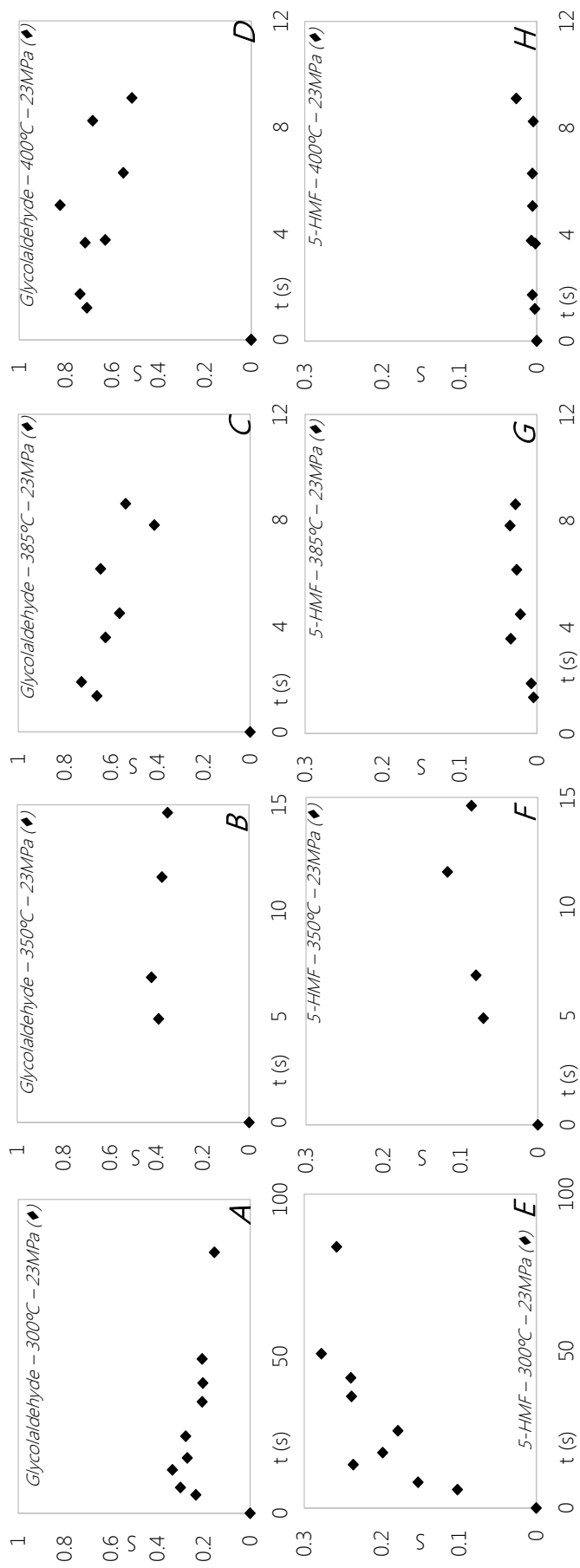
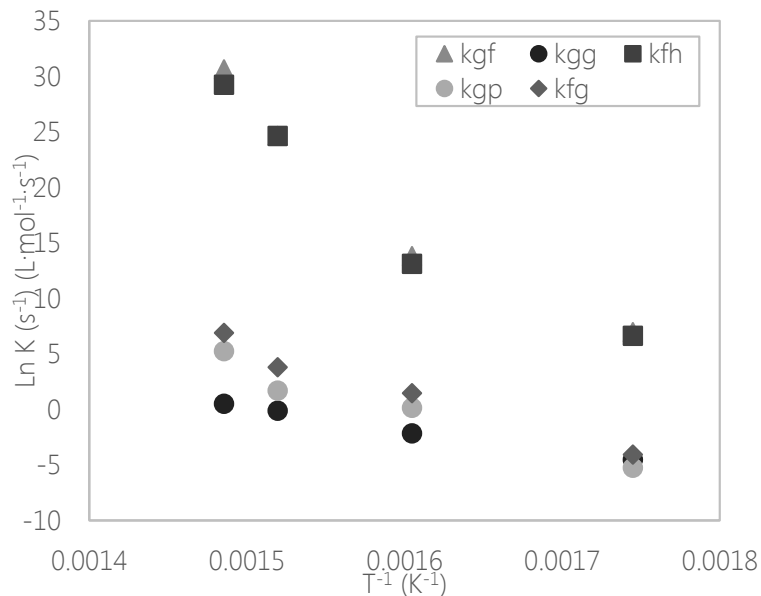


Fig. 5. Selectivity evolution along residence time of glycolaldehyde (A, B, C, D) and 5-HMF (E, F, G, H) at 300°, 350°C, 385°C and 400°C respectively.

### 3.2. Kinetic Analysis

The reaction rates obtained from the model resolution are shown in Figure 6. The activation energy ( $E_a$ ) and pre-exponential factor ( $\ln k_0$ ) according the Arrhenius relationship were calculated and are shown in Table 2. It is observed that the fitted values for the kinetics of glucose isomerization to fructose ( $k_{gf}$ ) and fructose dehydration to 5-HMF ( $k_{fh}$ ) are higher than the others. This is because these kinetics were calculated taking into account the hydroxide anions and glucose or fructose concentration as reagents (Chapter 3). The hydroxide anions concentration at supercritical conditions is extremely low due to almost no-dissociation of water ( $pK_w=20.8$ ). Therefore, the values of  $k_{gf}$  or  $k_{fh}$  should be high in order to fit the concentration profiles with the model. In addition, these units are like kinetic constants of the second order reactions ( $L \cdot mol^{-1} \cdot s^{-1}$ ). Equation 3 shows the evolution of fructose molar concentration along residence time calculated in the used model.

$$\frac{dF}{dt} = k_{gf} n_{OH} n_G - (k_{fh} n_{OH} + k_{fa} + k_{fg}) n_F \quad (3)$$



**Fig. 6.** Reaction rate of: (▲) glucose isomerization to fructose ( $k_{gf}$  -  $L \cdot mol^{-1} \cdot s^{-1}$ ); (■) fructose dehydration ( $k_{fh}$  -  $L \cdot mol^{-1} \cdot s^{-1}$ ); (●) glucose retro-aldol condensation ( $k_{gg}$  -  $s^{-1}$ ); (◆) fructose retro-aldol condensation ( $k_{fg}$  -  $s^{-1}$ ); (●) glyceraldehyde isomerization to pyruvaldehyde ( $k_{gp}$  -  $s^{-1}$ ).

Where  $F$  is the molar flow of fructose;  $n_{OH}$  is the molar concentration of hydrolysis in the medium;  $n_G$  is the molar concentration of glucose;  $n_F$  is the molar concentration

of fructose and  $k_{fa}$  is the kinetics of fructose decomposition to organics acids. The kinetic constants of  $k_{gf}$ ,  $k_{fh}$ ,  $k_{gg}$ ,  $k_{fg}$  and  $k_{gp}$  are plotted in Figure 6 respectively.

**Table 2.** Fitted Arrhenius parameters for the reactions of glucose in pressurized water.

	Ea kJ·mol <sup>-1</sup>	Uncertainty Ea kJ·mol <sup>-1</sup>	Ln ko	Uncertainty Ln ko	R <sup>2</sup>
kgf	738	-144	159.9	27.5	0.93
kfh	721	-138	156.2	26.3	0.93
kgg	163	-9	29.5	1.8	0.99
kfg	329	-37	64.8	7.1	0.97
kgp	306	-49	58.9	9.4	0.95

### 3.3. Medium selectivity

The properties of the reaction medium are shown in Table 1. These properties were calculated according to IAPWS [17]. The density change from 350°C/23 MPa (616 kg/m<sup>3</sup>) to 400°C/23 MPa (133 kg/m<sup>3</sup>) implies that that density decreased almost 5 times, while the ionic product ( $pK_w$ ) is decreased 9 order of magnitude and the dielectric constant ( $\epsilon$ ) is decreased 7 times.

At 300°C, the selectivity of 5-HMF is higher than the glycolaldehyde selectivity (28% w·w<sup>-1</sup> vs 18% w·w<sup>-1</sup>). By rising temperature the selectivity of glycolaldehyde is increased while 5-HMF selectivity is decreased. Temperature would have a predominant effect in the selectivity due to the change in the identity of the medium (ionic product). At supercritical conditions, where ions concentration is low, the reaction pathway of glucose retro-aldol condensation is benefited over the other reactions. The maximum selectivity of glycolaldehyde achieved at supercritical conditions was 75% w·w<sup>-1</sup>.

### 3.4. Production of added value products: lactic acid

In a water medium, the reactions of glucose degradations did not produce lactic acid. In order to obtain lactic acid several catalyst combinations were experimented. The different experiments carried out are shown in Table 3.

**Table 3.** Different catalyst combinations used in the experimentation. The temperature of the experiments was kept constant at 400°C. NaOH was used with a concentration of 0.5 M. NaOH\* refers to the experiment in which sodium hydroxide was fed in an independent stream to the reactor. H<sub>2</sub>O<sub>2</sub> was used in a stoichiometric concentration. <sup>a</sup> The biomass was glucose. <sup>b</sup> The biomass was Fructose. <sup>c</sup> The biomass was cellulose.

Conditions			Selectivity, % w·w <sup>-1</sup> carbon basis		
P MPa	Residence time (s)	Catalyst	Glycolaldehyde	Lactic Acid	Acrylic Acid
23	20.0 ±0.3	-	0.85	0	0.01
23	43.5±1.7	NaOH	0	0.08	0.03
27	12.1±0.1	H <sub>2</sub> O <sub>2</sub>	0.26	0	0.14
27	10.0±0.1	H <sub>2</sub> O <sub>2</sub>	0.2	0	0.01
27	10.2±0.1	H <sub>2</sub> O <sub>2</sub>	0.11	0	0.03
27	10.2±0.1	NaOH	0.09	0	0.02
27	40.1±0.5	NaOH	0	0.41	0.05
27	30.0±0.5	NaOH + H <sub>2</sub> O <sub>2</sub>	0	0.05	0.01
27	20.6 ±0.3	NaOH* <sup>a</sup>	0.1	0.54	0.05
27	22.2 ±0.3	NaOH* <sup>b</sup>	0.05	0.57	0.07
27	21.6 ±0.3	NaOH* <sup>c</sup>	0.43	0.48	0.03

Reaction time was increased at 400°C in order to evaluate if lactic acid is produced at higher residence times. However, at 400°C and 23 MPa, the main product was glycolaldehyde with a selectivity of 85% at 20 s of residence time. No lactic acid was produced at those conditions. As it was discussed in Chapter 5, sodium hydroxide favors the isomerization of glucose to fructose. This is a desired reaction because fructose retro-aldol condensation produces pyruvaldehyde, which is a lactic acid precursor. The use of NaOH as catalyst would also favor the conversion of pyruvaldehyde into lactic acid [18, 19].

Sodium hydroxide and hydrogen peroxide were tested as catalyst and reagent respectively in the experiments in order to produce lactic acid. The catalyst was fed to the reactor together with glucose. The experiments using sodium hydroxide produce lactic acid with a selectivity of 8% w·w<sup>-1</sup> in a residence time of 43 s. When hydrogen peroxide was used injected together with glucose, the glycolaldehyde production was lower than without catalyst but no lactic acid was produced. The maximum selectivity (40% w·w<sup>-1</sup>) of lactic acid was achieved using sodium hydroxide at a pressure of 27 MPa and a residence time of 40 s. The lactic acid selectivity was increased from 5% to 40% when the residence time was increased from 30 s to 40 s. During

the experiments it was observed that glucose stream was degraded prior pumped when the solution was dosed with the catalyst. In order to avoid this phenomenon, the experimental setup was modified. In the new disposition (Figure1), the catalyst was fed to the reactor in an independent stream, so, the catalyst will acts only in the reactor. The selectivity of lactic acid was increased up to 54% w·w<sup>-1</sup> carbon basis when the catalyst was fed directly to the reactor (See Table 3 – NaOH\*<sup>a</sup>).

In order to evaluate the effect of the starting biomass fructose and cellulose were also evaluated at the same conditions than glucose. It was observed that the selectivity of lactic acid was slightly increased when the starting biomass was fructose (See Table 3 – NaOH\*<sup>b</sup>). The retro-aldol condensation of a six-carbon ketose (like fructose) produces two molecules of three carbons (glyceraldehyde). Glucose retro-aldol condensation produces two molecules: a two carbons molecule and a 4 carbons molecule. Lactic acid is also a three carbon molecule, so the production of lactic acid would be enhanced by using a ketose as starting material. When starting biomass was changed to cellulose, it was observed that the selectivity of lactic acid was decreased (48% w·w<sup>-1</sup> carbon basis) while the selectivity of glycolaldehyde was highly increased (See Table 3 – NaOH\*<sup>c</sup>). The HPLC chromatograms for these three experiments are shown in Figure 7. The blue line corresponds to lactic acid. Using these HPLC column the separation between area corresponding to glycolaldehyde and lactic acid areas in the chromatogram was not clear.

In order to accurately know the concentration of each peak, a mathematical treatment of the chromatogram was applied. In order to identify the main peaks and calculate the areas of the complex mixture that we obtained during the experiments we have used a band-analysis via Fast Fourier Transform (fft) and band-adjustment by Gaussian functions. The adjustment was done by minimizing the quadratic error using a Nelder-Mead algorithm. The HPLC chromatograms and the peak corresponding to lactic acid are plotted in Figure 5 for glucose (A), fructose (C) and cellulose (C) as starting material. The originals HPLC Chromatograms can be seen in the Supporting Information. It should be mentioned that the peak that appears in all chromatograms at an elution time of 7 minutes corresponds to sulfuric acid. Sulfuric acid was added to the sample in order to set an appropriate pH for the HPLC column.

The concentration of acrylic acid was also analyzed in the experiments using catalyst. Acrylic acid is a degradation product of lactic acid dehydration reaction [20]. The maximum selectivity of acrylic acid was obtained when H<sub>2</sub>O<sub>2</sub> was used as catalyst with a residence time of 12 s.

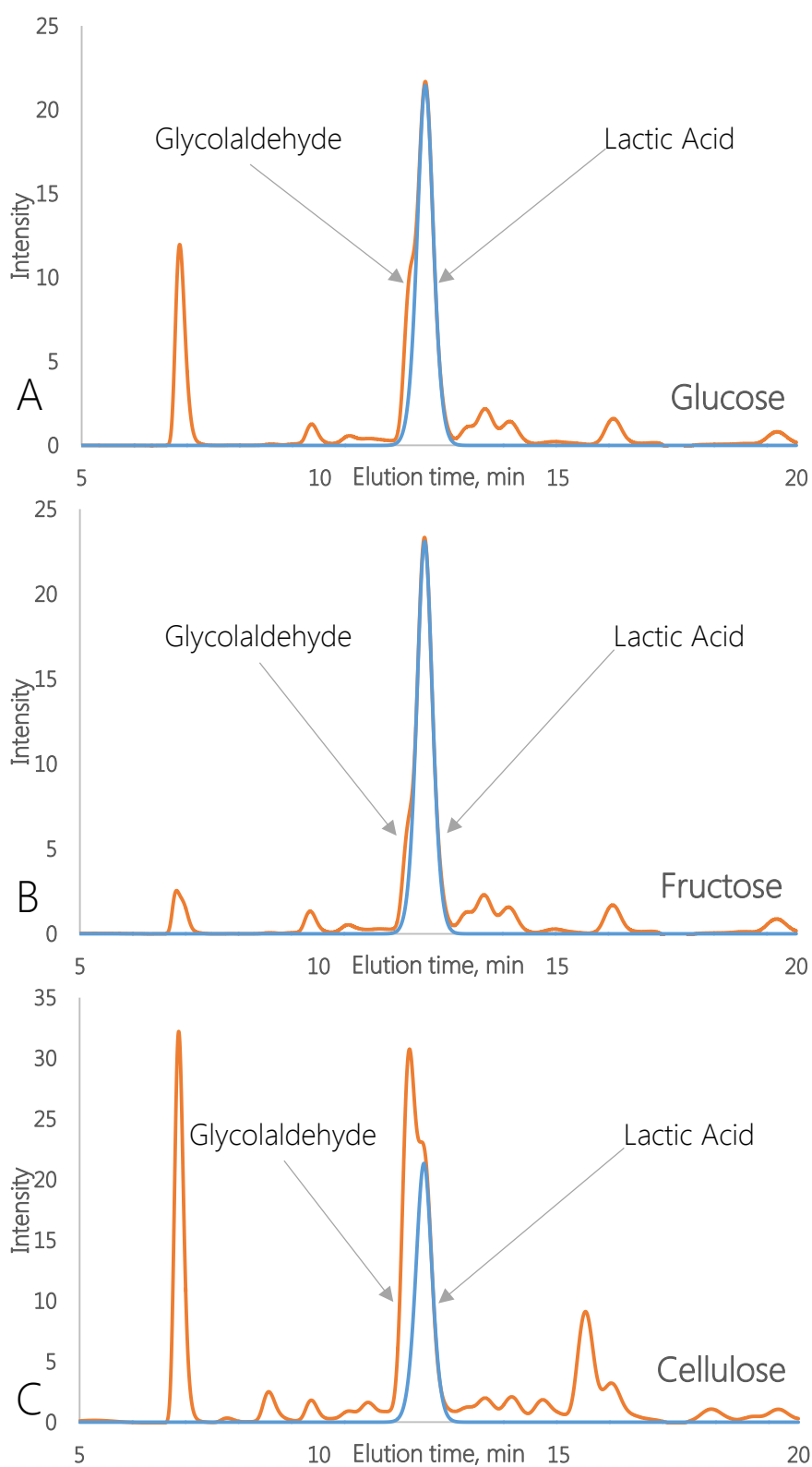


Fig. 7. RI HPLC chromatograms for different starting biomass (A) glucose; (B) fructose and; (C) cellulose. Orange line: original chromatogram. Blue line: Lactic acid peak.

#### 4. Conclusions

The selectivity of the reactions of glucose in pressurized water could be driven by managing the temperature and the density of the medium. The temperature would play an important role in the intensification of one of the following parallel reactions: production of 5-HMF via fructose dehydration; or glycolaldehyde formation via retro-aldol condensation of glucose. At low temperatures 5-HMF formation reactions are favored; at high temperatures the glycolaldehyde reactions are favored. The non-ionic medium induced at supercritical temperatures would favor the retro-aldol condensation of glucose instead isomerization or dehydration.

Lactic acid was studied as value added product formed from glucose hydrolysis. This compound was produced by using lactic acid as catalyst. A lactic acid selectivity of 57% w·w<sup>-1</sup> carbon basis was achieved using a continuous reactor at 400°C and 27 MPa and a residence time of 20 s. The maximum lactic acid production was reached using NaOH as catalyst. Sodium hydroxide enhanced the glucose isomerization to fructose as well as the pyruvaldehyde conversion into lactic acid.

#### Acknowledgements

The authors thank the Spanish Ministry of Economy and Competitiveness for the Project CTQ2011-23293 and ENE2012-33613. The authors thank Repsol for its technical support. D.A.C. thanks the Spanish Ministry of Education for the FPU fellowship (AP2009-0402).

## References

1. Arai, K., Smith Jr, R.L., and Aida, T.M., *Decentralized chemical processes with supercritical fluid technology for sustainable society*. The Journal of Supercritical Fluids, 2009. 47(3): p. 628-636.
2. Ragauskas, A.J., Williams, C.K., Davison, B.H., Britovsek, G., Cairney, J., Eckert, C.A., Frederick, W.J., Hallett, J.P., Leak, D.J., Liotta, C.L., Mielenz, J.R., Murphy, R., Templer, R., and Tschaplinski, T., *The Path Forward for Biofuels and Biomaterials*. Science, 2006. 311(5760): p. 484 -489.
3. Bobleter, O., *Hydrothermal degradation of polymers derived from plants*. Progress in polymer science, 1994. 19(5): p. 797-841.
4. Cantero, D.A., Bermejo, M.D., and Cocero, M.J., *High glucose selectivity in pressurized water hydrolysis of cellulose using ultra-fast reactors*. Bioresource Technology, 2013. 135: p. 697-703.
5. Tollefson, J., *Energy: Not your father's biofuels*. Nature News, 2008. 451(7181): p. 880-883.
6. Aida, T.M., Sato, Y., Watanabe, M., Tajima, K., Nonaka, T., Hattori, H., and Arai, K., *Dehydration of D-glucose in high temperature water at pressures up to 80 MPa*. The Journal of Supercritical Fluids, 2007. 40(3): p. 381-388.
7. Aida, T.M., Tajima, K., Watanabe, M., Saito, Y., Kuroda, K., Nonaka, T., Hattori, H., Smith Jr, R.L., and Arai, K., *Reactions of D-fructose in water at temperatures up to 400 °C and pressures up to 100 MPa*. The Journal of Supercritical Fluids, 2007. 42(1): p. 110-119.
8. Kabyemela, B.M., Adschiri, T., Malaluan, R.M., and Arai, K., *Glucose and Fructose Decomposition in Subcritical and Supercritical Water: Detailed Reaction Pathway, Mechanisms, and Kinetics*. Industrial & Engineering Chemistry Research, 1999. 38(8): p. 2888-2895.
9. Kabyemela, B.M., Adschiri, T., Malaluan, R.M., Arai, K., and Ohzeki, H., *Rapid and Selective Conversion of Glucose to Erythrose in Supercritical Water*. Industrial & Engineering Chemical Research, 1997. 36(12): p. 5063-5067.
10. Corma, A., Iborra, S., and Velty, A., *Chemical Routes for the Transformation of Biomass into Chemicals*. Chemical Reviews, 2007. 107(6): p. 2411-2502.

11. van Putten, R.-J., van der Waal, J.C., de Jong, E., Rasrendra, C.B., Heeres, H.J., and de Vries, J.G., *Hydroxymethylfurfural, A Versatile Platform Chemical Made from Renewable Resources*. Chemical Reviews, 2013. 113(3): p. 1499-1597.
12. Yan, X., Jin, F., Tohji, K., Moriya, T., and Enomoto, H., *Production of lactic acid from glucose by alkaline hydrothermal reaction*. Journal of Materials Science, 2007. 42(24): p. 9995-9999.
13. Cantero, D.A., Bermejo, M.D., and Cocero, M.J., *Kinetic analysis of cellulose depolymerization reactions in near critical water*. The Journal of Supercritical Fluids, 2013. 75: p. 48-57.
14. Kabyemela, B.M., Adschiri, T., Malaluan, R., and Arai, K., *Degradation Kinetics of Dihydroxyacetone and Glyceraldehyde in Subcritical and Supercritical Water*. Industrial & Engineering Chemistry Research, 1997. 36(6): p. 2025-2030.
15. Sasaki, M., Goto, K., Tajima, K., Adschiri, T., and Arai, K., *Rapid and selective retro-aldol condensation of glucose to glycolaldehyde in supercritical water*. Green Chem., 2002. 4(3): p. 285-287.
16. Holm, M.S., Saravanamurugan, S., and Taarning, E., *Conversion of Sugars to Lactic Acid Derivatives Using Heterogeneous Zeotype Catalysts*. Science, 2010. 328(5978): p. 602 -605.
17. Wagner, W, Cooper, J, R., Dittmann, et al., *The IAPWS industrial formulation 1997 for the thermodynamic properties of water and steam*. 2000, American Society of Mechanical Engineers: New York, N, ETATS-UNIS.
18. Watanabe, M., Aizawa, Y., Iida, T., Levy, C., Aida, T.M., and Inomata, H., *Glucose reactions within the heating period and the effect of heating rate on the reactions in hot compressed water*. Carbohydrate Research, 2005. 340(12): p. 1931-1939.
19. Wang, Y., Jin, F., Sasaki, M., Wahyudiono, Wang, F., Jing, Z., and Goto, M., *Selective conversion of glucose into lactic acid and acetic acid with copper oxide under hydrothermal conditions*. AIChE Journal, 2013. 59(6): p. 2096–2104.
20. Aida, T.M., Ikarashi, A., Saito, Y., Watanabe, M., Smith Jr, R.L., and Arai, K., *Dehydration of lactic acid to acrylic acid in high temperature water at high pressures*. The Journal of Supercritical Fluids, 2009. 50(3): p. 257-264.



# Chapter 7. Simultaneous and Selective Recovery of Cellulose and Hemicellulose Fractions from Wheat Bran by Supercritical Water Hydrolysis

## Abstract

In this study the conversion of wheat bran into soluble oligosaccharides and monosaccharide such as glucose, xylose and arabinose was analyzed in a supercritical water medium. The hydrolysis reactions were performed in a continuous pilot plant at 400 °C, 25 MPa and residence times between 0.1 and 0.7 seconds. The yield of the process was evaluated for different products, such as C-6 (glucose derived from cellulose) and C-5 sugars (saccharide derived from hemicellulose hydrolysis). The production of glycolaldehyde and 5-hydroxymethylfural (5-HMF) was analyzed as byproducts formation. Operating under supercritical conditions a biomass liquefaction of 84% w·w<sup>-1</sup> was achieved at 0.3 s of residence time. The obtained solid after the hydrolysis is composed of 86% w·w<sup>-1</sup> of lignin. The highest recovery of cellulose (C-6) and hemicellulose (C-5) as soluble sugars (76% w·w<sup>-1</sup>) was achieved at 0.19 s of residence time. An increase in the residence time decreased the yield of C-6 and C-5. A total recovery of C-5 was achieved at 0.19 s, however at longer residence times, the yield of C-5 decreased. On the other hand, the highest yield (65% w·w<sup>-1</sup>) of C-6 was achieved at 0.22 s of residence time. The main hydrolysis product of C-6 and C-5 was glycolaldehyde yielding the 20% w·w<sup>-1</sup> at 0.22 s of residence time. The 5-HMF production was highly inhibited in the experimented conditions obtaining yields lower than 0.5 % w·w<sup>-1</sup>.

**Keywords:** Biorefinery • Glucose • Glycolaldehyde • Lignin • Xylose



## 1. Introduction

The processes based on the conversion of biomass resources into fuels and chemicals have been intensively studied in the recent years due to the necessity of changing the current production philosophy based on oil to the bioeconomy [1, 2]. Vegetal biomass is a promising raw material for the production of chemicals and fuels because it is an abundant, renewable and world-wide distributed source of carbon [3]. The vegetal biomass is generally composed of: 40 – 45 % cellulose, 25 – 35 % hemicellulose and 15 – 30 % lignin [4]. One of the main challenges of biomass usage is the efficient depolymerization of cellulose and hemicellulose into its composing monomers [5].

The use of sub and supercritical water has been proposed as a promising solvent to process biomass due to its special properties very promising to perform the hydrolysis reactions [1, 3, 6]. The main variations in water properties are: (1) in the surrounding of the critical point, the dielectric constant decreases by increasing temperature, increasing in this way solubility of organic compounds and; (2) the ionic product of water varies from  $10^{-10}$  to  $10^{-22}$  when changing the temperature from 300°C to 400°C at 25 MPa, changing the benefited reaction mechanism from ionic to free-radical [7]. In addition, the hydrothermal processing presents the following advantages: (1) it is not necessary to reduce the water content in the raw material, what implies an important energy saving; (2) the same reaction medium is suitable for the transformation of the different biomass fractions; (3) mass transfer limitations are reduced or avoided, thus reaction rates are faster [6, 8-11].

The conversion of biomass components (cellulose, hemicellulose and lignin) into their constitutive monomers using supercritical water have been previously reported [12-14]. The challenge then is to apply this technology to complex biomass, in order to transform it in valuable products by using a clean, safe and environmentally benign technology. The fractionation and hydrolysis of vegetal biomass in a hydrothermal medium has been studied using different kinds of reactors: batch [15-19], semi continuous [20-25] and continuous reactors [26-28]. In the aforementioned works, the yields of cellulose recovery as soluble sugars are between 3% w·w<sup>-1</sup> – 15% w·w<sup>-1</sup>; 16% w·w<sup>-1</sup> – 22% w·w<sup>-1</sup> and; 2% w·w<sup>-1</sup> – 6% w·w<sup>-1</sup> for batch, semi continuous and continuous reactors respectively. The hemicellulose yields recovery are between 17% w·w<sup>-1</sup> – 97% w·w<sup>-1</sup>; 18% w·w<sup>-1</sup> – 95% w·w<sup>-1</sup> and 25% w·w<sup>-1</sup> – 95% w·w<sup>-1</sup> for batch, semi continuous and continuous reactors respectively. Finally, the lignin

compositions of the solids in the reactor are between 45% w·w<sup>-1</sup> – 53% w·w<sup>-1</sup> and 20% w·w<sup>-1</sup> – 50% w·w<sup>-1</sup> for batch and semi continuous reactors respectively.

Wheat bran is a by-product of the milling of wheat to produce white flour. Bran fraction constitutes around 11% of the total milling by-products and only 10% of wheat bran available is used as fiber supplement in breakfast cereals and bakeries (human consumption) while the remaining 90% is used as animal feed [29]. Compositional analysis suggests that wheat bran contains approximately 30% w·w<sup>-1</sup> – 40% w·w<sup>-1</sup> of hemicellulose, 15% w·w<sup>-1</sup> – 35% w·w<sup>-1</sup> of cellulose and 5% w·w<sup>-1</sup> – 25% w·w<sup>-1</sup> of lignin, depending on growing conditions and varieties [30, 31].

Traditional hydrolysis processes using acid catalysts or enzymes have been improved in last years but they still present limitations in providing high yield in moderate residence times. The hydrolysis of wheat bran was carried out combining acid hydrolysis (0.2 % w·w<sup>-1</sup> sulfuric acid, 160 °C for 20 min) with enzymatic hydrolysis (2 % enzymes, 50 °C for 72 h) obtaining a yield of 80% w·w<sup>-1</sup> of sugars [32]. Wheat bran hydrolysis can also be achieved exclusively by acid hydrolysis using sulfuric acid (1% w·w<sup>-1</sup>) as catalyst at temperatures between 110°C and 180°C for 40 min, obtaining around 80 % w·w<sup>-1</sup> of sugars [33]. Other methods were proposed in order to reduce the concentration of degradation products, such as a combined method of milling, acid hydrolysis and two steps enzymatic hydrolysis. In that case sulfuric acid (0.3% w·w<sup>-1</sup> 121 °C for 30 min) was used and also two kinds of enzymes obtaining a yield of 63% w·w<sup>-1</sup> in sugars and no degradation products [34].

In this work, a continuous micro-reactor was used to carry out the hydrolysis of wheat bran in supercritical water. This reactor has been previously used to hydrolyze pure cellulose in supercritical water, giving as a result a total conversion of cellulose in 0.02 s of residence time yielding a sugars production of 98% w·w<sup>-1</sup>[12]. The aim of this work was to test the capability of the aforementioned reactor to hydrolyze natural biomass.

## 2. Materials and methods

### 2.1. Materials

The wheat bran used in the experiments was supplied by a local supplier. The particle size of the biomass was 430 µm. In order to ensure a correct pumping, the particle size was reduced to 125 µm using a ball mill Retsch PM100. The standards used in High Performance Liquid Chromatography (HPLC) analysis were: cellobiose (≥ 98%), glucose (≥ 99%), xylose (≥ 99%),

galactose ( $\geq 99\%$ ), mannose ( $\geq 99\%$ ), arabinose ( $\geq 99\%$ ), glyceraldehyde ( $\geq 95\%$ ), glycolaldehyde dimer ( $\geq 99\%$ ), lactic acid ( $\geq 85\%$ ), formic acid ( $\geq 98\%$ ), acetic acid ( $\geq 99\%$ ), acrylic acid ( $\geq 99\%$ ) and 5-hydroxymethylfurfural ( $\geq 99\%$ ) purchased from Sigma. Distillated water was used to run the experiments.

For the determination of structural carbohydrates and lignin [35], sulfuric acid ( $\geq 96\%$ ) and calcium carbonate ( $\geq 99\%$ ) supplied by Sigma were used as reagents. Milli-Q water was used in this procedure.

## *2.2. Methods*

### *2.2.1. Chemical characterization for raw material*

Natural biomass (wheat bran) was used in the experiments, so first of all the composition of the sample was determined. For that purpose a Laboratory Analytical Procedure (LAP) from NREL was used to determine the structural carbohydrates and lignin in biomass [35]. Briefly, the sample was dried at 105 °C in an oven for 24 hours in order to obtain composition in dry basis. After that, the sample was subjected to a Soxhlet extraction using hexane as solvent in order to remove the extractives from the sample. For carbohydrates and lignin determination, 300 mg of solid sample were weighed and 3 mL of 72 % sulfuric acid were added. The sample was incubated at 30 °C for 30 minutes and after that, 84 mL of deionized water were added. Finally, the sample was heated at 120 °C for 60 minutes. The final product was vacuum filtered and a 50 mL liquid aliquot was used to determine soluble lignin as well as carbohydrates. The remaining solid was collected to analyze the insoluble lignin and ash content. The liquid aliquot was analyzed with UV-Visible spectrophotometer to determine soluble lignin. The wavelength was set at 280 nm and the used extinction coefficient had a value of  $18.675 \text{ L}\cdot\text{g}^{-1}\cdot\text{cm}^{-1}$  [36]. The same liquid aliquot was neutralized with calcium carbonate to a pH between 5 and 6 and then analyzed with HPLC to identify and quantify structural carbohydrates. The solid was dried at 110°C for 24 h and then cooled in a desiccator, weighting the solid. After that, the sample was placed in a muffle at 550 °C for 24 h and the remaining residue was weighed to obtain the ash content.

### *2.2.2. Analysis*

The solids in the product were separated by centrifugation and dried at 60 °C for 24 h and then, following the same procedure described in Section 2.2.1, total lignin content was

determined. The separated solids obtained after wheat bran hydrolysis were analyzed by spectroscopy Fourier Transform Infrared (FTIR) and scanning electron microscopy (SEM). The FTIR experiments were carried out using a Bruker Tensor 27. Samples were analyzed in the wavelength range of  $4000\text{ cm}^{-1}$  –  $600\text{ cm}^{-1}$  with a resolution of  $4\text{ cm}^{-1}$ . The number of scans per sample was 32 being the scanner velocity 10 KHz. The interferogram size was 14220 points. The SEM experiments were conducted in a JSM-820 (JOEL, Japan) operated at 20 kV of accelerating voltage. A gold evaporator Balzers SCD003 with a gold thickness of 25 nm – 30 nm was used.

The carbon content of the products was determined by total organic carbon (TOC) analysis with Shimadzu TOC-VCSH equipment. The composition of the liquid product was determined by using HPLC analysis. The column used for the separation of the compounds was Shodex SH-1011 at 50 °C, using sulfuric acid (0.01 N) as mobile phase with a flow of 0.8 mL/min. A Waters IR detector 2414 was used to identify the sugars and their derivatives and Water UV-Vis detector was used to determine the 5-hydroxymethylfurfural concentration at a wavelength of 254 nm.

The soluble oligosaccharides concentration in the samples was determined by acid hydrolysis to glucose and HPLC determination. Briefly, to 10 mL of filtered liquid aliquots was added 4 mL of 96 % sulfuric acid. The sample was maintained at 30 °C during 60 min in an oven. Then it was diluted with 86 mL of deionized water and incubated at 121 °C for 60 min. Calcium carbonate was added to 20 mL of this sample to neutralize the medium and finally the supernatant was filtered and analyzed with HPLC.

### 2.2.3. Selectivity and residence time

In this work residence time is one of the main parameters for controlling the hydrolysis. It was calculated as shown in Equation 1, where ' $V$ ' is the volume of the reactor ( $\text{m}^3$ ), ' $\rho$ ' ( $\text{kg}/\text{m}^3$ ) is the density of the medium at the reactor conditions (considered as water due to the low concentration of biomass,  $\approx 1\%$  w•w-1) and ' $F_m$ ' is the mass flow in the reactor ( $\text{kg}/\text{s}$ ).

$$\tau = \frac{V\rho}{F_m} \quad (1)$$

The selectivity of main compounds (C-6 sugars, C-5 sugars, glycolaldehyde and 5-HMF) was determined by Equation 2, where ' $Y_s$ ' is the selectivity of the compound ' $s$ ', ' $C_s$ ' is the concentration of ' $s$ ' in the liquid product in ppm and ' $S_{in}$ ' is the concentration of sugars at the inlet of the reactor in ppm, calculated as shown in Equation 3. Soluble sugars derived from

cellulose (cellobiose and glucose) were called C-6, the derived from hemicellulose (xylose, mannose, galactose and arabinose) were called C-5 and the rest of compounds were organic acids (acetic, lactic and acrylic acid), glycolaldehyde, glyceraldehyde and 5-HMF.

$$Y_s = \frac{C_s}{S_{in}} \quad (2)$$

$$S_{in} = C_{in} \cdot S_T \quad (3)$$

In Equation 3, ' $C_{in}$ ' is the concentration of wheat bran at the reactor's inlet in ppm and ' $S_T$ ' is the cellulose and hemicellulose fraction in the raw material in mass fraction which represents the proportion of wheat bran susceptible of being hydrolyzed into sugars (see Table 1). When the yield was referred to each fraction, cellulose or hemicellulose, ' $S_T$ ' was the portion of each fraction in the raw material.

**Table 1.** Chemical composition of wheat bran.

Component	Moisture	Extractives	Cellulose	Hemicell.	Lignin	Ash	TOTAL
g / 100g wheat bran	8.2 ± 0.1	10.6 ± 0.8	31.4 ± 1.6	20.3 ± 1.0	22.3 ± 0.3	0.5 ± 0.1	93.4 ± 1.6

### 2.3. Experimental setup

The continuous pilot plant used for this work is shown in Figure 1. The hydrolysis pilot plant was designed to operate up to 400 °C and 30 MPa using a sudden expansion micro-reactor (SEMR) developed in a previous work [12].

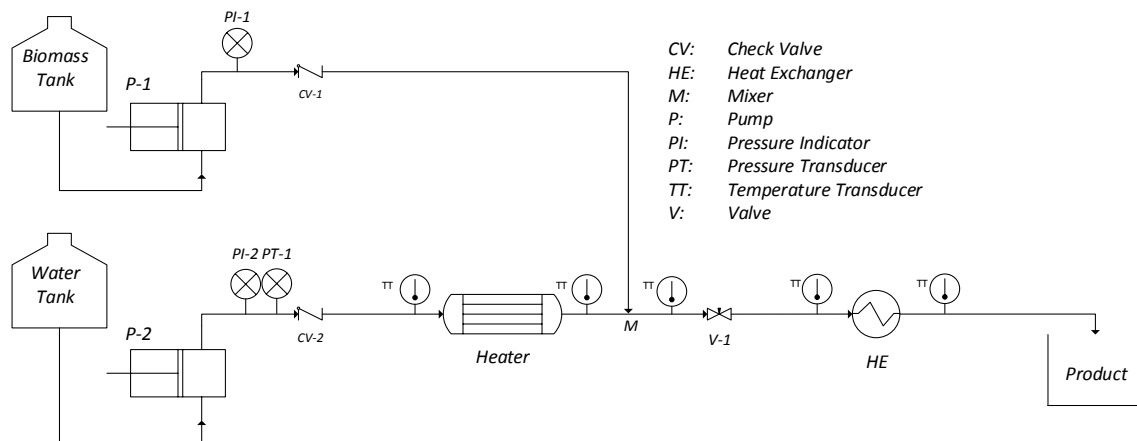


**Fig 1.** Experimental Setup.

The main advantage of this reactor is the instantaneous cooling of the products stopping efficiently the reactions of hydrolysis. This allows the precise evaluation of the residence time without diluting the products. In a similar way, the heating of the biomass stream is achieved

instantaneously by supercritical water injection at the reactor inlet. With this heating method, it is possible to change the temperature of a biomass particle from room temperature until 400°C in a mixer which is the reactor inlet. In addition, the reactor is thermally isolated which makes possible to consider it as isothermal. A detailed description of the pilot plant as well as the operation procedure is presented in a previous work [37].

In this case, a wheat bran suspension (5% w·w<sup>-1</sup>) was continuously compressed and pumped up to the operation pressure (25 MPa), remaining at room temperature until the inlet of the reactor. In that point the suspension was instantaneously heated by mixing it with a supercritical water stream and the hydrolysis reactions start. Then the effluent was suddenly depressurized at the outlet of the reactor without previous cooling in order to instantaneously stop the hydrolysis. In this setup, a modification from the previous pilot plant [12] was tested. In this setup, the reactor outlet stream was driven to a heat exchanger (HE-1) to pre-heat the supercritical water stream. In order to ensure the cooling of the sample, a cooler (HE-2) was set after HE-1.

### 3. Results and Discussion

From compositional analysis of the raw material it was determined that the percentage of moisture was  $8.2 \pm 0.1\%$  w·w<sup>-1</sup> and the extractive fraction was  $10.6 \pm 0.8\%$  w·w<sup>-1</sup>. The content of lignin was  $22.3 \pm 0.3\%$  w·w<sup>-1</sup>, being  $19.6 \pm 0.3\%$  w·w<sup>-1</sup> due to soluble lignin and  $2.7 \pm 0.1\%$  w·w<sup>-1</sup> due to insoluble lignin. The content of cellulose and hemicellulose were  $31.4 \pm 1.6\%$  w·w<sup>-1</sup> and  $20.3 \pm 1.0\%$  w·w<sup>-1</sup> respectively and the ash represented  $0.5 \pm 0.1\%$  w·w<sup>-1</sup> of the wheat bran (Table 1).

The wheat bran was hydrolyzed at 400°C and 25 MPa at different residence times. These conditions were chosen because they were optimized in a previous work for cellulose hydrolysis [12]. Because of the fast hydrolysis, the residence time was evaluated between 0 s and 1 s. Each experimental point is a result of five repetitions of the analyzed conditions. In Figure 2 it is shown a typical temperature and pressure profile for an experiment. The pressure variations along residence time would be produced due to a partial solid deposition near the depressurization valve. The reactor was maintained at  $400 \pm 5^\circ\text{C}$  and the pressure at  $25 \pm 1\text{MPa}$ . The temperature of the reactor outlet (after depressurization) was around 160°C. This stream was fed to the HE-1 and leave it at a temperature of 150°C. So, a post cooling was needed to take the sample at 25°C. On the other hand, the water stream pumped to the HE-

1 was heated from 20°C to 155°C. That was the temperature which the water stream entered to the heater to be further heated until 450°C. The use of this heat exchanger allowed the reduction of the heat requirements in 20%.

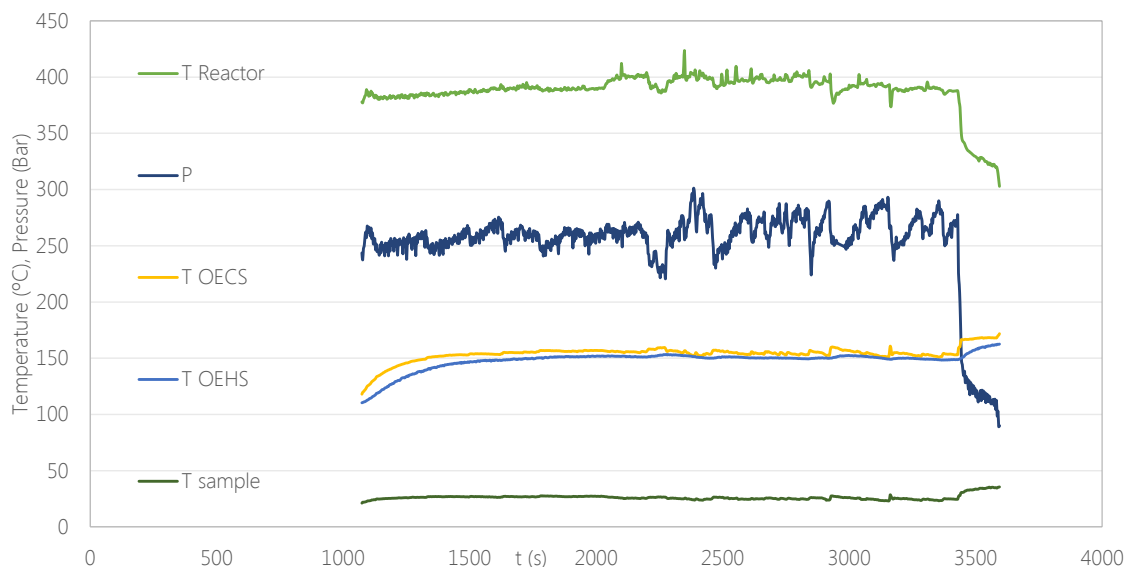


**Fig 2.** Temperature and pressure profile during a typical experiment. 'T Reactor' is the temperature in the middle of the reactor in °C. 'P' is the pressure in bar. 'T OECS' is the temperature of the outlet cold stream of the HE. 'T OEHS' is the temperature of the outlet hot stream of the HE. 'T Sample' is the temperature of the sample.

The lignin composition of the solids (soluble lignin -SL- and insoluble lignin -IL-) obtained after hydrolysis is shown in Figure 3.

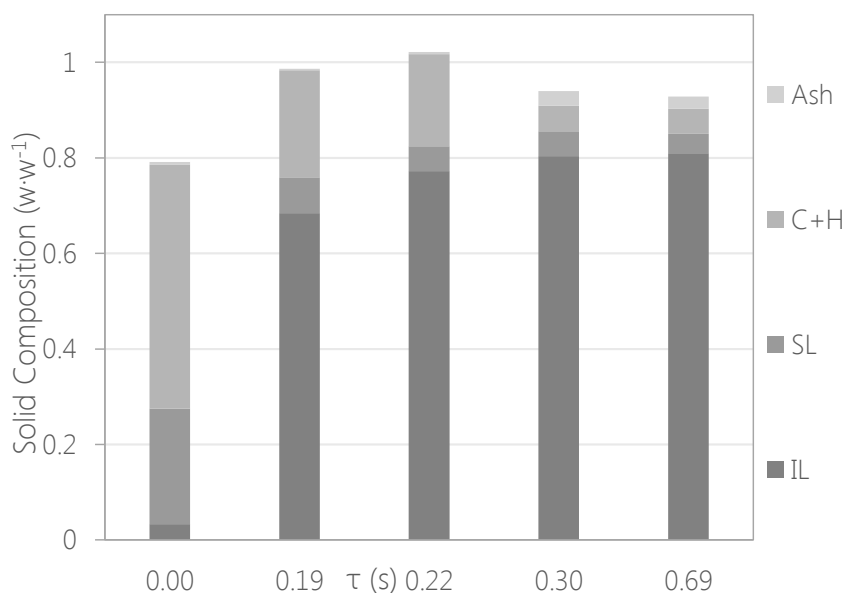


**Fig 3.** Solid composition of the solids products after hydrolysis in supercritical water. The residence time of 0 s refers to the composition of the raw material. 'C+H' is the solid composition in cellulose and hemicellulose in % w-w<sup>-1</sup>. 'SL' is the solid composition in soluble lignin in % w-w<sup>-1</sup>. 'IL' is the solid composition in insoluble lignin in % w-w<sup>-1</sup>.

The initial lignin composition was around 22% w·w<sup>-1</sup>. The lignin fraction was increased while residence time was. At 0.3 s of residence time, the lignin content reached a value of 85% w·w<sup>-1</sup>. This values was not enhanced by increasing the residence time until 0.69 s. It would occur because of the less accessibility of inners fractions of cellulose and hemicellulose linked to lignin [38]. The ash content was increased from 0.5% w·w<sup>-1</sup> in the raw material up to 3% w·w<sup>-1</sup> after hydrolysis. Although the lignin composition of the solids was increased from 22 % to 85% w·w<sup>-1</sup>, the soluble lignin fraction was decreased from 19% w·w<sup>-1</sup> to 5% w·w<sup>-1</sup>. This phenomenon would occur due to the lignin hydrolysis, which would occur firstly in the sites where lignin interacts with hemicellulose [38]. However, lignin remain in the solid as the main component after fractionation. The cellulose and hemicellulose fractions in the solids were decreased as the residence time was increased. However, these fractions remained constant at a value near to 5% w·w<sup>-1</sup> when the residence time was increased from 0.3 s to 0.7 s. In order to evaluate the solid characteristics after hydrolysis, SEM and FTIR analysis were carried out to them. In Figure 4, it is observed the spectrum comparison between the raw material (wheat bran) and the solid product after hydrolysis. The bands at 1135 cm<sup>-1</sup> are indicative of the aromatic C–H in-plane deformation for syringyl type [39]. This suggest that syringyl type lignins were present in the raw material as well as in the solid product. However, aromatic C–H out of bending exhibits at 844 cm<sup>-1</sup> [39]. This band was observed in the raw material but not in the solid product, suggesting that a fraction of lignin is decomposed after supercritical water hydrolysis. This agree with the results presented in Figure 3, in which the soluble lignin content is decreased after the process. Aromatic skeleton vibrations occurred at 1510 cm<sup>-1</sup> and 1460 cm<sup>-1</sup> [39]. The absorbance for these bands appeared at both, raw material and product, suggesting that the aromaticity properties remained in the solid products. The band at 1720 cm<sup>-1</sup> is originated from the carbonyl group, including unconjugated ketone and carbonyl group stretching [39]. This band was observed in the raw material but not in the product, so this suggest that typical cellulose bonds were broken or they were not present in the solid. In addition, the disappearance of the band at 1747 cm<sup>-1</sup> would indicated the rupture of the ester link of acetyl, feruloyl and p-coumaroyl between hemicellulose and lignin [40]. It can be also observed that the O–H and aliphatic C–H (2870 cm<sup>-1</sup>) bonds which are the basic function groups in biomass were present in the raw material as well as in the products.

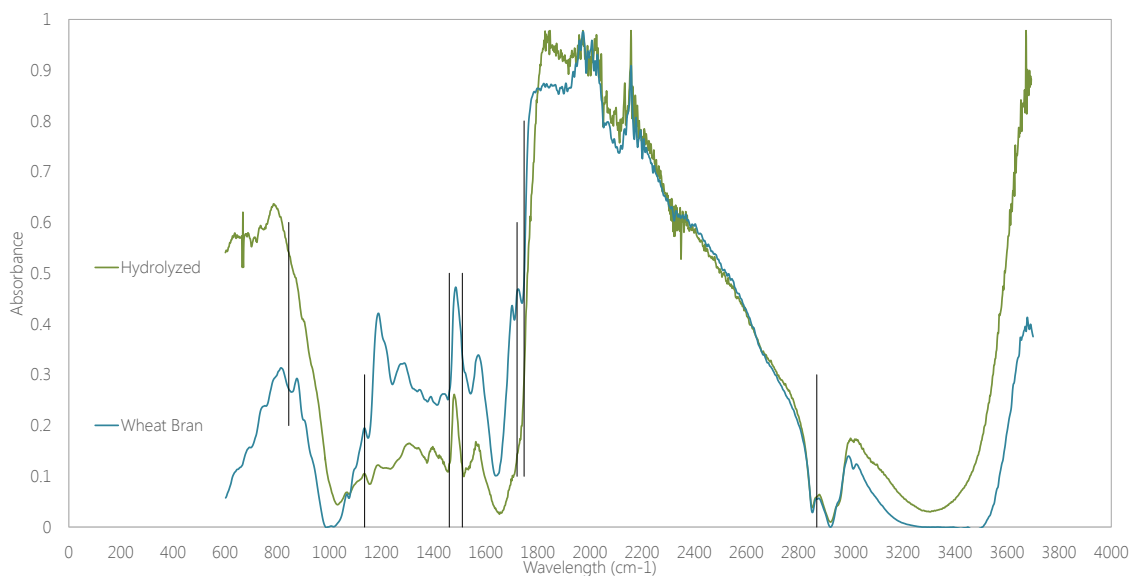


**Fig 4.** FTIR spectrums of wheat bran and the solid after 0.69 s of hydrolysis at 400°C and 25 MPa.

In order to analyze the structure of the hydrolyzed products, SEM microscopy was applied to the samples. SEM images of the raw material are shown in Figure 5-A and 5-C for a zoom of 5000X and 5-E for a zoom of 1000X. The images corresponding to the solids obtained after hydrolysis are shown in Figure 5-B and 5-D for a zoom of 5000X and 5-F for a zoom 1000X. In Figure 5, it is observed that the raw material presented a shape like spheres with a smooth surface. After hydrolysis, the remaining solid showed an amorphous shape. In addition, Figures 5-D and 5-F suggest that a porous solid was obtained after hydrolysis. Cellulose and hemicellulose that are located in the outer area of the particle would be rapidly hydrolyzed in the process. However, the fractions of cellulose and hemicellulose situated in the inner part of the porous net of lignin would be the reason of the remaining 5% w·w<sup>-1</sup> found (see Figure 3) at high residence times (0.69 s).

The recovery of soluble sugars in the liquid products decreased while residence time was increased from 0.19 s to 0.69 s. In Figure 6, the yield of C-5 and C-6 obtained as soluble sugars after supercritical water hydrolysis is shown. The maximum recovery of soluble sugar reached was 73% w·w<sup>-1</sup> at 0.19 s of residence time. Although the highest yield of sugars was achieved at the lowest residence time, a decrease in the residence time would not produce a higher yield due to the uncompleted hydrolysis of cellulose and hemicellulose. In fact, the solid products after hydrolysis at 0.19 had a C-6 and C-5 composition of 22% w·w<sup>-1</sup>. The recovery of cellulose and hemicellulose fractions as soluble sugars along residence time are shown in Figure 7-A and 7-B respectively.

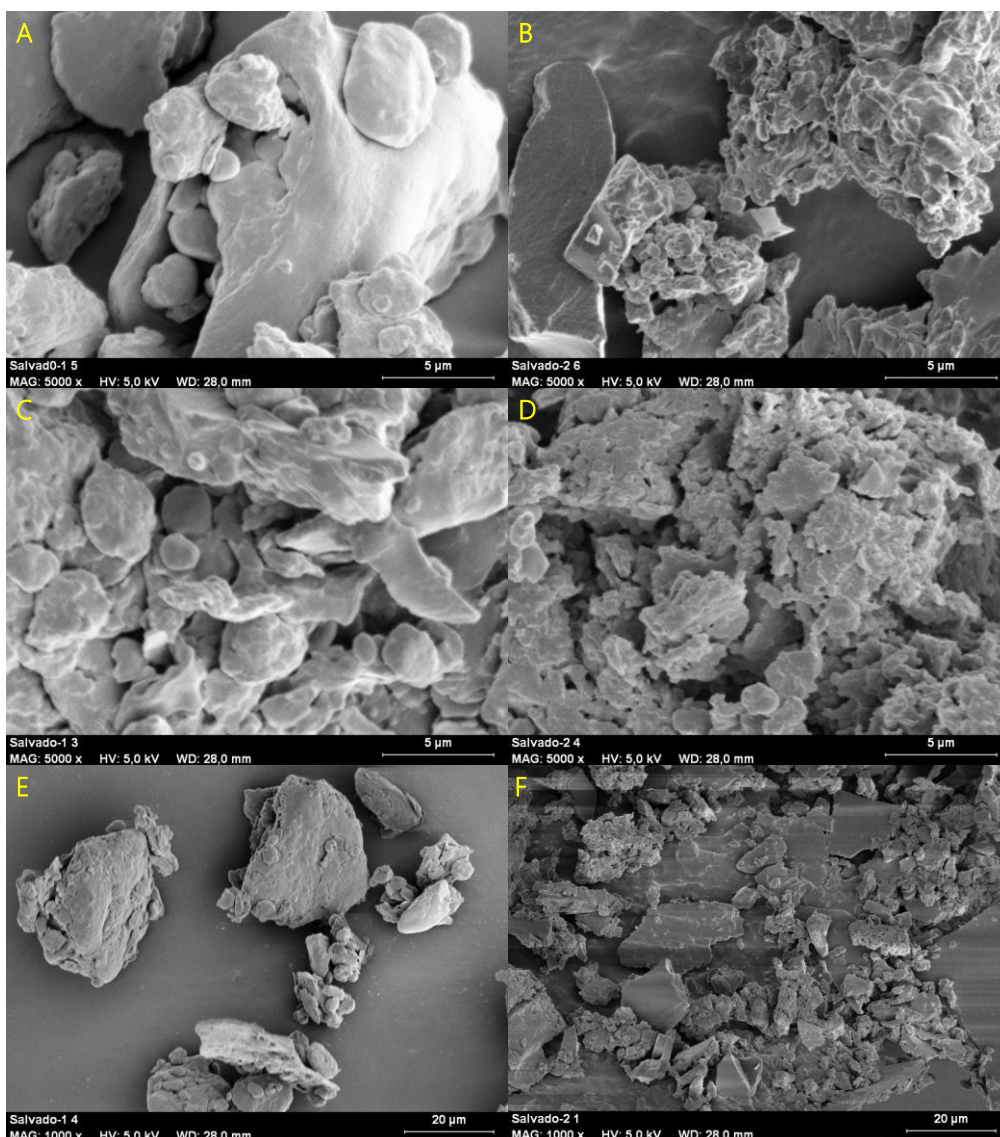


**Fig 5.** SEM images of the solids before and after hydrolysis. (A) Wheat straw at 5000X; (B) hydrolysed product at 5000X; (C) Wheat straw at 5000X; (D) hydrolysed product at 5000X; (E) Wheat straw at 1000X; (F) hydrolysed product at 1000X.

The maximum yield of cellulose derived sugars ( $63\% \text{ w}\cdot\text{w}^{-1}$ ) was achieved at  $0.22 \text{ s}$  of residence time. The hydrolysis of pure cellulose at the same conditions that the experimented in this work was able to produce a yield of  $98\% \text{ w}\cdot\text{w}^{-1}$  at  $0.02 \text{ s}$  of residence time [12]. The difference in the yields of cellulose hydrolysis, suggest a strong effect of the cellulose interaction with the other components of the biomass over the kinetic. In fact, pure cellulose would be completely dissolved in supercritical water [14, 37]. This phenomenon might not occur when cellulose is interacting with other components of biomass like lignin or when it is located inside a lignin net. Despite of the difference between pure cellulose and wheat bran, the results obtained in this work improves those found in literature ( $<25\% \text{ w}\cdot\text{w}^{-1}$ ) for batch,

semi-continuous or continuous fractionation [15-28]. Hemicellulose seems to be completely hydrolyzed and recovered as sugars at residence time of 0.19 s. The increase in the residence time produced a lower yield of C-5. In this case, similar values of C-5 was found in literature [15, 20].

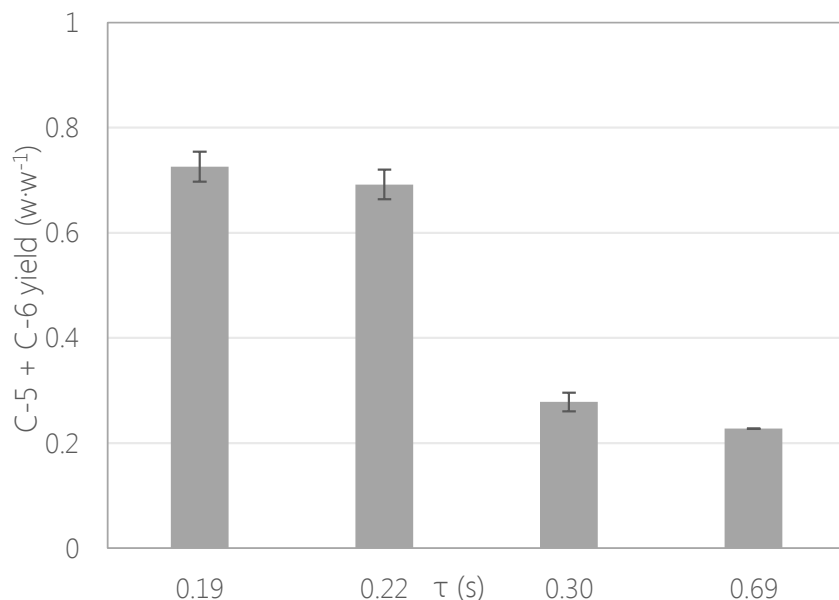


**Fig 6.** Yield of cellulose and hemicellulose recovered along residence time after supercritical water hydrolysis at 400°C and 25 MPa.

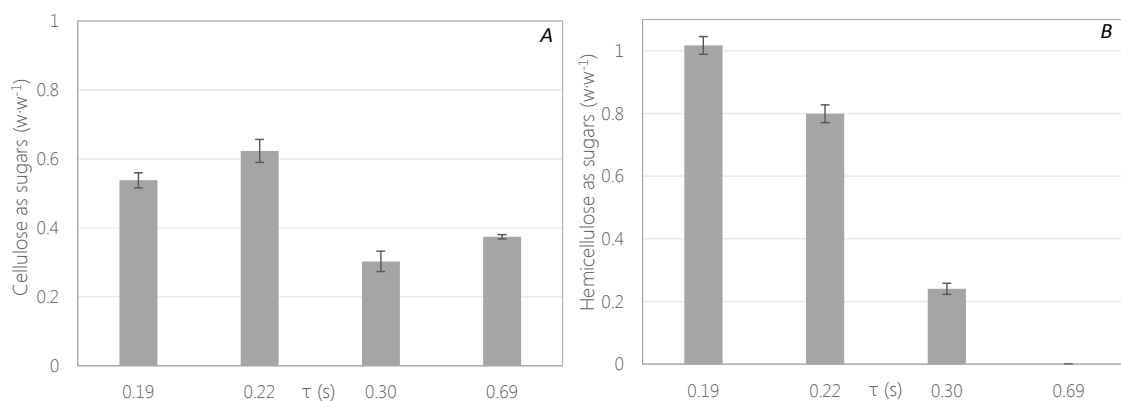


**Fig 7. (A)** Cellulose recovery along residence time. **(B)** Hemicellulose recovery along residence time.

The sugars produced after cellulose and hemicellulose hydrolysis can follow different reaction in supercritical water, such as retro-aldol condensation or dehydration [41]. The main products of glucose retro-aldol condensation is glycolaldehyde (see Figure 8). The yield of this compound at 0.19 s (highest yield of C-5 and C-6 recovery) was 14%  $w \cdot w^{-1}$ . The maximum amount of glycolaldehyde was 20%  $w \cdot w^{-1}$  at 0.22 s of residence time. On the other hand, 5-HMF is a dehydration product of C-6 sugars. This compound would be undesired in a

microorganism post-processing of the obtained sugars is needed [21]. In Figure 9 it is shown the obtained yields of 5-HMF in the experimented conditions. In the same way that it was developed in a previous work [12], the yield of 5-HMF over the whole range of residence time was lower than 0.05% w·w<sup>-1</sup>.

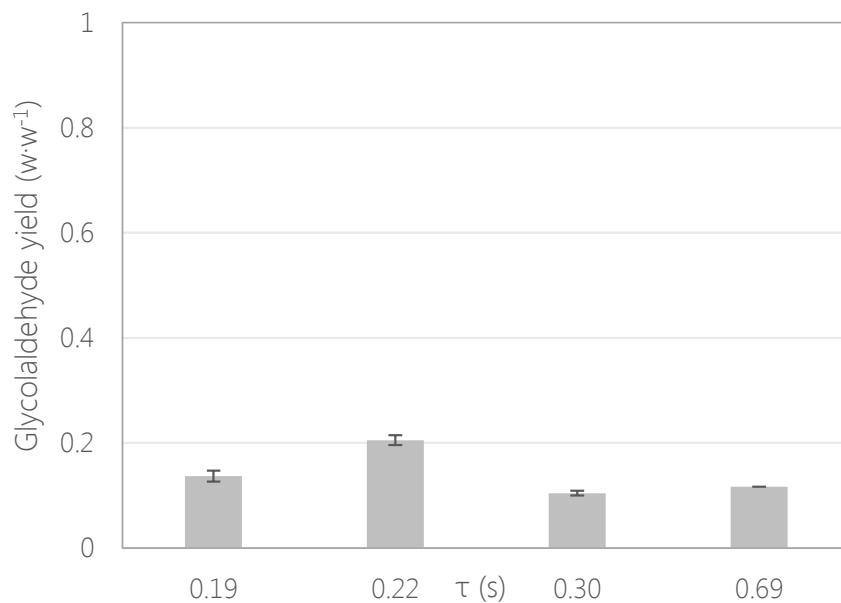


**Fig 8.** Yield of glycolaldehyde along residence time after supercritical water hydrolysis at 400°C and 25 MPa.

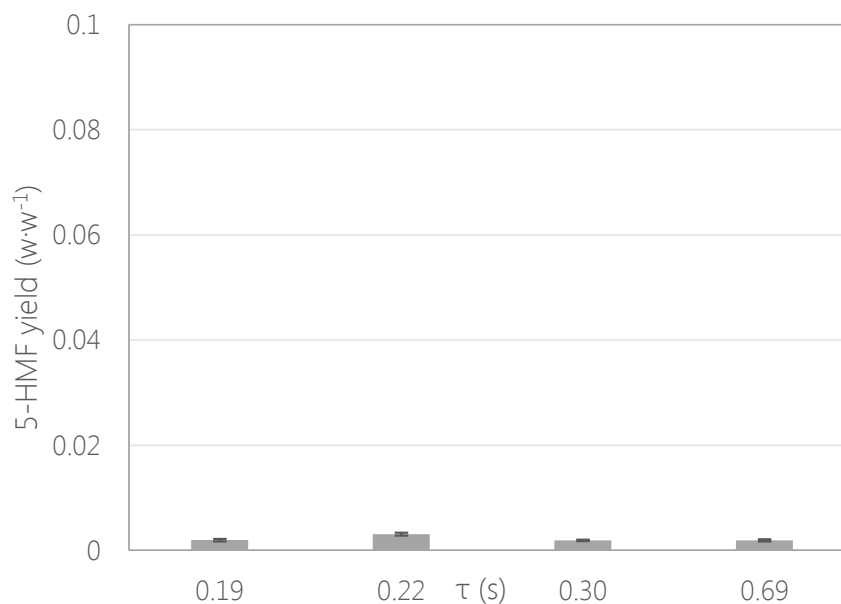


**Fig. 9.** Yield of 5-HMF along residence time after supercritical water hydrolysis at 400°C and 25 MPa.

#### 4. Conclusions

Wheat bran hydrolysis in supercritical water was analyzed at 400°C and 25 MPa at residence times lower than 1 s. This method showed to be an effective procedure to hydrolyze both, cellulose and hemicellulose, at the same time with low concentration of degradation products. This result was achieved by working at high temperature (400°C) and low residence time (0.19 s). The control of the residence time was the key factor to stop the reaction before sugars degradation.

The recovery yield of cellulose and hemicellulose as C-6 and C-5 was 76 % w·w<sup>-1</sup>. The solid after the hydrolysis was composed of 80% w·w<sup>-1</sup> of lignin. An increase in residence time increased the lignin content of the solid. However, a cellulose fraction (5% w·w<sup>-1</sup>) seems to remain occluded inside a lignin network after a residence time increment. The obtained solid product after hydrolysis consisted of an amorphous and porous material.

#### Acknowledgements

The authors thank the Spanish Ministry of Economy and Competitiveness for the Project CTQ2011-23293 and ENE2012-33613. The authors thank Repsol for its technical support. D.A.C. thanks the Spanish Ministry of Education for the FPU fellowship (AP2009-0402).

## References

1. Arai, K., Smith Jr, R.L., and Aida, T.M., *Decentralized chemical processes with supercritical fluid technology for sustainable society*. The Journal of Supercritical Fluids, 2009. 47(3): p. 628-636.
2. BECOTEPS. *European Technology Platforms for the FP7. The European Bioeconomy 2030. Delivering Sustainable Growth by addressing the Grand Societal Challenges 2013 - 10/04/2014 10/04/2014*].
3. Ragauskas, A.J., Williams, C.K., Davison, B.H., Britovsek, G., Cairney, J., Eckert, C.A., Frederick, W.J., Hallett, J.P., Leak, D.J., Liotta, C.L., Mielenz, J.R., Murphy, R., Templer, R., and Tschaplinski, T., *The Path Forward for Biofuels and Biomaterials*. Science, 2006. 311(5760): p. 484 -489.
4. Bobleter, O., *Hydrothermal degradation of polymers derived from plants*. Progress in polymer science, 1994. 19(5): p. 797-841.
5. Tollefson, J., *Energy: Not your father's biofuels*. Nature News, 2008. 451(7181): p. 880-883.
6. Peterson, A.A., Vogel, F., Lachance, R.P., Fröling, M., Michael J. Antal, Jr., and Tester, J.W., *Thermochemical biofuel production in hydrothermal media: A review of sub- and supercritical water technologies*. Energy & Environmental Science, 2008. 1(1): p. 32-65.
7. Akiya, N. and Savage, P.E., *Roles of Water for Chemical Reactions in High-Temperature Water*. Chemical Reviews, 2002. 102(8): p. 2725-2750.
8. Bröll, D., Kaul, C., Krämer, A., Krammer, P., Richter, T., Jung, M., Vogel, H., and Zehner, P., *Chemistry in Supercritical Water*. Angewandte Chemie International Edition, 1999. 38(20): p. 2998–3014.
9. Loppinet-Serani, A., Aymonier, C., and Cansell, F., *Supercritical water for environmental technologies*. Journal of Chemical Technology & Biotechnology, 2010. 85(5): p. 583–589.
10. Akizuki, M., Fujii, T., Hayashi, R., and Oshima, Y., *Effects of water on reactions for waste treatment, organic synthesis, and bio-refinery in sub- and supercritical water*. Journal of Bioscience and Bioengineering, 2014. 117(1): p. 10-18.

11. Machida, H., Takesue, M., and Smith Jr, R.L., *Green chemical processes with supercritical fluids: Properties, materials, separations and energy*. The Journal of Supercritical Fluids, 2011. 60(0): p. 2-15.
12. Cantero, D.A., Bermejo, M.D., and Cocero, M.J., *High glucose selectivity in pressurized water hydrolysis of cellulose using ultra-fast reactors*. Bioresource Technology, 2013. 135: p. 697-703.
13. Fang, Z., Sato, T., Smith Jr, R.L., Inomata, H., Arai, K., and Kozinski, J.A., *Reaction chemistry and phase behavior of lignin in high-temperature and supercritical water*. Bioresource Technology, 2008. 99(9): p. 3424-3430.
14. Sasaki, M., Adschiri, T., and Arai, K., *Kinetics of cellulose conversion at 25 MPa in sub- and supercritical water*. AIChE Journal, 2004. 50(1): p. 192-202.
15. Alfaro, A., López, F., Pérez, A., García, J.C., and Rodríguez, A., *Integral valorization of tagasaste (*Chamaecytisus proliferus*) under hydrothermal and pulp processing*. Bioresource Technology, 2010. 101(19): p. 7635-7640.
16. Lee, J.Y., Ryu, H.J., and Oh, K.K., *Acid-catalyzed hydrothermal severity on the fractionation of agricultural residues for xylose-rich hydrolyzates*. Bioresource Technology, 2013. 132: p. 84-90.
17. Yáñez, R., Garrote, G., and Díaz, M.J., *Valorisation of a leguminous specie, *Sesbania grandiflora*, by means of hydrothermal fractionation*. Bioresource Technology, 2009. 100(24): p. 6514-6523.
18. Zhao, Y., Lu, W.-J., Wang, H.-T., and Yang, J.-L., *Fermentable hexose production from corn stalks and wheat straw with combined supercritical and subcritical hydrothermal technology*. Bioresource Technology, 2009. 100(23): p. 5884-5889.
19. Rodríguez, A., Moral, A., Sánchez, R., Requejo, A., and Jiménez, L., *Influence of variables in the hydrothermal treatment of rice straw on the composition of the resulting fractions*. Bioresource Technology, 2009. 100(20): p. 4863-4866.
20. Ingram, T., Rogalinski, T., Bockemühl, V., Antranikian, G., and Brunner, G., *Semi-continuous liquid hot water pretreatment of rye straw*. Journal of Supercritical Fluids, 2009. 48(3): p. 238-246.
21. Rogalinski, T., Ingram, T., and Brunner, G., *Hydrolysis of lignocellulosic biomass in water under elevated temperatures and pressures*. The Journal of Supercritical Fluids, 2008. 47(1): p. 54-63.

22. Merali, Z., Ho, J.D., Collins, S.R.A., Gall, G.L., Elliston, A., Käsper, A., and Waldron, K.W., *Characterization of cell wall components of wheat straw following hydrothermal pretreatment and fractionation*. *Bioresource Technology*, 2013. 131: p. 226-234.
23. Pronyk, C. and Mazza, G., *Fractionation of triticale, wheat, barley, oats, canola, and mustard straws for the production of carbohydrates and lignins*. *Bioresource Technology*, 2012. 106: p. 117-124.
24. Pronyk, C. and Mazza, G., *Optimization of processing conditions for the fractionation of triticale straw using pressurized low polarity water*. *Bioresource Technology*, 2011. 102(2): p. 2016-2025.
25. Liu, C. and Wyman, C.E., *Partial flow of compressed-hot water through corn stover to enhance hemicellulose sugar recovery and enzymatic digestibility of cellulose*. *Bioresource Technology*, 2005. 96(18): p. 1978-1985.
26. Mosier, N., Hendrickson, R., Ho, N., Sedlak, M., and Ladisch, M.R., *Optimization of pH controlled liquid hot water pretreatment of corn stover*. *Bioresource Technology*, 2005. 96(18): p. 1986-1993.
27. Schacht, C., Zetzl, C., and Brunner, G., *From plant materials to ethanol by means of supercritical fluid technology*. *The Journal of Supercritical Fluids*, 2008. 46(3): p. 299-321.
28. Rogalinski, T., Herrmann, S., and Brunner, G., *Production of amino acids from bovine serum albumin by continuous sub-critical water hydrolysis*. *The Journal of Supercritical Fluids*, 2005. 36(1): p. 49-58.
29. Hossain, K., Ulven, C., Glover, K., Ghavami, F., Simsek, S., Alamri, M.S., Kumar, A., and Mergoum, M., *Interdependence of cultivar and environment on fiber composition in wheat bran*. *Australian Journal of Crop Science*, 2013. 7(4): p. 525-531.
30. Lamsal, B.P., Madl, R., and Tsakpunidis, K., *Comparison of Feedstock Pretreatment Performance and Its Effect on Soluble Sugar Availability*. *Bioenergy Research*, 2011. 4(3): p. 193-200.
31. Seyer, M.È. and Gélinas, P., *Bran characteristics and wheat performance in whole wheat bread*. *International Journal of Food Science and Technology*, 2009. 44(4): p. 688-693.

32. Palmarola-Adrados, B., Chotěborská, P., Galbe, M., and Zacchi, G., *Ethanol production from non-starch carbohydrates of wheat bran*. *Bioresource Technology*, 2005. 96(7): p. 843-850.
33. Chotěborská, P., Palmarola-Adrados, B., Galbe, M., Zacchi, G., Melzoch, K., and Rychtera, M., *Processing of wheat bran to sugar solution*. *Journal of Food Engineering*, 2004. 61(4): p. 561-565.
34. Favaro, L., Basaglia, M., and Casella, S., *Processing wheat bran into ethanol using mild treatments and highly fermentative yeasts*. *Biomass and Bioenergy*, 2012. 46: p. 605-617.
35. Sluiter, J.B., Ruiz, R.O., Scarlata, C.J., Sluiter, A.D., and Templeton, D.W., *Compositional Analysis of Lignocellulosic Feedstocks. 1. Review and Description of Methods*. *J. Agric. Food Chem.*, 2010. 58(16): p. 9043-9053.
36. Fukushima, R.S. and Hatfield, R.D., *Comparison of the acetyl bromide spectrophotometric method with other analytical lignin methods for determining lignin concentration in forage samples*. *Journal of Agricultural and Food Chemistry*, 2004. 52(12): p. 3713-3720.
37. Cantero, D.A., Bermejo, M.D., and Cocero, M.J., *Kinetic analysis of cellulose depolymerization reactions in near critical water*. *The Journal of Supercritical Fluids*, 2013. 75: p. 48-57.
38. Gullón, P., Romani, A., Vila, C., Garrote, G., and Parajó, J.C., *Potential of hydrothermal treatments in lignocellulose biorefineries*. *Biofuels, Bioproducts and Biorefining*, 2012. 6(2): p. 219-232.
39. Zhang, J., Deng, H., Sun, Y., Pan, C., and Liu, S., *Isolation and characterization of wheat straw lignin with a formic acid process*. *Bioresource Technology*, 2010. 101(7): p. 2311-2316.
40. Xu, Y. and Chen, B., *Investigation of thermodynamic parameters in the pyrolysis conversion of biomass and manure to biochars using thermogravimetric analysis*. *Bioresource Technology*, 2013. 146: p. 485-493.
41. Sasaki, M., Goto, K., Tajima, K., Adschiri, T., and Arai, K., *Rapid and selective retro-aldol condensation of glucose to glycolaldehyde in supercritical water*. *Green Chem.*, 2002. 4(3): p. 285-287.



# Chapter 8. On the Energetic Approach of Biomass Hydrolysis in Supercritical Water

## Abstract

Production of glucose through hydrolysis from vegetal biomass is of interest because it can be used as starting point in the production of chemicals, materials and bio-fuels. Cellulose hydrolysis can be performed in supercritical water with a high selectivity of soluble sugars. This reaction yield can be achieved using a continuous reactor with instantaneous heating and cooling methods that allow the precise control of the residence time. Operation can be carried out by adding a stream of supercritical water to the cellulose stream and by cooling the reactor outlet by sudden decompression. With this technology it is possible to greatly decrease the temperature in a fraction of a second. The process produces a high pressure steam that can be integrated, from an energy point of view, with the global biomass treating process. This work investigate the integration of biomass hydrolysis reactors with commercial Combined Heat and Power (CHP) schemes, with special attention to reactor outlet streams. Temperature of the flue gases from CHP around 500 °C and the use of direct shaft work in the process offer adequate energy integration possibilities for feed preheating and compression. The integration of biomass hydrolysis with a CHP process allow the selective conversion of biomass into sugars without any extra heat requirements. The wide range of commercially available GT sizes allows widespread process scaling.

**Keywords:** Biomass • Biorefinery • Glucose • Flash • Steam Injection Gas  
Turbine



## 1. Introduction

In the current society, there is a tendency in changing the production methods in order to achieved a development supported in the bioeconomy [1]. This goal would be reached by using energy efficient processes treating renewable raw materials.

Vegetal biomass is probably the most useful and widely available renewable raw material. For example, there are some kinds of biomass which cannot be used for human consumption, which are a viable alternative source of chemicals and energy [2, 3]. The annual biomass growth on the continents is estimated to be 10,000 dry tons·ha<sup>-1</sup> [2]. Taking into account the crude oil production and the energy equivalence between biomass and oil (2.5 times higher for oil), less than 10% of the annual growth of vegetal biomass is needed to replace the petroleum production [4]. Biomass is composed of 34-50% cellulose, 16-34% hemi-cellulose and 11-29% of lignin [4]. As the most important skeletal component in plants, the cellulose is an almost inexhaustible polymeric raw material [5]. The challenging step in the processing of biomass is the production of sugars such as glucose [3]. Glucose is a target product because it can be used as a raw material in the production of chemicals, materials and bio-fuels [6-9]. Hydrolysis leads to cleavage of ether and ester bonds by the addition of one molecule of water for every broken linkage which results in the production of simpler sugars as glucose [10].

The current manufacturing philosophy is based on the mass production of throw-away products using high density energy sources. On the other hand, for a biomass chemical industry, the philosophy may be moved to a local production of reusable products from low energy density sources taking in advance the distributed nature of biomass resource. This environmental philosophy imposes substantial changes in production, moving from centralized large scale plants to decentralized plants on a scale according to the biomass availability in each neighborhood [11].

The reduction in equipment cost, environmental compatibility and the hydrolysis at high temperatures can be reached using supercritical fluids, mainly supercritical CO<sub>2</sub> and H<sub>2</sub>O. The properties of water at conditions near and above its critical point of water (374°C, 22.1MPa) constitute new forms of byproducts recovery from industries like waste of food industry [11, 12]. The main reasons that make the hydrothermal medium a promising alternative for biomass processing are as follows [13] (1) it is not necessary to reduce the water content in

the raw material, thus avoiding energy losses; (2) the reaction media permits the transformation of the different biomass fractions; (3) the mass transfer limitations are reduced or avoided, thus allowing faster reaction rates. Furthermore, it is possible to control the reaction selectivity adjusting the properties of the reaction media, which is useful to avoid the generation of by-products. In addition, biofuels and chemical products produced would be free of biologically active organism and compounds, including bacteria, viruses and even prion proteins [13] because of the high temperatures involved. For these reasons, the use of supercritical fluids has been proposed as a clean technology to integrate the depolymerization-reaction-separation processes and this technology can be considered as fundamental for decentralizing chemical processes.

Nowadays, the biomass hydrolysis under hydrothermal conditions is starting to be applied in an industrial scale. Renmatix [14] is North American company dealing with the hydrothermal conversion of lignocellulosic biomass into sugars. Although this company is under production, operation data about process conditions, energy integration and flows are not available. In this work, it has been studied three energetic alternatives to develop the process of biomass hydrolysis in an energetically efficient way. Two alternatives deal with the integration of the hydrolysis process to a process of electrical energy production using a gas turbine with or without steam injection. The other alternative was supposed to be fossil fuels independent, using a biomass burner to obtain the heat requirements.

The objective of this work is the thermodynamic analysis of the processes integration between: (1) cellulose hydrolysis in supercritical water and; (2) gas turbine with steam injection. The thermal energy produced in the gas turbine is used to heat up a pressurized stream of water which will reach supercritical conditions to carry out the hydrolysis process. Moreover, the produced vapor fraction in the cellulose hydrolysis is used to enhance the efficiency of the gas turbine.

## **2. SCW Biomass Hydrolysis: Process description**

The hydrolysis of biomass in supercritical water can be analyzed in different stages as it is shown in Figure 1. As starting point, cellulose and water should be pressurized up to the reactor pressure. For this purpose, positive displacement pump can be used to increase the pressure from atmospheric until 25 MPa (or desired pressure). Special attention should be played in the biomass pumping. Biomass is composed of diverse materials and it not soluble

in water. This is because a suspension of biomass should be able to be pumped. Although this issue would produce troubles of clogging at lab scale, this problem can be overcome in the scaling up [13].

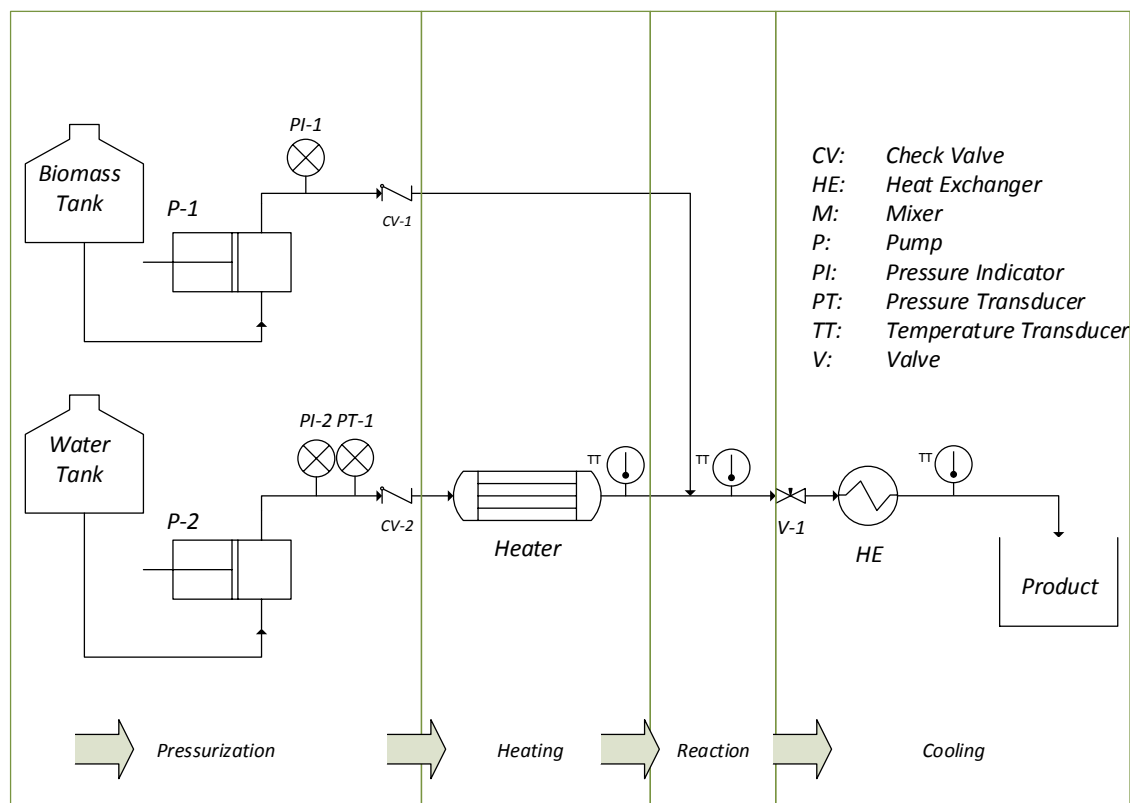


Fig 1. Experimental setup of biomass hydrolysis process in supercritical water.

In a previous work of our research group [15], a pilot plant was designed and built in order to perform biomass hydrolysis. In the aforementioned setup (see Figure 1), two pumps were used to impulse water and a biomass suspension ( $5\% \text{ w}\cdot\text{w}^{-1}$ ). The second stage in the process is the heating of the biomass stream which coincides with the start of the reactions. In order to avoid uncontrolled reactions, it is important to heat up the cellulose stream as fast as possible avoiding heating ramps. The heating of biomass stream was achieved by mixing it with supercritical water in a tee junction. This heating method is almost instantaneous. The biomass stream pumped by P-1 reaches the reactor at room temperature. On the other hand, water pumped by P-2 is heated up to  $450^\circ\text{C}$  in a furnace to be finally mixed with biomass. The third important stage is the reaction. After the desired temperature is reached, the residence time of biomass at the reaction conditions is critical in the selectivity of the process. Supercritical water hydrolysis is fast, so residence time higher than  $0.3 \text{ s}$  would lead to a product with high rate of degradation products [16]. The residence time was changed in the

designed setup by modifying the flows and the reactor volumes (length in tubular reactors). Finally, after the desired residence time is achieved, the products should be rapidly cooled in order to stop the hydrolysis reactions. The cooling of the products was achieved by sudden decompression of the reactor products. With this method it is possible to decrease the temperature of the stream from 400°C to 150°C between the inlet and outlet of the valve. After this, the products were cooled down to room temperature in a heat exchanger.

In the setup described above, the cellulose hydrolysis can be performed in supercritical water with a selectivity of soluble sugars as high as 98% w·w<sup>-1</sup> [15]. This reaction yield can be achieved using a continuous reactor with instantaneous heating and cooling methods that allow the precise control of the residence time [16]. The most frequently method for instantaneous heating is the mixing of the cellulose stream with supercritical water [15-20]. On the other hand, the most frequently method for the instantaneous cooling in the cool water injection in the reactor outlet [17-20]. However, a novel method was used to stop the reaction by cooling the reactor outlet by sudden decompression of the stream [15, 16]. With this technology it is possible to decrease the temperature from 400°C to 100°C immediately. In addition, this cooling method allow the control of the reactions without dilute the products. After the isenthalpic expansion, a two phase stream is produced: liquid and vapor. These two phases can be separated in a flash chamber in order to obtain as products a vapor phase without sugars and a liquid phase with high concentration of sugars.

### **3. Energy Integration**

The use of supercritical water requires high pressures and temperatures. Water as a liquid, can be compressed using a pump with affordable costs. The use of supercritical fluids makes necessary to supply heat of high quality ( $\approx 400^\circ\text{C}$ ). For this reason it is necessary to study reasonable solutions which are able to solve this part of the process with an affordable efficiency. One solution could be the integration of supercritical processes with energy production in cogeneration cycles. Cogeneration is defined as the simultaneous production of various forms of energy from one power source. The engine produces primary electrical power whereas thermal energy in the exhaust gases is converted into steam in the heat recovery boiler [21]. The implementation of cogeneration processes is joined with the use of gas turbines. Nowadays, the most extended fuel used in gas turbines is natural gas. This kind of turbines own several advantages over steam turbines and diesel engines, such as, higher

yields, better flexibility and higher efficiency [22]. Additionally, it is a compact engine, with lower manpower operating needs and ready availability [23]. Also, the gas turbine is further recognized for its better environmental performance manifested in curbing of air pollution and reducing the greenhouse effect [24]. For all these reasons it is proved that over the last two decades, the gas turbine has seen tremendous development and market expansion. Whereas gas turbines represented only twenty percent of the power generation market twenty years ago, they now claim approximately forty percent of new capacity additions [25].

As it was mentioned above, the biomass hydrolysis process at supercritical conditions produces a high pressure steam stream. This stream can be thermally integrated if there is a necessity of heat in other processes. If there are no other heat requirements, it is possible to implement a steam injection in the gas turbine, which will improve the efficiency of the global process. This mechanism links the process of cellulose hydrolysis with the cogeneration process. Steam injection is a technique which can increase the ability of a plant to generate extra power without burning extra fuel and requiring moderate capital investment. Furthermore a decrease in NO<sub>x</sub> emissions from the gas turbine is produced and also the electric generation efficiency of the simple and regenerative cycles is improved [26]. Steam Injected Gas Turbines (STIG) systems operate as an enhancement to the Brayton cycle. High quality steam is used to increase the power output and improve operating efficiency of the basic Brayton cycle. In general, the amount of steam injected can vary at a rate of between 2% and 10 % related to the compressed air [25]. The site at which this steam is injected differs according to the design of the particular gas turbine; however, mainly, high pressure steam is injected into the high-pressure sections of the gas turbine via the combustor fuel nozzles [25]. In its most basic form, steam injection works by increasing general mass flow through the gas turbine without increasing the mass of air compressed. This increase in the expanded mass flow generates an increase in the rotational torque and power output. Steam injection technology offers a clear improvement over the Brayton cycle while providing a fully flexible operating cycle. For all these reason it has been selected to be implemented in the process of hydrolysis.

#### **4. Methods – ASPEN simulation of biomass hydrolysis plant**

The simulation of all the processes has been carried out using ASPEN PLUS software. ASPEN PLUS is a chemical engineering simulation software which allows the study of several processes

including the analysis of flows, thermodynamic properties, kinetic properties, work and energy balance as some of the multiple possibilities provided by ASPEN. To execute the simulations, Peng Robinson property package has been selected. It has been necessary to introduce the interaction parameter between glucose and water, which constitute the main raw materials in the simulation. This parameter was experimentally analyzed and calculated by Abderafi et al [27, 28] at 0.1 MPa of pressure and temperatures between 100 and 113 °C. This value has been accepted because is more restrictive than the one at the operation conditions which is not available in literature up to best of our knowledge. The vapor-liquid equilibrium of the system glucose-water should be measured at the range of 1.5 MPa to 2.0 MPa in order to obtain the accurate interaction parameters of glucose and water.

The three analyzed options are: (1) Hydrolysis + Gas Turbine + Vapor injection; (2) Hydrolysis + Gas turbine and; (3) Hydrolysis + Biomass Burner. These option are analyzed and compared in sections 2.1, 2.2 and 2.3. When gas turbine was used in the process, the flows have been adjusted to similar values than those used in commercial gas turbines (e.g. SGT-100) [29].

#### 4.1. Hydrolysis + Gas turbine process + Vapor injection

The first alternative analyzed here was the combination of supercritical hydrolysis of cellulose process with the generation of electrical power using a cogeneration plant formed by a gas turbine plus steam injection. The ASPEN process flow diagram used in this simulation is shown in Figure 2. This option uses a gas turbine with steam injection. There are three main sections which will be explained in order to understand in a better way the simulation. These sections are the gas turbine section (2.1.1), the reactants conditioning section (2.1.2) and the reaction and separation section (2.1.3).

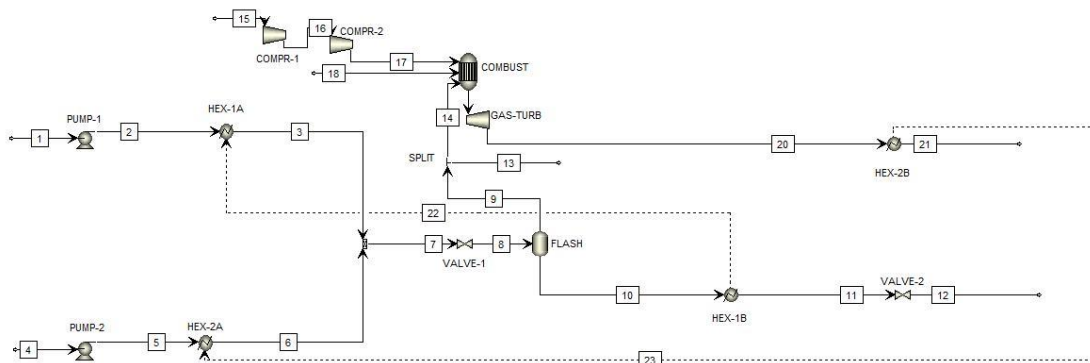


Fig 2. ASPEN process flow diagram, gas turbine & steam injection process.

##### 4.1.1. Gas turbine

The necessary air flow of the turbine is first compressed in two stages until 1.56 MPa. This compression has been simulated using two isentropic compressors (COMPR-1, COMPR-2). There is no intercooling between the two stages of compression because a higher temperature increases the work generated in the expansion. The air is fed to the combustion chamber (COMBUST), simulated as a stoichiometric reactor. Natural gas is the fuel used in the process. It is supplied at 20°C and 1.56 MPa. It is completely consumed in the process. Also one part of the flow of water steam generated in the separation section of the process (see section 2.1.3) is injected in the combustion chamber at 2 MPa of pressure. The relationship between the mass flow of steam injected and the mass flow of compressed air must be between 2 and 10 % [25]. The high specific heat of water benefits a higher generation of work in the expansion although it decreases the temperature of the outlet stream of the combustion chamber. The gases produced in the combustion chamber are expanded in the gas turbine (GAS-TURB), where the pressure decreases to 0.1 MPa. The enthalpy decrease of the gases after expansion in the gas turbine, generates work which is used to compress the necessary air flow of the process. The rest of the work can be used to produce power in an electric generator. The flue gases of the gas turbine have a higher temperature, so they are introduced in a heat exchanger (HEX-2) in order to heat up the process water stream (stream 5). The flue gases are cooled down until 120°C to avoid the possible condensation.

#### *4.1.2. Reactants*

The reactions of cellulose hydrolysis in sub and supercritical water were intensively studied in previous works of our research group [15, 16, 30]. These kinetics parameters were used in order to calculate reaction times and conversion in the process. In order to simplified the simulation, it was considered that the reactor outlet was the same than the experimentally determined in a previous work [15]. Thus, glucose is used as the biomass in the inlet stream of the reactor (stream 7). The feed stream (stream 1) has a mass concentration of 20% w·w<sup>-1</sup> of glucose. Its pressure is increased until 23 MPa using a pump (PUMP-1). It is also heated in a heat exchanger (HEX-1) using the product stream. It has to be taken into account that this stream must not be heated at temperatures higher than 250°C because at temperature above this value, the reaction of cellulose hydrolysis become faster and undesired reactions would occur. A detailed analysis of possible undesired reaction in the heat exchanger is presented in section 3. The process water stream used to carry out the reaction is pumped until 23 MPa in

the pump (PUMP-2). It is heated in a heat exchanger (HEX-2) using the flue gases of the gas turbine (GAS-TURB). Once the two streams are joined, the final temperature must be 400°C and the pressure 23 MPa, which are the conditions in which the reactions proceed in the reactor. It has been simulated a concentration of glucose in the inlet stream of the reactor of 4% w-w<sup>-1</sup>. The total flow of raw material fed to the reactor is a function of the available enthalpy of the flue gases.

#### 4.1.3. Reaction and separation

The reactions are stopped by sudden cooling of the reactor outlet as it was experimentally determined in previous works [15, 16]. Sudden decompression of the products showed to be an effective alternative to stop the reactions of cellulose hydrolysis. The reaction products, represented as glucose, are expanded in a valve (VALVE-1) until 2.0 MPa in order to stop the reactions (the reactions of cellulose hydrolysis are intensively retarded at temperature below 250°C, which correspond with a pressure of 4.0 MPa). Additionally, the expansion process produces a high pressure steam which can be injected in the turbine after separation in a flash chamber. Thus, the reaction products are introduced in a flash unit (FLASH). The vapor stream of the flash is split in two sub-streams. One is directly feed to the combustion chamber of the gas turbine and the other is removed of the process. The possible rests of sugars are considered to be totally combusted inside the combustion chamber. It is cooled down until 45°C in the heat exchanger (HEX-1) preheating too the biomass feed stream of the process. Finally, it is expanded until atmospheric pressure using a valve (VALVE-2).

#### 4.2. Hydrolysis + Gas turbine process

The ASPEN process flow diagrams of the gas turbine without steam injection process is shown in Figure 3.

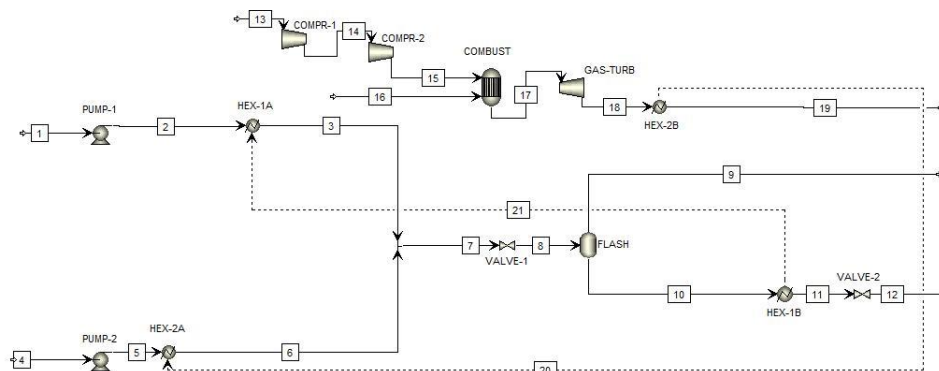


Fig 3. ASPEN process flow diagram, gas turbine without steam injection process

The main difference between this process and the process with steam injection is that the vapour stream of the flash (stream 9) is removed from the system without being partially injected in the turbine. The temperature of the flue gases is higher than in the process with steam injection if no extra natural gas is injected in this last one. However, less work per unit of product is produced as a consequence of the decrease in the mass flow injected in the turbine in comparison with the steam injection process. On the other hand, in this process it is possible to control the concentration of sugars in the product stream changing the pressure of expansion of the valve before the flash.

#### 4.3. *Hydrolysis + Biomass Burner*

The ASPEN process flow diagrams of the biomass burner process is shown in Figure 4. In contrast with steam injection process, a gas turbine is not used in this alternative. The heating of the pressurized water stream is carried out using a biomass burner which implies the use of higher amount of fuel as a consequence of the lower LHV (lower heating value of biomass) in comparison to natural gas. Furthermore, the process is simpler of be operated since there is not necessary to control a gas turbine and the possible failures are easy to be fixed. As in the process with gas turbine without steam injection, it is possible to control the concentration of sugars in the product stream changing the pressure of expansion of the valve before the flash. Finally, as the only fuel source is biomass, the life cycle assessment will be better than in the other proposed processes which use natural gas as fuel [31].

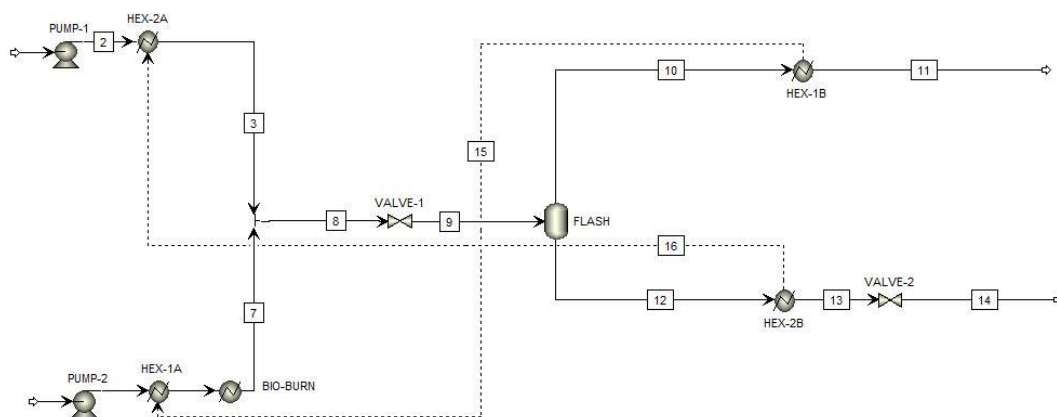


Fig 4. ASPEN process flow diagram, biomass burner process.

## 5. Simulation results

The process of cellulose hydrolysis was energetically evaluated by thermodynamic simulation of the three different alternatives presented in section 4. The main results for these three alternatives are summarized sections 5.1, 5.2 and 5.3 for option 1, 2 and 3 respectively.

### 5.1. Gas turbine + steam injection

The main parameter obtained from the simulation of cellulose hydrolysis linked to a gas turbine with vapor injection is shown in Table 1. This setup consumes 73 tons·h<sup>-1</sup> of air, 1.23 tons·h<sup>-1</sup> of natural gas and 13.68 tons·h<sup>-1</sup> of water. The process produces 554 kg·h<sup>-1</sup> of sugars (from cellulose hydrolysis) and 8.9 tons·h<sup>-1</sup> of available steam at 215°C and 2.0 MPa. In addition, the gas turbine produces 5.12 MW of work.

**Table 1.** Summary of the main condition operations of Gas turbine with steam injection.

<i>Description</i>	Value	Units
<i>Air Flow</i>	73000	kg·h <sup>-1</sup>
<i>Natural gas flow</i>	1230	kg·h <sup>-1</sup>
<i>Process water</i>	13680	kg·h <sup>-1</sup>
<i>Biomass feed stream concentration</i>	0.2	w·w <sup>-1</sup>
<i>Biomass inlet concentration in the reactor</i>	0.04	w·w <sup>-1</sup>
<i>Reactor Temperature</i>	400	°C
<i>Reactor Pressure</i>	23	MPa
<i>Product expansion pressure</i>	2.0	MPa
<i>Product expansion temperature</i>	215	°C
<i>L/V flash relationship</i>	0.11	w·w <sup>-1</sup>
<i>Product sugars concentration</i>	0.39	w·w <sup>-1</sup>
<i>Sugars product flow</i>	554	kg·h <sup>-1</sup>
<i>Gas turbine inlet pressure</i>	1.56	MPa
<i>Work required in compression</i>	10.78	MW
<i>Work produced in expansion</i>	15.90	MW
<i>Work balance</i>	5.12	MW
<i>Flue gasses outlet pressure</i>	0.1	MPa
<i>Flue gasses outlet temperature</i>	507.8	°C
<i>Steam availability flow</i>	8900	kg·h <sup>-1</sup>
<i>Steam availability temperature</i>	215	°C
<i>Steam availability pressure</i>	2.0	MPa

Another important unit of this process is the flash operation. The relationship between the outlet stream of liquid and the outlet stream of vapor in the flash is L/V = 0.1. The liquid stream

has a mass concentration of glucose of 39% w·w<sup>-1</sup>. In this stream it is recovered the 97 % w·w<sup>-1</sup> of the glucose fed to the flash.

## 5.2. Gas turbine

The main parameter obtained from the simulation of cellulose hydrolysis in combination with a gas turbine with vapor injection is shown in Table 2. This setup consumes 73 tons·h<sup>-1</sup> of air, 1.1 tons·h<sup>-1</sup> of natural gas and 12.6 tons·h<sup>-1</sup> of water. The process produces 509 kg·h<sup>-1</sup> of sugars (from cellulose hydrolysis) and 11.9 tons·h<sup>-1</sup> of available steam at 215°C and 2.0 MPa. In addition, the gas turbine produces 4 MW of work.

**Table 2.** Summary of the main condition operations of Gas turbine without steam injection.

<i>Description</i>	Value	Units
<i>Air Flow</i>	73000	kg·h <sup>-1</sup>
<i>Natural gas flow</i>	1100	kg·h <sup>-1</sup>
<i>Process water</i>	13100	kg·h <sup>-1</sup>
<i>Biomass feed stream concentration</i>	0.2	w·w <sup>-1</sup>
<i>Biomass inlet concentration in the reactor</i>	0.04	w·w <sup>-1</sup>
<i>Reactor Temperature</i>	400	°C
<i>Reactor Pressure</i>	23	MPa
<i>Product expansion pressure</i>	2.0	MPa
<i>Product expansion temperature</i>	215	°C
<i>L/V flash relationship</i>	0.06	w·w <sup>-1</sup>
<i>Product sugars concentration</i>	0.42	w·w <sup>-1</sup>
<i>Sugars product flow</i>	509	kg·h <sup>-1</sup>
<i>Gas turbine inlet pressure</i>	1.56	MPa
<i>Work required in compression</i>	10.8	MW
<i>Work produced in expansion</i>	14.8	MW
<i>Work balance</i>	4	MW
<i>Flue gasses outlet pressure</i>	0.1	MPa
<i>Flue gasses outlet temperature</i>	529	°C
<i>Steam availability flow</i>	11900	kg·h <sup>-1</sup>
<i>Steam availability temperature</i>	215	°C
<i>Steam availability pressure</i>	2.0	MPa

About the flash unit, the relationship between the outlet stream of liquid and the outlet stream of vapor in the flash is L/V = 0.1. The liquid stream has a mass concentration of glucose of 42% w·w<sup>-1</sup>. In this stream it is recovered the 97 % w·w<sup>-1</sup> of the glucose fed to the flash.

### 5.3. Biomass burner

The main parameter obtained from the simulation of cellulose hydrolysis in combination with a gas turbine with vapor injection is shown in Table 3. This setup consumes 1.66 Gcal·h<sup>-1</sup> of burnable biomass (the mass of required biomass will depend on the heat capacity and humidity of the biomass) and 3.6 tons·h<sup>-1</sup> of water. The process produces 144 kg·h<sup>-1</sup> of sugars (from cellulose hydrolysis) with a concentration of 45% w·w<sup>-1</sup> and 3.4 tons·h<sup>-1</sup> of available steam at 215°C and 2.0 MPa. In this case there is not production of work.

**Table 3.** Summary of the main condition operations of Cellulose hydrolysis and biomass burner.

<i>Description</i>	Value	Units
<i>Air Flow</i>	-	kg·h <sup>-1</sup>
<i>Burning biomass flow</i>	1.66	Gcal·h <sup>-1</sup>
<i>Process water</i>	3600	kg·h <sup>-1</sup>
<i>Biomass feed stream concentration</i>	0.2	w·w <sup>-1</sup>
<i>Biomass inlet concentration in the reactor</i>	0.04	w·w <sup>-1</sup>
<i>Reactor Temperature</i>	400	°C
<i>Reactor Pressure</i>	23	MPa
<i>Product expansion pressure</i>	2.0	MPa
<i>Product expansion temperature</i>	215	°C
<i>L/V flash relationship</i>	0.09	w·w <sup>-1</sup>
<i>Product sugars concentration</i>	0.45	w·w <sup>-1</sup>
<i>Sugars product flow</i>	144	kg·h <sup>-1</sup>
<i>Gas turbine inlet pressure</i>	-	MPa
<i>Work required in compression</i>	-	MW
<i>Work produced in expansion</i>	-	MW
<i>Work balance</i>	-	MW
<i>Flue gasses outlet pressure</i>	-	MPa
<i>Flue gasses outlet temperature</i>	-	°C
<i>Steam availability flow</i>	3400	kg·h <sup>-1</sup>
<i>Steam availability temperature</i>	212	°C
<i>Steam availability pressure</i>	2.0	MPa

## 6. Discussion

### 6.1. Alternatives evaluation

As it was previously explained, it has been developed the study of three different options to implement a biomass hydrolysis plant. In Table 4, it is shown the energy consumption of the analyzed processes. It has not been considered the work requirement in the pumps due to the fact that is the same in the three processes. The process with steam injection requires less

amount of work in compression per kg of product and produces a higher amount of work in the turbine per kg of product. This alternative presents the highest work balance per kilogram of product obtained.

**Table 4.** Work comparative of the three simulated alternatives.

<i>Process</i>	Work requirement / kg of product (kW·kg <sup>-1</sup> )	Work production / kg of product (kW·kg <sup>-1</sup> )	Work balance / kg of product (kW·kg <sup>-1</sup> )
<i>Gas turbine &amp; steam injection</i>	19.5	28.7	9.2
<i>Gas turbine no steam injection</i>	21.2	29.4	7.8
<i>Biomass Burner</i>	0.0	0.0	0.0

In Table 5, it is shown the flows comparative. The two processes with turbine, requires the same amount of air. However, the steam injection process is able to produce more product per kilogram of air. On the other hand, it is necessary to introduce a higher amount of natural gas in the process with steam injection in order to maintain the temperature of combustion so as to be able to heat up the process water stream. Finally, the rate between the mass of sugars in the product stream and the mass of biomass in the feed is similar for the three experimented processes 97% w-w<sup>-1</sup>.

**Table 5.** Flows comparative of the three simulated alternatives. The biomass burner will require available atmospheric air.

<i>Process</i>	kg compressed air / kg product	kg natural gas / kg product	kg product / kg sugar in the feed
<i>Gas turbine &amp; steam injection</i>	131.8	2.22	0.97
<i>Gas turbine no steam injection</i>	143.4	2.16	0.97
<i>Biomass Burner</i>	0.0	0.00	0.96

The heat requirements of the three process are summarized in Table 6. Although in the biomass burner process is not necessary to use natural gas, the required amount of heat has to be supplied with biomass. It has to be taken into account that biomass has a lower heating value [4] ( $LHV_{\text{biomass}} = 2500\text{-}4000 \text{ kcal}\cdot\text{kg}^{-1}$ , dependent of the type of biomass and the humidity) than the natural gas ( $LHV_{\text{natural gas}} = 13000 \text{ kcal/kg}$ ), so it is necessary to use a higher amount of biomass than if the process would be carried out with natural gas. Biomass also leaves a solid residue which has to be processed. In the processes in which gas turbines are

used, the heat requirements are provided by the flue gases of the turbine resulting in a non-extra heat supplies.

**Table 6.** Heat requirement and sugar concentration in the outlet stream comparative.

<i>Process</i>	Heat requirement / kg product (kW·kg <sup>-1</sup> )	Sugar concentration (w·w <sup>-1</sup> ) outlet stream
<i>Gas turbine &amp; steam injection</i>	0	0.39
<i>Gas turbine no steam injection</i>	0	0.42
<i>Biomass Burner</i>	13	0.45

Regarding to the sugar concentration in the outlet stream, in the three processes the concentration is similar ( $\approx 40\%$  w·w<sup>-1</sup>). Nevertheless, this value can be modified in the processes of gas turbine without steam injection and biomass burner. These two processes do not require the vapor stream at high pressure and temperature, so the pressure after the expansion valve can be varied in order to achieved the best separation in the flash unit. In the process with steam injection the flash conditions cannot be modified because high pressure steam is needed to be injected in the turbine. The flash unit was also simulated at lower pressure than the previous ones. At 1.5 MPa, the relationship between the outlet stream of liquid and the outlet stream of vapor in the flash is  $L/V = 0.05$ . At this condition, the liquid stream has a mass concentration of glucose of 51% w·w<sup>-1</sup>. In this stream it would be recovered the 98 % w·w<sup>-1</sup> of the glucose fed to the flash. However, it is important to take into account that a high concentration value in the product stream could cause problems in the flow as a consequence of a high viscosity.

The process of hydrolysis using biomass as fuel, which will achieve the independence of fossil fuels, can be developed if biomass is available in high amounts. Finally, there are other process options such as the use of gasified biomass in biomass turbines or the expansion of air heated in a biomass burner. However, these technologies have not reached the necessary development to be capable of replacing natural gas as fuel. When gasification and biomass turbines processes are enhanced in efficiency, the total independence of fossil fuels and the use of biomass as the unique raw material and fuel in this process will be reached.

### *6.2. Effects of pre-heating and post-cooling ramps*

In order to evaluate the effects of the heating and cooling ramps in the reaction of cellulose hydrolysis, the heat exchanger of the biomass stream was calculated. The goal was to know

the temperatures profiles and the residence times in the heat exchanger. With these parameters and the kinetic constants of cellulose and glucose hydrolysis it is possible to determine the proportion of undesired reactions.

The heat exchanger has been designed applying Kern method of shell and tubes heat exchangers [32]. The values of the heat exchanged and the inlet and outlet temperatures of the cold and hot streams have been provided by ASPEN simulator. The total heat exchanged was 343kW. The hot fluid (the product stream of the process) flows through the tubes while the cold fluid (biomass raw material stream) flows in the shell. The cold fluid is heated from 36.7°C to 118°C while the hot fluid is cooled from 215°C to 45°C. The global transfer coefficient is 960 W·m<sup>-2</sup>·K<sup>-1</sup>. The total area required is 2.2 m<sup>2</sup>. The tubes have a diameter of 20 mm and a length of 1.83 m. The heat exchanger was designed so that the fluid in the tubes passes four times for them. It was necessary to use 20 tubes to cover the area requirements. The shell has 0.15 m of diameter. The pressure drop in the tubes and the shell is 0.02 bar. The residence time in the heat exchanger of the solution of biomass is 14s. On the other hand, the residence time of the product stream is 21 s.

The kinetic of cellulose and glucose hydrolysis were obtained from a previous work of our research group [16, 30]. The values of activation energy (E<sub>a</sub>) and pre-exponential factor (Ln k<sub>0</sub>) of cellulose hydrolysis at subcritical temperature are 154.5 kJ·mol<sup>-1</sup> and 29.6 respectively [16]. On the other hand, the values of E<sub>a</sub> and Ln k<sub>0</sub> are 123.3 kJ·mol<sup>-1</sup> and 23.1 respectively [30].

The conversion of cellulose along residence time can be calculated by Equation 1 [16, 33], where 'x' is the cellulose conversion, 't' is the time (s) and 'k' is the kinetic constant of cellulose hydrolysis (s<sup>-1</sup>).

$$\frac{dx}{dt} = 2k(1-x)^{1/2} \quad (1)$$

The conversion of glucose along residence time can be calculated by Equation 2, where 'x<sub>g</sub>' is the glucose conversion, 't' is the time (s) and 'k' is the kinetic constant of glucose hydrolysis (s<sup>-1</sup>).

$$\frac{dx_g}{dt} = k_g(1-x_g) \quad (2)$$

This equation were evaluated together with the Arrhenius relationship between the kinetic constant and the temperature shown in Equation 3, where ' $E_a$ ' is the activation energy in  $\text{kJ}\cdot\text{mol}^{-1}$ ; ' $R$ ' is the universal constant of gases in  $\text{kJ}\cdot\text{mol}^{-1}\cdot\text{K}^{-1}$  and ' $T$ ' is the temperature in K.

$$k = k_0 e^{\frac{-E_a}{RT}} \quad (3)$$

The resolution of these equation at the same time allow knowing the amount of cellulose that is hydrolyzed before entering to the reactor as well as the amount of glucose that is hydrolyzed during the cooling. Because of the low temperature and residence times required in the heat exchanger, less than 0.004%  $\text{w}\cdot\text{w}^{-1}$  of cellulose would be degraded before entering the reactor. After the reaction, less than 0.004%  $\text{w}\cdot\text{w}^{-1}$  of glucose would be hydrolyzed in the heat exchanger.

## 7. Conclusions

The integration of cellulose hydrolysis in supercritical water with the electrical power generation by gas turbines with steam injection showed to be a promising alternative for the production of sugars from a renewable raw material, using compact equipment and energetically efficient processes.

In this work, it was thermodynamically calculated that cellulose hydrolysis could be done selectively (98%  $\text{w}\cdot\text{w}^{-1}$ ) without any energy demand if the process is linked to a gas turbine with steam injection. In addition the production of work by a gas turbine is enhanced ( $\approx 10\%$ ) by injecting the steam produced in the process of cellulose hydrolysis. In addition, the use of a flash chamber after the reactor allows the concentration of the products from 0.04%  $\text{w}\cdot\text{w}^{-1}$  to 0.37%  $\text{w}\cdot\text{w}^{-1}$ .

The experimental setup calculated as the integration of the cellulose hydrolysis process with a gas turbine without steam injection allows the development of the hydrolysis process without any demand of heat or power. However, this alternative produce less energy than the use of a gas turbine with steam injection. Finally, the setup analyzed in combination with a biomass burner allows the operation without any demand of fossil fuels. However, this process do not produce extra power availability like in the previous alternatives.

## Glossary

COMBUST	Combustion chamber
COMPR	Isentropic compressors
Ea	Activation Energy
FLASH	Flash Chamber
GAS-TURB	Gas turbine
HEX	Heat exchanger
LHV	Lower Heating Value
$\ln k_0$	Pre-exponential factor of Arrhenius relationship
P	Pressure
PUMP	Pump
STIG	Steam Injected Gas Turbines
T	Temperature
VALVE	Valve

## Acknowledgements

The authors thank the Spanish Ministry of Economy and Competitiveness for the Project CTQ2011-23293 and ENE2012-33613. The authors thank Repsol for its technical support. D.A.C. thanks the Spanish Ministry of Education for the FPU fellowship (AP2009-0402).

## References

1. BECOTEPS. *European Technology Platforms for the FP7. The European Bioeconomy 2030. Delivering Sustainable Growth by addressing the Grand Societal Challenges* 2013 - 10/04/2014 10/04/2014].
2. Ragauskas, A.J., Williams, C.K., Davison, B.H., Britovsek, G., Cairney, J., Eckert, C.A., Frederick, W.J., Hallett, J.P., Leak, D.J., Liotta, C.L., Mielenz, J.R., Murphy, R., Templer, R., and Tschaplinski, T., *The Path Forward for Biofuels and Biomaterials*. Science, 2006. 311(5760): p. 484 -489.
3. Tollefson, J., *Energy: Not your father's biofuels*. Nature News, 2008. 451(7181): p. 880-883.
4. Bobleter, O., *Hydrothermal degradation of polymers derived from plants*. Progress in polymer science, 1994. 19(5): p. 797-841.
5. Klemm, D., Heublein, B., Fink, H.P., and Bohn, A., *Cellulose: Fascinating Biopolymer and Sustainable Raw Material*. Angewandte Chemie International Edition, 2005. 44(22): p. 3358-3393.
6. Huber, G.W., Iborra, S., and Corma, A., *Synthesis of Transportation Fuels from Biomass: Chemistry, Catalysts, and Engineering*. Chemical Reviews, 2006. 106(9): p. 4044-4098.
7. Huber, G.W. and Corma, A., *Synergies between Bio- and Oil Refineries for the Production of Fuels from Biomass*. Angewandte Chemie International Edition, 2007. 46(38): p. 7184-7201.
8. Corma, A., Iborra, S., and Velty, A., *Chemical Routes for the Transformation of Biomass into Chemicals*. Chemical Reviews, 2007. 107(6): p. 2411-2502.
9. van Putten, R.-J., van der Waal, J.C., de Jong, E., Rasrendra, C.B., Heeres, H.J., and de Vries, J.G., *Hydroxymethylfurfural, A Versatile Platform Chemical Made from Renewable Resources*. Chemical Reviews, 2013. 113(3): p. 1499-1597.
10. Brunner, G., *Near critical and supercritical water. Part I. Hydrolytic and hydrothermal processes*. The Journal of Supercritical Fluids, 2009. 47(3): p. 373-381.
11. Arai, K., Smith Jr, R.L., and Aida, T.M., *Decentralized chemical processes with supercritical fluid technology for sustainable society*. The Journal of Supercritical Fluids, 2009. 47(3): p. 628-636.

12. Cocero, M.J., Cantero, D.A., Bermejo, M.D., and García-Serna, J., *Nuevas tendencias en el diseño de procesos para aprovechamiento de residuos alimentarios dirigidas a conseguir una sociedad sostenible*, in *Retos Medioambientales de la Industria Alimentaria*. 2010. p. 89-100.
13. Peterson, A.A., Vogel, F., Lachance, R.P., Fröling, M., Michael J. Antal, Jr., and Tester, J.W., *Thermochemical biofuel production in hydrothermal media: A review of sub- and supercritical water technologies*. *Energy & Environmental Science*, 2008. 1(1): p. 32-65.
14. Renmatix. 2013 - 10/04/2014 10/04/2014].
15. Cantero, D.A., Bermejo, M.D., and Cocero, M.J., *High glucose selectivity in pressurized water hydrolysis of cellulose using ultra-fast reactors*. *Bioresource Technology*, 2013. 135: p. 697-703.
16. Cantero, D.A., Bermejo, M.D., and Cocero, M.J., *Kinetic analysis of cellulose depolymerization reactions in near critical water*. *The Journal of Supercritical Fluids*, 2013. 75: p. 48-57.
17. Sasaki, M., Adschiri, T., and Arai, K., *Kinetics of cellulose conversion at 25 MPa in sub- and supercritical water*. *AIChE Journal*, 2004. 50(1): p. 192-202.
18. Aida, T.M., Tajima, K., Watanabe, M., Saito, Y., Kuroda, K., Nonaka, T., Hattori, H., Smith Jr, R.L., and Arai, K., *Reactions of D-fructose in water at temperatures up to 400 °C and pressures up to 100 MPa*. *The Journal of Supercritical Fluids*, 2007. 42(1): p. 110-119.
19. Aida, T.M., Shiraishi, N., Kubo, M., Watanabe, M., and Smith, R.L., *Reaction kinetics of d-xylose in sub- and supercritical water*. *The Journal of Supercritical Fluids*, 2010. 55(1): p. 208-216.
20. Aida, T.M., Sato, Y., Watanabe, M., Tajima, K., Nonaka, T., Hattori, H., and Arai, K., *Dehydration of D-glucose in high temperature water at pressures up to 80 MPa*. *The Journal of Supercritical Fluids*, 2007. 40(3): p. 381-388.
21. Najjar, Y.S.H., *Gas turbine cogeneration systems: a review of some novel cycles*. *Applied Thermal Engineering*, 2000. 20(2): p. 179-197.
22. McKay, M.E. and Rabl, A., *A case study on cogeneration*. *Energy*, 1985. 10(6): p. 707-720.

23. Langston, L., *Market drivers for electric power gas turbines: reasons for the revolution*. Global Gas Turbine News, 1996: p. 36.
24. Najjar, Y.S.H., Akyurt, M., Al-Rabghi, O.M., and Alp, T., *Cogeneration with gas turbine engines*. Heat Recovery Systems and CHP, 1993. 13(5): p. 471-480.
25. Koivu, T.G., *New Technique for Steam Injection (STIG) Using Once Through Steam Generator (GTI/OTSG) Heat Recovery to Improve Operational Flexibility and Cost Performance*. Industrial Application of Gas Turbines Committee: p. Paper No: 07-IAGT-2.2.
26. Nishida, K., Takagi, T., and Kinoshita, S., *Regenerative steam-injection gas-turbine systems*. Applied Energy, 2005. 81(3): p. 231-246.
27. Abderafi, S. and Bounahmidi, T., *Measurement and estimation of vapor-liquid equilibrium for industrial sugar juice using the Peng-Robinson equation of state*. Fluid Phase Equilibria, 1999. 162(1-2): p. 225-240.
28. Abderafi, S. and Bounahmidi, T., *Measurement and modeling of atmospheric pressure vapor-liquid equilibrium data for binary, ternary and quaternary mixtures of sucrose, glucose, fructose and water components*. Fluid Phase Equilibria, 1994. 93: p. 337-351.
29. Siemens. *Siemens Gas Turbines*. 2014 - 10/04/2014.
30. Cantero, D.A., Álvarez, A., Bermejo, M.D., and Cocero, M.J., *Transformation of glucose in high added value compounds in a hydrothermal reaction media*. III Iberoamerican Conference on Supercritical Fluids, 2013.
31. Gasafi, E., Meyer, L., and Schebek, L., *Using Life-Cycle Assessment in Process Design.: Supercritical Water Gasification of Organic Feedstocks*. Journal of Industrial Ecology, 2003. 7(3-4): p. 75-91.
32. Kern, D.Q., *Process heat transfer*, ed. T.M.-H. Education. 1950.
33. Sasaki, M., Fang, Z., Fukushima, Y., Adschiri, T., and Arai, K., *Dissolution and Hydrolysis of Cellulose in Subcritical and Supercritical Water*. Industrial & Engineering Chemistry Research, 2000. 39(8): p. 2883-2890.



# Conclusions

Intensification of Cellulose  
Hydrolysis Process by  
Supercritical Water.  
Obtaining of Added Value  
Products



The overall conclusions of this PhD Thesis are presented below. The specific conclusions of each research are presented in the chapter conclusions.

The process of cellulose hydrolysis was intensively studied in near critical water. A new concept of reactors for reactions in supercritical water was developed. The used experimental setup is able to operate up to 425°C, 30 MPa with residence times between 0.004 and 50 s. The used method to start and finish the reaction is by applying sudden changes in temperature, obtaining an isothermal reactor. In this kind of reactor is easy to determine the residence time of the reagents in the reactor, which will drive to precise results. The continuous operation mode of the reactors showed to be adequate for the selective hydrolysis of biomass. The hydrolysis selectivity obtained in this PhD Thesis was higher than the process selectivity presented in literature for batch or semi-continuous reactors.

Cellulose hydrolysis was studied at temperatures between 275°C and 400°C and pressures between 10 MPa and 27 MPa. It was observed that cellulose hydrolysis kinetic is much accelerated by rising temperature than glucose hydrolysis does. This difference is accentuated at temperatures above the critical point of water, however, both reactions are enhanced. From this phenomenon it can be taken benefit if an adequate control on residence time is applied. The total conversion of cellulose at 400°C and 25 MPa takes 0.013 s, if the reaction is stopped at residence times between 0.013 s and 0.03 s the yield of sugars will be higher than 98% w-w<sup>-1</sup>. The pressure effect on the kinetics of cellulose is less marked than temperature and residence time effects. Nevertheless, it plays an important role in the composition of the hydrolysis products. An increment in pressure will produce sugars of higher molecular weights.

The variation of temperature and pressure together allows the modification of the chemical and physical properties of water, thus, the reaction medium. The main properties of water that will affect the kinetics of the process are density and ionic product. It was observed that the hydroxide ion concentration in the medium is a driven factor in the reactions in which glucose is converted. At low ion concentrations, the reactions of glucose-fructose isomerization and dehydration are diminished while retro-aldol condensation reactions are benefited.

The kinetics of cellulose hydrolysis as well as glucose and fructose hydrolysis were studied and the Arrhenius parameters were calculated for each one. Also, the kinetics were analyzed with pressure, obtaining the activation volume of the reaction kinetics.

The reactions of fructose and glucose hydrolysis were studied and the main reaction pathways were developed. Firstly, it was found that the main reaction at supercritical conditions is retro-aldol condensation. This reaction produces two-carbon or three-carbon molecules when glucose or fructose is converted respectively. The main product of glucose hydrolysis at 400°C, 27 MPa and 20 s of residence time was glycolaldehyde (>80% w·w<sup>-1</sup>). On the other hand, when fructose was hydrolyzed at the same conditions, the main product was pyruvaldehyde. The reaction of the glucose and fructose mixture produced a combination of glycolaldehyde and pyruvaldehyde as main products.

The effect of homogeneous catalyst was tested in glucose conversion. It was observed that sodium hydroxide favors the reaction of glucose isomerization to fructose as well as the reaction of pyruvaldehyde conversion into lactic acid.

#### *Future Work*

From the studies developed in this PhD, it can be concluded that the field of biomass conversion in supercritical water is a promising research area with several interesting topics to address. In the next paragraphs, the main topics to be developed in the research of biomass upgrading are presented.

It was observed that continuous operation is useful for reducing the reactor volume. Furthermore, the process control is better than in semi or discontinuous processes. However, the management of solids inputs and solids output to the reactor are two important topic that should be completely developed. The solids pumping can be overcome to be successful in scaling up the process. Nevertheless, at lab scale is important to develop feeding system capable of impelling concentrated sludge. On the other hand, the separation of unreacted solids should be done just before the reaction end at extremely low residence times. The temperature and residence time proposed in this PhD Thesis for the cellulose hydrolysis process makes necessary the development of an apparatus capable of being a reactor and a separator with a particle residence time lower than 0.1 seconds.

If we attend to lactic acid production, it would be interesting the development of a selective catalyst capable of enhancing the reaction of glucose into one of the optical active isomers of lactic acid (L +).

# Resumen

Intensificación del Proceso de  
Hidrólisis de Celulosa para la  
Obtención de Productos de Valor  
Añadido mediante el uso de Agua  
Supercrítica.



En el último siglo, la producción de productos químicos ha estado basada en la disponibilidad de grandes cantidades de petróleo a precios bajos. Estos procesos son llevados a cabo en grandes plantas de producción a gran escala, permitiendo así la reducción del coste de obtención del producto. Este tipo de producción ha permitido un fuerte crecimiento económico mundial en el siglo XX. Sin embargo, en los últimos años ha habido una tendencia generalizada en hacia el desarrollo de una sociedad basada en la *Bio-Economía*. Este tipo de producción se refiere a la producción y conversión de biomasa en distintos tipos de alimentos, fibras, productos industriales y energía. Este cambio en la filosofía de producción implica una renovación sustancial en el concepto de generación de productos. La utilización de biomasa vegetal como fuente de materia prima se podría llevar a cabo en plantas de producción descentralizadas que sean versátiles y eficientes. Este tipo de planta química podría estar ubicada en las cercanías de producción de la materia prima.

Las industrias basadas en la utilización de biomasa como fuente de materias primas no están aun totalmente desarrolladas para ser capaces de afrontar una producción descentralizada. Para alcanzar este desafío es necesario orientar el desarrollo de nuevas tecnologías basados en procesos compatibles con el medio ambiente que utilicen eficientemente la energía a la vez que permitan una reducción del coste de las instalaciones. Los procesos *amigables* con el medioambiente están caracterizados por tener alta selectividad y rendimiento. Esto puede ser alcanzado simplificando el número de etapas del proceso, buscando alternativas entre nuevas fuentes de materias primas y utilizando disolventes *limpios* como el agua o el dióxido de carbono. La reducción de los costes de instalación implica el desarrollo de equipos compactos con pequeños tiempos de operación, una disminución en el tiempo de residencia desde minutos a milisegundos permite una disminución en el volumen de reactor desde  $m^3$  hasta  $cm^3$ .

El uso de fluidos presurizados ha sido propuesto como método compatible con el medio ambiente capaz de integrar el proceso de despolimerización – reacción – separación de la biomasa. Particularmente el agua presurizada es un disolvente limpio, seguro y compatible medio ambientalmente para llevar a cabo reacciones orgánicas.

El **OBJETIVO DE ESTA TESIS DOCTORAL** es desarrollar un proceso capaz de convertir celulosa (o biomasa vegetal) en productos de valor añadido como compuestos químicos o combustibles utilizando agua supercrítica como medio de reacción.

Este objetivo se desarrolla en los objetivos concretos que se presentan a continuación:

- Diseño y construcción de una planta piloto para el estudio de la hidrólisis de celulosa en un medio hidrotermal. Los principales requerimientos de la planta piloto son:
  - Máxima temperatura de operación: 425°C;
  - Máxima presión de operación: 30 MPa;
  - Versatilidad en el tiempo de residencia. Desde milisegundos hasta 1 minuto;
  - Calentamiento y enfriamiento rápido;
  - Alimentación. Bomba capaz de bombear suspensiones de celulosa de hasta un 20 % de concentración en masa.
- Modelado cinético de la hidrólisis de celulosa:
  - Desarrollo de un modelo matemático para estimar la conversión de celulosa así como también la concentración de los productos derivados de su hidrólisis;
  - Determinación de las constantes de energía de activación y factor pre-exponencial de las reacciones estudiadas (parámetros de Arrhenius);
  - Determinación del volumen de activación de las constantes cinéticas implicadas en el proceso;
  - Análisis del proceso cinético junto con las propiedades del medio de reacción.
- Estudio de la hidrólisis de celulosa:
  - Efecto del tiempo de residencia, temperatura y presión sobre las reacciones de hidrólisis de celulosa y glucosa.
- Estudio de la hidrólisis de fructosa:
  - Determinación de los principales caminos de reacción en la hidrólisis de fructosa en un medio hidrotermal;
  - Efecto de modificadores del medio de reacción sobre las reacciones de fructosa en agua presurizada.
- Estudio de la hidrólisis de glucosa:
  - Determinación de los principales caminos de reacción de la hidrólisis de glucosa en agua presurizada;
  - Producción de ácido láctico a partir de glucosa.
- Estudio de la hidrólisis de biomasa vegetal: salvado de trigo:

- o Estudio del comportamiento del reactor desarrollado utilizando biomasa natural como alimentación.
- Estudio energético del proceso de hidrólisis en agua supercrítica:
  - o Análisis de diferentes alternativas energéticas para la producción de compuestos de valor añadido en agua supercrítica.

Esta tesis doctoral ha sido estructurada en una revisión bibliográfica sobre el tema y ocho capítulos. En cada uno de los capítulos se han presentado los objetivos parciales así como una revisión bibliográfica sobre el tema en cuestión. Los principales logros de están descriptos a continuación por capítulos.

La planta piloto diseñada y construida para realizar la experimentación fue capaz de operar a temperaturas de hasta 425°C, presiones de hasta 30 MPa con tiempos de residencia entre 0.004 s y 50 s. Las principales ventajas del dispositivo experimental son: (a) el reactor puede ser considerado isotérmico debido a los instantáneos métodos de calentamiento y enfriamiento; (b) los productos del reactor no se diluyen en el proceso de enfriamiento y (c) es posible variar el tiempo de residencia desde 0.004 s hasta 50 s utilizando reactores tubulares de aleación de Níquel de diferente longitud.

En el **Capítulo 1**, "High glucose selectivity in pressurized water hydrolysis of cellulose using ultra-fast reactors", se presentan y discuten las principales ventajas del método de calentamiento y enfriamiento. En este estudio, se mejoró la producción de glucosa usando celulosa como material de partida mediante la utilización de reactores ultra rápidos. Para ellos se combinó la utilización de un medio de reacción selectivo (400°C y 25 MPa) donde el tiempo de residencia fue crítico para el control de la selectividad. Un rendimiento azúcares solubles mayor al 98% w·w<sup>-1</sup> fue obtenido en 0.03 s de tiempo de residencia. El rendimiento de glucosa, fructosa y celobiosa fue de 50% w·w<sup>-1</sup> en ese tiempo de residencia. La celulosa fue completamente hidrolizada a tiempos de residencia mayores a 0.015 s. Además, el medio de reacción aplicado sumado al control del tiempo de residencia permitió que la obtención producción de productos de degradación como el 5-hydroxymethylfurfural sea menor a 5 ppm. En este capítulo se ha demostrado que es posible reducir el tiempo de residencia de las reacciones de hidrólisis de celulosa. Una reducción del tiempo desde minutos a milisegundo implica una reducción en el tamaño de los reactores desde los convencionales reactores de volúmenes de m<sup>3</sup> a reactores de volúmenes de cm<sup>3</sup>.

En la Figura 1 se puede observar la influencia del tiempo de residencia sobre la selectividad obtenida en el proceso de azúcares solubles.

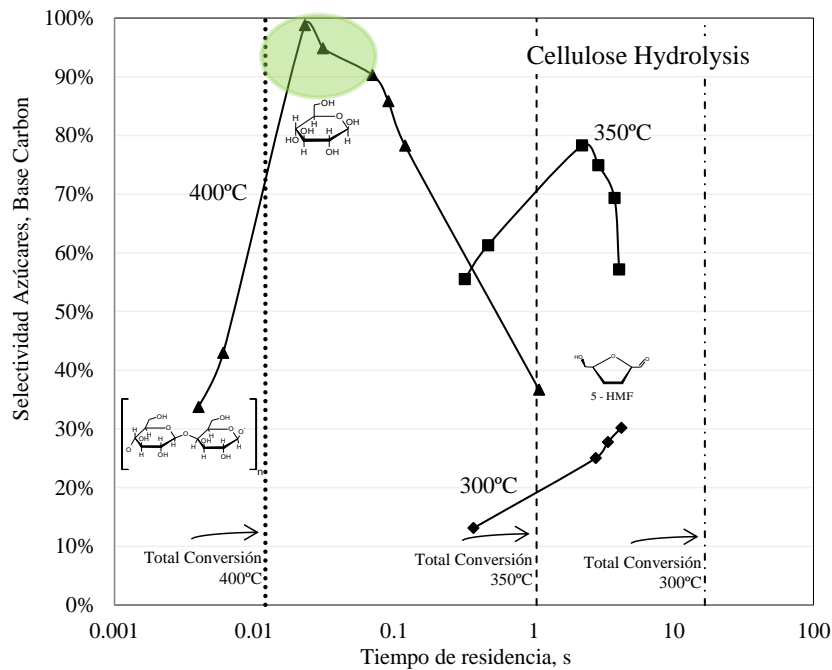


Fig. 1. Efecto del tiempo de residencia y la temperatura sobre la selectividad en la hidrólisis de celulosa en agua presurizada.

En el **Capítulo 2**, “Kinetics analysis of cellulose depolymerization reactions in near critical water”, se presenta un estudio sobre el efecto de la temperatura y el tiempo de residencia sobre las cinéticas de hidrólisis de celulosa y glucosa. Se desarrolló un modelo matemático para predecir la concentración de celulosa y sus productos de hidrólisis a lo largo del tiempo de reacción. Para ello, se propuso una ruta de reacción y se realizó una búsqueda bibliográfica de los parámetros de reacción involucrados en el proceso. Las constantes cinéticas de hidrólisis de celulosa, hidrólisis de oligosacáridos, isomerización de glucosa y formación de 5-HMF se ajustaron mediante la comparación de los perfiles de concentraciones experimentalmente obtenidas y los modelados. La cinética de hidrólisis de celulosa mostró un cambio en su comportamiento en las cercanías del punto crítico del agua. La energía de activación  $154.4 \pm 9.5 \text{ kJ}\cdot\text{mol}^{-1}$  y  $430.3 \pm 6.3 \text{ kJ}\cdot\text{mol}^{-1}$  por debajo y encima del punto crítico respectivamente. La energía de activación de la cinética de hidrólisis de oligosacáridos fue  $135.2 \pm 9.2 \text{ kJ}\cdot\text{mol}^{-1}$  mientras que la energía de activación de la reacción de isomerización de glucosa a fructosa fue  $111.5 \pm 9.1 \text{ kJ}\cdot\text{mol}^{-1}$ . Como puede observarse en la Figura 2, la cinética de formación de 5-HMF sufre un cambio drástico a 330°C. La energía de activación de esta reacción es de  $285 \pm 34 \text{ kJ}\cdot\text{mol}^{-1}$  y  $-61.3 \pm 15.7 \text{ kJ}\cdot\text{mol}^{-1}$  a temperaturas menores y mayores a

330°C respectivamente. Cuando se incorporó la concentración de agua como reactivo en el ajuste cinético de esta reacción ( $k_{hmf,w}$ ) se observó que el valor de la constante cinética no decrecía, sino que siguió aumentando con la temperatura aunque en menor medida. A temperaturas mayores a 330°C la reacción de formación de 5-HMF podría estar influenciada por la densidad y producto iónico del medio de reacción.

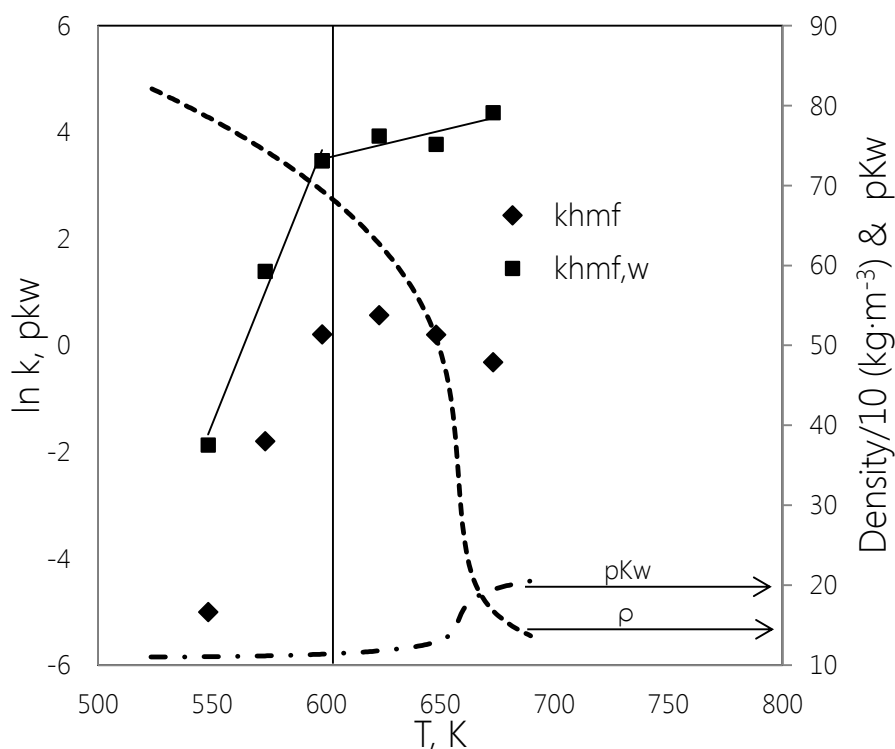
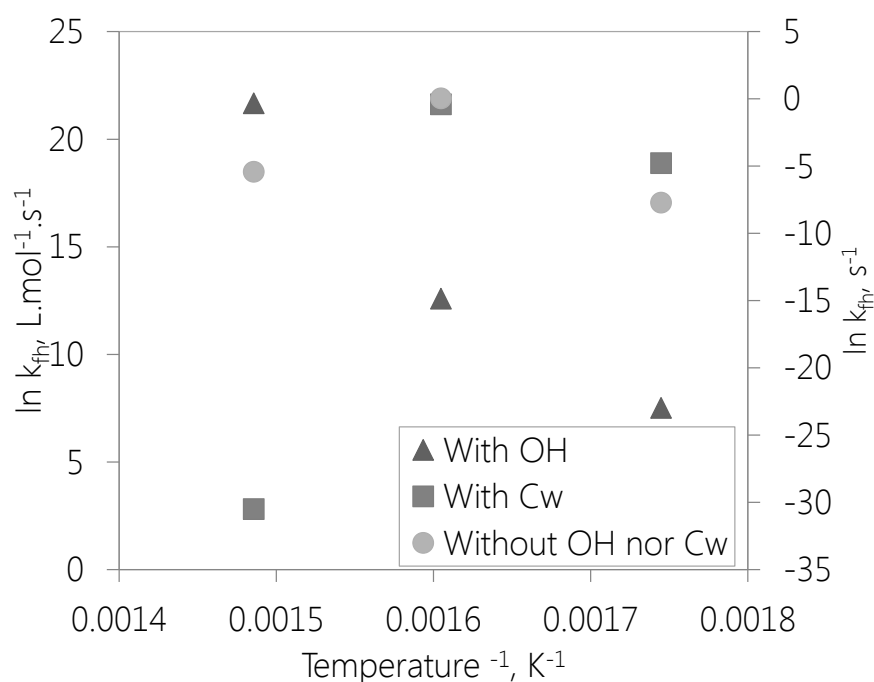


Fig. 2. Efecto de la temperatura sobre las cinéticas de producción de 5-HMF en agua presurizada. Variación de la densidad y el producto iónico del agua con la temperatura a 25 MPa.

En el **Capítulo 3**, "Tunable Selectivity on Cellulose Hydrolysis in Supercritical Water", se estudió el efecto del medio de reacción en la selectividad del proceso de hidrólisis. Se observó en los trabajos anteriores (Capítulos 2 y 3) que trabajando a tiempos de residencia bajos (0.02 s), la selectividad de azúcares solubles fue mayor al 98%  $w \cdot w^{-1}$  a una temperatura y presión de trabajo de 400°C y 23 MPa respectivamente. La concentración de 5-HMF en esas condiciones fue menor que 0.1%  $w \cdot w^{-1}$ . Cuando el tiempo de residencia fue aumentado hasta 1 s, la selectividad de glicolaldehído fue del 60%  $w \cdot w^{-1}$  a las mismas condiciones de presión y temperatura. El control del tiempo de residencia es clave en la producción selectiva de azúcares o glicolaldehído. En este Capítulo se experimentó el proceso de hidrólisis de celulosa a temperaturas entre 300°C y 400°C, presiones entre 10 y 27 MPa y tiempos de residencia entre 0.02 y 50 s. Se desarrolló un nuevo modelo cinético incluyendo una modificación del

presentado en el Capítulo 2. Se encontró que la concentración de iones hidroxilos y protones del medio de reacción debido a la disociación del agua en un parámetro clave en la selectividad del proceso. Como se puede observar en la Figura 3, la reacción de isomerización de glucosa a fructosa y su posterior deshidratación para producir 5-HMF son fuertemente dependientes de la concentración de iones en el medio (H/OH). Mediante un incremento del pH/pOH, se minimizan estas reacciones permitiendo controlar la formación de 5-HMF. En cambio, en estas condiciones se vieron favorecidas las reacciones de condensación retroaldólica sobre las reacciones de isomerización y deshidratación.



**Fig. 3.** Cinéticas de producción de 5-HMF en agua Sub- y Supercrítica (27 MPa). (▲) Corresponde al modelo resultado incluyendo la concentración de oxidrilos en el medio. (■) Corresponde al modelo resultado incluyendo la concentración del agua en el medio (densidad). (●) Corresponde al modelo resultado sin incluir la concentración del agua ni la concentración de oxidrilos en el medio.

En el **Capítulo 4**, "Pressure and Temperature Effect on Cellulose Hydrolysis Kinetic in Pressurized Water", se estudió el efecto de la temperatura y presión sobre las reacciones de hidrólisis de celulosa y glucosa en un medio hidrotermal. El proceso de hidrólisis de celulosa produjo oligosacáridos, celobiosa, glucosa y fructosa. En general, los perfiles de concentración fueron similares a distintas presiones y temperaturas. Sin embargo, los productos de hidrólisis de glucosa y fructosa se vieron fuertemente afectados por el cambio en la presión y la temperatura. La reacción de isomerización de glucosa a fructosa y la reacción de deshidratación de la fructosa para producir 5-HMF se inhiben cuando se incrementó la

temperatura. Por otro lado, la producción de 5-HMF se favorece a altas concentraciones de iones (H/OH) en el medio de reacción. Por lo tanto, a una temperatura constante, la producción de 5-HMF aumenta cuando aumenta de la densidad. La producción de glicolaldehído mediante la reacción de condensación retro-aldólica de la glucosa se ve beneficiada al incrementar la presión y la temperatura. Las constantes cinéticas de hidrólisis de celulosa fueron ajustadas utilizando los datos experimentales. La presión mostró no tener un efecto apreciable sobre las cinéticas de producción de azúcares. A temperaturas subcríticas, las cinéticas de hidrólisis de glucosa no mostraron cambios significativos cuando se aumenta la presión. Sin embargo, las reacciones de isomerización y deshidratación de glucosa fueron desfavorecidas mediante el incremento de la presión mientras que las reacciones de condensación retro-aldólica fueron beneficiadas (Figura 4).

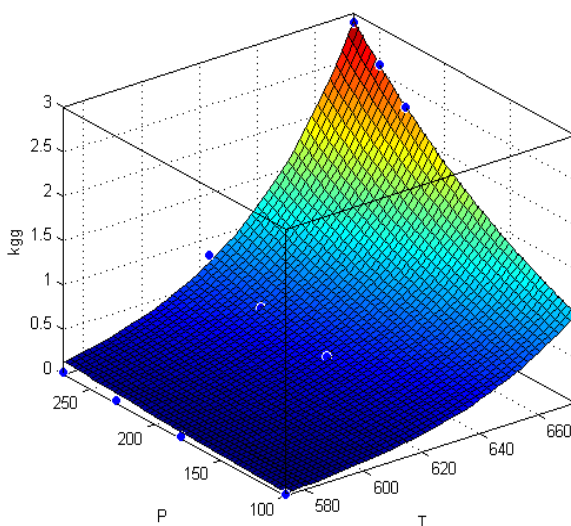


Fig. 4. Constante cinéticas ( $s^{-1}$ ) de la reacción de condensación retro-aldólica de la glucosa ( $k_{gg}$ ) a lo largo de la presión (bar) y temperatura (K).

En el **Capítulo 5**, "Selective Transformation of Fructose into Pyruvaldehyde in Supercritical Water. Reaction Pathway Development", se estudiaron las reacciones de fructosa en agua sub- y supercrítica. Para ello se realizaron experimentos a distintas temperaturas y utilizando aditivos en el medio de reacción para modificar sus propiedades (pH y secuestradores de radicales libres). Las reacciones se llevaron a cabo a temperaturas de 260°C, 330°C y 400°C a 23 MPa. Se modificó el pH del medio mediante el uso de ácido oxálico e hidróxido de sodio. Compuestos llamados *Scavengers* fueron utilizados como secuestradores de radicales libres para analizar su influencia en este tipo de reacciones (TEMPO y BHT). El producto principal

de la hidrólisis de fructosa fue el piruvaldehído (>80% w-w<sup>-1</sup>) a 400°C y 23 MPa en un tiempo de residencia de 0.7 s. Además las reacciones de fructosa fueron analizadas en combinación con glucosa. Como se muestra en la Figura 5, diferentes productos de la reacción de condensación retro-aldólica fueron obtenidos dependiendo del material que se hidrolice. La fructosa produjo principalmente compuestos de 3 carbonos (C-3, piruvaldehído) y la glucosa produjo compuestos de 2 carbonos (C-2, glicolaldehído). La isomerización de fructosa a glucosa resultó ser despreciable y por lo tanto la producción de compuestos C-2 cuando el material de partida es fructosa. Por otro lado, la producción de 5-HMF fue despreciable cuando el material de partida es glucosa.

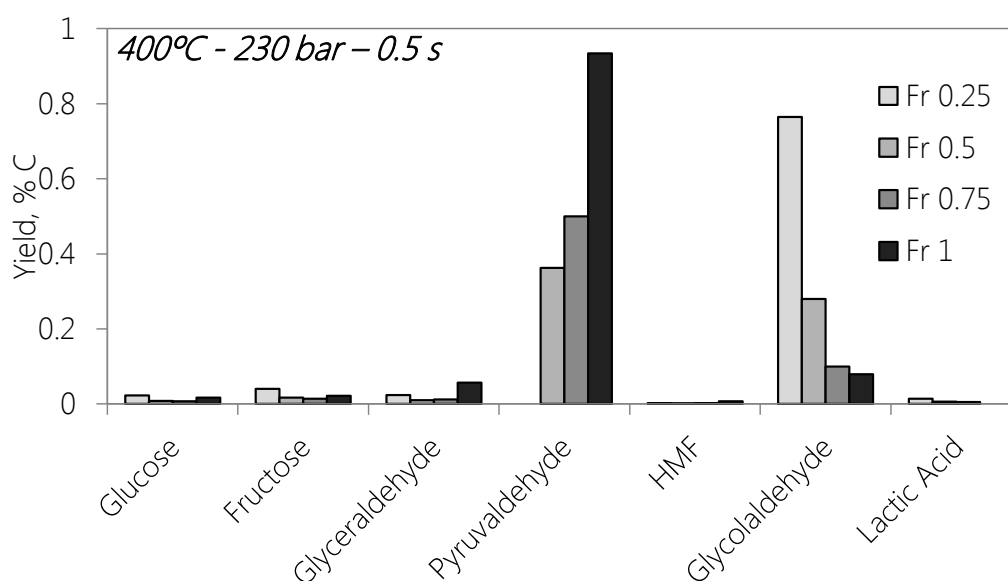


Fig. 5. Reacciones de hidrólisis de distintas mezclas de glucosa y fructosa a 400°C y 23 MPa.

En el **Capítulo 6**, "Transformation of Glucose in Added Value Compounds in Supercritical Water", se analizó la conversión de glucosa en compuestos de valor añadido utilizando como medio reacción el agua hidrotermal. Las reacciones de hidrólisis de glucosas fueron llevadas a cabo a temperaturas de 300°C, 350°C, 385°C y 400°C. La presión de los experimentos fue 23 y 27 MPa. Uno de los mayores productos de interés que se pueden obtener de la hidrólisis de glucosa es el ácido láctico. En las condiciones experimentadas no se ha logrado la producción de este compuesto. El compuesto principal de la hidrólisis de glucosa fue el glicolaldehído (80% w-w<sup>-1</sup>) a una temperatura y presión de trabajo de 400°C y 27 MPa respectivamente con un tiempo de residencia de 20 s. En la búsqueda de producción de ácido láctico se probaron hidróxido de sodio y agua oxigenada como aditivos al medio de reacción

(Tabla 1). La mayor concentración de ácido láctico fue lograda utilizando hidróxido de sodio (0.5 M) como catalizador a 27 MPa, 400°C y 20 s de tiempo de residencia. Se observó que el pH del medio es influyente en la selectividad del proceso. Un modelo del proceso cinético ha sido desarrollado con la finalidad de identificar los factores más influyentes en la selectividad.

**Tabla 1.** Diferentes catalizadores utilizados en la experimentación. La temperatura de los experimentos fue 400°C. NaOH se utilizó a una concentración de 0.5 M. NaOH\* se refiere a los experimentos en los cuales el hidróxido de sodio se alimentó en una corriente separada. H<sub>2</sub>O<sub>2</sub> fue utilizado en una concentración estequiométrica. <sup>a</sup> La biomasa fue glucosa. <sup>b</sup> La biomasa fue fructosa. <sup>c</sup> La biomasa fue celulosa.

Condiciones			Selectividad, % w·w <sup>-1</sup>		
P MPa	Tiempo de Residencia (s)	Catalizador	Glicolaldehído	Ácido Láctico	Ácido Acrílico
23	20.0 ±0.3	-	0.85	0	0.01
23	43.5±1.7	NaOH	0	0.08	0.03
27	12.1±0.1	H <sub>2</sub> O <sub>2</sub>	0.26	0	0.14
27	10.0±0.1	H <sub>2</sub> O <sub>2</sub>	0.2	0	0.01
27	10.2±0.1	H <sub>2</sub> O <sub>2</sub>	0.11	0	0.03
27	10.2±0.1	NaOH	0.09	0	0.02
27	40.1±0.5	NaOH	0	0.41	0.05
27	30.0±0.5	NaOH + H <sub>2</sub> O <sub>2</sub>	0	0.05	0.01
27	20.6 ±0.3	NaOH* <sup>a</sup>	0.1	0.54	0.05
27	22.2 ±0.3	NaOH* <sup>b</sup>	0.05	0.57	0.07
27	21.6 ±0.3	NaOH* <sup>c</sup>	0.43	0.48	0.03

En el **Capítulo 7**, "Simultaneous and Selective Recovery of Cellulose and Hemicellulose Fractions from Wheat Bran by Supercritical Water Hydrolysis", se estudió la conversión en un medio hidrotermal del salvado de trigo en oligosacáridos solubles, y monómeros de glucosa, xilosa y arabinosa. Las reacciones de hidrólisis se llevaron a cabo a una temperatura de 400°C, una presión de 25 MPa con tiempos de residencia entre 0.1 s y 0.7 s. el rendimiento del proceso fue evaluado para diferentes productos como C-6 (productos derivados de la hidrólisis de celulosa) y C-5 (sacáridos derivados de la hidrólisis de hemicelulosa). La producción de glicolaldehído y 5-HMF fue analizada como formación de subproductos. Operando en las mencionadas condiciones se logró una licuefacción de la biomasa en un

85% w·w<sup>-1</sup> en 0.3 s de tiempo de residencia. Los sólidos obtenidos del proceso de hidrólisis estaban compuestos por un 86% w·w<sup>-1</sup> de lignina. Como se puede observar en la Figura 6, la mayor recuperación de celulosa (C-6) y hemicelulosa (C-5) como azúcares (76% w·w<sup>-1</sup>) fue alcanzada a 0.19 s de tiempo de residencia. Un incremento en el tiempo de residencia resultó en una disminución en el rendimiento de recuperación de las fracciones C-6 y C-5. Una recuperación total de C-5 fue alcanzada a 0.19 s de tiempo de reacción, sin embargo, a mayores tiempos el rendimiento fue menor. Por otro lado, el mayor rendimiento de C-6 fue del 65% w·w<sup>-1</sup> a 0.22 s. El principal producto de hidrólisis de los compuestos C-6 y C-5 fue el glicolaldehído con un rendimiento del 20% w·w<sup>-1</sup> a 0.22 s de tiempo de residencia. La producción de 5-HMF fue altamente inhibida en las condiciones experimentadas obteniendo rendimientos menores al 0.5% w·w<sup>-1</sup>.

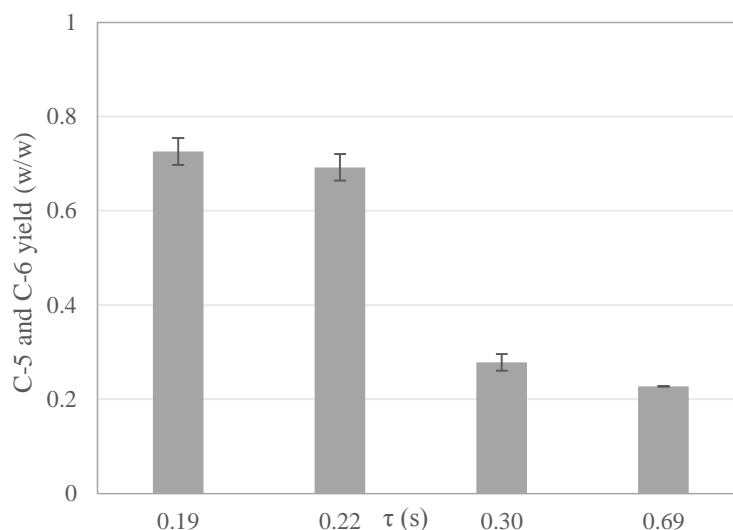


**Fig 6.** Rendimiento de hidrólisis de celulosa y hemicelulosa a lo largo del tiempo de residencia después de hidrólisis en agua supercrítica a 400°C y 25 MPa.

En el **Capítulo 8**, “On the Energetic Approach of Biomass Hydrolysis in Supercritical Water”, se estudiaron tres posibles alternativas para llevar a cabo la hidrólisis de biomasa en agua supercrítica de una manera energéticamente eficiente. El efluente del reactor de la etapa de hidrólisis presentado en el Capítulo 1 (Hidrólisis de celulosa, glucosa, fructosa o biomasa) se puede despresurizar formando una corriente de vapor que permite ser integrada energéticamente en el proceso. En este Capítulo se estudió la integración del proceso de hidrólisis de biomasa con los esquemas comerciales de plantas combinadas de producción de calor y potencia (CHP), prestando especial atención a la corriente de salida del reactor. La temperatura de los gases de salida del proceso CHP con una temperatura aproximada a

500°C y el trabajo producido en el proceso presentan unas adecuadas posibilidades de integración energética para el precalentamiento y compresión. Se analizaron 3 diferentes opciones: (a) Hidrólisis de biomasa + Turbina de gas con inyección de vapor; (b) Hidrólisis de biomasa + Turbina de gas sin inyección de vapor; (c) Hidrólisis de biomasa + calor disponible por un quemador de biomasa. Los requerimientos de calor y la concentración en azúcares del producto obtenido para las tres opciones se muestran en la Tabla 2. La integración del proceso de hidrólisis de biomasa con los procesos CHP permite la obtención de azúcares de manera selectiva sin requerimientos de calor. El amplio rango disponible de turbinas de gas permite un escalado flexible del proceso.

**Table 6.** Requerimiento de calor y concentración de azúcares en la corriente de salida de las diferentes alternativas energéticas analizadas.

<i>Proceso</i>	Requerimiento de Calor / kg producto (kW·kg <sup>-1</sup> )	Concentración Azúcares (w·w <sup>-1</sup> ) corriente salida
<i>Turbina de Gas &amp; Inyección de vapor</i>	0	0.39
<i>Turbina de Gas sin Inyección de vapor</i>	0	0.42
<i>Quemador de biomasa</i>	13	0.45

Las **CONCLUSIONES GENERALES** de esta tesis doctoral se presentan a continuación. Las conclusiones específicas de cada objetivo de la investigación realizada están presentes en las conclusiones de cada capítulo.

El proceso de hidrólisis de celulosa fue estudiado en un medio hidrotermal. Un nuevo concepto de reactor para reacciones en agua supercrítica fue desarrollado. El dispositivo experimental utilizado es capaz de operar hasta temperaturas de 425°C, presiones de 30 MPa con tiempos de residencia de entre 0.004 s y 50 s. El método desarrollado para iniciar y terminar las reacciones se consigue mediante la aplicación de cambios instantáneos en la temperatura de la corriente de biomasa, obteniendo así un reactor isotérmico. En este tipo de reactores es fácil determinar el tiempo de residencia de los reactivos en el reactor, lo cual conducirá a resultados precisos. La operación en continuo de los reactores mostró ser adecuada para la hidrólisis de biomasa. La selectividad en las reacciones lograda en esta Tesis Doctoral fue mayor a la presentada en bibliografía para reactores batch y semi-continuos.

La hidrólisis de celulosa fue estudiada a temperaturas entre 275°C y 400°C y presiones entre 10 MPa y 27 MPa. Se observó que las cinéticas de hidrólisis de celulosa son mucho más rápidas que las reacciones de hidrólisis de glucosa. Esta diferencia se acentúa a temperaturas por encima del punto crítico del agua, de todas formas, ambas reacciones son muy rápidas. De este fenómeno puede obtenerse beneficio si se aplica un adecuado control del tiempo de residencia. Una conversión total de celulosa puede alcanzarse a 400°C y 25 MPa en 0.013 s de tiempo de residencia. Si las reacciones de hidrólisis son detenidas en tiempos de residencia entre 0.013 s y 0.03 s el rendimiento en azúcares solubles será mayor al 98% w·w<sup>-1</sup>. El efecto de la presión sobre las reacciones de hidrólisis de celulosa son menores que el efecto de la temperatura y el tiempo de residencia. Sin embargo, la presión juega un importante rol en la composición de los productos de hidrólisis. Un incremento en la presión producirá azúcares de mayor peso molecular.

La variación de la temperatura y la presión permiten modificar las propiedades químicas y físicas del agua y por lo tanto del medio de reacción. Las principales propiedades que afectan las cinéticas del proceso son la densidad y el producto iónico. Se observó que la concentración de oxidrilos en el medio es un factor decisivo en las reacciones de transformación glucosa. A bajas concentraciones de iones, las reacciones de isomerización de glucosa a fructosa y de deshidratación de fructosa son desfavorecidas mientras se potencian las reacciones de condensación retro-aldólica.

Las cinéticas de hidrólisis de celulosa, glucosa y fructosa fueron estudiadas y se presentan los parámetros de la ecuación de Arrhenius para cada una de ellas. Además, las cinéticas fueron analizadas a distintas presiones obteniendo los volúmenes de activación.

Se han estudiado las reacciones de hidrólisis de glucosa y fructosa y se han desarrollado los principales caminos de reacción. En primer lugar, se encontró que el principal tipo de reacción en agua supercrítica es la condensación retro-aldólica. Esta reacción produce moléculas de dos carbonos o tres carbonos cuando se hidroliza la fructosa o glucosa respectivamente. El producto principal de la hidrólisis de glucosa es el glicolaldehído (>80% w·w<sup>-1</sup>) en las siguientes condiciones: 400°C, 27 MPa y 20 s de tiempo de residencia. Por otro lado, cuando la fructosa fue hidrolizada a las mismas condiciones, el producto principal fue el piruvaldehído. Las reacciones de hidrólisis de mezclas de glucosa y fructosa producen una combinación de glicolaldehído y piruvaldehído como productos.

El efecto de utilizar catalizadores homogéneos fue analizado para la conversión de glucosa. Se observó que el hidróxido de sodio favorece la reacción de isomerización de glucosa a fructosa así como también la conversión de piruvaldehído en ácido láctico.

Se ha estudiado el funcionamiento del reactor desarrollado con biomasa vegetal natural, el salvado de trigo. Se observó que el dispositivo experimental construido en esta Tesis Doctoral es capaz de recuperar el 76%  $w \cdot w^{-1}$  de los azúcares presentes en la materia prima en un tiempo de residencia de 0.19 s. Los sólidos obtenidos en la hidrólisis están compuestos por un 85%  $w \cdot w^{-1}$  de lignina en forma de material poroso.

Por último se han estudiado distintas alternativas energéticas para llevar a cabo el proceso de hidrólisis de biomasa en agua supercrítica. Se ha determinado mediante el cálculo termodinámico del proceso que, el proceso de hidrólisis de biomasa puede llevarse a cabo sin requerimientos extras de calor o trabajo si el proceso se integra con una planta combinada de producción de calor y potencia. Además, el proceso de hidrólisis produce una corriente vapor que puede ser utilizada para mejorar el rendimiento de las turbinas de gas utilizadas en los procesos de ciclo combinado de generación de calor y potencia.

#### *Trabajo Futuro*

De los estudios desarrollados en esta Tesis doctoral, se puede concluir que el campo de investigación de conversión de biomasa en agua supercrítica es un área con numerosos temas de estudio que deben ser desarrollados y optimizados. En los párrafos siguientes se presentan los principales temas a estudiar en el refinado de biomasa.

Se observó que la operación en continuo de los reactores hace posible la reducción de los volúmenes de reactor. Además, el control del proceso es mejor que en los reactores semi-continuos o discontinuos. Sin embargo, la manipulación de los sólidos de entrada y salida del reactor son dos puntos muy importantes que deben ser estudiados. El bombeo de sólidos puede lograrse satisfactoriamente en el escalado del proceso. Sin embargo, en escala laboratorio es importante desarrollar un sistema de bombeo capaz de impulsar suspensiones concentradas. Por otro lado, la separación de los sólidos que no han reaccionado debería llevarse a cabo antes de la salida del reactor en tiempos extremadamente bajos para evitar degradación de los productos. La temperatura y el tiempo de residencia obtenidos en esta

Tesis Doctoral para la hidrólisis de celulosa hacen necesario el desarrollo de un equipo capaz de ser un reactor y separador a la vez, con un tiempo de residencia cercano a 0.1 s.

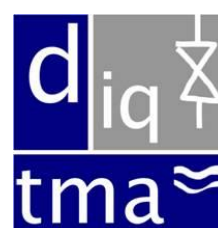
Para la producción de ácido láctico, sería interesante desarrollar un catalizador selectivo capaz de mejorar la reacción de conversión de glucosa en uno de los isómeros ópticos activos del ácido láctico (L+).

# Anexo

Manual de prevención de riesgos y operación en planta de hidrólisis de biomasa en agua presurizada.



GRUPO DE PROCESOS A ALTA PRESIÓN.  
DEPARTAMENTO DE INGENIERÍA QUÍMICA Y  
TECNOLOGÍA DEL MEDIOAMBIENTE  
UNIVERSIDAD DE VALLADOLID



---

## Universidad de Valladolid

MANUAL DE PREVENCIÓN DE RIESGOS Y  
OPERACIÓN EN PLANTA DE HIDRÓLISIS DE BIOMASA  
EN AGUA PRESURIZADA.

RESPONSABLE,



María José Cocero Alonso  
Catedrática del Departamento de  
Ingeniería Química y Tecnología del Medioambiente

**Universidad de Valladolid**

Personas que han leído y comprendido el manual previo a operar en la planta piloto de hidrólisis de biomasa;

NOMBRE	FECHA	FIRMA

## 1. INTRODUCCIÓN

La planta de hidrólisis de biomasa en agua presurizada a alta temperatura, situada en las instalaciones de la Escuela de Ingenierías Industriales sede Doctor Mergelina en el Departamento de Ingeniería Química y Tecnología del medioambiente, está diseñada para experimentar en las reacciones de hidrólisis y descomposición de material celulósico a partir de distintas materias primas en un medio de agua subcrítica o supercrítica. Las condiciones de alta presión y temperatura en las que se trabaja junto con las sustancias que se pretenden tratar son los principales riesgos con los que se puede encontrar un operario que trabaje en la instalación.

## 2. DIAGRAMA DE FLUJO Y DESCRIPCIÓN DE LA PLANTA

Esta planta, que opera en continuo y tiene una capacidad de tratamiento de hasta 3,6 kg/día de material celulósico seco, ha sido diseñada para trabajar a presiones de hasta 30 MPa y temperaturas de reactor 425°C.

La planta de hidrólisis se divide en cuatro zonas, la zona de presurización, la zona de calentamiento, la zona de reacción y la zona de enfriamiento de los productos como se muestra en la figura 2.1.

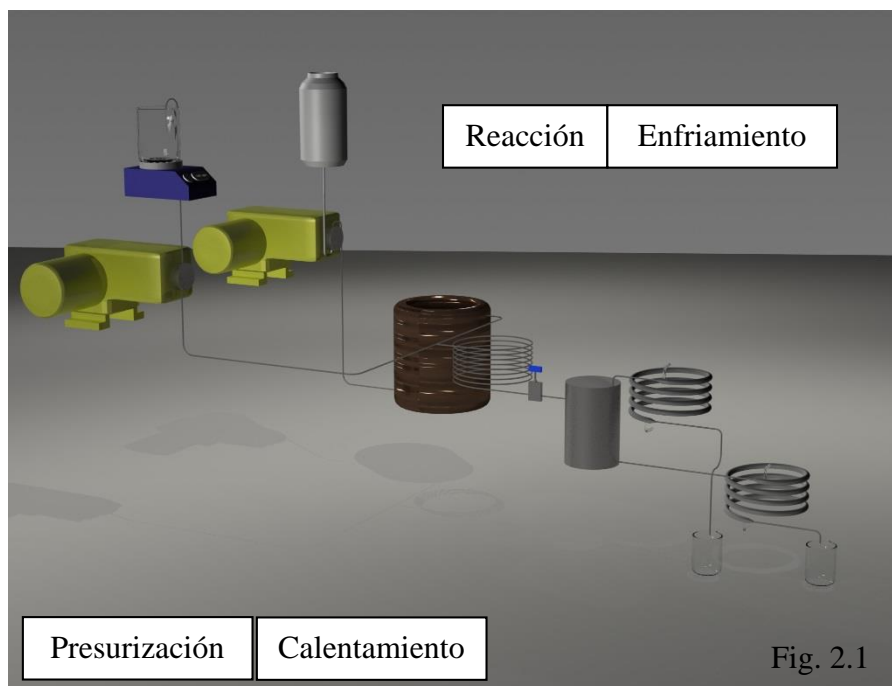
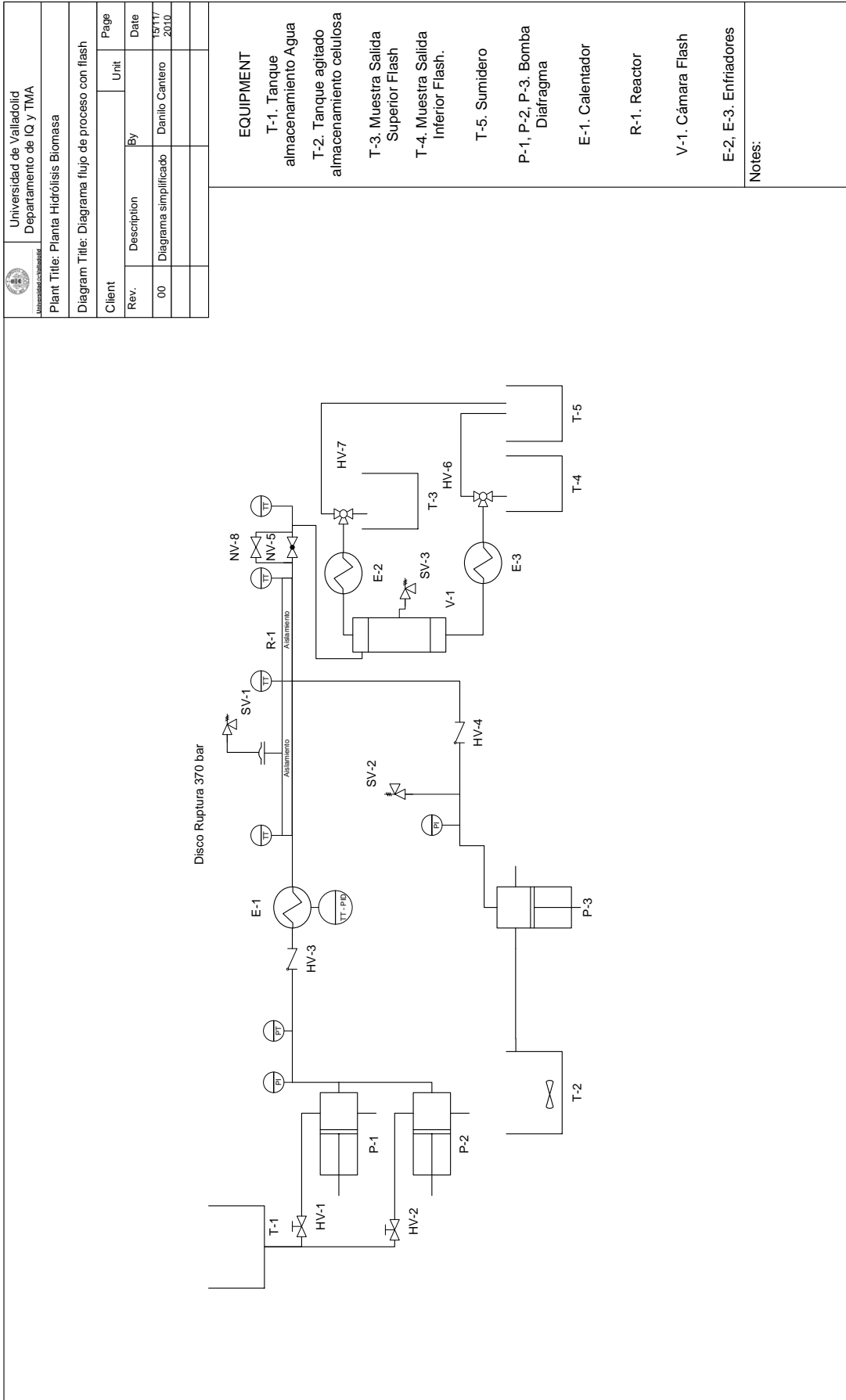


Figura 2.1. Esquema de la planta. Etapas de Presurización, Calentamiento, Reacción y enfriamiento.

En la figura 2.2 se muestra el diagrama de flujo del proceso con una cámara de flash. En la figura 2.3 se muestra el diagrama de flujo de proceso sin cámara de flash. En la figura 2.4 se muestra una imagen de la planta construida. Por la parte frontal se tiene acceso al manejo y control del proceso. Las etapas de elevada presión (250 bar) y temperatura (400°C) se encuentran dentro de un "bunker" y solo se tiene acceso por la parte posterior de la planta con el fin de evitar el contacto directo entre el operario y esta zona.



EQUIPMENT
T-1. Tanque almacenamiento Agua
T-2. Tanque agitado almacenamiento celulosa
T-3. Muestra Salida Superior Flash
T-4. Muestra Salida Inferior Flash.
T-5. Sumidero
P-1, P-2, P-3. Bomba Diafragma
E-1. Calentador
R-1. Reactor
V-1. Cámara Flash
E-2, E-3. Enfriadores

Notes:

Figura 2.2. Diagrama de flujo simplificado. Instalación con cámara de flash





Figura 2.4. Imagen de la planta construida. Sector de manejo y control y sector posterior de acceso a la zona de presión y temperatura.

### 2.1. Descripción del funcionamiento de la planta

La celulosa es un sólido cristalino que no se disuelve en agua a temperatura ambiente, puede mantenerse en suspensión mediante agitación. La suspensión se prepara al 10% p/p y se mantiene agitada mediante un agitador magnético en el tanque T-2 que tiene una capacidad de 3 litros. El agitador cuenta además con una plancha calefactora. La suspensión se calienta hasta 45°C y esta temperatura se mantiene con un termostato del agitador magnético. Desde el tanque T-2 se realiza la impulsión de la suspensión al interior del reactor con la bomba P-3, la cual tiene un flujo máximo de 1,5 L/h. el control del flujo se realiza desde la misma bomba.

El flujo de celulosa llega a temperatura de reacción a la entrada del reactor por inyección de vapor en una unión T. El vapor se genera con el calentador E-1 hasta una temperatura de 550°C. Este calentador es un sistema eléctrico formado por un conjunto de 4 resistencias de 2500 W de potencia cada una, insertadas en un cilindro metálico que lleva enrollado en espiral 6 metros de tubo de Inconel® 625. El dispositivo está aislado y dispone de un termopar en el interior del bloque macizo central para caracterizarlo y controlarlo mediante un termostato. A la salida del equipo hay otro termopar conectado a la tubería del vapor mediante una T, lo que permite determinar la temperatura de salida del vapor del calentador. El calentador es

alimentado por las bombas P-1 y P-2 con una capacidad máxima de 5 L/h cada una. El flujo de estas bombas se fija mediante su carrera, existiendo curvas de calibrado realizadas a la presión de operación que se incluyen en el suplemento 3. En el tanque T-1 se almacena agua destilada que se utiliza para la generación de vapor.

El reactor con el que se opera es tubular y su longitud variará según el experimento que se desee realizar para lograr distintos tiempos de residencia. La longitud del reactor puede variar desde 0,1 – 6 metros. El reactor es de Inconel® 625 y se encuentra aislado con lana de roca para disminuir la pérdida de calor.

El sistema de enfriamiento es un punto importante de la planta debido a que la reacción de hidrólisis y descomposición ocurre a velocidad alta a temperaturas mayores de 250°C. El fin de la reacción se realiza mediante un enfriamiento de la corriente de salida del reactor por descompresión súbita mediante la válvula NV-5. El flujo a la salida de la válvula tiene una temperatura de  $100 \pm 10$  °C suficiente para considerar que las reacciones han sido frenadas. En el caso de la disposición con flash (figura 2.1) la válvula NV-5 está conectada a una cámara flash V-1 en el cual se separan la fase vapor de la fase líquida las cuales se acondicionan hasta temperatura ambiente mediante los enfriadores E-2 y E-3. En el caso de la disposición sin flash (figura 2.2) la corriente de salida de la válvula se conecta al enfriador E-2 el cual acondiciona el flujo hasta temperatura ambiente.

El enfriador E-2 es de tubos concéntricos de cobre, en los que por la sección anular circula agua corriente de refrigeración y por la sección interior la corriente a refrigerar. El enfriador E-3 es de análoga disposición pero el tubo interno es de Inconel® 625 de diámetro y el tubo externo es de acero inoxidable AISI 316.

La hoja de especificaciones de los principales equipos de la planta se encuentra en el SUPLEMENTO II.

### 3. OPERACIÓN EN PLANTA DE HIDRÓLISIS DE BIOMASA

#### 3.1. Personal de trabajo en la planta

La planta de hidrólisis requiere de un mínimo de un operario para su manejo. El operario debe controlar de forma manual la presión del sistema mediante la válvula NV-5, el nivel de los tanques T-1 y T-2 y la toma de muestras.

#### 3.2. Funciones a realizar durante la operación

En la operación de la planta pueden distinguirse algunas de las funciones siguientes.

Planificación de la experiencia

Objetivos de la misma.

Cambios a realizar durante la operación en las distintas variables.

Estimación de la cantidad de suspensión a utilizar en función de los flujos y tiempos de residencia que se deseen experimentar y los objetivos que se persigan.

Puesta en marcha de la planta siguiendo el protocolo de arranque que está descrito en el siguiente apartado.

Seguimiento y control de las variables de operación e introducción de medidas correctoras en las variables de actuación de la planta. Estas variables son los flujos de alimentación de vapor, flujo de suspensión que entran al reactor y la presión del sistema.

Toma de muestras.

Parada de la forma en que se detalla en el protocolo de parada de la planta

### 3.3. Equipos de protección personal necesarios (EPIS)

Durante la operación de la planta será necesario que los operarios usen diferentes equipos de protección individual (EPIS), tal como figura en la Tabla 3.1.

Tabla 3.1. EPIS que se deben utilizar

GAFAS	Uso durante la operación. Imprescindible toma de muestras.
MASCARILLAS ESPECÍFICAS PARA TÓXICOS	Uso de mascarilla para sustancias en polvo: Al preparar o cargar la suspensión de celulosa. Manipulación lana de vidrio.
GUANTES	<b>Latex</b> Al preparar o cargar la suspensión de celulosa. En la manipulación de la lana de vidrio. <b>Piel flor vacuno natura 406vrw/t10</b> En la actuación sobre la válvula NV-5.
BATA	Durante la operación. Manipulación lana de vidrio (ropa desechable).

### 3.4. Especificaciones del equipo de trabajo

Antes de poner en marcha la instalación los responsables de la misma durante el periodo de funcionamiento deberán comprobar que todos los equipos se encuentran en correcto estado. Los equipos y sus variables a controlar se muestran en la tabla 3.2.

Tabla 3.2. Verificación previa del estado de la planta

COMPROBACIONES PREVIAS DE LOS EQUIPOS DE LA PLANTA					
<b>LÍNEA DE ALIMENTACIÓN</b>					
TANQUE ALIMENTACIÓN T-1	DE	Verificar el nivel de agua destilada	Verificar el estado de las válvulas	Observar la posible existencia de fugas	Comprobar el correcto funcionamiento y cebado de las bombas
TANQUE ALIMENTACIÓN T-2	DE	Verificar el correcto preparado de la suspensión de celulosa	Verificar el nivel de suspensión de celulosa	Comprobar que el agitador esté funcionando (agitación y calentamiento)	Comprobar el correcto funcionamiento y cebado de las bombas
BOMBAS		Verificar que se encuentran abiertas las válvulas de impulsión y aspiración	Verificar que el caudal configurado sea el deseado		Verificar que se encuentra cebada
<b>LÍNEA DE CALENTAMIENTO</b>					
CALENTADOR E-1		Comprobar el funcionamiento de las resistencias	Comprobar el funcionamiento del controlador de temperatura del calentador y de la temperatura de flujo de vapor		Observar el correcto estado de todas las conexiones y juntas
<b>LÍNEA DE DE SALIDA</b>					
VÁLVULA NV-5		Verificar estado. Verificar que no existan taponamientos	Comenzar en posición abierto 100%		Observar posibles fugas.
VÁLVULA NV-8		Verificar estado. Verificar que no existan taponamientos			Observar posibles fugas.
<b>REFRIGERACIÓN</b>					
ENFRIADOR E-2		Prestar atención a posibles fugas.		Verificar que este circulando el agua de refrigeración.	
ENFRIADOR E-3		Prestar atención a posibles fugas.		Verificar que este circulando el agua de refrigeración.	
TOMA MUESTRA		Verificar estado y si existen taponamientos en válvulas HV-6 y HV-7.		Verificar que los dos conductos de salida de las válvulas HV-6 y HV-7 están limpios.	

#### 4. PROTOCOLOS DE ARRANQUE Y PARADA DE LA PLANTA

##### 4.1. Protocolo de arranque planta de hidrólisis de biomasa.

El protocolo de arranque se muestra en la tabla 4.1.

Tabla 4.1. Protocolo de arranque

SECUENCIAS DE ACCIONES PARA LA PUESTA EN MARCHA DE LA PLANTA	Check
<b>ENCENDIDO DE LOS PRECALENTADORES</b>	
Encender el sistema de ventilación, en el laboratorio anexo.	
Encendido de las resistencias del precalentador de la alimentación 30 minutos antes de la puesta en marcha. Temperatura deseada para el arranque (T=450°C).	
<b>PREPARAR LA ALIMENTACIÓN DE BIOMASA</b>	
Elegir la concentración con la que se desea trabajar.	
Calcular la masa de biomasa y agua necesaria para el volumen de suspensión a tratar.	
Agregar un 30% del agua necesaria en el tanque T-1.	

Insertar la sonda de medida de temperatura del termostato del la plancha calefactora en el seno del líquido.	
Encender agitación y plancha calefactora con una temperatura objetivo de 45°C.	
Incorporar en fracciones la mitad de la masa de celulosa necesaria en el tanque T-1.	
Incorporar un 40% del agua necesaria en el tanque T-1.	
Incorporar en fracciones la masa de celulosa restante en el tanque T-1.	
Incorporar el agua restante en el tanque T-1.	
Aguardar que se alcance la temperatura objetivos.	
<b>ENCENDIDO DE LOS ENFRIADORES</b>	
Abrir las válvulas de circulación de agua de refrigeración en los enfriadores E-2 o E-a y E-3 según sea el caso	
<b>COMPROBAR ALIMENTACIONES</b>	
Comprobar que haya agua suficiente para la operación en el tanque T-2.	
Comprobar posición de las válvulas HV-1 y HV-2 según las bombas que se utilicen. (Que estén abiertas).	
Comprobar que la temperatura de la suspensión de celulosa es igual a la temperatura objetivo.	
<b>INICIO OPERACIÓN</b>	
Encender el ordenador y abrir el programa de adquisición de datos Picolog recorder. Crear un archivo para guardar los datos del experimento. Comenzar la toma de datos de presión y temperatura. Una serie de datos cada segundo. Detalles del programa en suplemento 4.	
Colocar en la posición sumidero las válvulas de selección HV-6 y HV-7.	
Cerrar laválvula NV-8 y abrir la válvula NV-5.	
Comenzar el bombeo con las bombas P-1 y P-2.	
Cerrar gradualmente la válvula NV-5 para que la presión del sistema comience a subir. Alcanzar una presión de 150 bares.	
Iniciar la impulsión con la bomba P-3.	
Mediante el accionamiento gradual de la válvula alcanzar la presión de trabajo lentamente.	
<b>REACCIÓN EN ESTADO ESTACIONARIO</b>	
Una vez alcanzada la estabilidad de las variables de temperatura y presión del sistema, dejar el sistema estable por 1 hora.	
Tomar muestras de 100 mL de cada una de las salidas de la planta accionando las válvulas HV-6 y HV-7. Tomar el tiempo en que se recogen los 100 mL. Tomar 3 muestras de cada estado estacionario cada 10 minutos.	

#### 4.2. Protocolo de parada y limpieza

El protocolo de parada y limpieza se muestra en la tabla 4.2.

Tabla 4.2. Protocolo de parada y limpieza.

Desconectar resistencias del calentador.	
Cambiar la alimentación de la bomba P-3 por agua destilada. Desconectar el agitador. NUNCA PARAR LA BOMBA CON LA TUBERÍA DE IMPULSIÓN LLENA DE SUSPENSIÓN DE CELULOSA.	

Descomprimir el sistema lentamente abriendo válvula NV-5. Cuando P=50 bar mantener esta presión durante 30 minutos para enfriamiento y limpieza del sistema.	
Verificar temperaturas en calentador, reactor y tuberías	
Verificar que la salida de los productos es cristalina. En caso contrario continuar pasando agua destilada para la limpieza.	
Desconexión de las bombas P-1 y P-2. Descompresión hasta presión atmosférica mediante válvula NV-5.	
Verificar que la temperatura en el reactor sea menor a 50°C.	
Cambiar la alimentación de la bomba P-3 por acetona. Impulsar 250 mL de acetona a un caudal de 10 ml/min con P-3.	
Cambiar la alimentación de P-3 por agua destilada. Impulsar 2 litros de agua destilada a flujo máximo.	
Desconectar la bomba P-3.	
Abrir válvulas NV-5 y NV-8 totalmente.	
Desconectar la circulación de agua de refrigeración.	
Desconectar el sistema de ventilación.	

## 5. ÁRBOL DE FALLOS

El árbol de fallos se muestra en la tabla 5.1.

Tabla 5.1. Árbol de fallos.

POSIBLE FALLO	ACTUACIÓN
No hay cambio en la presión del sistema cuando se acciona la válvula de descompresión NV-5.	Detener la planta (Según 4.2) y descomprimir abriendo lentamente la válvula de seguridad NV-8. Revisar el estado de la válvula NV-5.
No se consigue hacer bajar la presión abriendo la válvula de descompresión.	Tratar de controlar la presión con la válvula de seguridad NV-8. Si es imposible mantener el control, detener la planta (según 4.2), y descomprimir.
La temperatura sube por encima de los 500°C de forma incontrolada	Detener la planta, según 4.2
La temperatura de salida de los enfriadores es muy alta	Comprobar circuito de refrigeración. Comprobar que hay suficiente circulación de agua de refrigeración por los cambiadores de calor. Si es posible aumentar el flujo de agua de refrigeración. En el caso de que esta se haya cortado, detener la planta según 4.2
Problemas de taponamiento en la bomba de impulsión de biomasa.	Detener la impulsión de la bomba P-3. Limpiar la válvula de admisión de la bomba y el tubo de conexión entre T-2 y P-3. Recomenzar el bombeo con P-3. En caso de continuar sin impulsar, descomprimir y limpiar la válvula de salida de la bomba P-3.
Se rompe el disco de ruptura.	Detener la planta según 4.2. Esperar que el sistema adquiera temperatura ambiente. Cambiar el disco de ruptura y buscar el problema de sobrepresión.
Tapones en las tuberías	Aumenta la presión, abrir la válvula de descompresión. Detener las bombas. En caso necesario cambiar el tramo de tubería afectado.
Mal funcionamiento de las válvulas antirretorno.	Cambiarlas

## 6. SEGURIDAD EN EL MANTENIMIENTO DE LA PLANTA

### 6.1 Pruebas que se realizarán en la instalación

Durante la vida útil de la instalación, se realizarán pruebas así como un registro y documentación de las comprobaciones que se realicen.

Estas pruebas se realizarán:

- Tras la instalación y antes de la puesta en marcha.
- Después de cada montaje o cambio de lugar de emplazamiento.
- Periódicamente, conforme a las instrucciones de mantenimiento.
- Tras una transformación de algún tipo o accidentes.
- Después de un largo periodo de no uso.
- Cuando se cambia de reactor.

#### Prueba de presión

Todos los equipos de presión (reactor, cambiadores y enfriadores) se probarán al terminar su montaje o modificaciones, para verificar la no existencia de fugas. Estas pruebas se realizarán con agua fría, nunca en caliente. Para ello se aislará la parte del circuito que se quiere probar retirando los dispositivos de seguridad susceptible de abrirse o resultar dañados (válvulas de alivio, discos de ruptura) y el aislante cuando impida ver las zonas susceptibles de haber fuga. A continuación se da presión hasta alcanzar una presión de 1,5 veces la presión de diseño (si ha de utilizarse empleando las bombas de la instalación,  $P_{max}=300$  bar). No habrá fugas si la presión se mantiene constante durante un periodo de tiempo. En el caso de que no sea posible aislar una parte del circuito sin que se produzcan fugas por elementos de la planta como válvulas o pistones de las bombas, se verificará que el equipo pasa la prueba de presión haciendo circular agua a la presión mencionada y mediante la inspección visual buscando fugas de agua.

Se comprueba el estado de los cierres de la bomba observando la lectura del manómetro instalado y comprobando las oscilaciones de la aguja. Ésta ha de mantenerse estable en torno a la presión de trabajo. Cuando estas oscilaciones se mantengan en un nivel razonable cerca de la presión que marca el otro manómetro será señal de buen funcionamiento. De lo contrario si estas son muy pronunciadas puede ser señal de que existe un problema de cierre en las válvulas antirretorno.

Periódicamente se revisarán los racores prestando especial atención a aquellos que se han manipulado recientemente. Estas revisiones nunca se realizarán en caliente.

## 6.2. Protocolo de limpieza de la planta

Comprobar que no hay presión en la línea. Comprobar que las válvulas de descompresión estén abiertas y los manómetros no marquen presión.

Verificar que la temperatura en el reactor sea menor a 50°C.

Cambiar la alimentación de la bomba P-3 por acetona. Impulsar 250 mL de acetona a un caudal de 10 ml/min con P-3.

Cambiar la alimentación de P-3 por agua destilada. Impulsar 2 litros de agua destilada a flujo máximo.

Desconectar la bomba P-3.

Abrir válvulas NV-5 y NV-8 totalmente.

Desconectar la circulación de agua de refrigeración.

Finalizado de la operación.

Dejar las bombas apagadas.

Volver todas las válvulas a su posición inicial. Abrir las válvulas de descompresión.

## 6.3. Manipulación del aislamiento de lana de vidrio

La lana de vidrio y de roca es un producto de forma similar al amianto que se emplea como aislamiento del reactor, los calentadores y las tuberías, y está clasificado como cancerígeno. Normalmente se encuentra cubierto por papel de aluminio y no se desmonta frecuentemente.

Debe evitarse la dispersión de fibras al ambiente, por lo que no se deberá realizar ningún tipo de trabajo mediante herramienta de giro: radial, taladro o similar. Si se precisa cortarlo se deben emplear sistemas mediante cizalla como tijeras o similar que no produzcan dispersión de fibras.

Para su manipulación conviene:

Emplear material de protección de vías respiratorias compuesto por mascarilla auto filtrante FFP3 (según EN-149), o máscara tipo filtro tipo P3 según EN-420.

Emplear guantes para evitar el contacto con la piel de forma directa y ropa de trabajo desechable preferentemente.

Empleo de pantalla facial o gafas cerradas.

La eliminación de la sustancia si fuera necesaria se realizará según reglamentación vigente.

El trabajo con esta sustancia hace conveniente la aplicación de lo dispuesto en el R.D. 665/97 sobre sustancias cancerígenas.

#### 6.4. Instalación de tuberías

Las conducciones del agua son de 1/4" de acero inoxidable 316, norma ASTM A-249, con espesor de pared de 0.049", excepto en los casos donde la temperatura sea alta (calentadores). Cuando la tubería va a estar a más de 400° C se emplea tubo de inconel 625 de diámetro 1/4" y 0,09 mm de espesor.

Los racores, válvulas de regulación, válvulas de seguridad, están fabricados en acero inoxidable 316 norma ASTM A-213. Los cierres se realizan por uniones con conos, contraconos y tuerca de presión.

Para la instalación de tuberías estas se cortan empleando un cortatubos. Hay que prestar especial atención a los bordes interiores y exteriores del tubo, avenallandolos si es necesario. Se unen empleando las uniones de cono y contracono. Para ello en primer lugar se introduce la tuerca seguida del contracono y el cono. Se rosca a mano hasta que se pueda y después se hace una marca en la tuerca y en la unión con un rotulador indeleble, y se gira sujetando con dos llaves o llaves inglesas 1 vuelta y 1/4 de vuelta en el caso de los racores de 1/4" y 3/4 de vuelta en el caso de los de 1/8". Hay que asegurarse que la tubería no se desplace hacia fuera al apretar. A continuación se suelta la tuerca para verificar que el cono y contracono estén correctamente fijados.

Se debe comprobar antes de unir un racor que la rosca está limpia por ambos lados.

Si es necesario realizar algún cambio en la red de tuberías asegurarse que la tubería está fría y sin presión antes de soltar ningún racor. Es recomendable utilizar guantes al apretar los racores y gafas de seguridad anti-impacto al soltar una tubería que pudiese contener presión.

#### 6.5. Discos de ruptura

Estos sistemas constan de un disco de Niquel y Cromo principalmente tarado a una presión, por encima de la cual este disco rompe y habilita una salida para el fluido contenido. El modo correcto de instalarlos es en serie con una válvula de alivio y tarado a una presión ligeramente superior a la de la válvula. El objetivo de esta disposición es dar una opción de salida primero al fluido hacia una zona de escape controlada.

Los discos utilizados son de la casa Autoclave engineer (P-7321-CE) y rompen en un rango de presión de 334,9 y 365,42 barg. Han sido tarados a 22°C pero funcionan bien hasta temperaturas de hasta 427°C a partir de aquí, la presión que pueden aguantar disminuye.

En esta instalación existe un disco de ruptura en la corriente de vapor. Con esta disposición se protege a la instalación de posibles subidas bruscas de presión.

## 7. RESUMEN DE RIESGOS Y MEDIDAS PREVENTIVAS DETECTADAS EN LA PLANTA

<b>MEDIDAS DE SEGURIDAD PLANTA HIDRÓLISIS DE BIOMASA</b>			
<b>LÍNEA DE ALIMENTACIÓN</b>			
<b>Elementos</b>	<b>Descripción</b>	<b>Riesgos</b>	<b>Precauciones</b>
Tanques de alimentación	Tanques de vidrio agitados y calefactados donde se almacena la suspensión biomasa/agua para su adecuación antes de entrar al reactor	Salpicaduras y derrames derivados del exceso nivel de suspensión o elevada agitación.	Bata, guantes y gafas de protección. EPIs necesarias para la biomasa.
Bomba impulsión de suspensión de celulosa	Bomba de membrana de alta presión Pmax 300 bar	Sobrepresión Goteos en la zona de impulsión y aspiración Fugas en el sistema de purga para la eliminación del aire y cebado	Realizar las operaciones de ajuste de estas fugas con los EPIs necesarios (guantes, gafas y mascarilla en caso de manipulación de residuo peligroso. Válvula de alivio tarada a 320 bar
<b>LÍNEA DE VAPOR</b>			
Bomba de impulsión de agua.	Bomba de membrana de alta presión Pmax 300 bar	Sobrepresión Goteos en la zona de impulsión y aspiración Fugas en el sistema de purga para la eliminación del aire y cebado	Realizar las operaciones de ajuste de estas fugas con los EPIs necesarios (guantes, gafas y mascarilla en caso de manipulación de residuo peligroso. Válvula de alivio tarada a 320 bar
Calentador	Pre calentador eléctrico de 10000 W. T < 550°C	Superficie caliente: quemaduras Derivaciones T excesiva	Aislamiento del pre calentador y las tuberías de salida NO ACCEDER A LA ZONA CALIENTE DURANTE LA OPERACIÓN. Regulación automática. Apagado a T max Conexión a tierra.
Disco de ruptura	Se rompe cuando hay una sobrepresión por encima de 330 bar liberando vapor que puede estar hasta a 550°C	Liberación súbita, violenta y masiva de vapor	Colocar las tuberías de salida del disco de ruptura hacia arriba. Anclarlas bien. NUNCA ACERCARSE A LA ZONA DE SALIDA DEL DISCO DE RUPTURA SI SE SOSPECHA QUE HA SALTADO UN DISCO DE RUPTURA.
<b>REACTOR</b>			
<b>Elementos</b>	<b>Descripción</b>	<b>Riesgos</b>	<b>Precauciones</b>
Tubería a presión	Recipiente tubular a presión. Tmax= 425°C, Pmax=300 bar	Sobrepresión en el interior Exceso de temperatura en la pared del reactor Quemaduras	Control de P maxima en la línea. Aislamiento

			No es una zona de trabajo habitual durante la operación
Aislante	Carcasa de aluminio y material aislante: lana de vidrio y lana de roca de propiedades similares al amianto	Inhalación de partículas del aislante o contacto cutáneo que irrita la piel y es susceptible de causar daños en las vías respiratorias	Uso de ropa desechable, mascarilla, gafas y guantes. Evitar el contacto con la piel y vías respiratorias

### LÍNEA DE SALIDA

Elementos	Descripción	Riesgos	Precauciones
Tubería caliente	Tubería acero inoxidable ¼" Pmax 400 bar	Quemaduras, sobrepresión	Aislamiento tuberías NO ACCEDER DURANTE OPERACIÓN
Válvula de descompresión	Válvula de aguja	Atasco	Existencia de una válvula auxiliar

### ENFRIADORES

Elementos	Descripción	Riesgos	Precauciones
Enfriador	Cambiador de calor con adecuación de la temperatura del efluente	Vapores calientes procedentes de fugas	NO PERMANECER CERCA DEL CIRCUITO DE REFRIGERACIÓN DURANTE LA OPERACIÓN

### ZONA DE CONTROL

Elementos	Descripción	Riesgos	Precauciones
Manómetros, válvulas y ordenador		Rotura de cristales de manómetros. Fugas de residuo en la zona de válvulas	Gafas de seguridad Protección de panel y pantalla de metacrilato Revisión y reparación de posibles fugas

## 8. FICHAS DE SEGURIDAD DE LOS PRODUCTOS EMPLEADOS



Health	1
Fire	1
Reactivity	0
Personal Protection	B

### Material Safety Data Sheet Cellulose MSDS

Section 1: Chemical Product and Company Identification	
<b>Product Name:</b> Cellulose <b>Catalog Codes:</b> SLC4804 <b>CAS#:</b> 9004-34-6 <b>RTECS:</b> FJ5691460 <b>TSCA:</b> TSCA 8(b) inventory: Cellulose <b>CI#:</b> Not available. <b>Synonym:</b> Cellulose, Microcrystalline <b>Chemical Name:</b> Cellulose <b>Chemical Formula:</b> POLYMER	<b>Contact Information:</b> <b>Sciencelab.com, Inc.</b> 14025 Smith Rd. Houston, Texas 77396 <b>US Sales: 1-800-901-7247</b> <b>International Sales: 1-281-441-4400</b> Order Online: <a href="http://ScienceLab.com">ScienceLab.com</a> <b>CHEMTREC (24HR Emergency Telephone), call:</b> 1-800-424-9300 <b>International CHEMTREC, call:</b> 1-703-527-3887 <b>For non-emergency assistance, call:</b> 1-281-441-4400

Section 2: Composition and Information on Ingredients		
<b>Composition:</b>		
<b>Name</b>	<b>CAS #</b>	<b>% by Weight</b>
Cellulose	9004-34-6	100
<b>Toxicological Data on Ingredients:</b> Not applicable.		

Section 3: Hazards Identification
<b>Potential Acute Health Effects:</b> Slightly hazardous in case of eye contact (irritant), of ingestion, of inhalation. Non-irritant for skin. <b>Potential Chronic Health Effects:</b> CARCINOGENIC EFFECTS: Not available. MUTAGENIC EFFECTS: Not available. TERATOGENIC EFFECTS: Not available. DEVELOPMENTAL TOXICITY: Not available. Repeated or prolonged exposure is not known to aggravate medical condition.

Section 4: First Aid Measures
<b>Eye Contact:</b> Check for and remove any contact lenses. In case of contact, immediately flush eyes with plenty of water for at least 15 minutes. Get medical attention if irritation occurs. <b>Skin Contact:</b> Wash with soap and water. Get medical attention if irritation develops.

**Serious Skin Contact:** Not available.

**Inhalation:**

If inhaled, remove to fresh air. If not breathing, give artificial respiration. If breathing is difficult, give oxygen. Get medical attention if symptoms appear.

**Serious Inhalation:** Not available.

**Ingestion:**

Do NOT induce vomiting unless directed to do so by medical personnel. Never give anything by mouth to an unconscious person. Loosen tight clothing such as a collar, tie, belt or waistband. Get medical attention if symptoms appear.

**Serious Ingestion:** Not available.

### Section 5: Fire and Explosion Data

**Flammability of the Product:** May be combustible at high temperature.

**Auto-Ignition Temperature:** Not available.

**Flash Points:** Not available.

**Flammable Limits:** Not available.

**Products of Combustion:** Not available.

**Fire Hazards in Presence of Various Substances:**

Slightly flammable to flammable in presence of open flames and sparks, of heat. Non-flammable in presence of shocks.

**Explosion Hazards in Presence of Various Substances:**

Risks of explosion of the product in presence of mechanical impact: Not available. Risks of explosion of the product in presence of static discharge: Not available.

**Fire Fighting Media and Instructions:**

SMALL FIRE: Use DRY chemical powder. LARGE FIRE: Use water spray, fog or foam. Do not use water jet.

**Special Remarks on Fire Hazards:**

Damp cellulose can be a significant fire hazard since it may undergo spontaneous combustion. Fire and explosions may occur from reactions involving pentafluoride, acetic acid and cellulose. Contact between cellulose and sodium nitrite at elevated temperatures results in vigorous burning from decomposition reaction.

**Special Remarks on Explosion Hazards:**

Fire and explosions may occur from reactions involving pentafluoride, acetic acid and cellulose. Contact between cotton and fluorine may result in violent explosion. Excess dust generation may create explosion hazard.

### Section 6: Accidental Release Measures

**Small Spill:**

Use appropriate tools to put the spilled solid in a convenient waste disposal container. Finish cleaning by spreading water on the contaminated surface and dispose of according to local and regional authority requirements.

**Large Spill:**

Use a shovel to put the material into a convenient waste disposal container. Finish cleaning by spreading water on the contaminated surface and allow to evacuate through the sanitary system. Be careful that the product is not present at a concentration level above TLV. Check TLV on the MSDS and with local authorities.

### Section 7: Handling and Storage

**Precautions:**

Keep away from heat. Keep away from sources of ignition. Empty containers pose a fire risk, evaporate the residue under a fume hood. Ground all equipment containing material. Do not ingest. Do not breathe dust. If ingested, seek medical advice immediately and show the container or the label.

**Storage:** Keep container tightly closed. Keep container in a cool, well-ventilated area. Do not store above 25°C (77°F).

### Section 8: Exposure Controls/Personal Protection

**Engineering Controls:**

Use process enclosures, local exhaust ventilation, or other engineering controls to keep airborne levels below recommended exposure limits. If user operations generate dust, fume or mist, use ventilation to keep exposure to airborne contaminants below the exposure limit.

**Personal Protection:** Safety glasses. Lab coat. Gloves (impervious).

**Personal Protection in Case of a Large Spill:**

Splash goggles. Full suit. Boots. Gloves. Suggested protective clothing might not be sufficient; consult a specialist BEFORE handling this product.

**Exposure Limits:**

TWA: 10 (mg/m<sup>3</sup>) from ACGIH (TLV) [United States] Inhalation Total. TWA: 10 (mg/m<sup>3</sup>) from British Columbia Occupational Exposure Limit [Canada] Inhalation Total. TWA: 3 from British Columbia Occupational Exposure Limit [Canada] Inhalation Respirable. TWA: 5 (mg/m<sup>3</sup>) from OSHA (PEL) [United States] Inhalation Respirable. TWA: 15 (mg/m<sup>3</sup>) from OSHA (PEL) [United States] Inhalation Total. TWA: 10 STEL: 20 (mg/m<sup>3</sup>) [United Kingdom (UK)] Inhalation Total. TWA: 4 (mg/m<sup>3</sup>) [United Kingdom (UK)] Inhalation Respirable. Consult local authorities for acceptable exposure limits.

### Section 9: Physical and Chemical Properties

**Physical state and appearance:**

Solid. (A polymer consisting of linked glucose units (cellobiose) in unbranched linear chains. It may exist as a fibrous or white crystalline solid. Microcrystalline cellulose consists of rigid rods. It is the main constituent of plant fiber.)

**Odor:** Odorless.

**Taste:** Tasteless.

**Molecular Weight:** Not available.

**Color:** Off-white.

**pH (1% soln/water):** Not applicable.

**Boiling Point:** Decomposes.

**Melting Point:** 500°C (932°F) - 518 C

**Critical Temperature:** Not available.

**Specific Gravity:**

1.27 - 1.61@ 0 C (32 F)(Water = 1) 0.28-.032 (temperature not listed)

**Vapor Pressure:** Not applicable.

**Vapor Density:** Not available.

**Volatility:** Not available.

**Odor Threshold:** Not available.

**Water/Oil Dist. Coeff.:** Not available.

**Ionicity (in Water):** Not available.

**Dispersion Properties:** Not available.

**Solubility:**

Insoluble in cold water, hot water. Insoluble in organic solvents. It will swell in dilute alkaline solutions such as sodium hydroxide and will dissolve in caustic alkali with carbon disulfide. It is soluble in ammoniacal copper hydroxide solution (Schweitzer's reagent) and concentrated zinc chloride solution.

### Section 10: Stability and Reactivity Data

**Stability:** The product is stable.  
**Instability Temperature:** Not available.  
**Conditions of Instability:** Excess heat, incompatible materials  
**Incompatibility with various substances:** Not available.  
**Corrosivity:** Non-corrosive in presence of glass.  
**Special Remarks on Reactivity:** Not available.  
**Special Remarks on Corrosivity:** Not available.  
**Polymerization:** Will not occur.

### Section 11: Toxicological Information

**Routes of Entry:** Inhalation. Ingestion.  
**Toxicity to Animals:**  
WARNING: THE LC50 VALUES HEREUNDER ARE ESTIMATED ON THE BASIS OF A 4-HOUR EXPOSURE. Acute oral toxicity (LD50): >5000 mg/kg [Rat]. Acute dermal toxicity (LD50): >2000 mg/kg [Rabbit]. Acute toxicity of the dust (LC50): 5800 mg/m<sup>3</sup> 4 hours [Rat]. 3  
**Chronic Effects on Humans:** Not available.  
**Other Toxic Effects on Humans:**  
Slightly hazardous in case of ingestion, of inhalation. Non-irritant for skin.  
**Special Remarks on Toxicity to Animals:** Not available.  
**Special Remarks on Chronic Effects on Humans:** Not available.  
**Special Remarks on other Toxic Effects on Humans:**  
Acute Potential Health Effects: Skin: It is not known to cause skin irritation. Ingestion: Ingestion of large amounts of cellulose may cause digestive tract irritation. Eyes: Dust may cause mechanical irritation. To the best of our knowledge, there are no known cases of adverse effects or disease in humans from exposure to cellulose. Health effects from cotton fibers, wood, flax, jute, and hemp are usually due to other substances. Purified cellulose is known to be essentially inert. Pure cellulose dust is not known to be irritating or toxic. Chronic Potential Health Effects: Chronic inhalation from cellulose-containing fibers can cause byssinosis. Allergies can develop to cellulose-containing fibers, but these are probably due to plant proteins or other components. In chronic feeding studies with purified cellulose in mice and rats, no significant adverse reactions were seen.

### Section 12: Ecological Information

**Ecotoxicity:** Not available.  
**BOD5 and COD:** Not available.  
**Products of Biodegradation:**  
Possibly hazardous short term degradation products are not likely. However, long term degradation products may arise.  
**Toxicity of the Products of Biodegradation:** The product itself and its products of degradation are not toxic.  
**Special Remarks on the Products of Biodegradation:** Not available.

### Section 13: Disposal Considerations

**Waste Disposal:**

Waste must be disposed of in accordance with federal, state and local environmental control regulations.

#### Section 14: Transport Information

**DOT Classification:** Not a DOT controlled material (United States).

**Identification:** Not applicable.

**Special Provisions for Transport:** Not applicable.

#### Section 15: Other Regulatory Information

**Federal and State Regulations:**

Illinois toxic substances disclosure to employee act: Cellulose Rhode Island RTK hazardous substances: Cellulose  
Pennsylvania RTK: Cellulose Minnesota: Cellulose Massachusetts RTK: Cellulose TSCA 8(b) inventory: Cellulose

**Other Regulations:** EINECS: This product is on the European Inventory of Existing Commercial Chemical Substances.

**Other Classifications:**

**WHMIS (Canada):** Not controlled under WHMIS (Canada).

**DSCL (EEC):**

This product is not classified according to the EU regulations. Not applicable.

**HMIS (U.S.A.):**

**Health Hazard:** 1

**Fire Hazard:** 1

**Reactivity:** 0

**Personal Protection:** B

**National Fire Protection Association (U.S.A.):**

**Health:** 1

**Flammability:** 1

**Reactivity:** 0

**Specific hazard:**

**Protective Equipment:**

Gloves (impervious). Lab coat. Not applicable. Safety glasses.

#### Section 16: Other Information

**References:** Not available.

**Other Special Considerations:** Not available.

**Created:** 10/11/2005 11:34 AM

**Last Updated:** 11/06/2008 12:00 PM

*The information above is believed to be accurate and represents the best information currently available to us. However, we make no warranty of merchantability or any other warranty, express or implied, with respect to such information, and we assume no liability resulting from its use. Users should make their own investigations to determine the suitability of the information for their particular purposes. In no event shall ScienceLab.com be liable for any claims, losses, or damages of any third party or for lost profits or any special, indirect, incidental, consequential or exemplary damages, howsoever arising, even if ScienceLab.com has been advised of the possibility of such damages.*

## Fichas Internacionales de Seguridad Química

**ACETONA**

ICSC: 0087

 <p style="text-align: center;"> <b>MINISTERIO DE TRABAJO Y ASUNTOS SOCIALES ESPAÑA</b>                  ACETONA                  Propanona                  Propan-2-ona                  Dimetil cetona  <math>C_3H_6O/CH_3-CO-CH_3</math>                  Masa molecular: 58.1             </p>			
N° CAS 67-64-1 N° RTECS AL3150000 N° ICSC 0087 N° NU 1090 N° CE 606-001-00-8			
			
TIPOS DE PELIGRO/ EXPOSICION	PELIGROS/ SINTOMAS AGUDOS	PREVENCION	PRIMEROS AUXILIOS/ LUCHA CONTRA INCENDIOS
<b>INCENDIO</b>	Altamente inflamable.	Evitar las llamas, NO producir chispas y NO fumar.	Polvo, espuma resistente al alcohol, agua en grandes cantidades, dióxido de carbono.
<b>EXPLOSION</b>	Las mezclas vapor/aire son explosivas.	Sistema cerrado, ventilación, equipo eléctrico y de alumbrado a prueba de explosión. NO utilizar aire comprimido para llenar, vaciar o manipular.	En caso de incendio: mantener fríos los bidones y demás instalaciones rociando con agua.
<b>EXPOSICION</b>			
• <b>INHALACION</b>	Salivación, confusión mental, tos, vértigo, somnolencia, dolor de cabeza, dolor de garganta, pérdida del conocimiento.	Ventilación, extracción localizada o protección respiratoria.	Aire limpio, reposo y proporcionar asistencia médica.
• <b>PIEL</b>	Piel seca, enrojecimiento.	Guantes protectores.	Quitar las ropas contaminadas y aclarar la piel con agua abundante o ducharse.
• <b>OJOS</b>	Enrojecimiento, dolor, visión borrosa. Posible daño en la córnea.	Gafas de protección de seguridad o pantalla facial. No llevar lentes de contacto.	Enjuagar con agua abundante durante varios minutos (quitar las lentes de contacto, si puede hacerse con facilidad) y proporcionar asistencia médica.
• <b>INGESTION</b>	Náuseas, vómitos (para mayor información, véase Inhalación).	No comer, ni beber, ni fumar durante el trabajo.	Enjuagar la boca y proporcionar asistencia médica.
DERRAMAS Y FUGAS	ALMACENAMIENTO	ENVASADO Y ETIQUETADO	
Ventilar. Recoger el líquido procedente de la fuga en recipientes precintables, absorber el líquido residual en arena o absorbente inerte y trasladarlo a un lugar seguro. NO verterlo al alcantarillado. (Protección personal adicional: equipo autónomo de respiración).	A prueba de incendio. Separado de oxidantes fuertes.	símbolo F símbolo Xi R: 11-36-66-67 S: (2-)-9-16-26 Clasificación de Peligros NU: 3 Grupo de Envasado NU: II CE:	
 			
<b>VEASE AL DORSO INFORMACION IMPORTANTE</b>			

## Fichas Internacionales de Seguridad Química

## ACETONA

ICSC: 0087

<b>D A T O S  I M P O R T A N T E S</b>	<p><b>ESTADO FISICO; ASPECTO</b> Líquido incoloro, de olor característico.</p> <p><b>PELIGROS FISICOS</b> El vapor es más denso que el aire y puede extenderse a ras del suelo; posible ignición en punto distante.</p> <p><b>PELIGROS QUIMICOS</b> La sustancia puede formar peróxidos explosivos en contacto con oxidantes fuertes tales como ácido acético, ácido nítrico y peróxido de hidrógeno. Reacciona con cloroformo y bromoformo en condiciones básicas, originando peligro de incendio y explosión. Ataca a los plásticos.</p> <p><b>LIMITES DE EXPOSICION</b> TLV (como TWA): 750 ppm; 1780 mg/m<sup>3</sup> (ACGIH 1993-1994).</p>	<p><b>VIAS DE EXPOSICION</b> La sustancia se puede absorber por inhalación y a través de la piel.</p> <p><b>RIESGO DE INHALACION</b> Por evaporación de esta sustancia a 20°C, se puede alcanzar bastante rápidamente una concentración nociva en el aire alcanzándose mucho antes, si se dispersa.</p> <p><b>EFFECTOS DE EXPOSICION DE CORTA DURACION</b> El vapor de la sustancia irrita los ojos y el tracto respiratorio. La sustancia puede causar efectos en el sistema nervioso central, el hígado, el riñón y el tracto gastrointestinal.</p> <p><b>EFFECTOS DE EXPOSICION PROLONGADA O REPETIDA</b> El contacto prolongado o repetido con la piel puede producir dermatitis. El líquido desengrasa la piel. La sustancia puede afectar a la sangre y a la médula ósea.</p>
	<p><b>PROPIEDADES FISICAS</b></p> <p>Punto de ebullición: 56°C Punto de fusión: -95°C Densidad relativa (agua = 1): 0.8 Solubilidad en agua: Miscible Presión de vapor, kPa a 20°C: 24 Densidad relativa de vapor (aire = 1): 2.0</p>	<p>Densidad relativa de la mezcla vapor/aire a 20°C (aire = 1): 1.2 Punto de inflamación: -18°C c.c. Temperatura de autoignición: 465°C Límites de explosividad, % en volumen en el aire: 2.2-13 Coeficiente de reparto octanol/agua como log Pow: -0.24</p>
<b>DATOS AMBIENTALES</b>		
<b>NOTAS</b>		
<p>El consumo de bebidas alcohólicas aumenta el efecto nocivo. Antes de la destilación comprobar si existen peróxidos; en caso positivo, eliminarlos.</p> <p style="text-align: right;">Ficha de emergencia de transporte (Transport Emergency Card): TEC (R)-30 Código NFPA: H 1; F 3; R 0; .</p>		
<b>INFORMACION ADICIONAL</b>		
FISQ: 3-004 ACETONA		
ICSC: 0087		ACETONA
© CCE, IPCS, 1994		
<b>NOTA LEGAL IMPORTANTE:</b>	<p>Ni la CCE ni la IPCS ni sus representantes son responsables del posible uso de esta información. Esta ficha contiene la opinión colectiva del Comité Internacional de Expertos del IPCS y es independiente de requisitos legales. La versión española incluye el etiquetado asignado por la clasificación europea, actualizado a la vigésima adaptación de la Directiva 67/548/CEE traspuesta a la legislación española por el Real Decreto 363/95 (BOE 5.6.95).</p>	

**FICHA DE DATOS DE SEGURIDAD**

Redactada y presentada con arreglo a lo especificado en la norma ISO 11014-1 (Noviembre 1994)

I. IDENTIFICACION DEL PRODUCTO Y DE LA EMPRESA				
<b>Nombre del producto:</b>		Lana de roca		
<b>Fabricante:</b>		Rockwool Isolation, S.A. (Francia) Rockwool Peninsular, S.A. (España)		
<b>Distribuidor en España:</b>		Rockwool Peninsular, S.A. Calle Bruc, 50 3º 08010 Barcelona	Tel: 93.318.90.28 Fax 93.317.89.66	
<b>Utilización:</b>		Aislamiento térmico y acústico.		
II. COMPOSICION / INFORMACION SOBRE LOS COMPONENTES				
Substancia <sup>(1)</sup>	Nº C.A.S. <sup>(2)</sup>	Contenido % en peso	Clasificación y etiquetado <sup>(3)</sup>	Valor límite de exposición VLE VME
Fibra de roca	No asignado	99,5 a 96 %	Xi, Irritante para la piel (R:38)	1 fibra / ml <sup>(4)</sup>
<p><b>Elementos susceptibles de provocar peligro:</b> ninguno según el anexo I de la Directiva 67/548 CEE.</p> <p><sup>(1)</sup></p> <p><sup>(2)</sup> C.A.S.: Chemical Abstract Service.</p> <p><sup>(3)</sup> Directiva 97/69/CE del 5 de Diciembre de 1997 publicada en el DOCE del 13 de Diciembre de 1997</p> <p><sup>(4)</sup> Circular DRT nº 95/4 del 12 de Enero de 1995 modificando y completando la circular del 19 Julio de 1982 modificada relativa a los valores límite admitidos para las concentraciones de ciertas substancias peligrosas en la atmósfera de los puestos de trabajo (No publicado en el DOCE).</p> <p><b>Revestimientos y adhesivos:</b> No aplicable (producto desnudo). Velo de vidrio, kraft, aluminio, mallas (productos revestidos).</p>				

### III. IDENTIFICACION DE LOS RIESGOS

- Principales riesgos:** Las fibras minerales han sido clasificadas por la U.E. como productos irritantes para la piel. La exposición a niveles altos de polvo pueden irritar la garganta.
- Riesgos específicos:** No aplicable.

### IV. PRIMEROS AUXILIOS

**Medidas a tomar como primeros auxilios:**

**Informaciones en función de las diversas formas de exposición**

- **Inhalación:** Conducir al afectado al aire libre. Sonarse para evacuar el polvo.
- **Contacto con la piel:** Lavar con abundante agua templada y jabón. En caso de alergia consultar al médico.
- **Contacto con los ojos:** Limpiarlos con abundante agua limpia y templada durante 15 minutos como mínimo, opcionalmente consultar al médico.
- **Ingestión:** Sin objeto.

### V. MEDIDAS DE LUCHA CONTRA INCENDIOS

**Medios de extinción:** Agua, agua pulverizada, espumas para los productos desnudos, CO<sub>2</sub> y extintores en seco para los productos revestidos.

<b>VI. MEDIDAS A TOMAR EN CASO DE DISPERSION ACCIDENTAL</b>	
<b>Precauciones individuales:</b>	En caso de presencia abundante de polvo, utilizar el mismo equipamiento de protección individual que el mencionado en el párrafo VIII.
<b>Precauciones para la protección del medioambiente:</b>	No aplicable.
<b>Métodos de limpieza:</b>	Aspiración.
<b>VII. MANIPULACION Y ALMACENAMIENTO</b>	
<b>Manipulación</b>	
<ul style="list-style-type: none"><li>• <b>Medidas técnicas:</b></li><li>• <b>Precauciones:</b></li><li>• <b>Consejos de uso:</b></li></ul>	No hay medidas específicas. No aplicable. No aplicable.
<b>Almacenamiento</b>	
<ul style="list-style-type: none"><li>• <b>Medidas técnicas:</b></li><li>• <b>Condiciones de almacenaje recomendadas:</b></li><li>• <b>Materiales incompatibles:</b></li><li>• <b>Materiales de embalaje:</b></li></ul>	No hay medidas específicas. Proteger el material de la intemperie. Ninguno. Se suministra embalado en polietileno, cartón y/o madera.
<ul style="list-style-type: none"><li>• <b>Recomendaciones:</b></li></ul>	No hay recomendaciones específicas.

**VIII. CONTROL A LA EXPOSICION / PROTECCION INDIVIDUAL**

<b>Medidas de orden técnico:</b>	Para cortar utilizar preferentemente un cuchillo a una sierra.
<b>Equipamiento de protección individual</b>	
• <b>Protección respiratoria:</b>	Llevar una máscara tipo P1 es recomendable en caso de instalaciones en espacios cerrados, o durante la ejecución de una operación que implique la producción de polvo.
• <b>Protección de manos:</b>	Guantes.
• <b>Protección de la piel y del cuerpo aparte de las manos:</b>	Utilizar ropa ancha y con los cierres de las muñecas cerrados.
• <b>Protección de los ojos:</b>	Gafas de protección.
<b>Medidas de higiene:</b>	Tras un contacto prolongado, lavarse las manos con abundante agua y jabón.

**IX. PROPIEDADES FISICAS Y QUIMICAS**

<b>Estado físico:</b>	Sólido.
<b>Forma:</b>	Lana mineral, de textura homogénea, presentada en forma de paneles, fieltros, coquillas, etc.
<b>Diámetro aproximado de las fibras:</b>	3 a 5 micras.
<b>Diámetro medio geométrico:</b> <small>Ponderado por la longitud</small>	< 6 micras.
<b>Color de la lana:</b>	Tostado
<b>Olor:</b>	No aplicable.
<b>PH (a 1000 g/l H<sub>2</sub>O, 25°C):</b>	7 a 8 (DIN 54275)
<b>Temperatura de desvitrificación:</b>	Alrededor de los 1400 ° C.
<b>Ebullición:</b>	No aplicable.
<b>Chispas:</b>	No aplicable.
<b>Explosión:</b>	No aplicable.
<b>Solubilidad en el agua:</b>	Nula.
<b>Masa volumétrica aparente:</b>	Variable según aplicaciones y productos.

<b>X. ESTABILIDAD REACTIVA</b>	
<b>Estabilidad:</b>	Estabilidad de sus características iniciales hasta 750 ° C
<b>Reacciones peligrosas:</b>	No aplicable
<b>Productos de descomposición Peligrosa:</b>	No aplicable
<b>XI. INFORMACIONES TOXICOLÓGICAS</b>	
<b>Toxicidad aguda:</b>	No aplicable.
<b>Toxicidad crónica:</b>	Ningún efecto crónico en las condiciones normales de uso. La vida media medida por inhalación es inferior a 10 días, (según resultados obtenidos con el test realizado de acuerdo con el protocolo europeo, adoptado por los expertos europeos).
<b>Efectos puntuales</b>	
• <b>Inhalación:</b>	Riesgo de picor en la garganta y las fosas nasales.
• <b>Contacto con la piel:</b>	Riesgo de escozor pasajero debido a una irritación mecánica. Estos efectos cesan al cabo de pocos días. Excepcionalmente, riesgo de alergia. No es irritante para la piel según el método B4 de la Directiva europea 67/548/CEE.
• <b>Contacto con los ojos:</b>	Riesgo de picor pasajero o de inflamación.
• <b>Ingestión:</b>	Riesgo de irritación de las vías aerodigestivas superiores.
<b>XII. INFORMACIONES ECOLÓGICAS</b>	
Ningún riesgo de contaminación sobre el medio ambiente para el material instalado. El material es reciclable.	
<b>XIII. CONSIDERACIONES RELATIVAS A LA ELIMINACIÓN DE RESIDUOS</b>	
<b>Restos de residuos:</b>	Aplicar las normas en vigor para la evacuación y eliminación de residuos. Los residuos de estos productos forman parte de la lista verde de residuos (GE-020) Directiva europea nº 259/93 modificada por la decisión nº 96/660).
<b>Embalaje sucio:</b>	Aplicar las normas en vigor para la evacuación y eliminación de los embalajes.
Para mayor información contacte con el fabricante.	

**XIV. INFORMACIONES RELATIVAS AL TRANSPORTE**

**Reglamentaciones internacionales:** No hay recomendaciones especiales.

**XV. INFORMACIONES REGLAMENTARIAS**

La Directiva europea 97/69CE, adaptada en 23ª versión, al progreso de la técnica, la Directiva 67/548/CEE relativa a la clasificación, embalaje y etiquetado de sustancias peligrosas, define los criterios que permiten exonerar a las fibras de las lanas minerales de vidrio o de roca de la clasificación cancerinógena (categoría 3) si éstas cumplen como mínimo con uno de los cuatro tests practicados sobre animales.

Estos tests se realizan exponiendo a los animales a muy fuertes dosis, por ejemplo, a concentraciones cerca de 100 veces superiores a las medidas, normalmente en los lugares de trabajo durante la producción o tras la instalación de los productos. Los protocolos que describen estos tests han sido adoptados por los expertos europeos el 25 de Febrero de 1998.

Las fibras de lana de roca de este producto están exoneradas de la clasificación cancerinógena de las sustancias en los términos de la nota Q de la Directiva 97/69/CE.

Las fibras de las lanas minerales de vidrio, o de roca están consideradas como irritantes para la piel.

**XVI. OTRAS INFORMACIONES**

Las personas que deseen informaciones más detalladas pueden dirigirse al fabricante, cuyos datos se encuentran indicados en la primera página de este documento.

Esta ficha contiene las informaciones basadas en el estado de nuestros conocimientos relativos al producto en fecha 28 de diciembre de 1998. Estos se dan de buena fe.

Llamamos la atención a los usuarios sobre el eventual riesgo desconocido que se asume en el caso de utilizar el producto, para otras aplicaciones diferentes para las que ha sido concebido el producto.

## 9. SEGURIDAD EN EL DISEÑO

El reactor fue diseñado para unas condiciones de  $P_{max} = 30 \text{ MPa}$  y  $T_{max} = 400^\circ\text{C}$ .

Será necesario incluir en el diseño de la planta elementos de seguridad en los casos en los que prevea la normativa o que la persona que diseña piense que pueden ser críticos. Para ello es conveniente realizar algún tipo de análisis de la instalación, por ejemplo un análisis de riesgos y operabilidad HAZOP.

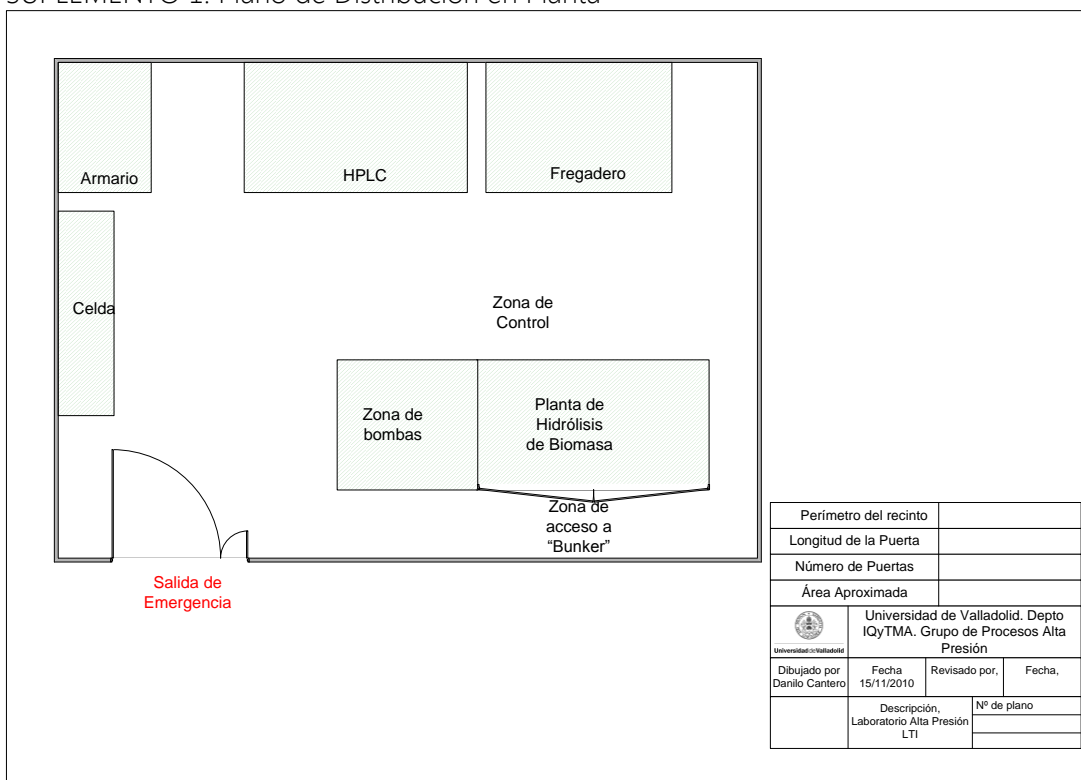
También será importante prever en el diseño una correcta ubicación de los equipos atendiendo a la seguridad, operabilidad, accesibilidad y ergonomía.

Es conveniente respetar las distancias de seguridad en el diseño. En este caso, también ha sido crítico el situar la zona de mayor riesgo: caliente y a presión en una zona donde no es necesario el acceso durante la operación.

El reactor según las recomendaciones de seguridad dadas para equipos a presión, está situado en el interior de un "bunker" de madera de 30 mm de espesor de pared al que se tiene acceso por la parte opuesta a la zona de control donde se encuentra el operario.

## SUPLEMENTOS

### SUPLEMENTO 1. Plano de Distribución en Planta



### SUPLEMENTO 2. Hojas de Especificaciones

Hojas de especificaciones: bombas, reactores, recipientes, válvulas de descompresión Y precalentadores y enfriadores.



Universidad de Valladolid

# EQUIPMENT LIST

REV.	0				JOB NO.	
DATE	17/11/2010				UNIT	
BY	DC				CLIENT	Uva
APPR'V	YES				LOCATION	Dr. Mergelina S/N. Esc. Ings. Inds. Depto IQyTMA

REV.	ITEM NO.	QUANTITY	DESCRIPTION	ORIGIN (1)	DRIVER (1)	REMARKS
1	P-1	1	Bomba abastecimiento de Agua Destilada	O	M	
2	P-2	1	Bomba abastecimiento de Agua Destilada	O	M	
3	P-3	1	Bomba alimentaci3n de suspensi3n de Celulosa	O	M	
4	T-1	1	Tanque almacenamiento de Agua	E		
5	T-2	1	Tanque almacenamiento de Suspensi3n	E		
6	T-3	1	Tanque de toma de muestra	E		
7	T-4	1	Tanque de toma de muestra	E		
8	T-5	1	Tanque de almacenamiento de residuos	E		
9	HV-1	1	V3lvula l3nea de P-1	O		
10	HV-2	1	V3lvula l3nea de P-2	O		
11	HV-3	1	V3lvula antirretorno l3nea de agua	O		
12	HV-4	1	V3lvula antirretorno l3nea de celulosa	O		
13	NV-5	1	V3lvula regulaci3n de la Presi3n	O		
14	HV-6	1	V3lvula de selecci3n de toma muestra	O		
15	HV-7	1	V3lvula de selecci3n de toma muestra	O		
16	NV-8	1	V3lvula de descompresi3n de seguridad	O		
17	SV-1	1	V3lvula de seguridad	O		
18	SV-2	1	V3lvula de seguridad	O		
19	E-1	1	Calentador	E		
20	E-2	1	Enfriador	E		
21	E-3	1	Enfriador	E		
22	V-1	1	C3mara de Flash	E		
23	SV-3	1	V3lvula Seguridad Flash	O		
24	R-1	1	Reactor	E		
25						
26						
27						
28						
29						
30						
31						
32						
33						
34						
35						
36						
37						
38						
39						
40						
41						

**LEGEND:**

1- DRIVER: M - ELECTRIC MOTOR T - TURBINE

ORIGIN: E - SPAIN O - OTHERS

HOJA DE ESPECIFICACIONES				
	BOMBA DE DESPLAZAMIENTO POSITIVO (ÉMBOLO)		Nº EQUIPO	P-1
			Hoja Nº	1/1
	SERVICIO		Bombeo flujo de agua al calentador	
CARACTERÍSTICAS DEL EQUIPO				
1	Marca	DOSAPRO MILTON ROY		
2	Modelo	C 99 07279.01		
3	Nº Serie	55900141		
4	Carcasa	Hierro Fundido		
5	Émbolo	Acero AISI 316-L		
6	Asiento válvulas y rodamiento			
7				
CONDICIONES DE SERVICIO				
8	Fluido	Agua		
9	Caudal (L/h)	4,70		
10	Temperatura (°C)	20		
11	Presión Aspiración (MPa)	0,1		
12	Presión Impulsión (Mpa)	30		
ACCIONAMIENTO				
13	TIPO	Motor Eléctrico		
14	POTENCIA	0,37 kW		
17	VOLTAJE	380 - 420		
18	FASES	3		
19	CICLOS	50		



## HOJA DE ESPECIFICACIONES

BOMBA DE DESPLAZAMIENTO  
POSITIVO (ÉMBOLO)

N° EQUIPO

P-2

Hoja N°

1/1

SERVICIO

Bombeo flujo de agua al calentador

### CARACTERÍSTICAS DEL EQUIPO

1	Marca	DOSAPRO MILTON ROY
2	Modelo	C 0327719/01
3	N° Serie	55040014
4	Carcasa	Hierro Fundido
5	Émbolo	Aceros AISI 316-L
6	Asiento válvulas y rodamiento	
7		

### CONDICIONES DE SERVICIO

8	Fluido	Agua
9	Caudal (L/h)	4,79
10	Temperatura (°C)	20
11	Presión Aspiración (MPa)	0,1
12	Presión Impulsión (Mpa)	30

### ACCIONAMIENTO

13	TIPO	Eléctrico
14	POTENCIA	0,55 kW
17	VOLTAJE	230 - 400
18	FASES	3
19	CICLOS	50

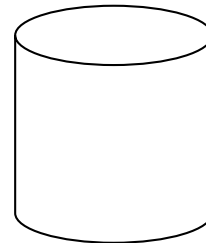
	HOJA DE ESPECIFICACIONES		
	BOMBA DE DESPLAZAMIENTO POSITIVO (ÉMBOLO)	Nº EQUIPO	P-3
		Hoja Nº	1/1
	SERVICIO	Bombeo flujo de suspensión de celulosa	
CARACTERÍSTICAS DEL EQUIPO			
1	Marca	GILSON	
2	Modelo	305	
3	Nº Serie	360G8C342	
4	Carcasa	Hierro	
5	Émbolo	AISI 316-L	
6	Asiento válvulas y rodamiento		
7			
CONDICIONES DE SERVICIO			
8	Fluido	Agua	
9	Caudal (L/h)	1,5	
10	Temperatura (°C)	20	
11	Presión Aspiración (MPa)	0,1	
12	Presión Impulsión (Mpa)	30	
ACCIONAMIENTO			
13	TIPO	Eléctrico	
14	POTENCIA	120VA	
17	VOLTAJE	220 - 240	
19	CICLOS	50	



Storage Tank  
Process Data Sheet

REV.					JOB N°	
DATE	17/11/10				UNIT	
BY	DC				CLIENT	UVa
APRV					UBICATION	DR. MERGELINA S/N. DEPTO IQyTMA

1	Item n°	T-1	Quantity	1
2	Service	Water Supply		
3	Fluid	Distilled water		
4	Capacity	Nominal	5	L
5		Net	7	L
6	Diameter	250	mm	Height
				250
				mm
7	Pressure in tank	Operating	1	Atm
8		Design	1	Barg
9		Vacuum D		
10	Temperature in Tank	Operating	20	°C
11		Design	20	°C
12	Coil	Op. Press.	0	Barg
13		Op. Temp.	20	°C
14		Design P.	0	Barg
15		Design T.	20	°C
16		Nominal D.	0,2	inch
17		Length	1	M
18		Material	Corr. Allow.	
19	Shell/Roof	Plastic		
20	Cladding	-		
21	Coil	Plastic		
22				
23	Type	Conical Roof	Floating Roof	
24		API	Refrigerated	
25	Bottom	x	Flat	
26			Conical pointing Downwards	
27			Conical pointing Upwards	
28	Code	API Std. 620		
29	Stress relieve for process reasons			
30	Insulation	Type		
31		Thickness		mm



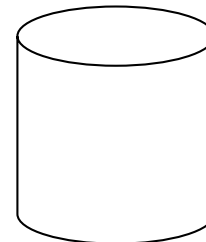
32	Notes				Nozzles			
33					Mark n°	Quantity	Size	Service
34								
35								
36								
37								
38								



## Storage Tank Process Data Sheet

REV.					JOB Nº	
DATE	17/11/10				UNIT	
BY	DC				CLIENT	UVa
APRV					UBICATION	DR. MERGELINA S/N. DEPTO IQyTMA

1	Item nº	T-2	Quantity	1		
2	Service	Feed Supply				
3	Fluid	Distilled water + cellulose				
4	Capacity	Nominal	3	L		
5		Net	3	L		
6	Diameter	170	mm	Height	250	mm
7	Pressure in tank			Operating	1	Atm
8				Design	1	Barg
9			Vacuum D			
10	Temperature in Tank			Operating	45	°C
11				Design	80	°C
12	Coil			Op. Press.	0	Barg
13				Op. Temp.	45	°C
14				Design P.	0	Barg
15				Design T.	20	°C
16				Nominal D.	1/16	inch
17				Length	1	M
18	Material		Corr. Allow.			
19	Shell/Roof	Glass				
20	Cladding	-				
21	Coil	Plastic				
22						
23	Type		Conical Roof	Floating Roof		
24			API	Refrigerated		
25	Bottom	x	Flat			
26			Conical pointing Downwards			
27			Conical pointing Upwards			
28	Code	API Std. 620				
29	Stress relieve for process reasons					
30	Insulation	Type				
31		Thickness				mm

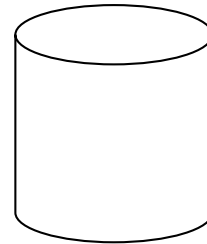


32	Notes	Nozzles			
33		Mark nº	Quantity	Size	Service
34					
35					
36					
37					
38					



Storage Tank  
Process Data Sheet

REV.					JOB N°	
DATE	17/11/10				UNIT	
BY	DC				CLIENT	UVa
APRV					UBICATION	DR. MERGELINA S/N. DEPTO IQYTMA
1	Item n°	T-3/T-4	Quantity	2		
2	Service	Samples				
3	Fluid	Cellulose derivates				
4	Capacity	Nominal	0.1	L		
5		Net	0.1	L		
6	Diameter	50	mm	Height	70	mm
7	Pressure in tank			Operating	1	Atm
8				Design	1	Barg
9				Vacuum D		
10	Temperature in Tank			Operating	20	°C
11				Design	20	°C
12	Coil			Op. Press.		Barg
13				Op. Temp.		°C
14				Design P.		Barg
15				Design T.		°C
16				Nominal D.		inch
17				Length		M
18		Material	Corr. Allow.			
19	Shell/Roof	Plastic				
20	Cladding	-				
21	Coil	-				
22						
23	Type		Conical Roof	Floating Roof		
24			API	Refrigerated		
25	Bottom	x	Flat			
26			Conical pointing Downwards			
27			Conical pointing Upwards			
28	Code	API Std. 620				
29	Stress relieve for process reasons					
30	Insulation	Type				
31		Thickness				mm
32	Notes					Nozzles
33				Mark n°	Quantity	Size Service
34						
35						
36						
37						
38						

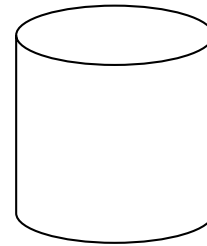




Storage Tank  
Process Data Sheet

REV.					JOB N°	
DATE	17/11/10				UNIT	
BY	DC				CLIENT	UVa
APRV					UBICATION	DR. MERGELINA S/N. DEPTO IQyTMA

1	Item n°	T-5	Quantity	1
2	Service	Liquid waste		
3	Fluid	Cellulose derivates		
4	Capacity	Nominal	20	L
5		Net	20	L
6	Diameter	250	mm	Height
				700
				mm
7	Pressure in tank	Operating	1	Atm
8		Design	1	Barg
9		Vacuum D		
10	Temperature in Tank	Operating	20	°C
11		Design	20	°C
12	Coil	Op. Press.	0	Barg
13		Op. Temp.	20	°C
14		Design P.	0	Barg
15		Design T.	20	°C
16		Nominal D.	0,25	inch
17		Length	1	M
18		Material	Corr. Allow.	
19	Shell/Roof	Plastic		
20	Cladding	-		
21	Coil	Plastic		
22				
23	Type	Conical Roof	Floating Roof	
24		API	Refrigerated	
25	Bottom	x Flat		
26		Conical pointing Downwards		
27		Conical pointing Upwards		
28	Code	API Std. 620		
29	Stress relieve for process reasons			
30	Insulation	Type		
31		Thickness		mm
32	Notes			
33				Nozzles
34				Mark n°
35				Quantity
36				Size
37				Service
38				





## Control Valves

REV.					JOB N°	
DATE	17/11/10				UNIT	
BY	DC				CLIENT	UVa
APRV					UBICATION	DR. MERGELINA S/N. DEPTO IQyTMA

1	Item n°	NV-5		Quantity	1	
2	Model	30VRMM4812				
3	Service	Pressure Control				
4	Fluid	Cellulose derivates				
5	Total Flow	10	kG/h			
6	In. liq. Flow	10	kG/h	Out Li. Flow	3	kG/h
7	In. vap. Flow		kG/h	In. vap. Flow	7	kG/h
8	DP at normal flow	250		bar		
9	Normal inlet Pressure, asb	300		Max		
10	Critical pressure, abs	221				
11	Vapor Pressure abs.					
12		max		min		
13	Normal Temperature (°C)	425		20		
14	Liquid density (kg/m <sup>3</sup> )	126		1009		
15	Viscosity, (cP)	,028		,99		
16	GAS, molecular W					
17	GAS composition					
18	Leaks					
19	Action on air failure					
20	Material	AISI 316				
21	Packing	graphite braided yarn				
22						
23						
24						
25						
26						
27						
28						
29						
30						
31						
32						
33						
34						
35						
36						
37						
38						
39						





## Control Valves

REV.				JOB N°	
DATE	17/11/10			UNIT	
BY	DC			CLIENT	UVa
APRV				UBICATION	DR. MERGELINA S/N. DEPTO IQYTMA

1	Item n°	NV-8		Quantity	1	
2	Model					
3	Service	Pressure Control				
4	Fluid	Cellulose derivates				
5	Total Flow	10	kg/h			
6	In. liq. Flow	10	kg/h	Out Li. Flow	3	kg/h
7	In. vap. Flow		kg/h	In. vap. Flow	7	kg/h
8	DP at normal flow	250		bar		
9	Normal inlet Pressure, asb	300		Max		
10	Critical pressure, abs	221				
11	Vapor Pressure abs.					
12		max		min		
13	Normal Temperature	425		300		
14	Liquid density	7.039		41.244		
15	Viscosity,	28.455		91.649		
16	GAS, molecular W					
17	GAS composition					
18	Leaks					
19	Action on air failure					
20	Material	AISI 316				
21						
22						
23						
24						
25						
26						
27						
28						
29						
30						
31						
32						
33						
34						
35						
36						
37						
38						
39						





Universidad de Valladolid

## HEAT EXCHANGER PROCESS DATA SHEET

REV.	0				JOB Nº	
DATE	17-nov				UNIT	
BY	DC				CLIENT	Uva
APPRV					LOCATION	Depto IQyTMA
REV.						
1	ITEM NUMBER	E-2			QUANTITY	1
2	SERVICE	Enfriamiento corriente salida reactor				
3	OPERATING CASE					
4	<b>TEMA Type</b>		Units	SHELL SIDE	TUBE SIDE	
5	FLUID CIRCULATED			Agua refrigeracion	Agua + derivados de cel.	
6	<b>FLOW TOTAL.</b>	Normal (Máx.)	kg/h	108	7	
7	Gas			0	0	
8	Liquid			108	0	
9	Steam			0	7	
10	Incondensables			0	0	
11	Vaporized or condensate			0	0	
12	Steam or condensate			0	0	
13	LIQUID DENSITY (Inlet/Outlet)		kg/m <sup>3</sup>	998	992	0,58 (Vap) 992
14	VISCOSITY-LIQUID (Inlet/Outlet)		cP	1	0,65	0,012 0,65
15	MOLECULAR WEIGHT-GAS (Inlet/Outlet)					
16	SPECIFIC HEAT (Inlet/Outlet)		J/mol K	75,37	75,29	37,41 75,29
17	ENTHALPY (Inlet/Outlet)		kJ/mol	1,51	3	48,2 3
18	THERMAL CONDUCTIVITY		W/m . K	0,61		,02 (vap)
19	SURFACE TENSION		dyna/cm			
20	<b>TEMPERATURE INLET</b>		°C	20 100		
21	<b>OUTLET</b>		°C	40 25		
22	OPERATING PRESSURE (Normal, Inlet)		barg	2 0,5		
23	ALLOWABLE PRESSURE DROP		bar	1 0,1		
24	FOULING FACTOR		h m <sup>2</sup> °C/kcal			
25	<b>DUTY</b>		kcal/h	4270		
26	SURFACE OVERDESIGN		%			
27	<b>DESIGN CONDITIONS</b>					
28	PRESSURE (MAX)		barg	5 5		
29	TEMPERATURE		°C	40 100		
30	<b>MATERIALS</b>					
31	Shell and cover	Copper + isolation		Tubes	Copper	
32	Floating head and cover			Channel and cover		
33	Fixed tubesheet			Floating tubesheet		
34	Wear plate			Baffles		
35	Joint type	Gaskets				
36	Dimensions	Shell side	0,75 inch	Tube side	0,5 inch	
37	NOZZLES	Shell side	Inlet	inch	Outlet	inch
38		Tube side	Inlet	inch	Outlet	inch
39	CODE REQUIREMENTS					
40	<b>NOTES</b>					
41						
41						
42						
43						
44						



Universidad de Valladolid

## HEAT EXCHANGER PROCESS DATA SHEET

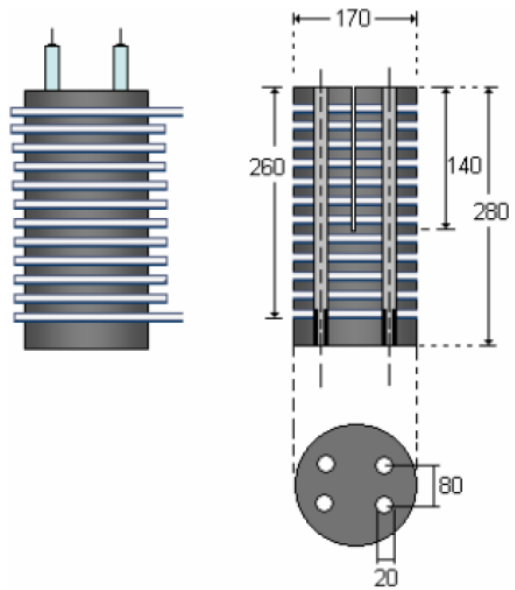
REV.	0				JOB Nº	
DATE	17-nov				UNIT	
BY	DC				CLIENT	Uva
APPRV					LOCATION	Depto IQyTMA
REV.						
1	ITEM NUMBER	E-3			QUANTITY	1
2	SERVICE	Enfriamiento corriente salida reactor				
3	OPERATING CASE					
4	<b>TEMA Type</b>		Units	SHELL SIDE	TUBE SIDE	
5	FLUID CIRCULATED			Agua refrigeracion	Agua + derivados de cel.	
6	<b>FLOW TOTAL.</b>	Normal (Máx.)	kg/h	14	2	
7	Gas			0	0	
8	Liquid			14	2	
9	Steam			0	0	
10	Incondensables			0	0	
11	Vaporized or condensate			0	0	
12	Steam or condensate			0	0	
13	LIQUID DENSITY (Inlet/Outlet)		kg/m <sup>3</sup>	998	995	960 998
14	VISCOSITY-LIQUID (Inlet/Outlet)		cP	1	0,65	0,28 0,65
15	MOLECULAR WEIGHT-GAS (Inlet/Outlet)					
16	SPECIFIC HEAT (Inlet/Outlet)		J/mol K	75,37	75,29	75,926 75,29
17	ENTHALPY (Inlet/Outlet)		kJ/mol	1,51	2,27	7,47 2,27
18	THERMAL CONDUCTIVITY		W/m . K	0,61		0,678
19	SURFACE TENSION		dyna/cm			
20	<b>TEMPERATURE INLET</b>		°C	20		99
21	<b>OUTLET</b>		°C	30		30
22	OPERATING PRESSURE (Normal, Inlet)		barg	2		0,5
23	ALLOWABLE PRESSURE DROP		bar	1		0,1
24	FOULING FACTOR		h m <sup>2</sup> °C/kcal			
25	<b>DUTY</b>		kcal/h	138		
26	SURFACE OVERDESIGN		%			
27	<b>DESIGN CONDITIONS</b>					
28	PRESSURE (MAX)		barg	300		300
29	TEMPERATURE		°C	40		100
30	<b>MATERIALS</b>					
31	Shell and cover	AISI 316		Tubes	Inconel 625	
32	Floating head and cover			Channel and cover		
33	Fixed tubesheet			Floating tubesheet		
34	Wear plate			Baffles		
35	Joint type	Gaskets				
36	Dimensions	Shell side	0,5 inch	Tube side	0,25 inch	
37	NOZZLES	Shell side	Inlet	inch	Outlet	inch
38		Tube side	Inlet	inch	Outlet	inch
39	CODE REQUIREMENTS					
40	<b>NOTES</b>					
41						
41						
42						
43						
44						



# Heater

REV.				JOB N°	
DATE	17/11/10			UNIT	
BY	DC			CLIENT	UVa
APRV				UBICATION	DR. MERGELINA S/N. DEPTO IQyTMA

1	Item n°	E-1	Quantity	1
2	Model	Resistance- conduction-pipe		
3	Service	Heater		
4	Type	Electric		
5	Support for resistences	Brass, resin		
6	Resistances	4 x 2500 W		
7	Outlet D pipe (in)	¼ "		
8	Thickness (mm)	0.035		
9	Material pipe	Inconel 600		
10	Isolation	Rock wool		
11	Support for isolation	Aluminum shell		
12	Work fluid	Water		
13	Cp ave. (kJ/kG)	4		
14	Work pressure (bar)	250		
15	Lowest Temperature (°C)	25		
16	Highest Temperature (°C)	550		
17	U (W/m²)	3310		
18	Thermometer	Type K		
19				
20				
21				
22				
23				
24				
25				
26				
27				
28				
29				
30				
31				
32				
33				
34				
35				
36				



### SUPLEMENTO 3. Flujos de las bombas P-1 y P-2

Bomba P-1		
Recorrido	Flujo mL/min	desvío mL/min
100%	89,0	2,2
75%	62,4	2,3
50%	36,2	2,2

Bomba P-2		
Recorrido	Flujo mL/min	desvío mL/min
100%	91,2	2,0
75%	70,2	1,7
50%	44,8	1,6

### SUPLEMENTO 4. Programa Picolog Recorder.

#### Utilidades del programa

El programa permite realizar el seguimiento en línea de la temperatura y presión en la planta piloto de hidrólisis de celulosa en agua presurizada. Las variables que son seguidas son:

- Temperatura del calentador (E-1),
- Temperatura del vapor de inyección,
- Temperatura luego de la mezcla celulosa-vapor,
- Temperatura en el medio del reactor,
- Temperatura a la salida del reactor,
- Temperatura a la salida de la válvula NV-5,
- Presión del sistema.

De cada una de estas variables el programa registra 1 dato por segundo. El tiempo de toma de datos lo controla el operario dando inicio o fin a la toma de datos.

El programa permite realizar un seguimiento grafico de las variables ya los datos son mostrados en graficas en línea y en una tabla.

## Uso del programa

Inicio → Todos los programas → Pico Technology → Picolog Recorder

Se abren 2 ventanas (Datos y gráfica)

Guardar archivo

Archivo → Guardar como...

Si el archivo luego se desea exportar a Excel debemos guardarlo con extensión \*.txt; de lo contrario el formato por defecto es \*.plw.

Cuando se desea comenzar la toma de datos se debe hacer "click" en el icono "play" ►; si se quiere pausar la toma de datos se debe hacer "click" en el icono pausa y si se quiere detener la toma de datos se debe hacer "click" en "stop" ■.

Abrir archivo

Archivo → Abrir...

Configuración registro de datos

Configuración → Canales de entrada → Tipo TC-08 → Aceptar

Escoger los canales → Aceptar

Configuración grafica

Para seleccionar los canales que se deseen graficar, sobre la ventana del gráfico se debe hacer "click" sobre el icono: Seleccionar canales → se escogen → Aceptar.



# About the author

Danilo A. Cantero was born in Río Cuarto, Córdoba, Argentina on September 15, 1985. He grew up in Rio Cuarto, where he graduated from high school in 2003 from the ENET N° 1



Ambrosio Olmos obtaining the degree of technician of goods and services production in food industry. He, then, joined the Universidad Nacional de Córdoba where he studied Chemical Engineering for five years. Danilo graduated in April 2009 with the degree of Chemical Engineer. In April 2009 Danilo was appointed Assistant Professor of the Department of Applied Chemistry in the University of Córdoba, Argentina. In September 2009, Danilo joined the University of Valladolid, Spain, for a M.S. in Thermodynamic Engineering of Fluids, and continued with the Ph.D. starting September 2010. During the Ph.D. Thesis the author completed its

research work with a doctoral stay in the department of "*Lehrstuhl für Prozessmaschinen und Anlagentechnik*" in the University of Erlangen, Germany.

## List of Publication

(3) Danilo A. Cantero; M. Dolores Bermejo; M José Cocero. High glucose selectivity in pressurized water hydrolysis of cellulose using ultra-fast reactors. *Bioresource Technology*.135, pp. 697 - 703.El Servier, 2013. *Journal Article*

(2) Danilo A. Cantero; M Dolores Bermejo; M José Cocero. Kinetic analysis of cellulose depolymerization reactions in near critical water. *The Journal of Supercritical Fluids*.75, pp. 48 - 57.El Servier, 2013. *Journal Article*

(1) M José Cocero; Danilo A. Cantero; M. Dolores Bermejo; Juan García Serna. Nuevas tendencias en el diseño de procesos para aprovechamiento de residuos alimentarios dirigidos a conseguir una sociedad sostenible. Retos medioambientales de la industria alimentaria. pp. 89 - 102.IMC, 2012. *Book Chapter*

## Submitted / In preparation

(4) Tunable Selectivity on Cellulose Hydrolysis in Supercritical Water. *Angewanted Chemie International Edition*

(5) Biomass refining processes intensification by supercritical water. Review. *Journal of Supercritical Fluids – especial issue*.

(6) Selective Transformation of Fructose into Pyruvaldehyde in Supercritical Water. Reaction Pathway Development. *Bioresource Technology*

(7) Transformation of Glucose in Added Value Compounds in a Hydrothermal Reaction Media. *Journal of Supercritical Fluids*

(8) Pressure and Temperature Effect on Cellulose Hydrolysis Kinetic in Pressurized Water. *Chemical Engineering Journal*.

(9) Hydrothermal Fractionation of Grape Seeds with Subcritical Water to Produce Polyphenols, Sugars and Lignin. *Catalysis Today*

(10) Hydrothermal extraction and hydrolysis of grape seeds to produce bio-oil. *RSC Advances*

(11) On the Energetic Approach of Biomass Hydrolysis in Supercritical Water. *Applied Energy*

(12) Simultaneous and Selective Recovery of Cellulose and Hemicellulose Fractions from Wheat Bran by Supercritical Water Hydrolysis. *Bioresour Technology*

## Conference Contributions

### Oral presentations

(8) Danilo A Cantero; M. Dolores Bermejo; M José Cocero. Pressure Effect on Cellulose Hydrolysis in Pressurized Water. September 2013.

(7) Danilo A Cantero; M. Dolores Bermejo; M José Cocero. "Hydrolysis of cellulose in sub and supercritical water. Experimental results, modeling and reactor optimization". 30<sup>th</sup> International Exhibition-Congress on Chemical Engineering, Environmental Protection and Biotechnology. June 2012.

(6) Danilo A. Cantero; Ana Lorenzo Hernando; Juan García Serna; M. Dolores Bermejo; Pedro Fardim; M. José Cocero. "Selective depolymerization of lignin in sub and supercritical water". International Congress of Chemical Engineering. June 2012.

(5) Juan García Serna; Danilo A. Cantero; Francisco Sobrón; M. José Cocero. "Semi continuous fractioning of grape seed biomass in subcritical Water." International Congress of Chemical Engineering. June 2012.

(4) Danilo A. Cantero; M. Dolores Bermejo; M. José Cocero. "Experimental Study of Cellulose Depolymerization in Near Critical Water Using a Novel Facility". 13th European Meeting on Supercritical Fluids. Keynote Lecture. October 2011.

(3) Danilo A. Cantero; M. Dolores Bermejo; M José Cocero. "Optimizing cellulose hydrolysis process in hot pressurized water media. Reactor analysis". 8th European congress of chemical engineering. September 2011.

(2) Danilo A. Cantero; M. Dolores Bermejo; M. José Cocero. "Cellulose Hydrolysis in pressurized water: kinetics revision, reactor modeling and pilot plant design and construction". Second International seminar on Engineering Thermodynamics of Fluids. July 2011.

(1) Danilo A. Cantero; M. Dolores Bermejo; M. José Cocero. "Hidrólisis de celulosa en agua presurizada: modelado de reactor y análisis cinético experimental". 2<sup>nd</sup> Reunión Interdisciplinaria de Tecnología y Procesos Químicos (RITeQ). October 2010.

## Poster Presentations

(3) Cantero, Danilo A.; Álvarez, Ana; Bermejo, M. Dolores; Cocero, M. José. "Transformation of glucose in high added value compounds in a hydrothermal reaction media". III Iberoamerican Conference on Supercritical Fluids. April 2013.

(2) Danilo A. Cantero; M. Dolores Bermejo; Pablo Cabeza; M. José Cocero. "Hidrólisis de Celulosa en Agua Presurizada". 4<sup>a</sup> Reunión de Expertos en Tecnologías de Fluidos Compromisos. February 2010.

(1) Danilo A. Cantero; M Dolores Bermejo; M Jose Cocero. "Cellulose Depolymerization: Process Design in Pressurized Water". III Reunión de Jóvenes Investigadores iberoamericanos de la UVa. November 2009.